TECHNISCHE UNIVERSITÄT MÜNCHEN
Lehrstuhl für Experimentelle Genetik

Genome-wide association study to search for SNPs affecting gene expression in a general population

Divya Deepak Mehta

Vollständiger Abdruck der von der Fakultät Wissenschaftszentrum Weihenstephan für Ernährung, Landnutzung und Umwelt der Technischen Universität München zur Erlangung des akademischen Grades eines

Doktors der Naturwissenschaften

genehmigten Dissertation.

Vorsitzender: Univ.-Prof. Dr. A. Gierl

Prüfer der Dissertation:

1. Univ.-Prof. Dr. Th. Meitinger
2. apl. Prof. Dr. J. Adamski
3. Univ.-Prof. Dr. H -R. Fries

Die Dissertation wurde am 19.12.2008 bei der Technischen Universität München eingereicht und durch die Fakultät Wissenschaftszentrum Weihenstephan für Ernährung, Landnutzung und Umwelt am 10.10.2009 angenommen.

Table of Contents

Zusammenfassung

Die quantitative Erfassung von Gentranskription liefert wertvolle Hinweise bei der Untersuchung genetischer Risikofaktoren von haüfigen Erkrankungen. Ziel dieser Arbeit war es, DNA-Varianten in der Normalbevölkerung zu identifizieren, welche die Genaktivität beeinflussen. Dazu wurde eine genomweite Assoziationsstudie (GWAS) von 381 Individuen der KORA Kohorte durchgeführt. Expressionsmuster im Vollblut führten zur Identifikation von neuen eQTLs und halfen bei der funktionellen Validierung von Kandidatengenen, die durch GWAS für quantitative Phänotypen identifiziert wurden. Zudem konnten mit Hilfe der eQTLs neue regulatorische Zusammenhänge beschrieben werden. Insgesamt lieferten die funktionellen Daten der Genaktivität wertvolle Hinweise, um die Konsequenzen der genetischen Varianz besser zu verstehen.

1.0 Summary

The aim of this study was to identify SNPs affecting gene expression in the general population. To achieve this, a genome-wide association study (GWAS) was performed from peripheral blood of 381 individuals belonging to the German KORA (Kooperative Gesundheitsforschung in der Region Augsburg) cohort.

A total of 371 identified peripheral blood eQTLs (expression quantitative trait loci) were compared to published eQTLs from HapMap lymphoblast cell lines. An overlap of 30% of eQTLs between the KORA and HapMap could be demonstrated. The remaining 70% of identified KORA eQTLs indicate a high degree of tissue-specific expression. The expression profiles allowed functional inference of 5% of complex trait associated SNPs at the level of transcription. In addition to discovery of novel whole blood eQTLs, the expression profiles allowed functional validation of two candidate genes identified in independent GWAS for uric acid levels and mean platelet volume (Doring, Gieger et al. 2008). Interrogation of SNPs reported in published GWAS with expression profiles generated in this study allowed discovery of 11 novel eSNPs. Furthermore, the transcriptional profiles allowed identification of a novel mechanism of IgE regulation in whole blood (Weidinger, Gieger et al. 2008).

Integration of gene expression data with genotype data has the potential to directly identify experimentally supported candidate susceptibility genes for disease (Schadt, Lamb et al. 2005). The application of gene expression profiles to augment several genome-wide association results and to identify novel biological pathways was demonstrated in this study.

2.0 Introduction

The fundamental aim of genetics is to understand the relation between phenotypes and genotypes (Botstein and Risch 2003). It has long been recognized that inherited DNA polymorphisms are responsible for clustering of common diseases in families (Newton-Cheh and Hirschhorn 2005). The earliest reported association between inherited variation and disease risk in 1956 was that of individuals with duodenal ulcer being more likely to have blood type O (Willer, Sanna et al. 2008). In the 1970s it was proposed that common functional variation could explain some of the inherited variation in susceptibility to common diseases (Harris 1970). One such earliest identified effect still remains one of the strongest known associations between common genetic variation and complex traits: 90% of individuals with type 1 diabetes carried either a DR3 or a DR4 allele at the HLA locus as compared to 20% of controls (Redondo, Fain et al. 2001). This early identified strong effect set high expectations for the strength of effects to be found in subsequent genetic studies. In the 1980's linkage studies using DNA polymorphisms to connect Mendelian diseases with DNA of genes were first proposed (Figures 1 and 2) (Botstein, White et al. 1980). At that time, polymerase chain reaction and restriction fragment length polymorphisms were used for analyses. The early genetic studies being statistically underpowered, were conducted to detect signals in candidate genes only (Hirschhorn, Lohmueller et al. 2002).

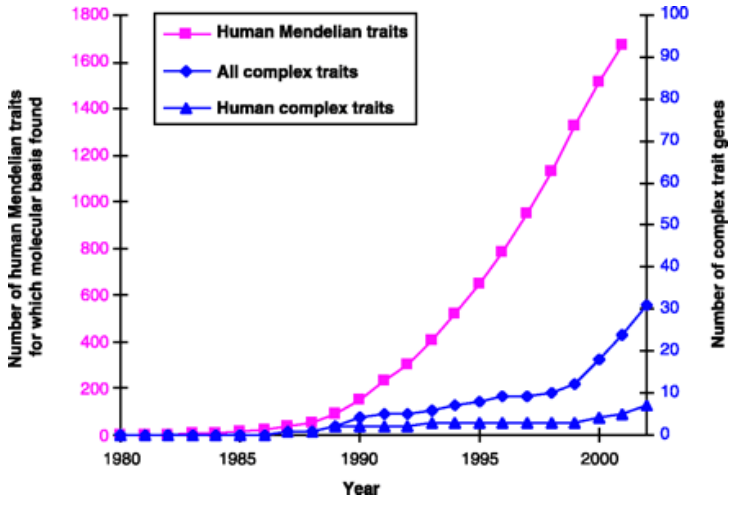

Figure 1-Progress in mapping of Mendelian and complex traits: Number of human traits for which molecular basis has been identified between the years 1980-2000 (Figure taken from Glazier et al. 2002).

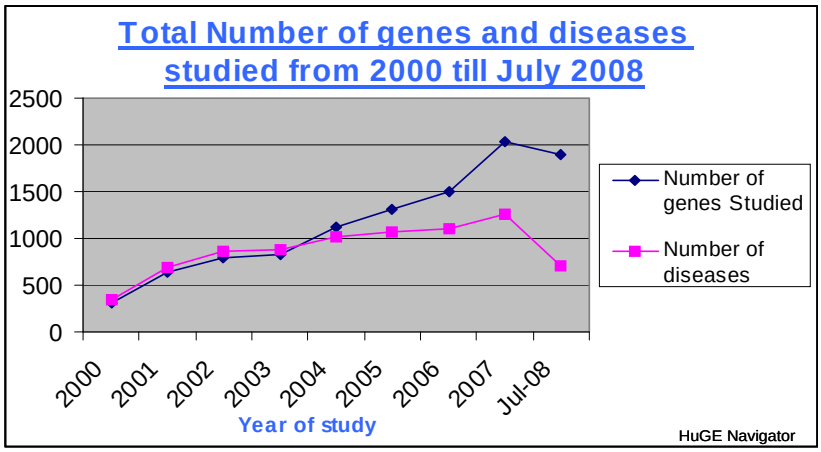

Figure 2-Number of genes and diseases studied from 2000 until July 2008: Until 2004 the number of identified genes corresponded to the number of diseases studied. In the later years, more genes per disease were identified, highlighting the complex nature of the studied diseases.

Today scientists benefit from an almost exhaustive list of common single nucleotide polymorphisms (SNPs), sites in the genome sequence of 3 billion nucleotide bases where individuals differ by a single base (Arking, Pfeufer et al. 2006). Roughly ten million such sites, an average of about one site per 300 bases are estimated to exist in the human population, a large number of which have been made available through the sequencing of the human genome (Venter, Adams et al. 2001; Tanaka 2005). Theoretically it is possible to type all ten million common SNPs in affected and unaffected individuals to locate sites differing in frequency between the two groups. Practically it is an expensive, labor-intensive and time-consuming endeavor and the possibility of not capturing rarer variants responsible for the effects is very high.

The pattern of association among SNPs in the genome can be derived on the basis of haplotypes and linkage disequilibrium (LD) (Takeuchi, Yanai et al. 2005). A haplotype is a combination of a set of alleles at a number of closely spaced sites on a single chromosome (Grapes, Firat et al. 2006). The rationale is that since for most SNPs, the rate of mutation is relatively low (roughly 10^{-8} per site per generation), nearby SNP alleles tend to be associated and inherited together more often that expected by chance (Gabriel, Schaffner et al. 2002). SNP alleles that are almost always inherited together are said to be in high LD. Hence the allele of one SNP in an individual is strongly predictive

of the allele of other SNPs located nearby in high LD (Enard, Khaitovich et al. 2002). In theory a small number of SNPs can produce several different combinations with other SNP alleles, but in reality fewer combinations make up the bulk of the haplotypes observed in humans (Gabriel, Schaffner et al. 2002). As a result, only a few carefully chosen representative "tag SNPs" need to be typed in order to predict the likely variants in that region (Halperin, Kimmel et al. 2005).

The International HapMap Consortium used tag SNPs to produce four human haplotype maps by genotyping lymphoblast cell lines of 270 people from four populations with diverse geographic ancestry (Tanaka 2005). Population-based genetic studies such as the HapMap have been successfully utilized to map genetic factors affecting gene expression and other cellular phenotypes (Cheung, Conlin et al. 2003; Stranger, Forrest et al. 2007).

The multifactorial nature of complex trait implies that each involved individual genetic variant generally has only a modest effect and the interaction of genetic variants with each other and with the environment determine the observed end phenotype (Newton-Cheh, Hirschhorn, 2005). Newly discovered genetic variants have the potential to explain at least some of the inherited variation in susceptibility to common disease and bring us one step closer to the elucidation of underlying biological causal mechanisms.

2.1 RNAissance and gene regulation

The accepted principle of unidirectional flow of genetic information from DNA to RNA to protein now forms the central dogma of molecular biology in almost all organisms (Crick 1970). It was evident that DNA was the carrier of genetic information containing the blueprints for proteins, but DNA itself could only have been formed with the aid of enzymes, which are proteins. Proteins, on the other hand, were the end products of the flow of genetic information that begins with DNA. The observation of DNA in the nucleus and synthesis of protein in the cytoplasm of eukaryotic cells suggested the possibility of something intermediate. In 1956, Volkin and Astrachan made a significant observation when they infected *E.coli* with T2 phage, inducing a rapid burst of RNA synthesis (Volkin and Astrachan 1956). The pulse-chase experiment could be demonstrated in eukaryotic cells pulsed with radioactive uracil transferred to a medium consisting of unlabelled uracil (Figure 3). The cells after pulsing had their labeled uracil

in the nucleus but the cells after the chase (removal) had their labeled RNA in the cytoplasm (Gros, Hiatt et al. 1961). This was a clear indication that RNA was first synthesized in the nucleus and later moved to the cytoplasm, making it an ideal candidate as an information- transfer intermediate between DNA and protein (Volkin 2001).

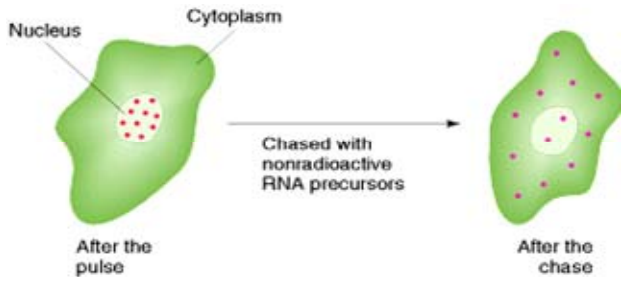

Figure 3-Pulse-chase experiment: The cells after pulsing had labeled uracil within the nucleus but after the chase have labeled RNA in the cytoplasm, indicating that RNA is synthesized in the nucleus and then moves to the cytoplasm (Figure taken from Griffiths 2005).

Transcription of DNA into RNA occurs in the nucleus and translation of RNA into protein occurs in the cytoplasm (Carmo-Fonseca 2007). Only a small portion of DNA in cells is transcribed into RNA and furthermore only a fraction of the RNA and proteins encoded in the genome are expressed. The control of a gene's transcript and its protein product is termed as gene regulation (Struhl 1999). Gene regulation is highly complex with an interplay of several combinatorial interactions and multiple components of the cell participating in the process (Chabot, Shrit et al. 2007). Mechanisms controlling mammalian gene expression can be categorized into two broad levels:

a. Transcriptional and post-transcriptional regulation of gene expression: Regulatory mechanisms at the transcriptional level include transcriptional initiation, chromatin condensation and DNA methylation (Bird 2002; Wray, Hahn et al. 2003). For most genes, transcriptional initiation appears to be the principal determinant of the overall mRNA gene expression profile (Jin, Riley et al. 2001). After DNA is transcribed and mRNA is formed, post-transcriptional mechanisms modulate how much of the mRNA is translated into proteins. This is moderated at the level of RNA processing (such as splicing), mRNA transport, mRNA stability, protein processing, targeting and stability.

b. Translational and post-translational regulation of gene expression : Translation is the first stage of protein biosynthesis comprising of four phases including activation, initiation, elongation and termination (Salehi and Mashayekhi 2007). Post- translational regulation includes chemical modifications of proteins after translation such as enzymatic processing of amino acids from the protein (Rucker and McGee 1993).

Most of the genetic regulation is thought to occur at the level of gene transcription (Holstege and Young 1999). Cellular abundance of RNA can be regulated at the level of transcription, processing and mRNA turnout (Figure 4). Traditional methods of gene expression analysis included Northern Blots, RT-PCR and *in-situ* hybridizations. Microarray technologies now allow parallel analysis of thousands of transcripts across many samples simultaneously. Microarrays measure steady state levels of a given transcript and do not examine the individual contributing components and post transcriptional changes (Raghavan and Bohjanen 2004). Despite this, expression levels serve as a good surrogate to study the activity of a gene. Variation in transcript levels is an interesting phenotype as it represents an intermediate stage between DNA sequence differences and complex human traits, thereby providing a snapshot of the consequences of DNA variance on cellular processes (Cheung, Jen et al. 2003).

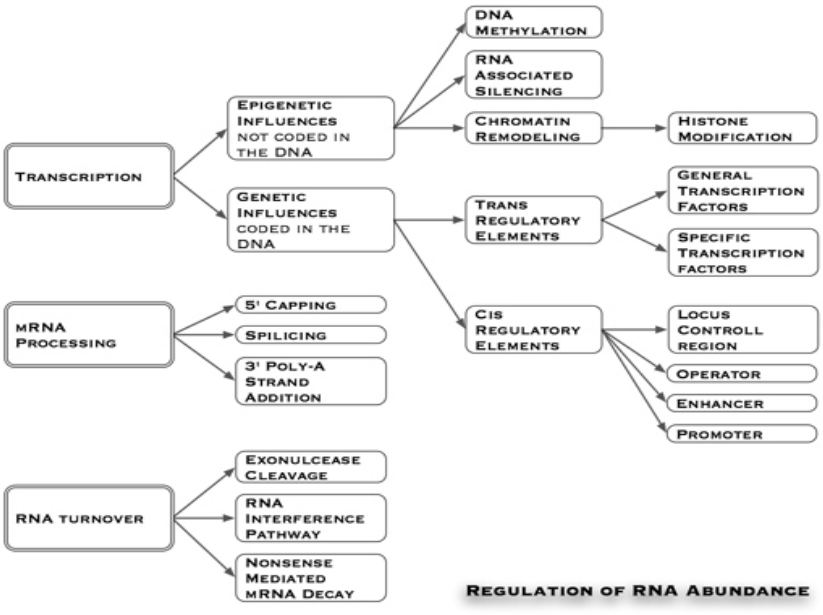

Figure 4-RNA abundance: RNA abundance at the levels of transcription, mRNA processing and RNA turnover (Figure taken from Sperling 2007).

2.2 Variation in human gene expression

The extent, nature and sources of variation in transcript levels across the entire human genome are largely unknown (Cheung, Conlin et al. 2003). Variation in gene expression may be a result of regulatory or environmental effects but usually it is a complex interplay between the two. The completion of the human genome project has resulted in greater attention to genetic variation among individuals and variations at the level of DNA sequence as well as gene expression levels are currently being investigated. Analyses of gene expression patterns have already been successful in definition of tumor types, prediction of cancer classes and identification of molecular markers for cancer (Golub, Slonim et al. 1999). Interrogation of gene expression phenotypes in humans will provide a resource that will greatly facilitate the fine mapping of disease variants in human populations.

2.2.1 Heritability of gene expression variation

The expression level of genes is known to be highly variable and heritable in humans (Cheung, Jen et al. 2003; Schadt, Monks et al. 2003) and other organisms such as yeast (Brem, Yvert et al. 2002), mice (Schadt, Monks et al. 2003) and rat (Petretto, Mangion et al. 2006). Natural variation in gene expression is an outcome of the complex interactions between genetic polymorphisms, physiological variations and environmental components. A fundamental question is what proportion of the variation of the gene expression can be attributed to genetic factors. It is inherently difficult to minimize the contribution of non-genetic factors in humans. An inference of variation in gene expression due to genetic determinants can be addressed by estimation of heritability of genes by familial aggregation studies (Cheung, Jen et al. 2003).

Evidence for familial aggregation of expression phenotype was observed when variation among unrelated individuals, siblings and monozygotic twins were compared in an experiment (Cheung, Jen et al. 2003). Cheung and colleagues analyzed 35 unrelated individuals from the Centre d'Etude du Polymorphisme Humain (CEPH) lymphoblast cell lines. To investigate the genetic basis of variation in gene expression, the authors examined the gene transcript levels of the 5 highest variable genes (ST3GALV1, ACTG2, GK, HNRPA2B1 and DHFR) among 49 unrelated individuals, 41 siblings from

CEPH family offspring and 10 sets of monozygotic twins using RT-PCR. The CEPH collection consists of DNA and lymphoblast cell lines (LCLs) of 61 reference multigenerational Caucasian families from Utah (Dausset, Cann et al. 1990). For the five genes examined, the variance among unrelated individuals was 3-11 times higher then that between monozygotic twins and the variance among siblings was 2-5 times higher than that between the twins. This was one of the first studies suggesting a genetic contribution to phenotypic variation at the level of gene expression (Figure 5).

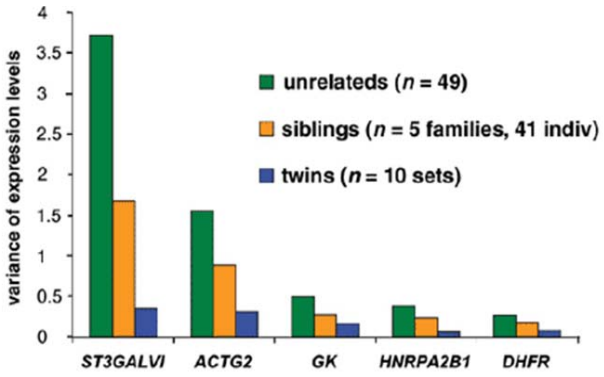

Figure 5-Heritability of gene expression: Quantitative RT-PCR showing that the variance among unrelated individuals is 3-11 times higher and the variance among siblings is 2-5 times higher than that between monozygotic twins (Figure taken from Cheung, Jen et al. 2003).

Recently, Emilsson and colleagues analyzed expression of 23,720 transcripts from blood (IFB=1002) and adipose tissue (IFA=673) in Icelandic subjects (Emilsson et al, 2008). The authors identified 13,910 significantly heritable traits in blood (58.6% of all assessed transcripts) and 16,825 significantly heritable traits in adipose tissue (70.9% of all analyzed transcripts). Furthermore, at least 50% of heritable traits in blood overlapped with those in adipose tissue. This demonstrated genetic factors to be significant contributors towards variation in gene expression in both blood and adipose tissues.

2.2.2 Cis and trans effects

A central question arising from heritability of gene expression relates to the relative contribution of gene-proximal (cis-acting) versus long-range (trans-acting) determinants. Most of the expression controlling elements are expected to be a combination of cis and

trans-acting sequences acting in concert to regulate expression levels (Cheung, Jen et al. 2003).

2.2.2.1 Cis-acting elements

A substantial proportion of variation in gene expression levels might be explained by variation in cis (Jin, Riley et al. 2001). Cis-elements are DNA sequences located within the promoter of a gene, just upstream of the transcriptional start site (Trinklein, Aldred et al. 2003). Vertebrate gene expression is regulated by different classes of cis-regulatory DNA sequences including enhancers, silencers, insulators and promoters (Butler and Kadonaga 2002; Felsenfeld 2003).

In humans, mice and maize, at least 30-50% of the genetic basis for differences in transcription level are cis to the coding locus (Schadt, Monks et al. 2003; Morley, Molony et al. 2004; Stranger, Forrest et al. 2005). Morley et al measured expression levels of 3,554 genes in 14 large CEPH families and found that 19% of significant gene expression phenotype associations mapped in cis (Morley, Molony et al. 2004). Unfortunately there is no golden standard to decide what cis-interval one should use for analysis. From various studies it was evident from the observed cis-associations that most of the cis-acting elements clustered within a 100kb interval from the center of the transcript (Figure 6).

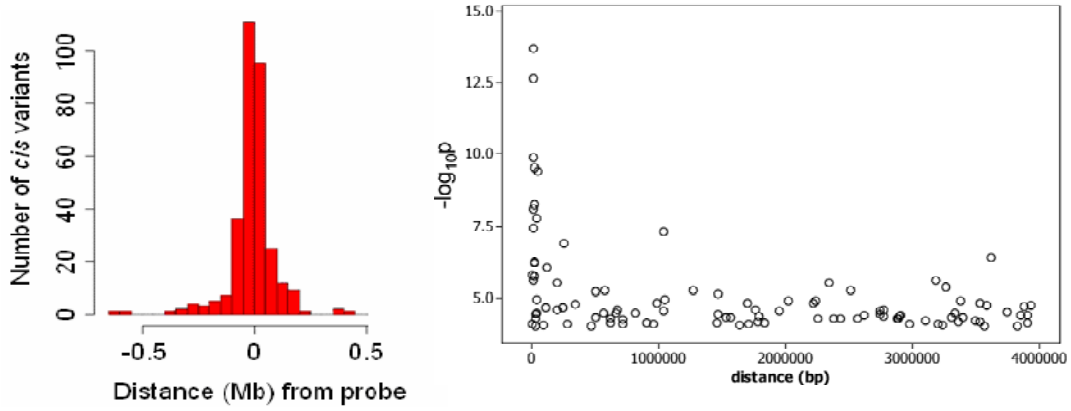

Figure 6-Cis associations: Studies indicating that most cis SNPs were located within 100kb upstream and downstream of the transcript midpoint (Figure taken from Stranger, Forrest et al. 2007; Emilsson, Thorleifsson et al. 2008).

2.2.2.2 Trans-acting factors

Trans factors are thought to bind to the cis-acting sequences to control gene expression. The detection of trans factors has not been very successful in humans due to the often indirect and weaker consequences of trans effects (Brem, Yvert et al. 2002). Trans effects are known to be sensitive to environmental regulation and hence have been shown to vary between experiments (Goring, Curran et al. 2007). In human studies most of the sample sizes do not provide enough power and are constrained by the multiple testing problems, which make finding trans-effects difficult. To combat this, Stranger et al analyzed trans effects by adopting a candidate variant approach. Prior relevance was assigned to SNPs known to be associated with cis regulation, protein sequence variation or mRNA structure. The authors demonstrated a 3-6 fold enrichment in the contribution of cis-regulatory variants among the trans variants, thereby suggesting that trans associations were largely cis-regulated effects (Stranger, Nica et al. 2007).

2.2.3 Gene expression variation at the level of isoforms

Sequencing of the human genome showed that humans have ~30,000 genes and this finding raised the possibility that alternative splicing rather than an increased number of expressed genomic loci was responsible for the functional complexity in vertebrates (Modrek and Lee 2002). Transcript alterations within coding regions of a gene may greatly alter protein sequences, structure and function. Changes in non-coding regions can have a wide-range of regulatory consequences (Liu and Altman 2003). Splicing effects in several genes such as CFTR and IRF5 result in both monogenic and complex disorders in humans (Field, Bonnevie-Nielsen et al. 2005). The estimate that 40-60% of human genes undergo alternative splicing, does not take into account how many different splice forms exist for each gene (Kim, Klein et al. 2004).

Recent advances in microarray technology allow investigation of genome-wide alternative splicing events (Lee and Roy 2004). Small to large scale microarrays have been designed utilizing probes spanning predicted exon junctions (Modrek, Resch et al. 2001), probes targeted toward individual exons (Frey, Mohammad et al. 2005) or a combination thereof (Srinivasan, Shiue et al. 2005). One of the leading microarray companies, Illumina, previously used target probes mapping to the 3'UTR of a gene and

hence using this microarray it was not possible to identify specific isoform changes. However, the updated microarray has newly designed probes, allowing discrimination of different transcripts for the same gene. Another leading microarray company, Affymetrix, released Affymetrix Gene Chip Exon 1.0 ST arrays designed to interrogate exon-level expression for human, mouse and rat, thereby allowing an even higher resolution of gene expression at the level of the isoform (Gardina, Clark et al. 2006).

Recently, Kwan and colleagues performed a genome-wide analysis of common genetic variation controlling differential expression of transcript isoforms in the HapMap population using a comprehensive exon tiling microarray containing 17,897 genes (Kwan, Benovoy et al. 2008). They detected 324 genes showing significant associations between the flanking SNPs and transcript levels. Of these, 39% reflected changes in whole genome gene expression and 55% reflected transcript isoform changes such as splicing variants and differential 3' and 5' untranslated regions (Kwan, Benovoy et al. 2008). This finding indicated that further investigation into alternative splicing was required to obtain an accurate picture of the true complexity of variation in gene expression.

2.3 Genetic mapping of gene expression variation

Variation in gene expression indicates the presence of regulatory effects and the mapping of these effects in the genome provides evidence for a genetic basis in gene expression variation (Deutsch, Lyle et al. 2005). Recent genetic studies in model organisms such as yeast, maize and mice have discovered extensive functional genetic variation than previously estimated (Brem, Yvert et al. 2002; Bystrykh, Weersing et al. 2005; Schadt, Molony et al. 2008).For genetic analysis, gene expression is considered to be a typical quantitative trait locus and there are 2 major methods used for mapping of these traits in humans: linkage and association (Cheung, Jen et al. 2003).

2.3.1 Linkage studies

Linkage is defined as "the existence or establishment of connection of two things (Elston 1998). Thomas Hunt Morgan observed that the amount of crossing over between linked genes differed and this led him to the idea that crossover frequency might indicate the distance separating genes on the chromosome (Allen 1978; Skaletsky, Kuroda-

Kawaguchi et al. 2003). His student Albert Sturtevant proposed that the greater the distance between linked genes, the greater the chance that non-sister chromatids would cross over in the region between the genes (Morgan 1915). This idea set the foundation for the first linkage map. Linkage studies rely on the use of pedigrees to map co segregation of particular markers with specific phenotypic characteristics (Figure 7). Linkage mapping is powerful when functional variants are rare and there is allelic heterogeneity but the small sizes of most families constitute a major disadvantage.

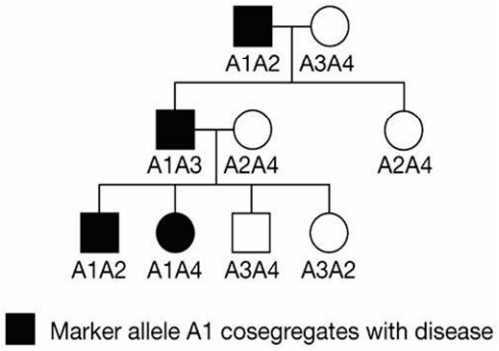

Figure 7-A typical linkage study design: Co-segregation of marker A1 with the disease in a family with 3 generations. The squares denote males and the circles denote females. The coloured squares and circles indicate the affected individuals (Figure taken from Kullo and Ding 2007).

2.3.2 Association studies

The term association owes its name to a medieval Latin word associare which means “to connect”. Association measures deviation from independent transmission of a locus with a disease. Genetic association studies determine whether a genetic variant is associated with a disease or trait: if association is present then a particular allele, genotype or haplotype of a polymorphism will be seen more often than expected by chance in individuals carrying the trait (Giordano, Godi et al. 2008). Association is a powerful method to identify susceptibility genes for common diseases and involves scanning thousands of samples. Most widely used association study designs are case-control and quantitative trait models.

2.3.2.1 Population-based association studies

Population-based association studies can be cohort and/or case-control studies. In population-based cohort studies, samples of a defined population are selected for longitudinal assessment of exposure-outcomes or merely quantitative traits (Szklo 1998). Advantages of using cohorts include estimations of distributions and prevalence of risk factors in a defined population, comparison of future distributions to the baseline measurements and finally an unbiased setting to evaluate all variables of interest.

Case-control is a classical epidemiological study design using subjects having the disease and determining if there are characteristics of these patients that differ from those who do not have the disease or trait (Tsai, Keller et al. 1994). Differences between allele frequencies and/or genotypic polymorphisms and/or haplotypes indicate that the genetic marker may increase risk of disease or likelihood of the trait or be in linkage disequilibrium with a polymorphism which does.

One major problem arising with population-based study designs is that of confounding due to population stratification (Hopper, Bishop et al. 2005).

2.3.2.1.1 Population stratification: lookout for “SUSHI” genes

Population stratification is a situation arising when a study population contains two or more ethnic subgroups having different allele frequencies, and coincidently different levels of a phenotype (Hamer and Sirota 2000).

An example highlighting the problem of population stratification is that of a geneticist aiming to study the "trait" of ability to eat with chopsticks in the San Francisco population. He discovers that allele HLA-A1 was positively associated with ability to use chopsticks and names the gene “SUSHI” (successful use of selected hand instruments). The reason for this false association was simply that the allele HLA-AI was more common among Asians than Caucasian (Hamer and Sirota 2000).

Population stratification can be overcome by using homogeneous populations, matched case-control pairs, exclusion of genetic markers whose allele frequencies differ between populations and applying statistical methods like genomic control (Hoggart, Parra et al. 2003).

2.3.2.2 Genome-wide association studies

The key concern in association studies is to harness recent improvements in our knowledge of the human genome sequence together with advances in genotyping technologies to accelerate discovery of susceptibility loci in a cost-effective manner (Wang, Barratt et al. 2005). The prospect of testing virtually all ~10 million common SNPs in the human genome for association with a given disease was first made public in 1996 (Figure 8).

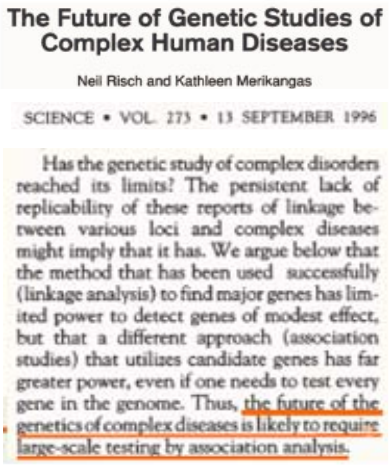

The Future of Genetic Studies of Complex Human Diseases

Neil Risch and Kathleen Merikangas

SCIENCE • VOL. 273 • 13 SEPTEMBER 1996

Has the genetic study of complex disorders reached its limits? The persistent lack of replicability of these reports of linkage between various loci and complex diseases might imply that it has. We argue below that the method that has been used successfully (linkage analysis) to find major genes has limited power to detect genes of modest effect, but that a different approach (association studies) that utilizes candidate genes has far greater power, even if one needs to test every gene in the genome. Thus, the future of the genetics of complex diseases is likely to require large-scale testing by association analysis.

Figure 8-GWAS: First proposal for a GWAS in 1996 (Figure adapted from Risch and Merikangas 2003).

Genome wide association studies (GWAS) represent an hypothesis-free approach "unbiased by prior assumptions of DNA alterations" for identification of genetic variants influencing common human diseases (Figure 9), being (Newton-Cheh and Hirschhorn 2005; Reiman, Webster et al. 2007). Such studies have been particularly useful in finding genetic variations contributing to common, complex diseases such as asthma and Parkinson as well as detection of genetic contribution to natural variation in gene expression (Fung, Scholz et al. 2006; Dixon, Liang et al. 2007).

The common disease common variant (CDCV) hypothesis has been the scientific paradigm for GWAS conducted for many common diseases (Hemminki, Forsti et al. 2008). The CDCV hypothesis proposed that most of the genetic variation in common complex diseases were due to relatively few common variants (Pritchard and Cox 2002). The complimentary hypothesis to CDCV is the classical disease heterogeneity hypothesis

(multiple rare-variant hypothesis) in which disease susceptibility is due to distinct genetic variants in different individuals and disease-susceptibility alleles have low population frequencies (Smith and Lusis 2002). Whether common variants or alternatively many independent rare variants will account for the contributions of specific genes in diseases is still unknown (Ji, Foo et al. 2008).

GWAS have successfully identified a number of common variants associated with quantitative traits but the signals collectively explained only a small fraction of inter-individual risk (Skaletsky, Kuroda-Kawaguchi et al. 2003; Frayling 2007). For example, a GWAS using a total of 30147 subjects identified 20 variants associated with adult height (Weedon, Lango et al. 2008). Combined, the 20 SNPs explained only ~3% of height variation resulting in height alteration between 0.2-0.6 cm per allele.

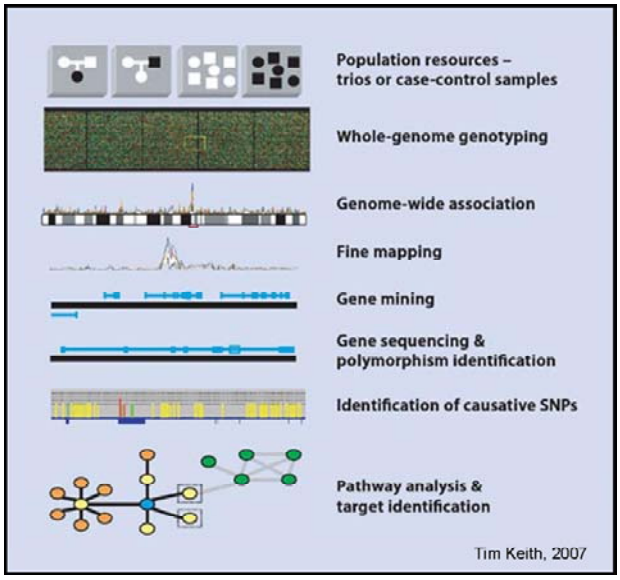

Figure 9-GWAS design: Schematic workflow of a GWAS from sample collection to pathway identification (Figure taken from Tim Keith 2007).

The performed GWAS do not imply that the CDCV hypothesis is false but instead suggest that the power is low for current study sizes to allow for detection of small effect variants (Bourgain, Genin et al. 2007). In addition, while many associated disease variants are frequent, there may be many more variants that are of moderate frequency but which current studies are not designed to find.

3.0 Aims of the Investigation

Alterations in the expression levels of genes are known to result in diseases such as Huntington disease (FitzPatrick, Ramsay et al. 2002; Deutsch, Lyle et al. 2005). An understanding of these putative changes could be beneficial for the detection and diagnosis of complex diseases. However one of the prerequisites of such studies is the knowledge of the magnitude and diversity of gene expression in the unperturbed state.

The KORA (Cooperative Health Research in the Region Augsburg) is a research platform for population based research in the fields of epidemiology, health economics and health care (Holle, Happich et al. 2005). This platform was established in 1996 and since then it has been successfully used in case-control and quantitative studies (Schiebel, Winkelmann et al. 1997; Pfeufer, Jalilzadeh et al. 2005; Arking, Pfeufer et al. 2006).

The goal of this investigation was to identify SNPs affecting gene expression in the KORA population. In order to accomplish this genome-wide gene expression data was generated from whole blood in 497 KORA individuals and was used to conduct the following studies:

1. Analysis of gene expression at the RNA level:

   a) Analysis of whole blood to assess variability in gene expression patterns within a normal population: To check for enrichment of functional categories of transcripts exhibiting the highest and lowest variable among the individuals.

   b) Analysis of gene expression profiles to confirm and propose new biochemical pathways: The goal was to utilize genome-wide expression profiles to confirm known regulatory pathways and possible identification of novel regulatory mechanisms

2. Analysis of gene expression at the phenotypic level:

   a) Identification of age and gender-specific expression: Analysis of expression profiles generated in this study to check for gender- and age-specific signatures. The aim was to question if small changes in expression levels could be used to predict gender and age in humans.

b) Functional validation of candidate genes identified in a genome-wide scan: The ability of transcriptional profiles to augment results from genome-wide association scans and to allow functional inference of the possible causal locus was interrogated.

3. Analysis of gene expression at the DNA level:

a) Identification of cis and trans regulators of expression: Cis and trans regulators usually act in concert to regulate expression of genes. The aim was to identify cis and trans expression quantitative trait loci (eQTLs) in whole blood.

b) Comparison of the resulting blood eQTL results with lymphoblast cell lines eQTL data available from the International HapMap project: The idea was to confirm and replicate identified eQTLs in a different tissue and another population which is a prerequisite for any successful association study.

c) Utilization of the KORA gene expression dataset to test for eSNPs: The goal was to test and confirm for the effects of published SNPs on gene expression to allow discovery of causal SNPs.

4.0 Materials and Methods

4.1 Materials

4.1.1 RNA resources

4.1.1.1 The KORA F3/S3 population

Study approval was obtained from the Ethics Committee of the Bavarian Medical Association (Bayerische Landesärztekammer) and the Bavarian commissioner for data protection and privacy (Bayerischer Datenschutzbeauftragter). In total, four surveys have been conducted. KORA S3 consists of representative samples of 4,856 subjects. In 2003/04, 2,974 participants returned for follow-up (KORA F3). All participants provided written consent after being informed about the study. The subjects came from the study region of Augsburg in the southern part of Germany. It has a population of about 600,000 inhabitants of which 430,000 are between the ages of 25 and 74. All participants underwent cross-sectional surveys and regular medical examination by trained staff. Blood was collected from the KORA cohort (n=497) in PAX tubes and couriered to the Helmholtz Research Center in Neuherberg within 3-4 hours of collection. RNA was extracted from whole blood and amplified, reverse transcribed and biotin-labeled to cRNA. The cRNA was quantified using Ribogreen and Bioanalyzer before it was hybridized on the Illumina Sentrix WG-6 v 2 microarray (Tables 1 and 2).

Table 1-The following kits and reagents were used for the gene expression experiments

Kit/Reagent	Company	Catalogue Number
PAXgene™ Blood RNA Tubes	Qiagen/BD Sciences	762125
PAXgene™ Blood RNA Kit	Qiagen/BD Sciences	762174
RediPlate™ 96 RiboGreen ® Kit	Invitrogen	R32700
Illumina® TotalPrep RNA Amplification Kit	Ambion/ Applied Biosystems	AMIL1791
HumanWG-6 v2 microarray	Illumina	BD-25-112
Cy3-Streptavidin	Amersham Biosciences	PA43001
Agilent RNA 6000 Nano Kit	Agilent	5067-1511
RNaseZap	Ambion	AM9780

Table 2-List of equipments used for the gene expression experiment

Equipment	Company	Catalogue Number
Orbital Shaker Incubator	IKA	VWR 260 basic
Centrifuge Rotana	Hettich	46 RS
Thermal cycler	MJ research	PTC-225
Centrifuge	Sigma Aldrich	6K15, rotor 11150/13350
Thermomixer Compact	Eppendorf	5350
Hybex Microsample Incubator 220V	Scigene	1057-30-2
FLUOstar Microplate Reader	BMG Labtech	413-101
2100 Bioanalyzer	Agilent	DE04700459
Neo block1	Neolab	2503

4.2 Methods

The blood was collected in PAX tubes at the KORA study center in Augsburg. After collection of blood, the PAX tubes were immediately couriered to us at the Institute of Human Genetics, Helmholtz Research Center in Munich. The PAX tubes were stored overnight at room temperature according to the manufacturer's instructions and then further stored at 4°C until required (Figure 10).

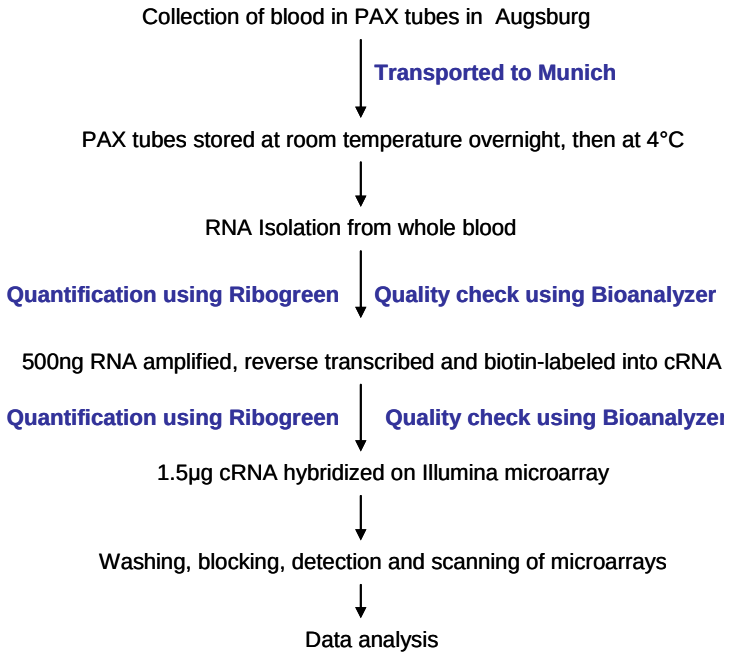

Figure 10-Experimental design: Schematic workflow of gene expression from whole blood in this study.

4.2.1 RNA isolation

The PAX tubes were stored at 4°C after overnight incubation at room temperature. For RNA isolation, the PAX tubes were removed from 4°C and placed at room temperature for 2-3 hours. All reagents were provided in the PAXgene™ Blood RNA Kit. All centrifugations were carried out at 20°C. Protocol (according to the manufacturer's instruction manual):

The PAXgene Blood RNA tubes were centrifuged for 10 minutes at 4000 x g. The supernatant was removed by decanting. 5ml RNase-free water was added to the pellet, thoroughly resuspended by vortexing and centrifuged for 10 minutes at 4000 x g. The supernatant was removed and discarded. The pellet was resuspended in 350µl resuspension buffer BR1 by vortexing. The sample was pipetted into a 1.5 ml microcentrifuge tube and 300µl Buffer BR2 and 40µl Proteinase K was added. The contents were mixed by vortexing for 5 seconds and incubated for 10 minutes at 55°C using a shaker–incubator at 1000rpm. The lysate was pipetted into the lilac coloured PAX gene shredder column placed in a microcentrifuge tube and centrifuged for 3 minutes at 14000 rpm. The supernatant was transferred to a 1.5 ml microcentrifuge tube without disturbing the pellet. 350µl 100% ethanol was added to the tubes, mixed by vortexing, and centrifuged briefly (1–2 seconds). The samples was added to the PAXgene column placed in a 2 ml processing tube and centrifuged for 1 minute at 14000 rpm. The PAXgene column was placed in a new 2ml processing tube and the old processing tube containing flow-through was discarded. The PAXgene column was placed in a new 2ml processing tube, and the old processing tube containing flow-through was discarded. 350µl buffer BR3 was added to the PAXgene spin column and centrifuged at 14000 rpm for 1 minute.

DNase Treatment - The solid DNase 1 (RNFD) was first dissolved in 550µl of the DNase resuspension buffer (DRB) to make the stock solution. For each sample, 10µl DNase I stock solution was added to 70µl buffer RDD, mixed by flicking the tube, and centrifuged briefly to bring to the bottom. 80µl DNase I incubation mix was added onto the PAXgene spin column membrane and incubated at room temperature for 15 minutes.

350µl buffer BR3 was added to the PAXgene spin column and centrifuged at 14000 rpm for 1 minute. The flow through was discarded and 500µl buffer BR4 was added to the column and centrifuged at 14000 rpm for 1 minute. After discarding the flow through, 500µl buffer BR4 was again added to the column and centrifuged at 14000 rpm for 2 minutes. The red spin column was transferred to a 1.5 ml elution tube, 40µl buffer BR5 was pipetted to the center of the column and the tube was centrifuged at 14000 rpm for 1 minute. Another 40µl buffer BR5 was added to the column and centrifuged at 14000 rpm for 1 minute to elute RNA. The eluate was incubated at 65°C for 5 minutes in a heating block (to denature the RNA for downstream applications) and then chilled immediately on ice. The RNA quality was checked for all samples after isolation using an Agilent Bioanalyzer and the stock RNA was stored at -80°C

4.2.2 RNA quality check using Agilent Bioanalyzer Nano 6000 kit

Agilent Nano chips contain an interconnected set of micro channels used for separation of nucleic acid fragments based on their size as they are driven through it electrophoretically. All reagents and samples were equilibrated at room temperature for 30 minutes before use. Procedure (according to the Agilent Bioanalyzer protocol)

The electrodes were decontaminated by washing with RNAse ZAP for 1 minute and with RNAse free water for 10 seconds. 550 of the red Agilent Nano gel matrix was added to the spin filter and centrifuged for 10 minutes at 5000 rpm. 65µl of the filtered gel was aliquoted in microcentrifuge tubes. For each use, 1µl of the blue dye was freshly added to the filtered 65µl gel aliquot and mixed by vortexing followed by a centrifugation step of 10 minutes at 5000 rpm. The chip was placed on the priming station and 9.0µl of the gel-dye mix was pipetted into the well marked. The plunger was positioned at 1 ml and the chip priming station was closed for 30 seconds. The syringe plunger was pressed down until it was held by the clip. After 30 seconds the plunger was released with the clip release mechanism. The priming station was opened and 9.0µl of the gel-dye mix was pipetted in each of the wells marked G. 5µl of the green Nano marker was added to the 12 probe wells and to the ladder well marked as. The RNA probes and the ladder was heat denatured at 70°C for 2 minutes to minimize secondary structures. 1µl of the mixture was added to the ladder well. 1µl of the RNA probes were added to the 12 wells. The chip

was placed in the adapter of the provided vortex mixer and vortexed for 1 minute at 2400 rpm. The chip was inserted in the Agilent 2100 Bioanalyzer and read.

4.2.3 The RIN (RNA Integrity Number)

The RNA integrity number (RIN) is an Agilent software tool designed to estimate the integrity of total RNA using the entire electrophoretic tracing (Schroeder, Mueller et al. 2006). The RIN number ranges from 1-10. A RIN number of 1 indicates totally degraded RNA while a RIN number of 10 indicated an intact RNA sample (Figure 11). After RNA isolation, the biological intactness of the sample was measured and only samples with RIN numbers more than 5.0 were used for subsequent analysis.

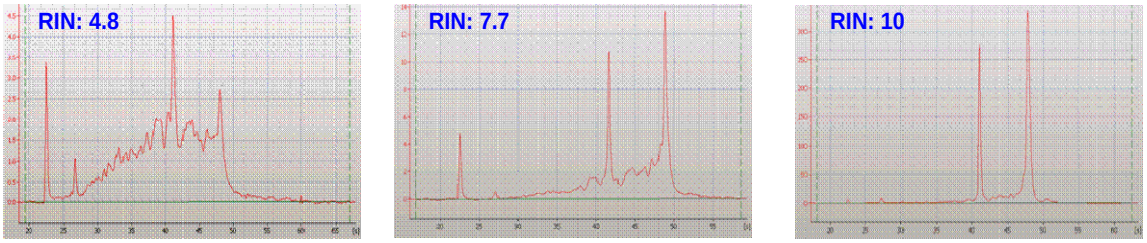

Figure 11-RNA integrity Number (RIN): Samples with different RINs, indicating different RNA qualities. A RIN of 1 indicates fully degraded RNA while a RIN of 10 indicates fully intact RNA.

4.2.4 RNA quantification using the Invitrogen Ribogreen kit

The Molecular Probes Invitrogen Ribogreen assay as the basis for quantification of cRNA samples is recommended by Illumina as it is relatively insensitive (unlike spectrophotometer measurements) to silica contamination after the cRNA filter cartridge cleanup (Bibikova, Talantov et al. 2004). Ribogreen® RNA quantization reagent is an ultrasensitive fluorescent nucleic acid stain for quantization RNA in solution. The RediPlate™ 96 Ribogreen ® RNA quantization kit is preloaded with the Ribogreen reagent. For an RNA determination the user adds buffer and samples to the micro-plate wells, waits 10 minutes, and then reads the fluorescence. The fluorescence of the sample is compared to that of a standard curve of RNA, prepared from RNA pre aliquoted into one column of the plate. Procedure (According to the Invitrogen protocol):

The kit components were incubated at room temperature for 20 minutes. The RNA standard samples were prepared by adding 100µl of RediPlate TE buffer (component B)

to each well in column 1 (with black tabs) and mixing by pipetting ~10 times. 180µl TE buffer (component B) was added to the required columns of the RediPlate and mixed well. 20µl of RNA standard (black strip) was added from each of the standard RNA wells (prepared above) into the assay wells and mixed well. The last RNA standard (well H) contained no RNA and served as the control to measure background fluorescence. 5µl of the RNA samples and 195µl TE buffer was added to the assay wells and well mixed. The loaded microplate was incubated for 10 minutes at room temperature protected from light.

Using a fluorescence-based microplate reader (excitation ~480 nm, emission ~520 nm), the Ribogreen plate was read. For each value of sample fluorescence, the value derived from the no-RNA control was subtracted. Using the data from the RNA standards, the amount of RNA versus the fluorescence intensity was plotted and a line was fitted to the data points. Using the standard curve, the amount of RNA was determined from the fluorescence intensity measured for each sample.

4.2.5 Globin reduction experimental procedure

The amount of input RNA was 4µg (volume up to 14µl).

Reagent preparation: 2ml of 100% isopropanol was added to the RNA binding buffer concentrate and stored at room temperature. 4ml of 100% ethanol was added to the RNA wash solution concentrate, mixed well and then stored at room temperature. The RNA bead buffer was combined with the RNA binding beads for each reaction as follows: 10µl RNA binding beads and 4µl RNA bead buffer and mixed briefly. To this mixture 6µl 100% isopropanol was added, mixed thoroughly by vortexing and stored at room temperature. This mixture was labeled as the bead resuspension mixture.

Preparation of streptavidin magnetic beads: The incubator was set to 50°C and the 2x hybridization buffer and the streptavidin bead buffer were heated at 50°C for at least 15 minutes. The streptavidin magnetic beads were vortexed and suspended and 30µl of the beads per sample was transferred into a 1.5ml non-stick tube provided in the kit. The mixture was centrifuged for 1 second at 2000 rpm. The tubes were placed on a magnetic stand for 5 minutes to allow complete capture of the beads. Once the solution turned transparent, the supernatant was carefully aspirated with a pipette without disturbing the

beads. The supernatant was discarded and the tubes were removed from the magnetic stand. 30µl of the streptavidin bead buffer was added to the magnetic beads and vortexed vigorously to resuspend the beads. The prepared streptavidin magnetic beads were placed at 50°C in an incubation oven for at least 15 minutes.

Hybridization of globin mRNA and globin capture oligonucleotides: 14µl of the starting RNA material (4µg) was placed in a 1.5ml non-stick tube and 1µl of capture oligo mix was added. 15µl of 50°C preheated 2x hybridization buffer was added to each sample, vortexed and centrifuged to collect at the bottom of the tube. The samples were incubated in a pre warmed 50°C incubator and the globin capture oligo mix was allowed to hybridize to the globin mRNA for 15 minutes.

Removal of globin mRNA: The streptavidin magnetic beads were removed from the 50°C incubator and resuspended by gently vortexing and centrifugation. 30µl of prepared streptavidin magnetic beads were added to the incubated samples. The mixture was vortexed, centrifuged, flicked gently to re suspend the beads and the RNA bead mixture was incubated at 50°C for 30 minutes. The samples were removed from the incubator, vortexed to mix and centrifuged. The tubes were placed on the magnetic stand to capture the streptavidin magnetic beads for 5 minutes until the solution turned transparent. The supernatant was carefully aspirated using a pipette without disturbing the streptavidin magnetic beads. The supernatant, containing the globin mRNA-depleted RNA was transferred to a new 1.5ml tube and placed on ice.

Purification of globinclear RNA: 100µl of prepared RNA binding buffer was added to each enriched RNA sample. 20µl of the bead resuspension mix was vortexed and immediately added to each sample. The mixture was vigorously vortexed for 10 seconds to fully mix the reagents and to allow the RNA binding beads to bind the RNA. The samples were briefly centrifuged for 1 second at 4000 rpm to collect at the bottom and then placed on a magnetic stand for 5 minutes to capture the beads. Once the solution turned transparent, the supernatant was carefully aspirated using a pipette without disturbing the RNA binding beads and was discarded.

The tubes were removed from the magnetic stand and 200µl of RNA wash solution was added to each sample, vortexed and briefly centrifuged for 1 second at 4000 rpm. The

RNA binding beads were captured on the magnetic stand, the supernatant was aspirated, discarded and the tube was removed from the magnetic stand. After brief centrifugation the tube was placed again on the magnetic stand and any remaining liquid was removed with a small bore pipette tip. The tubes were removed from the magnetic stand and the beads were allowed to air-dry for 5 minutes with the caps left open. 30µl of the elution buffer was added to each sample, vortexed vigorously to resuspend the beads and incubated at 58°C for 5 minutes. After incubation, the tubes were vortexed and centrifuged to collect the mixture at the bottom of the tube. The RNA binding beads were captured by placing the tubes on the magnetic stand for 5 minutes. The supernatant was transferred to a new 1.5ml tube and stored at -20°C.

4.2.6 RNA amplification, reverse transcription and labeling

The RNA obtained from whole blood is usually not enough for a microarray experiment and furthermore it is not labeled. Therefore, a step of amplification combined with reverse transcription and labeling with Biotin is required for the sample to be processed on the microarray. The Illumina® Total Prep RNA amplification kit generates biotinylated, amplified RNA for hybridization with Illumina Sentrix® arrays.

The experimental procedure was in accordance with the Ambion Illumina® Total Prep kit manual. The recommended amount of input RNA is between 50-500ng of total RNA. The minimum amount of input RNA which can be used is 25ng and the maximum volume of the RNA is 11µl.

A standardized amount of 500ng of total RNA was used as a starting material for all reactions. (Note: This amount was decided on after multiple test runs with different amounts of starting RNA. The efficiency of amplification between samples may differ so the maximum amount of starting total RNA was optimal to ensure enough final amount of labeled mRNA for the microarray procedures).

The RNA samples were concentrated or diluted as required to 11µl with nuclease free water in a nonstick sterile, RNase-free 0.5ml microcentrifuge tube. The reverse transcription master mix was prepared at room temperature in the following order: 1µl of T7 oligo (dT)primer, 2µl of 10x first strand buffer, 4µl of dNTP mix, 1µl of RNase inhibitor and 1µl of array script was added together.

The master mix was mixed well by gently vortexing, centrifuged briefly to collect at the bottom and then placed on ice. 9µl of the reverse transcription master mix was added to each RNA sample, mixed thoroughly by pipetting 2-3 times, flicking the tube 3-4 times and then centrifuging briefly. The samples were then incubated for 2 hours at 42°C. After incubation, the samples were centrifuged briefly and then placed on ice. On ice, the second strand master mix was prepared in the following order: 63µl of nuclease-free water, 10µlof 10x second strand buffer, 4µl of dNTP mix, 2µl of DNA polymerase and 1µl of RNase H was mixed well by gently vortexing, centrifuged briefly to collect at the bottom and then placed on ice:

80 µl of the second strand master mix was transferred to each sample, mixed thoroughly by pipetting 2-3 times, flicked 3-4 times and then centrifuged. The tubes were incubated for 2 hours at 16°C in a pre-cooled PCR incubator. During the incubation time, nuclease-free water was preheated to 55°C for 10 minutes for the elution steps and the cDNA elution columns were placed in the wash tubes for the next step. After the 2 hour incubation, the samples were placed on ice. 250µl of the cDNA binding buffer was added to each sample, mixed thoroughly by pipetting, flicked and then spun down to collect at the bottom. The samples were added to the center of a cDNA filet cartridge firmly placed in a wash tube and centrifuged at 14000 rpm for 1 minute. The flow-through was discarded and the cDNA filter cartridge was replaced in the wash tube. Note – At this point check that 24ml 100% Ethanol has been added to the wash buffer stock.

500µl of the wash buffer was added to the samples and then centrifuged at 14000 rpm for 1 minute. The flow-through was discarded and the cDNA filter cartridges were transferred to new cDNA elution tubes. 10µl of preheated nuclease-free water was added to the center of the cDNA filer, incubated for 2 minutes at room temperature and then centrifuged at 1400 rpm for 1 minute. An additional 10µl of preheated nuclease-free water was added to the center of the cDNA filer, incubated for 2 minutes at room temperature and then centrifuged at 1400 rpm for 1 minute. Note: The double stranded cDNA was now in the eluate

At room temperature, the *in vitro* transcription mix was prepared as follows: 2.5µl of T7 10x reaction buffer, 2.5µl of T7 enzyme mix and 2.5µl of biotin-NTP mix was added.

The master mix was gently vortexed and centrifuged briefly for 1-2 seconds 20 µl of the IVT master mix was added to each sample, mixed thoroughly by pipetting up and down, flicked 3-4 times and then centrifuged to collect the reaction to the bottom of the tube. Once assembled, the tubes were placed at 37°C in an incubator for 12 hours overnight.

Next day, 75µl of nuclease-free water was added to each sample to stop the reaction. 350µl cRNA binding buffer and 250µl 100% Ethanol was added to the tubes, pipetted 3 times to mix, transferred to the cRNA filters and centrifuged for 1 minute at 14000 rpm. The flow-through was discarded and the cRNA filter was replaced in the cRNA collection tube. 650µl of wash buffer was added to the filter and centrifuged for 1 minute at 14000 rpm. The cRNA filter was then transferred into a fresh labeled cRNA collection tube. 100 µl of preheated nuclease free water was added to the filter and incubated at room temperature for 2 minutes. The samples were then centrifuged for 1-2 minutes at 14000 rpm. The 100µl eluate contained the cRNA which was then stored at -80°C until further use.

4.2.7 Illumina microarray procedures

4.2.7.1 Whole genome gene expression with Sentrix bead chip

This system uses a “direct hybridization” assay, whereby gene-specific probes are used to detect labeled RNA. Each bead in the array contains a 50-mer; sequence-specific oligo probe synthesized using Illumina’s Oligator technology. The Sentrix bead platform offers three whole-genome formats: 6-sample (used in this study), 8-sample and 12-sample. Each array in the matrix holds thousands to tens of thousands of different oligonucleotide probe sequences that are attached to 3-micron beads assembled into the micro-wells of the bead chip substrate. Multiple copies of each bead type are present in the array, an average of ~30 copies per probe.

4.2.7.2 Microarray loading

GEX HYB (hybridization buffer) and GEX HCB (humidifying buffer) were part of the kit provided by Illumina. The GEX HYB and GEX HCB buffers were heated at 58°C in the Illumina hybridization oven for 10 minutes to dissolve any salts.

1.5µg of labeled cRNA was added unto 10µl of total sample volume in a 1.5ml microcentrifuge tube. 20µl of the HYB buffer was added to the samples and the assay was heated at 65°C for 5 minutes. The rubber hybridization chamber gaskets were placed into the hybridization chamber and 200µl GEX-HCB buffer was dispensed into the humidifying buffer reservoirs. The chamber was sealed by closing the clips. The bead chips were removed from their packages and placed in the hybridization chamber insert such that the microarray barcode was aligned with the barcode symbol on the insert. After the assay above was heated for 5 minutes, the tubes were vortexed, centrifuged and allowed to cool to room temperature. The samples were loaded on the right side of the microarray inlet port (Figure 12). The hybridization chamber inserts containing the loaded samples on the microarray were placed into the hybridization chamber. The lid was secured by closing down the clamps on the sides of the hybridization chamber. The hybridization chambers were placed into the preheated 58°C Illumina hybridization oven (provided by Illumina) with the rocker adjusted to a standard speed of 5.

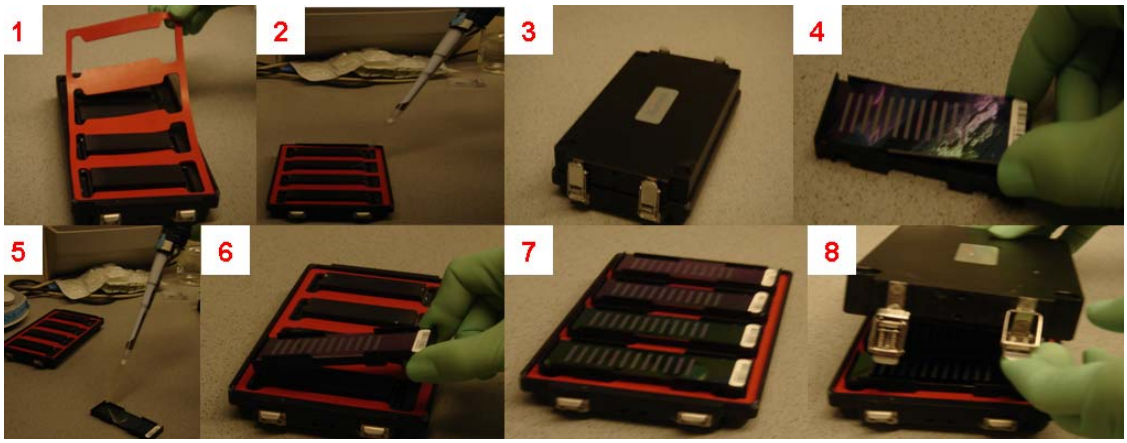

Figure 12-Illumina Sentrix Bead chip procedure: Setting up of the hybridization chamber and loading of the cRNA samples on the microarray (self-taken photographs to illustrate the microarray procedures).

Preparation of the high temperature wash buffer for the next day:

50ml of the high temperature wash buffer concentrate was diluted with 450ml RNase free water, placed into the Hybex water bath insert and heated to a temperature of 55°C overnight.

Day 2 Washing, blocking and detection procedure

Buffers, wash chambers, slide racks, wash beaker, staining dish, wash trays and tweezers were provided in the Illumina gene expression kit together with the microarrays.

7.25ml of E1BC wash buffer concentrate was added to 2.5l RNase free water to make the E1BC wash buffer. 250ml of this wash buffer was poured into the staining dish with the slide rack. The hybridization chamber was removed, opened, and the microarray was taken out and submerged in a wash beaker containing 1.5l E1BC wash buffer. The cover seal was gently and firmly pulled off and discarded. Bead chips were transferred to the slide rack submerged in the staining dish containing diluted wash E1BC buffer, then transferred into the overnight heated Hybex water bath insert containing high-temp wash buffer and incubated static at 58°C for 10 minutes. After the 10-minutes incubation in high-temp wash buffer, the slide rack was transferred to 250ml of the diluted E1BC in a clean staining dish using a rack handle. Using the slide rack handle, the rack was plunged in and out of the solution 10 times. The staining dish was placed on an orbital shaker set

to medium (so as not to allow for any spill) and shaken for 5 minutes. The rack was then transferred to a clean staining dish containing 250ml fresh 100% ethanol and placed on the orbital shaker and shaken at room temperature for 10 minutes. The rack was transferred to a staining dish containing 250ml fresh E1BC buffer and plunged in and out of the solution 10 times using the slide rack handle. The staining dish was placed on the orbital shaker and shaken at room temperature for 2 minutes. Using tweezers, the bead chips were then transferred into the wash trays facing upwards and 4ml block buffer was added to each tray. The trays were then placed in the hybridization oven and rocked at a speed of 5. 2ml of block buffer was prepared by addition of 2µl (1mg/ml) of streptavidin-Cy3 per chip. Note – The streptavidin-Cy3 is a powder which must be diluted with 1ml RNase free water to make a working solution of 1mg/ml streptavidin-Cy3. The Cy3 aliquots were stored at -20°C. 2ml block E1 buffer + streptavidin-Cy3 were pipetted into a new bead chip wash tray. Using tweezers, the bead chip was grasped at the barcode end via the well in the blocker wash tray, transferred to the wash tray containing the streptavidin-Cy3 and placed flat so that the barcode was again near the tweezers well. The wash tray was covered with the flat cover provided and placed on the rocker at medium speed for 10 minutes. 250ml E1BC was dispensed into a clean staining dish (with slide rack). Using tweezers, the bead chip was grasped at the barcode end and removed from the wash tray. The bead chip was transferred into the slide rack submerged in the staining dish and immediately submerged into the E1BC. Using the slide rack handle, the rack was plunged in and out of the solution ten times. The orbital shaker was set to medium-low and the staining dish was placed on the orbital shaker and mixed at room temperature for 5 minutes. The bead rack was pulled out of the E1BC buffer and transferred to the centrifuge rack containing paper towels. The centrifuge was balanced with equal weight and the microarrays were centrifuged for 4 minute at 275 rcf to dry the microarray. Once dry, the microarrays were stored in the dark until they were scanned.

Bead chips were imaged using the Illumina Bead Array reader, a two channel 0.8µm resolution confocal laser scanner. The decode data which comes with the microarray must first be loaded on the scanner computer. The chip was placed in the Bead Array reader and the barcode was scanned. After scanning, the raw data was imported from the Illumina Bead Studio software.

4.2.8 Illumina Bead studio control summary report

Bead chips have internal control features to monitor data quality. The controls consist of sample-independent oligonucleotides spiked into the hybridization solution. The results of these controls can be visualized in BEADSTUDIO software as a “control summary report”

The following control categories were present in the Illumina hybridization solution:

1. Cy3-labeled hybridization controls: - These controls consisted of six probes with corresponding Cy3-labeled oligonucleotides, producing a signal independent of both the cellular RNA quality and success of the sample preparation reactions. The Cy3 hybridization controls were present at three concentrations, yielding gradient hybridization responses.
2. Low stringency hybridization control: - This category contained four probes, corresponding to the medium and high-concentration Cy3 hybridization control targets. Each probe had two mismatch bases distributed in its sequence. If stringency was adequate, these controls yielded very low signal. If stringency was too low, they yielded signal approaching that of their perfect match counterparts in the Cy3 hybridization control category.
3. High stringency hybridization control: - The probe/target sequences had a very high G+C content, and should thus hybridize even if hybridization stringency was too high.
4. Biotin control: - This category consisted of two probes with complementary biotin-tagged oligonucleotides acting as secondary staining controls.
5. Negative controls: - This category consisted of probes of random sequence having no corresponding targets in the genomes. This provided a comprehensive measurement of background, representing the imaging system background as well as any signal resulting from non-specific binding of dye or cross-hybridization. The Bead Studio used the signals and standard deviation of these probes to establish gene expression detection limits: the detection p value.
6. Housekeeping controls: - The intactness of the biological specimen was monitored by housekeeping gene controls. These controls consisted of probes for housekeeping genes, two probes per gene that should be expressed in any cellular sample.

7. Sample Labeling Controls - These controls were optional, consisting of four probes corresponding to artificial polyadenylated spike RNA. These spike RNA are amplified and labeled in the same reaction as the sample, and thus acted as tracers for reaction success.

The Bead studio control summary report was used for comparison of samples across the listed control metrics to ensure a consistent ratio between relevant control values. Since Illumina does not provide a golden standard for the Quality Control (QC) measurements, we monitored these QC values over different experiments and noted an expected range of QC values (hybridization controls: high: 40000-60000, medium: 8,000-20000, low: 400-2000, low stringency: perfect match/ mismatch ratio >6, biotin: 6,000-20000, high stringency: >30000, housekeeping genes: >5000 and gene value: > background and noise values). A total of 386 whole-genome gene expression values were generated at the start. The QC report across all microarray experiments was used to exclude 5 sample outliers for further analysis, resulting in a total of 381 expression datasets.

4.2.9 Genotyping

Genotyping of the KORA S3/F3 individuals was performed by Dr. Peter Lichtner, Institute of Human Genetics at Helmholtz Research Center in Neuherberg. For 1644 of the KORA S3/F3 subjects, a genome-wide analysis was performed using Affymetrix 500K oligonucleotide array set consisting of two chips (Sty I and Nsp I) containing a total of 500,568 SNPs. 335,152 SNPs passed all quality control criteria, and were selected for the subsequent association analyses. Criteria leading to exclusion were genotyping efficiency < 95% (n = 49,325) and minor allele frequency (MAF) < 5% (n = 101,323). The microarrays were hybridized with genomic DNA in accordance with the manufacturer's standard recommendations. Genotypes were determined using the software BRLMM version 1.4.0 with standard settings proposed by Affymetrix.

4.2.10 Statistical analysis

The statistical analyses using R and PLINK were performed together with Diploma student Katharina Heim. The Beadstudio analyses, functional categorizations, extraction of genotypes using PLINK and HapMap database, generation of SNP lists, WG-PERMER permutations, genomic inflation factor calculations and merging of results

from different studies were performed by me. The raw data were exported from the Illumina Software BEADSTUDIO to R (http://www.R-project.org). The data were converted into logarithmic scores and normalized using LOWESS. The data were filtered using the BEADSTUDIO detection p-value < 0.01 in at least 5% of the individuals. Analysis was performed using a standard Welch t-test to determine effects of gender on expression of individual genes. Linear regression model with the dependent variable $\log_2$ (expression) and the independent variables sex and age was carried out. To adjust for multiple testing, the standard Bonferroni correction was used in which the adjusted p-value was obtained by dividing the observed p-value by the number of tests performed. The Prediction Analysis for Microarray (PAM) classification was used as an R function (pamr) to build a gender predictor. This carries out sample classification from gene expression data by the method of nearest shrunken centroids (Alizadeh, Eisen et al. 2000). Age prediction was done using a standard linear regression model. The PANTHER classification system was used for all functional annotation, pathway classification and analysis of gene enrichments. The binomial statistics tool compares classifications of transcript lists to a reference list to statistically determine over- or under- representation of PANTHER classification categories. Each list is compared to the reference list using the binomial test (Cho & Campbell, TIGs 2000) for each molecular function, biological process, or pathway term in PANTHER.

Graphs, histograms, boxplots and other figures were generated using R, Excel or SPSS. The cis and trans association analysis was performed using standard association commands in PLINK. For comparison of results, standard query language was used to query MYSQL database 5.0.60 and generate desired output files.

5.0 Results

In this project, I generated genome-wide expression data from whole blood of 497 individuals (261 males, 236 females) belonging to the German KORA cohort using the Illumina Sentrix WG6-v2 microarray. The statistical analyses were conducted together with Diploma student Katharina Heim. Prior to statistical analysis, the dynamic range of detection was calculated and preprocessing steps such as normalization and filtering were executed on the raw microarray data to get rid of noise and obtain reliable signals.

5.1 Dynamic range of detection

The dynamic range is the range between the signal intensities of the minimum and maximum fluorescent detection. Expression levels for each transcript were denoted by the logarithm base 2 (log_2) of the signal intensity of the transcript in fluorescent units. In this study a dynamic range of 3 – 16 was observed (corresponding to 1.9 – 4.9 on a logarithmic scale to the base 10), indicating a total dynamic range of 3 logs of magnitude. The log_2 expression levels of more than 75% of the 48,701 transcripts ranged from 6 – 8 (Figure 13). The dynamic range observed in this study was in accordance with previous studies using Illumina microarrays (Kuhn, Baker et al. 2004).

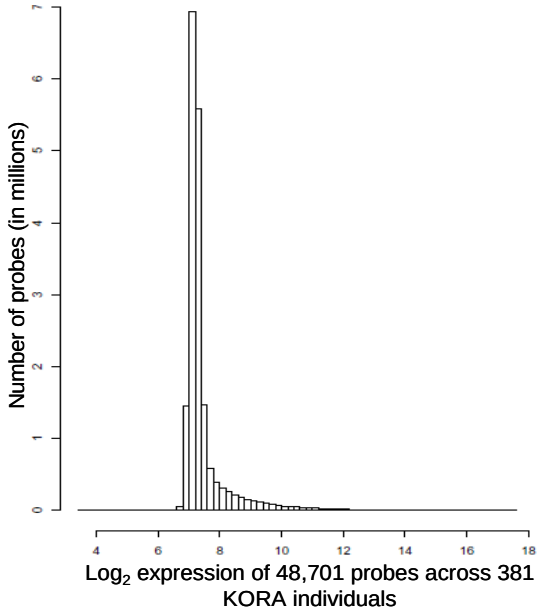

Figure 13-Dynamic range of detection: In this study a total dynamic range of 3 logs of magnitude was observed on the Illumina Sentrix WG6-v2 microarray.

5.2 Normalization of gene expression data

The purpose of normalization is to minimize systemic variations so that biological differences are clearly distinguishable. Rank invariant and locally weighted scatter plot smoothing (LOWESS) normalizations were applied to the data. For rank invariant normalization, a subset of probes whose rank does not change across the experiment are identified and these define the normalization parameters (Technical Note: Illumina RNA analysis, 2007). The LOWESS normalization is a moving average algorithm which smoothes all of the points (Yang, Dudoit et al. 2002). Normalization was combined with the scatter plot to allow better visualization of data points. Scatter plots are x versus y intensity plots. It is expected that the majority of unchanged genes should display a symmetrical distribution of data points and lie on the diagonal. How well the normalization equation fits to the data is expressed by the square of the coefficient of determination R. The closer R^2 is to 1.00, the better the fit. In this study, the data were normalized using the best-fitting LOWESS normalization, which resulted in an R^2 of 0.94 (Figure 14).

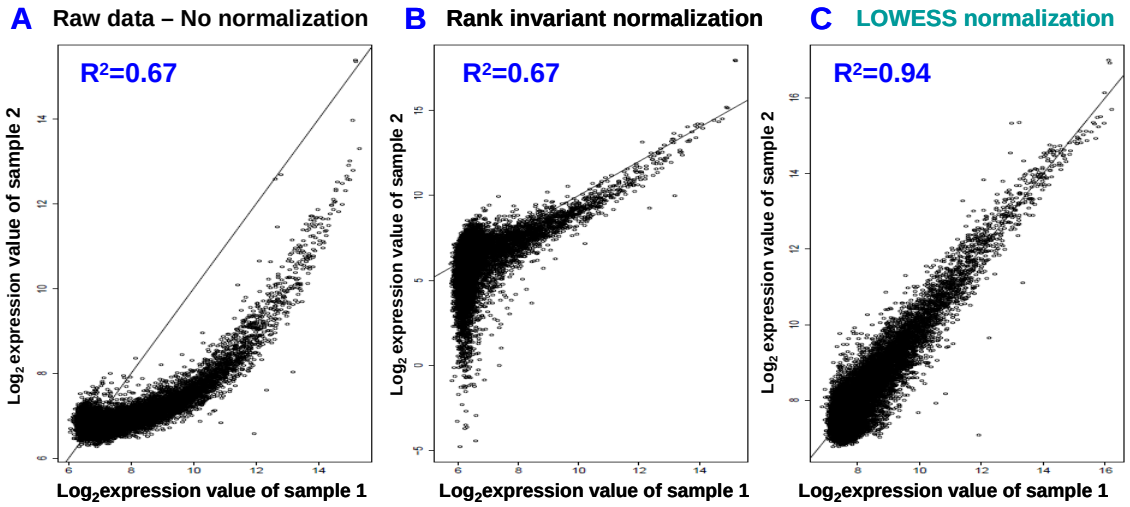

Figure 14-Scatter plots of log_2expression data of two individuals with (A) no normalization, (B) rank invariant normalization and (C) LOWESS normalization: Each black dot represents log_2 expression of a transcript. No normalization results in a banana curve such as seen in (A) above, which might bias the results. This indicates that normalization is required. The rank invariant normalization resulted in a square of coefficient of determination (R^2) of 0.64, indicating that the algorithm did not fit well to the data. The highest R^2 of 0.94 was obtained using LOWESS normalization.

5.3 Filtering of expression data

Filtering is a preprocessing step used to reduce noisy data. In this study filter criteria were applied at the level of the input RNA and at the level of the probes detected on the microarray. The quality of input RNA is crucial for gene expression results. The RNA quality was measured using the RNA Integrity Number (RIN) from Agilent based on a numbering system from 1-10, 1 depicting highly degraded RNA and 10 depicting intact RNA. According to previous reports, a threshold of RIN > 5 was used for microarray experiments (Schroeder, Mueller et al. 2006). Consequently a RIN threshold of >5 was applied to the input RNA. This resulted in the removal of 116 samples from a total of 497 RNA samples, allowing a remaining of 381 good quality RNA for further analyses.

The Illumina hybridization buffer contains ~ 1616 negative control probes lacking specific targets in the human transcriptome. The mean signal of these negative probes defines the signal background. A detection p-value represents the confidence that a given transcript is expressed above the background, thereby determining whether a transcript on the array is called “detected”. Several signals might result from high array background and/or low signal intensity hence the detection p-value acts as an overall quality control. The Illumina BEADSTUDIO calculates and reports detection p-value thresholds of 0.05 and 0.01 (Figure 15). Detection p-values are computed on the rank of the Z value of a probe relative to the Z values of the negative controls. Z value is calculated by subtraction of the mean of the negative controls from one and dividing this value by the standard deviation of negative control. A filter of detection p-value of <0.01 in at least one sample (corresponding to 1% false discovery rate) was applied to select for significantly detected probes. This resulted in reduction of the probes from 48,701 to 22,809. A further criterion of probes present in at least 5% of the individuals was applied, resulting in 13,767 probes which were used for subsequent analyses (Figure 16).

The low intensity signals generally corresponding to low-abundant transcripts are usually filtered as it is expected that the signal to noise ratio becomes too small. The data in this study were filtered using a filter criterion of probes significantly detected in at least 5% of individuals (19 individuals). This criterion was used so that all the weakly transcribed genes would not be filtered out and meaningful signals could still be retained.

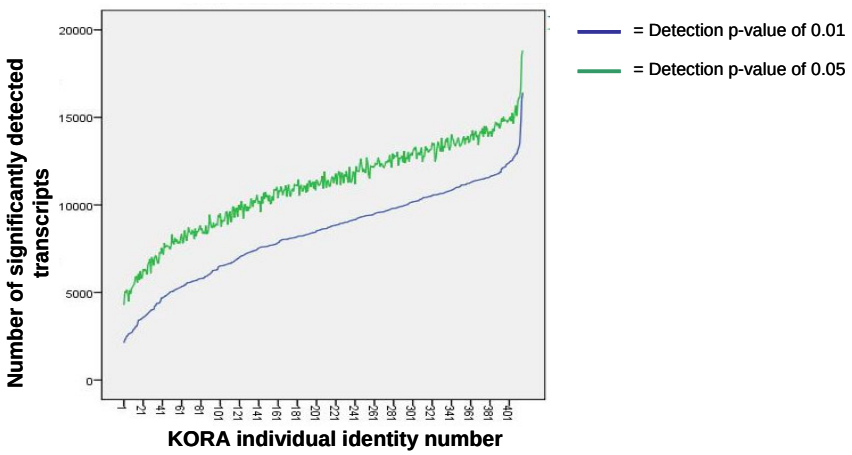

Figure 15-Number of probes significantly detected in each individual: The difference between the lines indicate the number of genes filtered out using the stringent filter of detection p-value<0.01. Using a detection p-value of <0.01, more than 6000 transcripts were detected in ~ 80% of the individuals sampled.

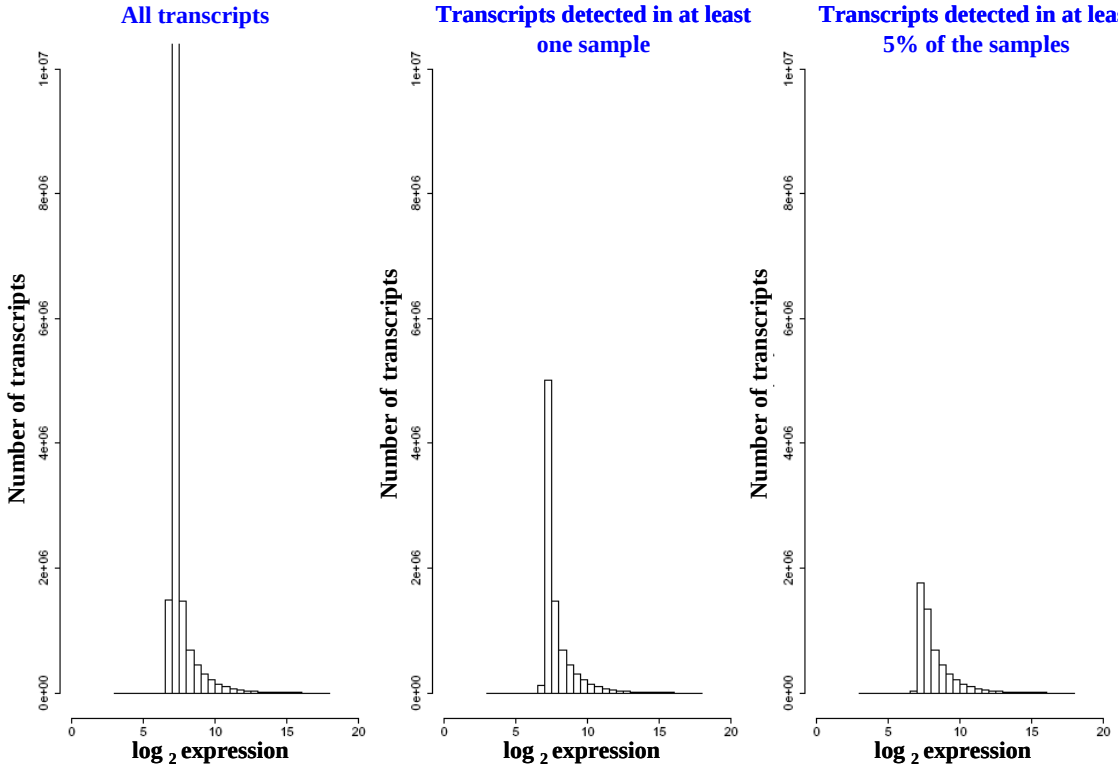

Figure 16-Filtering of the raw data: Distribution of gene expression intensities with most of its mass at small intensities and a long tail of high intensities to the right. The high peaks on the left (low intensities) were filtered out when the filter criterion of detection p-value <0.01 in at least 5% of individuals was used.

5.4 Technical and biological replicates

Reproducibility of the microarray data was tested by comparisons between technical replicates and biological replicates. Reproducibility of replicates provides confidence in conclusions drawn from the experiment.

The technical replicates consisted of the same RNA probe hybridized on two different arrays, thus testing only measurements due to technical differences in array processing. The biological replicates consisted of RNA extracted from whole blood of control individuals at different time points thus allowing exploration of differences in the underlying biological system such as variance in RNA isolation and amplification.

A total of 6 technical replicates and 9 biological replicates were used to test for reproducibility. Figure 17 shows an example of two technical and two biological replicates. Pearson correlation coefficient (r) is a measure of the strength of the association between two quantitative variables, the highest possible correlation being 1. The technical replicates were within the same range as the biological replicates, with a Pearson correlation coefficient of 0.96-0.99. The high correlation coefficient for the replicates demonstrates the reproducibility and robustness of the microarray for investigation of gene expression from whole blood in humans.

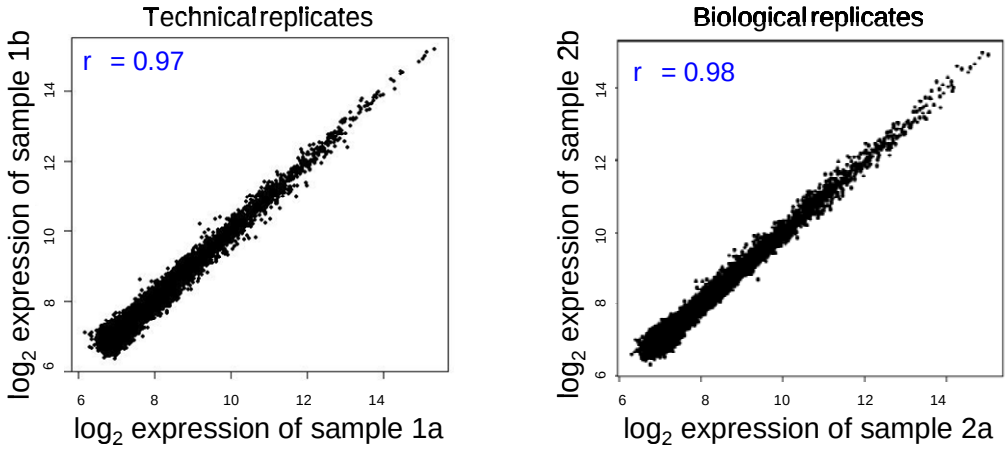

Figure 17-Reproducibility of microarray data: Scatter plots of two technical replicates and two biological replicates showing high Pearson correlation coefficients (r) of 0.97 and 0.98 respectively, indicating high reproducibility of data. Each black dot represents $\log_2$ expression level of a transcript in sample 1 on the x axis versus sample 2 on the y axis.

5.5 Variability in gene expression levels

The aim was to identify transcripts expressed in whole blood. The idea was to determine which transcripts exhibited variable gene expression among individuals, as these had the potential power to detect meaningful genetic associations. To test for variation between samples a variance score was calculated for each individual transcript using the R program. The variance score was calculated as the squared differences between expression levels and mean expression levels for each transcript, summed across all individuals and divided by the degrees of freedom (number of cases sampled minus one) The variance scores ranged from 0.0054-4.694, with a median variance score of 0.05. More than 80% of transcripts had variance scores between 0.0054-0.20 (Figure 18).

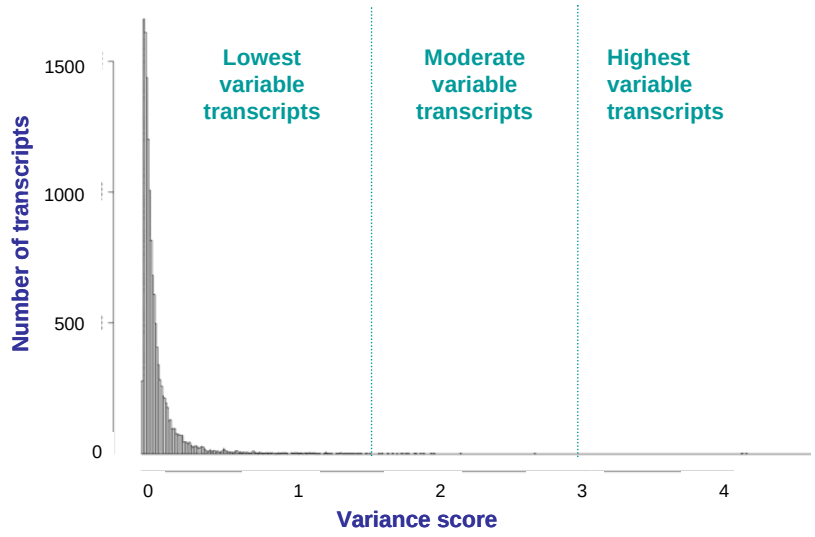

Figure 18-Variance of expression levels within individuals: The variance scores of 13,767 filtered transcripts ranged from 0.0054-4.694, with >80% transcripts having variance scores between 0.0054-0.20.

According to their variance scores, the differentially expressed transcripts were categorized into 3 groups – Highest variable (3.1 - 4.6), moderate variable (1.57 – 3.1) and lowest variable (0.0054 – 1.57) (Figure 19).

After categorization the 100 highest and lowest variable transcripts were investigated using the PANTHER classification system to check for gene enrichments and identify those functional categories which were overrepresented in the two groups. The PANTHER system uses the binomial statistics tool to compare transcript lists to a

reference list of 25,000 NCBI *Homo sapiens* genes and statistically determines over or under representation of PANTHER classification categories (Thomas, Campbell et al. 2003). In the binomial test it is assumed that genes in the uploaded list belong to the same population as genes from the reference set, so the probability of observing a gene from a particular category in the uploaded list is the same as that in the reference list (Cho and Campbell 2000). The p-value is calculated as an estimation of deviation from the null hypothesis. The binomial test is similar to the chi squared test but is more robust to small sample sizes. The results were corrected for multiple testing using the Bonferroni correction by dividing the p-value by the number of categories tested (Table 3).

Among the 3 highest variable transcripts, HBE1 and HLA-DRB5 are known to be polymorphic and highly variable among individuals while RPS4Y1is a male-specific transcript located on the Y chromosome and hence is highly variable. Among the 3 lowest variable transcripts, PIP5KIA is involved in phosphorylation and signal transduction (Pan, Choi et al. 2008) while M1A has melanoma inhibitory activity and was found to be significantly higher expressed in patients with malignant melanoma (Bosserhoff, Hauschild et al. 2000). The function of FLJ13273 is unclear (Figure 19).

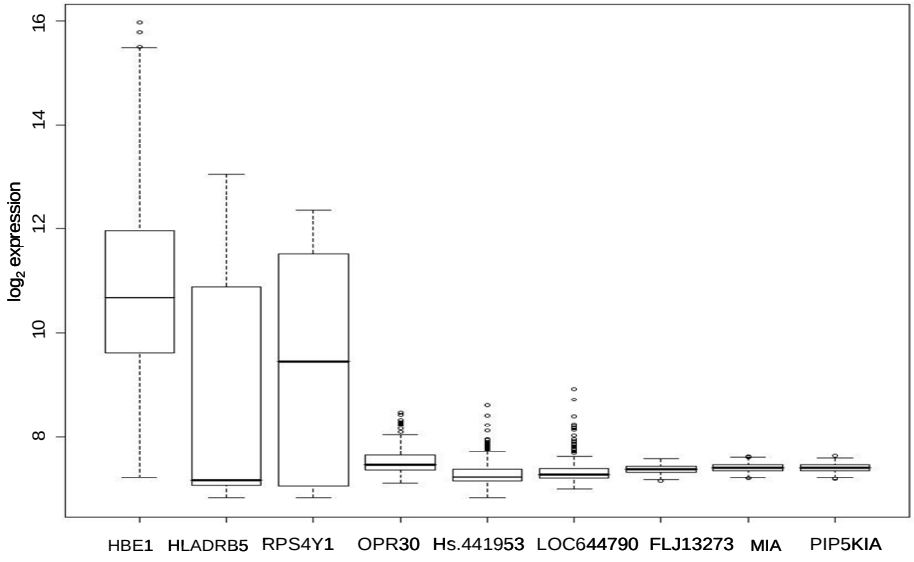

Figure 19-Box plots showing different degrees of variance among transcripts: $\log_2$ expression of 3 highest variable transcripts: HBE1, HLADRB5 and RPS4Y1, 3 moderate variable transcripts: OPR30, Hs.441953 and LOC644790 and 3 lowest variable transcripts: FLJ13273, MIA and PIP5KIA.

Table 3-PANTHER classification of the 100 highest and lowest variable transcripts based on biological function

Biological process	p-value	Category enriched in
Blood circulation and gas exchange	3.82×10^{-6}	Highest variable
Transport	6.72×10^{-4}	Highest variable
Immunity	7.58×10^{-4}	Highest variable
Mitosis	1.02×10^{-3}	Highest variable
Endocytosis	4.21×10^{-3}	Highest variable
Stress response	2.33×10^{-2}	Highest variable
Phospholipid metabolism	2.79×10^{-3}	Lowest variable
DNA repair	3.92×10^{-2}	Lowest variable
Gametogenesis	7.34×10^{-2}	Lowest variable
DNA recombination	7.82×10^{-2}	Lowest variable
Oncogenesis	1.20×10^{-2}	Lowest variable

Top categories enriched among the highest variable transcripts included blood circulation and gas exchange, transport and immunity. These can be expected since the expression profiles were generated from whole blood which is known to be involved in exchange of oxygen, transporter of nutrients and waste products from cells and also acts as an immune surveillance system.

Top categories enriched among the lowest variable transcripts included phospholipids metabolism, DNA repair and gametogenesis. Phospholipids are major structural components of cellular membranes and the regulation of phospholipid metabolism is known to be tightly maintained (Kent, Carman et al. 1991). The DNA repair system continuously monitors and repairs damaged DNA and is vital to the integrity of the genome. Previous reports have shown DNA repair genes to be housekeeping genes and demonstrated the expression of these genes to be tightly regulated (Iwanaga, Komori et al. 2004). Earlier studies have suggested a conserved overall expression profile of genes involved in gametogenesis in mammals (Baron, Houlgatte et al. 2005).

5.6 Genes expressed in whole blood

Out of 48,701 probes present on the Illumina microarray, 81% targeted a single transcript (Table 4). As mentioned in chapter 5.3, a stringent filter of detection p-value of <0.01 in at least 5% of the KORA individuals was used to identify 13,767 significantly detected probes which were used for downstream analysis. The aim was to check which probes exhibited detection p-value <0.01 and which probes exhibited detection p-value >0.01 in all 381 individuals. Of 48,701 probes, 25892 were always below the detection threshold and 642 probes were significantly detected in all 381 KORA individuals. Figure 20 depicts the number or probes significantly detected in each KORA individual.

Table 4-Number of probes specific to a transcript on the Illumina microarray

Number of transcripts	Number of probes
39665	1
1893	2
1245	3
262	4
53	5
16	6
9	7
3	8
1	9
1	10

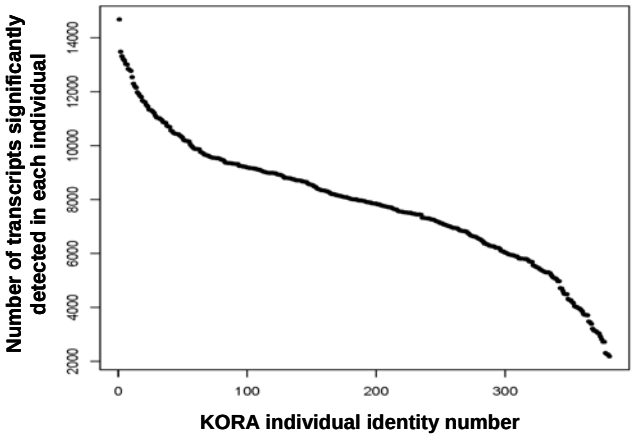

Figure 20-Number of probes detected in each of the KORA individuals: >8000 probes were detected in more than 50% of the KORA individuals sampled (n=200). Each black dot indicates the total number of probes detected in the corresponding KORA individual.

The PANTHER system was used for pathway classification to check for biological explanations of categories that were enriched among those probes significantly detected in all individuals and probes always detected below the threshold of significance. The results were corrected for multiple testing using Bonferroni correction (Table 5).

Table 5-Top 5 pathways enriched in KORA blood samples

642 always significantly detected probes		25892 never significantly detected probes	
Pathways	**p-value**	**Pathways**	**P value**
T cell activation	1.47×10^{-7}	Cadherin signaling pathway	1.38×10^{-18}
Inflammation	2.68×10^{-6}	Wnt signaling pathway	8.42×10^{-14}
Cytoskeletal regulation	7.21×10^{-6}	Alzheimer disease-presenilin pathway	1.34×10^{-3}
Parkinson disease	2.66×10^{-5}	Heterotrimeric G-protein signaling	2.53×10^{-3}
B cell activation	7.53×10^{-4}		

Top transcript categories enriched among probes never significantly detected include Cadherin and Wnt signaling pathways both known to be involved in developmental processes hence these transcripts might be expressed only during distinct developmental stages in humans or might not be expressed in whole blood at all (Dekel 2003).

Not surprisingly 3 of the 5 pathways enriched among the 642 probes that were always significantly detected were related to innate immune response such as T cell activation, B cell activation and inflammation. For other enriched pathways such as Parkinson and cytoskeleton regulation there was no plausible biological explanation. Enrichment of immune response transcripts among those always significantly detected indicated that the individuals studied might have had infections such as cold, cough or fever that contributed to differential expression of several immune-related transcripts. A large proportion of transcripts might be individual-specific, influenced by external factors (such as diet or smoking) or immune-dependent and hence might exhibit highly variable expression among the sampled individuals. Moreover, some probes present on the microarray might represent transcripts not be expressed in whole blood. Therefore it is not surprising that a large proportion of transcripts were not significantly detected in all 381 individuals. The results collected here could be an initial step towards establishing reference ranges for expression of genes related to inflammation and immunity in whole blood.

5.7 Cell-specific gene expression patterns

Blood is a complex tissue consisting of a heterogeneous population of cell types which can vary greatly between individuals. An increase or decrease in one cell type alters the overall proportion of that cell type's unique transcripts in the total pool of RNA from a given sample. These effects contribute to the overall variation in transcript abundances in whole blood. To find out if there was a correlation between gene expression and cell types, expression levels for all transcripts were correlated with each parameter in the partial blood count namely WBC, RBC and platelet counts. Linear regression models were built to test for association of each transcript level with the three available blood parameters – number of red blood cells (RBC) per nl, number of platelets per nl and number of white blood cells (WBC) per nl. After Bonferroni correction, 69 WBC-specific transcripts and one platelet-specific transcript were identified. No RBC-specific transcripts were obtained. The variance of the platelet-specific gene was 0.06 and the mean variance of the 69 WBC-specific transcripts was 0.22, indicating that they belonged to the lowest variable category and the moderate variable category. The distributions of the number of WBC, RBC and platelets are shown in Figure 21.

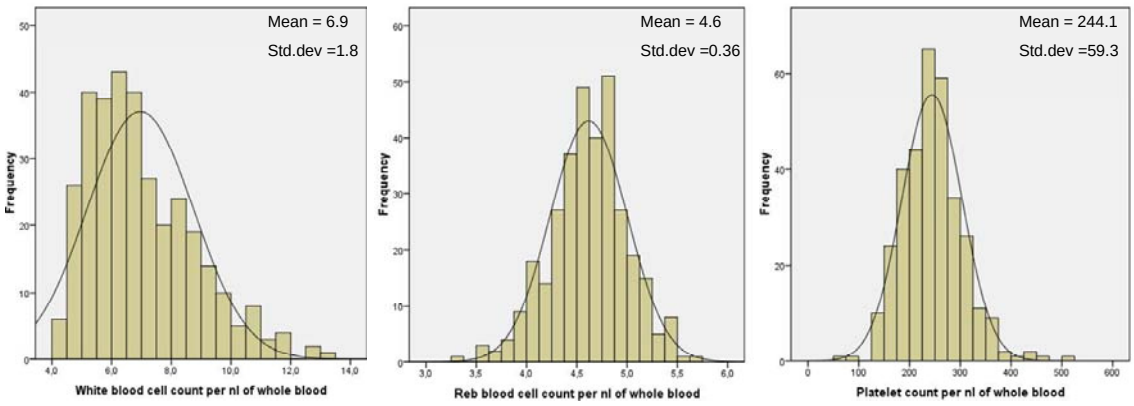

Figure 21-Distribution of WBC, RBC and platelets among KORA individuals: Histogram of frequencies of the number of WBC, RBC and platelets in blood. The curve depicts the normal distribution.

Pathway analysis of the 69 WBC-specific transcripts using PANTHER revealed overrepresentation of transcripts involved in transcriptional regulation, insulin pathway, interleukin pathway, muscarinic and nicotinic acetylcholine pathway, P13 pathway and TGF-beta pathway (Figure 22).

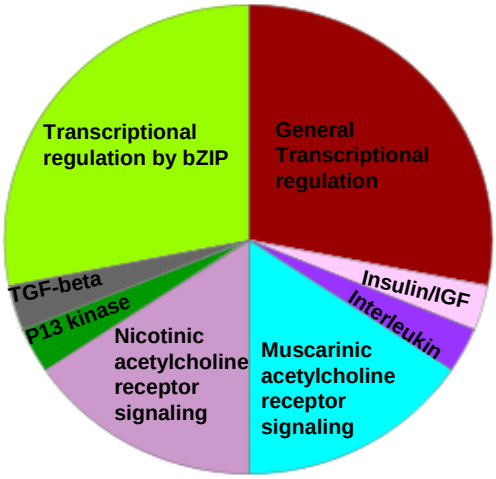

Figure 22-WBC-specific genes: PANTHER pathway analysis of 69 WBC-specific transcripts.

The top 15 significant WBC-specific transcripts and the platelet-specific transcript are shown in Table 6. Not surprisingly, the platelet-specific transcript was involved in blood coagulation and cell adhesion (Jeimy, Fuller et al. 2008).

Table 6-Top 15 WBC-specific and 1 platelet-specific transcript

	Gene	Probe ID	Chromosome	Function	p-value	Variance	Cell type	Correlation coefficient
1	NINJ2	770019	12	tissue regeneration, neuron adhesion	1.18×10^{-8}	0.35	wbc	-0.31
2	HS.234961	5340292	*	*	5.47×10^{-8}	0.34	wbc	-0.30
3	RALGPS2	2490091	1	signal transduction	8.24×10^{-8}	0.10	wbc	0.29
4	MBNL3	670735	X	development	8.83×10^{-8}	0.24	wbc	-0.29
5	LOC642464	1690156	12	*	9.07×10^{-8}	0.33	wbc	-0.29
6	HS.573549	70156	*	*	1.29×10^{-7}	0.13	wbc	-0.29
7	ATP6V0C	1170431	9	ATPase, H+ transporting	2.13×10^{-7}	0.17	wbc	-0.28
8	HS.563564	6840349	*	*	2.77×10^{-7}	0.16	wbc	-0.28
9	ZCCHC7	4560465	9	zinc finger, nucleic acid binding	2.85×10^{-7}	0.10	wbc	0.28
10	DPM2	7560390	9	macromolecule biosynthesis	3.05×10^{-7}	0.40	wbc	-0.28
11	PLVAP	5090242	19	*	3.13×10^{-7}	0.47	wbc	-0.28
12	PRSS36	630014	16	proteolysis and peptidolysis	3.70×10^{-7}	0.20	wbc	-0.28
13	HS.542295	3180468	*	*	3.76×10^{-7}	0.36	wbc	-0.28
14	39874	5310014	19	protein ubiquitination	4.18×10^{-7}	0.30	wbc	-0.28
15	KCNJ10	6480324	1	ion transport	5.01×10^{-7}	0.30	wbc	-0.28
1	MMRN1	940328	4	blood coagulation, cell adhesion	3.47×10^{-6}	0.06	platelet	0.26

* = unknown

If known, the number of WBCs, RBCs and platelets can be corrected for by adding them as covariables in the linear regression model. The 69WBC-specific transcripts and 1 platelet-specific transcript identified here might serve as biomarkers whose differential expression might represent a difference in proportion of WBCs and platelets in blood.

5.8 Globin – to reduce or not reduce?

Redundant globin mRNA in whole blood RNA might diminish transcript detection sensitivity and increase microarray signal variation (Liu, Walter et al. 2006). A pilot experiment was executed to evaluate the effect of globin reduction on gene expression. 5 RNA samples were globin reduced and the 10 RNA samples (5 samples before and after globin reduction) were hybridized on the Illumina microarray (Figure 23).

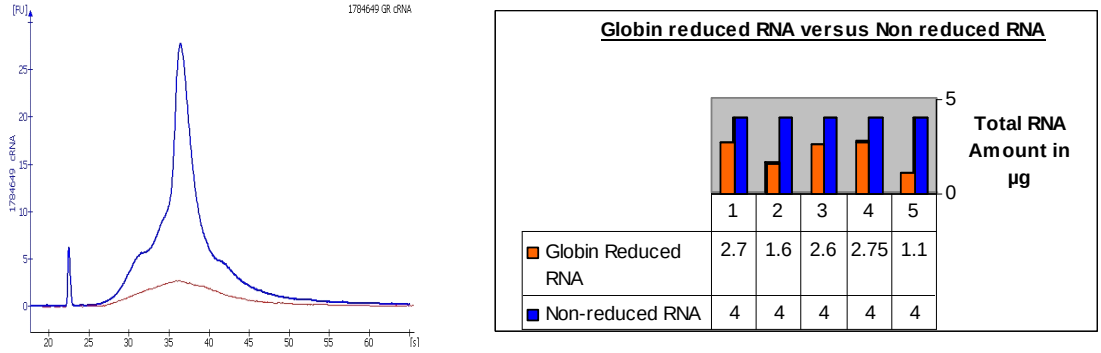

Figure 23-Globin reduction in whole blood: The left panel indicates efficient removal of the globin peak on the Bioanalyzer. The right panel indicates reduction in the amount of RNA after globin reduction.

The number of significantly detected transcripts also known as the present call rate increased considerably after globin reduction as indicated in Figure 24.

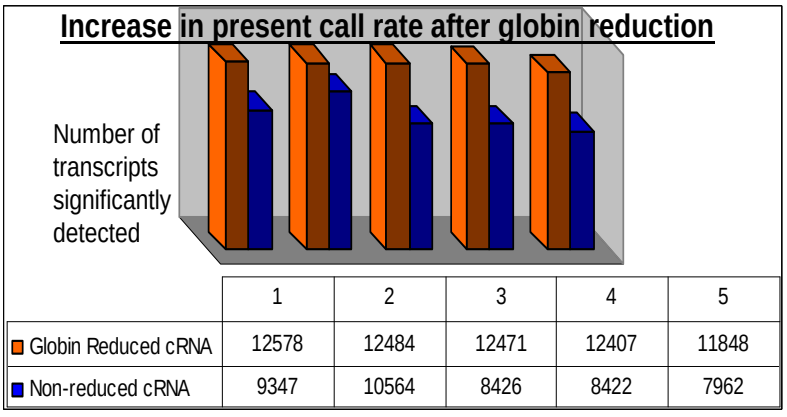

Figure 24-Present call rate in globin reduced versus non reduced RNA: Increase of 30-40% in the present call rate after globin reduction.

To test for differences due to the globin reduction procedure, the 10 samples were grouped under globin reduced and non reduced groups (n=5 in each group). A standard t-test was carried out to identify transcripts that were differentially expressed after globin reduction. Using the stringent Bonferroni correction 13 transcripts were found to be significantly different and using the Benjamini Hochberg 2425 significantly different transcripts were found between the two groups. For the 13 transcripts, globin reduction resulted in both increase (n=3) and decrease (n=10) in the mean expression levels (Table 7).

Table 7-Transcripts significantly different after globin reduction

	TargetID	Probe ID	Chromosome	p-value	log2 mean expression of globin-reduced group	log2 mean expression of non-reduced group
1	C14ORF2	240523	14	1.12×10^{-7}	9.68	10.22
2	TIAM2	1660035	6	2.53×10^{-7}	7.95	10.54
3	LOC643904	1170403	17	2.92×10^{-7}	9.60	16.25
4	ABCC6	3520091	*	4.63×10^{-7}	7.88	7.54
5	ROPN1B	5130435	3	5.90×10^{-7}	8.47	12.14
6	ARTN	7160022	1	7.85×10^{-7}	8.44	10.21
7	RGS19	290386	20	1.02×10^{-6}	13.38	11.68
8	SERPINA13	2630647	14	1.03×10^{-6}	8.86	14.02
9	LOC642724	3450731	11	1.33×10^{-6}	8.99	13.59
10	TNFAIP2	4210056	14	1.61×10^{-6}	12.49	13.16
11	LOC650472	1400097	*	1.92×10^{-6}	14.60	13.49
12	HS.583509	7210524	*	2.43×10^{-6}	7.82	9.66
13	HS.436060	940731	*	2.47×10^{-6}	8.15	10.40

* = unknown

The Illumina Sentrix WG6-v2 microarray has probes hybridizing to 6 human globin transcripts – HBA, HBB, HBD, HBE, HBGA1 and HBGA2. 4 of these 6 transcripts belonged to the list of transcripts significantly different between the globin reduced and non-reduced group using the Benjamini Hochberg correction (Table 8). Since HBA and HBB are the most abundant globin transcripts in blood, the globin reduction protocols are optimized for the removal of these (Affymetrix technical note, 2006). Significant reduction of the HBD and HBE1 transcripts could indicate a true reduction in transcript levels or might be an artifact of cross hybridization which may result due to the homology between the globin genes. The fact that the mean expression levels of HBA1 and HBB is only slightly reduced might be due to saturation of fluorescent signal

intensities on the microarray. HBG1 and HBG2 did not show a significant decrease in expression after globin reduction.

Table 8-Effect of globin reduction on expression levels for 6 globin genes

Target ID	Probe ID	Chromosome	p-value	log_2 mean expression of globin-reduced group	log_2 mean expression of non-reduced group
HBA1	360554	16	8.1×10^{-4}	16.31	16.83
HBB	5340674	11	1.5×10^{-3}	16.29	16.82
HBD	6250037	11	2.8×10^{-5}	12.46	16.40
HBE1	6520176	11	2.0×10^{-5}	9.39	12.05
HBG1	4150187	11	0.61	16.29	16.38
HBG2	6400079	11	0.66	16.24	16.32

To verify if the globin reduction-induced changes in expression levels were consistent across all samples, genes with the highest fold-change differences between the globin reduced and non-reduced RNA pairs were checked. Analysis of the fold-changes between sample pairs revealed several inconsistencies, denoted in red (Table 9).

Table 9-Examples of inconsistent fold changes across RNA pairs after globin reduction

Target ID	Probe ID	Chromosome	RNA 1 fold change before and after globin reduction	RNA 2 fold change before and after globin reduction	RNA 3 fold change before and after globin reduction
LOC44034	110468	16	- 6.29	- 6.87	**- 13.1**
IL6R	6250360	1	**+ 0.93**	- 0.8	**- 3.54**
SNF8	2650192	17	- 2.3	**- 4.44**	- 2.68
IIP45	4850692	1	- 2.61	**- 4.34**	- 2.27
DKFZP761	4290435	11	- 6.32	- 4.02	**- 2.65**

+ and - = indicates increase or decrease in expression after globin reduction

These results suggest that although globin reduction increased present call rates of expressed genes, it seemed to have introduced other artifacts which interfere with gene expression. This was in accordance with studies highlighting the problems of globin reduction resulting in loss of reproducibility at the cost of slight increase in sensitivity (Dumeaux, Borresen-Dale et al. 2008; Li, Ying et al. 2008) and reports from Illumina stating that globin reduction was not required for their microarray protocols (Illumina technical note, 2007).Therefore, the whole blood RNA samples were not globin reduced in this study.

5.9 Gender-specific differences in gene expression

Gender-specific differences are known to play an important role in the occurrence and susceptibility of several immunological diseases such as systemic lupus erythematosus (Verthelyi, Petri et al. 2001; Bouman, Heineman et al. 2005). One interesting aspect was to check expression of genes encoding the sex chromosomes in non-gonadal tissues such as peripheral blood. To achieve this, genes that were differentially expressed between males and females were investigated. Performing a Welch t-test with a Bonferroni correction, 24 genes were found to be significantly different between the two genders (Table 10).

Table 10-24 differentially expressed genes between males and females

	Target ID	Probe ID	Chromosome	Biological process	p-value
1	RPS4Y1	3180075	Y	protein biosynthesis	3.6×10^{-127}
2	SMCY	6560452	Y	regulation of transcription, spermatogenesis	1.75×10^{-60}
3	PRKY	2900048	Y	protein amino acid phosphorylation	2.99×10^{-51}
4	XIST	3390521	X	*	8.68×10^{-48}
5	HS.546019	7510292		*	1.92×10^{-43}
6	EIF1AY	1780270	Y	translational initiation, protein biosynthesis	3.37×10^{-40}
7	CYORF15A	2190192	Y	*	7.87×10^{-28}
8	HDHD1A	5820315	X	metabolism	4.71×10^{-22}
9	EIF2S3	5670521	X	protein biosynthesis	4.90×10^{-16}
10	LOC647322	4730600	2	*	7.08×10^{-15}
11	SEPT6.	20154	X	cytokinesis, cell cycle	1.63×10^{-12}
12	PRKX	2100187	X	protein amino acid phosphorylation	2.32×10^{-12}
13	LOC644670	4230376	X	*	5.08×10^{-8}
14	LOC284422	6760431		*	9.22×10^{-8}
15	TNFAIP6	2370524	2	cell-cell signaling, inflammatory response, cell adhesion	9.83×10^{-8}
16	ZBED1	520431	X	*	9.90×10^{-8}
17	OPLAH	5820348	8	*	2.24×10^{-7}
18	PTGDS	6960022	9	transport, regulation of circadian cycle	2.89×10^{-7}
19	LOC441528	4540403	X	*	4.02×10^{-7}
20	ELA2	1470554	19	proteolysis and peptidolysis	6.48×10^{-7}
21	CLCN7	450603	16	chloride transport, ion transport	9.45×10^{-7}
22	CA5B	7560162	X	one-carbon compound metabolism	1.31×10^{-6}
23	ALAS2	7560653	X	heme biosynthesis, biosynthesis	1.67×10^{-6}
24	RPS4X	6290274	X	protein biosynthesis	2.15×10^{-6}

* = unknown

Out of the 24 transcripts significantly different between males and females, 6 transcripts were located on autosomal chromosomes, while 18 of the transcripts were located on either X or Y chromosome (Figure 25). The most significant transcript differing between the two genders was RPS4Y1 on the Y chromosome with a p-value of 3.60×10^{-127}.

The autosomal genes included LOC647322 and TNFAIP6 (tumor necrosis factor, alpha-induced protein 6). TNFAIP6 is synthesized in the ovary prior to ovulation and is later released from the follicle at the ovarian surface. Female mice with a targeted disruption of the TNFAIP6 show severe defects in fertility (Wisniewski and Vilcek 2004). Another autosomal gene found to be gender-specific was PGD. PGD2 synthetases, and receptors for PGD2 had been discovered in testicular interstitial cells of men suffering from infertility (Kurimoto, Yabuta et al. 2007). Lipocalin-type PGD synthase, present in cerebrospinal fluid and seminal plasma, is thought to play an important role in male reproduction (Pinzar, Kanaoka et al. 2000). Hematopoietic PGD synthase, present in the spleen; fallopian tube, endometrial gland cells and trophoblasts has been suggested to play a role in female reproduction (Kurimoto, Yabuta et al. 2007).

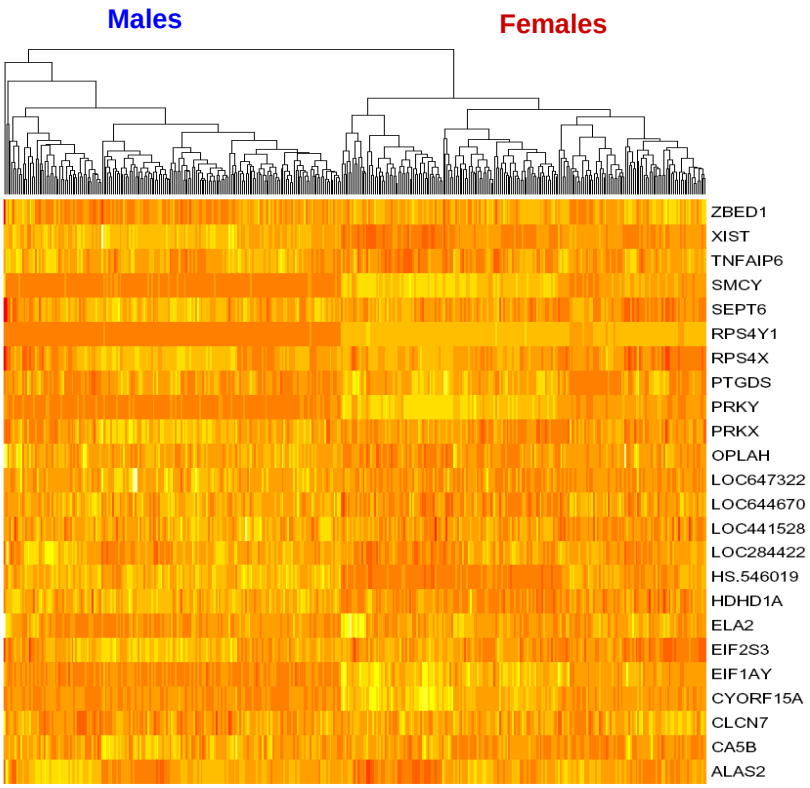

Figure 25-Gender-specific expression patterns: Heat map based on 24 genes differentially expressed between the two genders.

To check if changes in gene expression could clearly distinguish males from females a gender predictor was built based on the 24 gender specific genes using the Prediction of

Analysis of Microarray (PAM) algorithm in R. The best prediction was obtained using RPS4Y1, resulting in a prediction rate of 95% accuracy (Table 11).

Table 11-Gender prediction using RPS4Y1

	Predicted males	Predicted females	Class error rate
Males	186	14	0.07
Females	6	175	0.033
Overall error rate = 0.052			

The 6 misclassified females showed a high expression of RPS4Y1 while the 14 misclassified males showed a lower expression of RPS4Y1 gene relative to the other individuals within their gender (Figure 26).

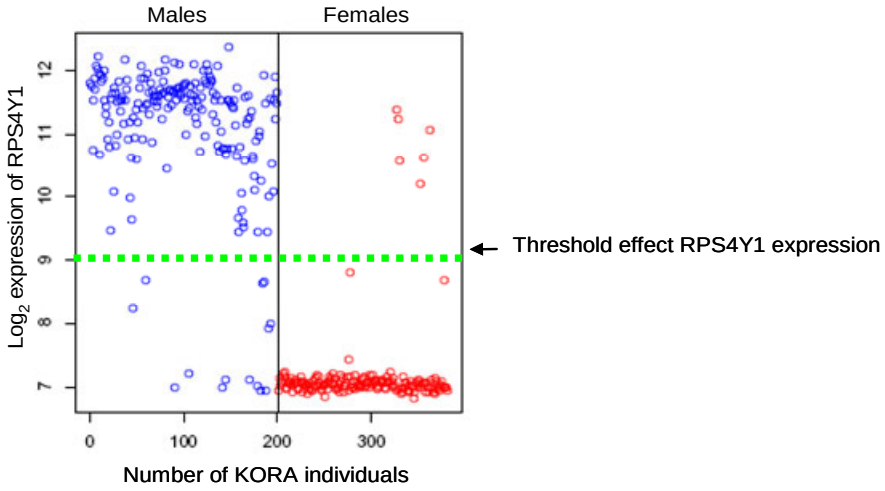

Figure 26-Gender prediction using the RPS4Y1 gene expression levels: 14 males (blue) lying below the green line and 6 females (red) lying above the green line were wrongly classified.

It was not unexpected that prediction of gender could be established using expression levels of a Y chromosomal gene. So another predictor was built using the 6 gender-specific autosomal genes (LOC647322, TNFAIP6, OPLAH, PTGDS, ELA2 and CLCN7). This resulted in an accuracy of 74% (Table 12). The numbers in blue indicate misclassified individuals using the RPSY41 gene for gender prediction.

Table 12-Gender prediction using six autosomal genes

	Predicted males	Predicted females	Class error rate
Males	156 (12)	44 (1)	0.22
Females	58 (4)	123 (5)	0.32
Overall error rate = 0.26			

5.10 Age-related gene expression patterns

The ages of the KORA individuals studied ranged from 50-83 years. The goal was to identify age-associated gene expression changes in peripheral blood. A gender stratified analysis was carried out to allow for sex related effects on age-related gene expression. Using a linear regression model and the Bonferroni correction, 11 genes were found to be significantly associated with age (Table 13).

Table 13-Age-specific gene expression profiles

	Target ID	Probe ID	Chromosome	Biological process	p-value
1	LRRN3	7380181	7	*	3.34×10^{-8}
2	DKFZP761P1	6420079	8	*	1.84×10^{-7}
3	GPR18	7050280	13	signal transduction	3.14×10^{-7}
4	CD248	2350292	11	*	4.46×10^{-7}
5	LOC389289	60470	5	*	6.05×10^{-7}
6	CCR7	6590561	17	chemotaxis, inflammatory response	7.43×10^{-7}
7	LOC387841	3800253	12	*	1.01×10^{-6}
8	OCIAD2	4560128	4	*	1.20×10^{-6}
9	VNN3	2810373	6	nitrogen compound metabolism	1.30×10^{-6}
10	LY9	450037	1	humoral defense mechanism, cell adhesion	1.56×10^{-6}
11	FAM113B	7200187	12	*	2.70×10^{-6}

* = unknown

The most significant association with age was observed with LRNN3 which encodes a neuronal leucine-rich repeat protein. Expression levels of 10 of the 11 age-specific genes showed a negative correlation with age. Only VNN3 expression showed a positive correlation with age (Figure 27). VNN3 belongs to the vanin family of proteins which possess pantotheinase activity and are thought to play a role in oxidative stress (Bomprezzi, Ringner et al. 2003).

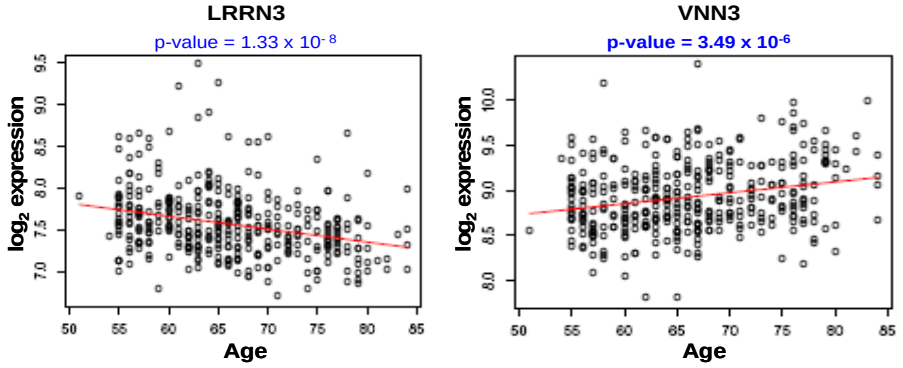

Figure 27-Age-specific gene expression patterns: Expression of LRNN3 is negatively correlated with age while expression of VNN3 is positively correlated with age.

5.11 Cis and trans regulators of gene expression

Affymetrix 500k genotypes were available for 320 KORA individuals. The 500,568 SNPs had been filtered using a minor allele frequency > 0.05, Hardy Weinberg p-value of $<10^{-6}$ and genotyping efficiency of >95%, resulting in 335,152 high-quality SNPs for further analysis (Winkelmann 2008). As described previously, 13767 filtered transcripts were used for analyses of gene expression.

A GWAS was performed to map SNPs influencing expression levels, referred to as expression quantitative trait loci (eQTLs). Cis SNPs refers to SNPs located within the vicinity of the transcript while trans SNPs refer to SNPs located at a distance from the transcript. For identification of cis SNPs, a cis-window of +/-100 kb from the probe end was defined based on previous reports demonstrating that >90% cis SNPs were situated within 100kb from the transcript (Stranger, Forrest et al. 2007; Emilsson, Thorleifsson et al. 2008). Due to the definition of the cis-window, depending on the density of SNPs within each cis-window, varying numbers of cis SNPs were tested for effects on transcript expression. On average, about 20 cis SNPs per transcript were tested. To achieve genome-wide significance, the Bonferroni adjusted p-value was computed as $0.05/ {}_{i=1}\Sigma^{13767}$, where N_i = number of SNPs tested for transcript i for 13767 transcripts. At this adjusted threshold of 1.8×10^{-7}, 1296 significant cis SNPs corresponding to 286 cis eQTLs were detected using a linear regression model.

To identify trans variants, 335,152 SNPs across all 13767 transcripts were investigated. The Bonferroni adjusted p-value was computed as $0.05/ (335{,}152 \times 13767) = 1 \times 10^{-11}$. At this threshold 1722 significant SNPs corresponding to 231 eQTLs were identified. Of these, 655 SNPs corresponding to 146 eQTLs (63%) were located +/- 100 kb from probe end and hence were also included in the cis eQTL analysis calculated above. The remaining 1067 SNPs (85 eQTLs) were trans effects. The top three cis and trans eQTLs are shown in Figure 28.

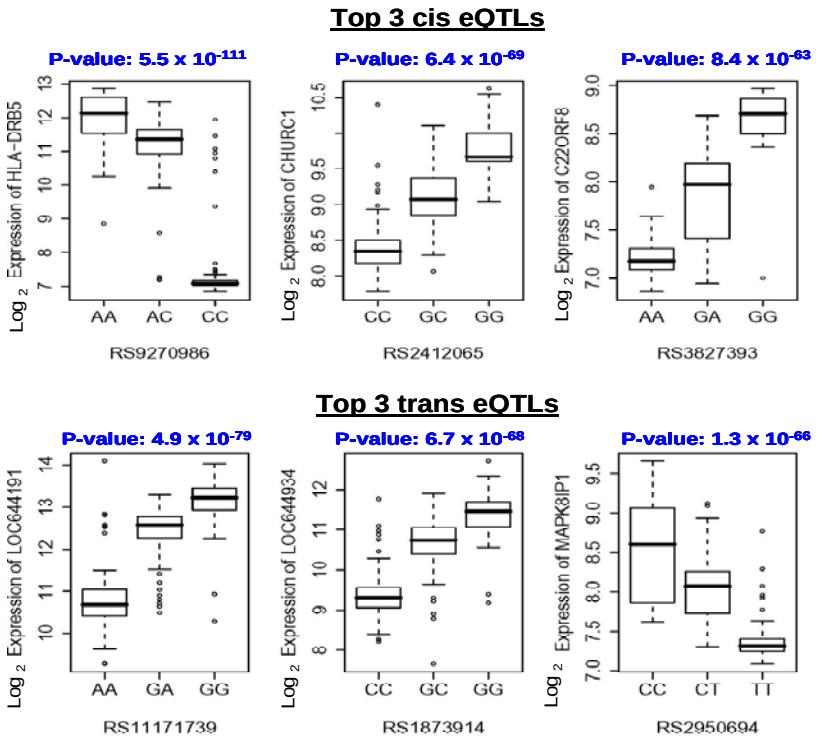

Figure 28-Top 3 cis and trans whole blood eQTLs: Of the top 3 cis eQTLs, HLA-DRB5 was categorized as one of the top 3 highest variable transcripts (according to the variance scores in chapter 5.5), hence strengthening the notion that the highest variable transcripts had the potential power to detect genetic associations. The functions of CHURC1 and C22ORF8 are unknown. Among the top 3 trans eQTLs, MAPK8IP1 is a regulator of the pancreatic beta cell function and is known to be mutated in type 2 diabetes (Waeber, Delplanque et al. 2000). The functions of LOC644191 and LOC644934 are not known.

Figures 29 and 30 depict the Manhattan plot and Q-Q plot of the 286 significant cis eQTLs identified in this study. For the cis eQTLs, only the SNPs within a 100kb region of the probe were tested. Since most of the cis variants are known to be in the vicinity of the transcript, this criterion is bound to introduce a selective bias for association. This bias is clearly visible on the skewed distribution of the Q-Q plot indicating inflated p-values.

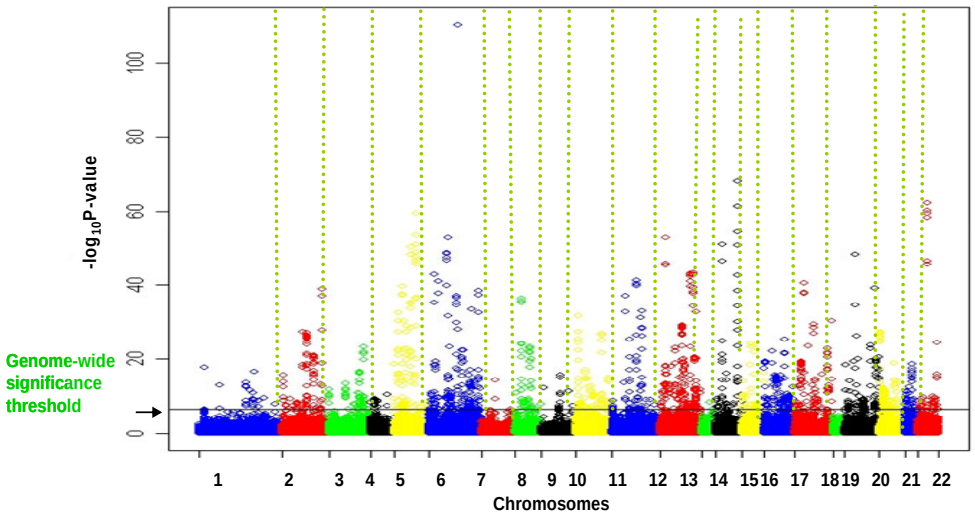

Figure 29-Cis eQTLs: A Manhattan plot showing the distribution of cis eQTLs across the chromosomes. The line indicates the genome-wide threshold of significance calculated for this study.

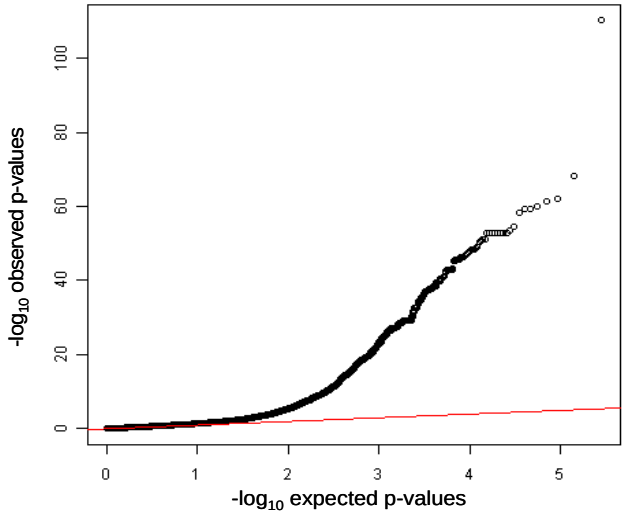

Figure 30-Q-Q plot of cis eQTLs: The Q-Q plot shows the distribution of the expected p-values on the x axis versus the observed p-values on the y axis. Each black dot denotes an eQTL. The Q-Q plot indicates a skewed distribution of the cis eQTL results indicating an inflated type 1 error.

Mapping of eQTLs poses some statistical challenges, some of which are visible in this study. One serious concern is the validity of assumption of normality of gene expression measurements in microarray data. Violation of the normality assumption might lead to

inflated type 1 error (false positives) as might be indicated by the top eQTL hit on chromosome 6 (p-value: 5.5 x 10^{-111}) in Figure 29.

One way to deal with the problem of non-normally distributed traits is to determine the empirical significance of the association results by performing simulation studies (Deutsch, Lyle et al. 2005). For the top eQTL which seemed to exhibit an inflated p-value, 1 million permutations were performed to test for associations between rs9270986 and HLA-DRB5 gene expression using WG-PERMER (http://www.wg-permer.org). WG-PERMER is a program for rapid permutations of genome-wide data using the Westfall-Young method of correction (Thoeringer, Ripke et al. 2009). The results for different models of association using the Fisher product method (Fisher, Immer et al. 1932) are indicated in Table 14. The best fitting models were the dominant and genotypic models with nominal p-values < 10^{-133}. Due to the high significance level of this eQTL, a large number of simulation tests would have to be performed to obtain a meaningful empirical p-value.

Table 14-Permutation results for rs9270986 and HLA-DRB5 expression

SNP	Chromosome	Gene	Permutation Model	Empirical p-value	Nominal p-value
rs9270986	6	HLA-DRB5	Dominant	1,00E-06	1.28 x 10^{-133}
rs9270986	6	HLA-DRB5	Genotypic	1,00E-06	5.75 x 10^{-133}
rs9270986	6	HLA-DRB5	Fisher model	1,00E-06	3.15 x 10^{-87}
rs9270986	6	HLA-DRB5	Het./Hom.	1,00E-06	3.65 10^{-86}
rs9270986	6	HLA-DRB5	Allelic/Additive	1,00E-06	2.39 10^{-75}
rs9270986	6	HLA-DRB5	Reccesive	1,00E-06	4.84 10^{-8}

Since performing large-scale simulations are computationally intensive, an alternative is to apply non-parametric tests to the expression data. Rank based non-parametric tests are used when the data do not conform to a normal distribution. Since the ranks of the genes are uniformly distributed, non-parametric tests are independent of any underlying assumptions of normal distribution. To evaluate if the HLA-DRB5 eQTL was a true positive, the non-parametric Kruskal Wallis test was applied to check for association between HLA-DRB5 expression and rs9270986. The Kruskal Wallis test is robust to trait distribution and has been used successfully in eQTL mapping in earlier studies (Schadt,

Molony et al. 2008). The Kruskal Wallis test resulted in a p-value of 3.3 x 10^{-43}, indicating that the association was a true one.

From the Manhattan plot in Figure 29, the solitary top eQTL on HLA-DRB5 seemed to be an artifact and had an inflated p-value of 5.5 x 10^{-111}. The minor allelic frequency of rs9270986 was 0.17, indicating that the allelic frequency did not contribute to the possible spurious association.

To interrogate other possible eQTLs in the region, a Manhattan plot was generated for HLA-DRB5 only. A close-up of the eQTL signals for the HLADRB5 transcript showed a clear peak of association at rs9270986 (Figure 31). Evaluation of the other SNPs in the region indicated high linkage disequilibrium between rs9280986 and the other significant SNPs associated with HLA-DRB5 expression (Table 15 and Figure 32).

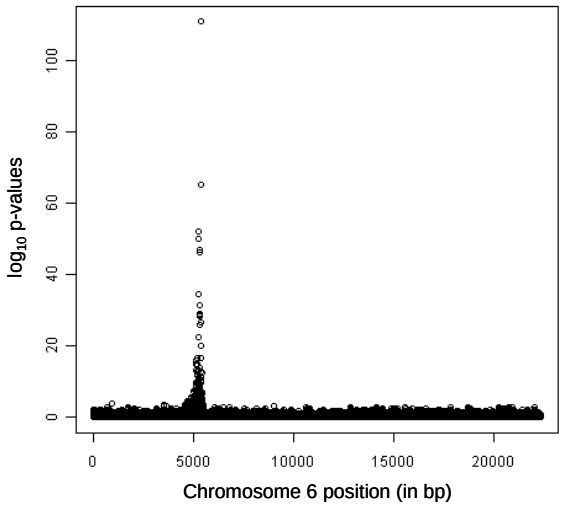

Figure 31-Zoomed-in Manhattan plot of HLA-DRB5 region: Clearly visible peak at rs9270986 was observed in the GWAS for HLA-DRB5 only.

Table 15-High linkage disequilibrium between rs9270986 and the top SNPs

SNP	Chromosome	Position in bp	p-value	R^2	D'
rs9270986	6	32682038	1.7 x 10^{-111}	1	1
rs3129768	6	32703061	5.17 x 10^{-66}	0.87	0.96
rs3131294	6	32288124	1 x 10^{-52}	0.58	0.78
rs3129900	6	32413957	1.33 x 10^{-47}	0.87	0.96
rs3129934	6	32444165	9.29 x 10^{-47}	0.87	0.96
rs3135377	6	32493377	3.84 x 10^{-32}	0.74	0.95
rs3132959	6	32406920	1.13 x 10^{-29}	0.64	0.91
rs2894249	6	32433813	2.16 x 10^{-29}	0.64	0.91
rs3129932	6	32444105	4.53 x 10^{-29}	0.64	0.91
rs910049	6	32423705	1.46 x 10^{-26}	0.64	0.91

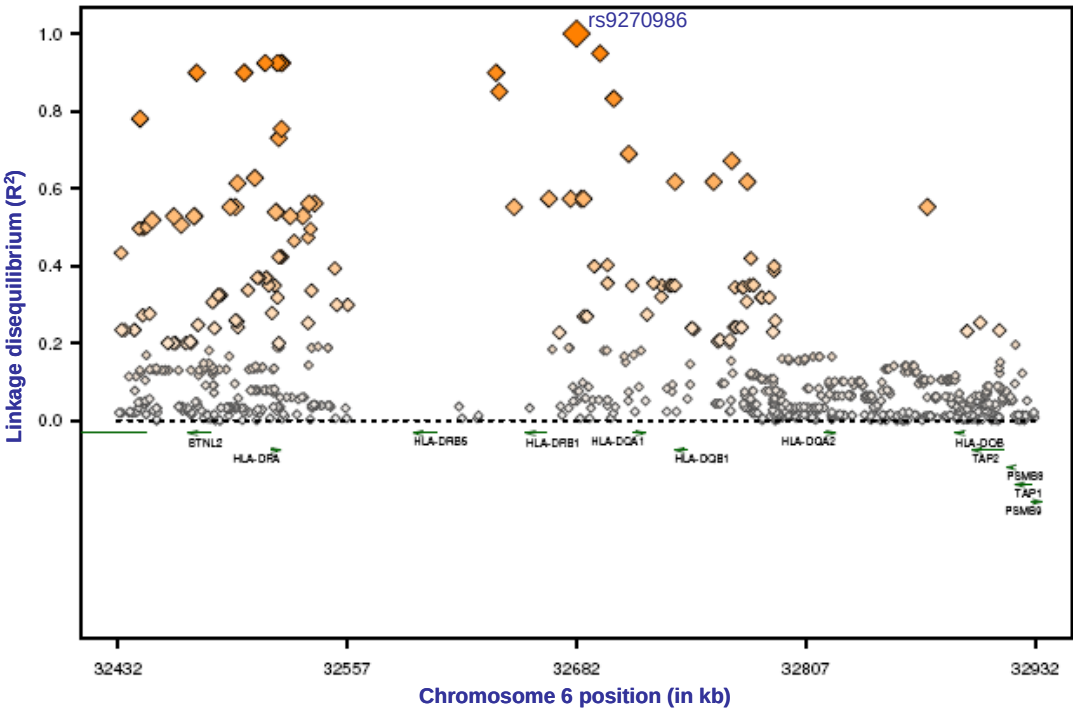

Figure 32-LD plot: High linkage disequilibrium was observed between rs9270986 and the other SNPs in the region, all which were significantly associated with HLA-DRB5 expression. The LD (R^2) is denoted on the left y axis. The base positions are indicated on the x axis. This figure was generated in SNAP tool version 2.1 (Johnson, Handsaker et al. 2008).

The genomic inflation factor compares the genome-wide distribution of the test statistic to the expected null distribution (de Bakker, Ferreira et al. 2008). The genomic inflation factor λ is defined as the ratio of the median of the empirically observed distribution of the test statistic to the expected median, thereby quantifying excessive false positives (Devlin and Roeder 1999). The genomic inflation factor for the GWAS was 1.2 across all chromosomes and reduced to 0.99 when eQTLs within chromosome 6 were excluded. Q-Q plots of HLA-DRB5 eQTLs both genome-wide and excluding chromosome 6 SNPs are indicated in Figure 33. The results suggest that a large portion of the bias in the eQTL seemed to localize within the major histocompatibility complex (MHC) on chromosome 6. The eQTL results were consistent with previous eQTL studies which demonstrated an inflation of p-values in the HLA locus (Dixon, Liang et al. 2007).

To my knowledge this is the first report of rs9270986 significantly influencing transcription levels of HLA-DRB5. According to the expression profiles, for individuals

homozygous for C allele of rs9270986, HLA-DRB5 expression is almost completely turned off (Figure 28). Previous studies have shown rs9270986 to be significantly associated with type 1 diabetes and multiple sclerosis (WTCCC 2007).

Inspection of eQTL results from LCLs in the HapMap dataset (Stranger, Nica et al. 2007) revealed significant association between rs9270986 and HLA-DRB5 (p-values: 0.001). Examination of eQTL results from LCLs in an asthma cohort (Dixon, Liang et al. 2007) revealed significant association between rs9267992 (high LD, R^2 of 0.91 with rs9270986) and HLA-DRB5 with a p-value of 1.2×10^{-5}. These eQTLs did not pass the genome-wide significance threshold in the above studies and hence had not been reported by the authors. Further inspection of published liver eQTL data (Schadt, Molony et al. 2008), revealed a significant correlation between rs9271366 (high LD, R^2 of 0.92 with rs9270986) and expression of HLA-DRB5 with a p-value of 5×10^{-45}.Taken together, these results suggest a true association between rs9270986 and HLA-DRB5 expression with a stronger effect in whole blood as indicated in this study.

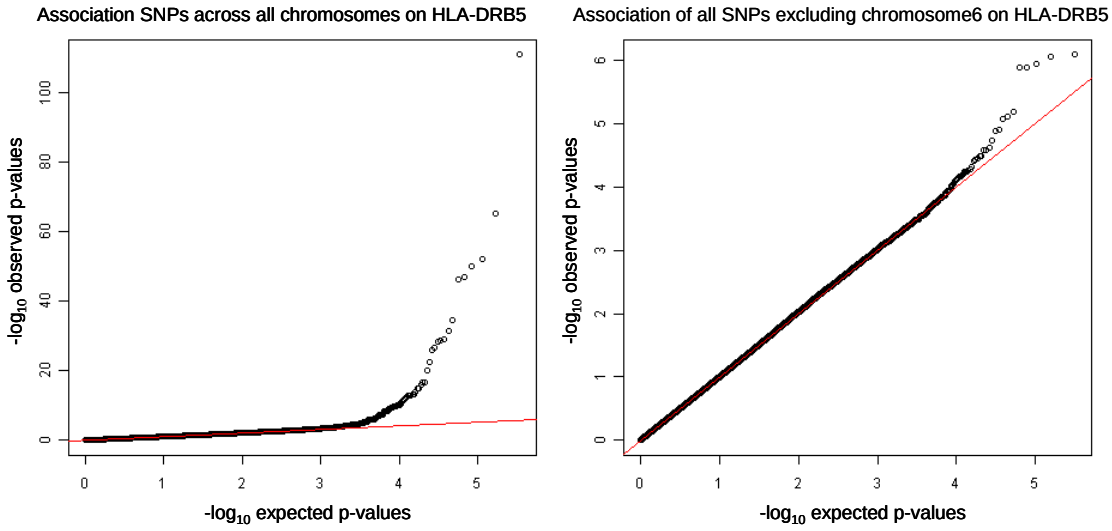

Figure 33-Q-Q plots of HLA-DRB5 with and without chromosome 6 SNPs: Genome-wide association of all 335,152 SNPs on HLA-DRB5 shows an inflated type 1 error indicated by the tail to the right. Removal of chromosomal 6 SNPs, results in a Q-Q plot showing a largely normal distributed result. The red line indicates the diagonal. Under the null distribution all points must lie on the diagonal.

A further method of validating the eQTLs identified in this study was to replicate these findings in another population and another tissue. Since the expression data generated in this study was from German individuals, the eQTL results were compared to the LCL expression from 90 Caucasians belonging to the HapMap to avoid population biases (Stranger, Nica et al. 2007) .

The filter criteria, cis-window, multiple testing correction and Illumina microarray versions used in both experiments differed therefore a direct comparison of the published data was not possible. For the HapMap dataset, the authors had analyzed eQTLs for 13647 transcripts which were found to be highly variable between the 4 HapMap populations in a previous study (Stranger, Forrest et al. 2005). For cis SNPs, the authors had selected a threshold of +/- 1Mb from the center of the probe. The results had been corrected for multiple testing based on a 0.001 permutation threshold in the HapMap. Finally, the HapMap used an older version of the Illumina Sentrix WG6 v1 microarray (Stranger, Forrest et al. 2005). Since the overlap between the filtered transcripts in KORA and HapMap was less than 50%, I decided to perform the same analysis using both KORA and HapMap datasets.

All tests were performed using linear regression and Bonferroni correction. Details of the comparisons between KORA and HapMap eQTLs are given in Table 16.

Overall, 119 cis eQTLs and 12 trans eQTLs were common between the two datasets. For the common eQTLs, the direction of effect was checked for all the overlapping eQTLs and was found to be the same in both the KORA and HapMap datasets for all except 7 transcripts (Supplementary Figure 1). For 5 of these 7 transcripts the difference in the direction of the SNP effect on gene expression could be explained by either the difference in DNA strand orientation or the frequency of the major allele in the dataset. For the remaining 2 eQTLs, the difference in SNP effect on expression were attributable to tissue-specific regulatory variation as has been observed in previous reports (Heap, Trynka et al. 2009). Details of the comparisons of direction of effect for these 7 transcripts are provided in Supplementary Table 1.

Table 16-Comparison of KORA blood and HapMap LCL eQTLs

		KORA	Overlap	HapMap CEU
a	Number of individuals surveyed	381		90
b	Tissue assayed for gene expression	whole blood		LCL
c	Criteria used to define cis-window	100kb		1Mb
d	Multiple testing correction used	Bonferroni		Permutation
e	Number of transcripts in raw data	48,701		47,296
	Overlapping transcripts in raw data		37,987	
f	Number of SNPs in raw data	500,568		2.2 million
	Overlapping SNPs in raw data		498,540	
g	Number of cis eQTLs identified	**286**		**299**
	Overlap of cis eQTLs		25	
	Confirmation of cis eQTLs using raw data from other study	**49 out of 299**		**45 out of 286**
	Total overlap of cis eQTLs		119	
h	Number of trans eQTLs identified	**85**		**44**
	Overlap of trans eQTLs		0	
	Confirmation of trans eQTLs using raw data from other study	**1 out of 44**		**11 out of 85**
	Total overlap of trans eQTLs		12	

Despite the large number of differences in the experimental designs between the two studies, a total of 131 KORA eQTLs (119 cis eQTLs and 12 trans eQTLs) could be reconfirmed and replicated in the HapMap data. This corresponds to a total overlap of 35% between whole blood and LCL eQTLs. The results presented here are in accordance with previous reports which have demonstrated a 30% overlap of eQTLs from different tissues such as blood, LCL and liver (Emilsson, Thorleifsson et al. 2008). In summary, at least 35% of the eQTLs identified in this study seem to be true positives. The remaining 65% of eQTLs identified here need to be independently verified.

An important observation from previous reports and this GWAS was the indication of increased type 1 errors in eQTL mapping (Deutsch, Lyle et al. 2005). This highlights the need to take correct measures such as simulations, non-parametric tests and replication of eQTLs to enable accurate interpretation of the significance of the results.

5.12 Functional validation of GWAS candidate SNPs using expression profiles

The principal outputs of GWAS are SNPs which are significantly correlated with complex traits. Based on known literature and available annotations of nearby genes most authors try to postulate the potential causal gene. However, very few of the SNPs are located in coding regions of genes. The majority of signals are located intronic or within intergenic regions of unknown function. One major challenge is the interpretation of GWAS and confident assignment of the true causal variant(s). Functional studies are required to pinpoint the causal variants and affected genes and allow transition from candidate gene identification to translational progress.

Integration of gene expression with genotypes and phenotypes allows prioritization of positional candidate genes, thereby providing a functional handle on understanding the etiology of complex traits (Figure 34).

• **GWAS SNP :** SNP identified in a published GWAS of a complex trait

• **eSNP :** a GWAS SNP found to significantly influence expression of the candidate gene in either KORA or HapMap datasets

• **cSNP and tSNP** : SNPs present in cis(+/-100kb from probe end) or trans significantly influencing expression of a GWAS candidate gene in the KORA dataset.

• *** * * :** Examples are given in sections 5.12.1, 5.12.3 , 5.12.4 and 5.12.5

Figure 34-Using gene expression to determine functionality: This cartoon depicts the possible associations between SNP, expression of a transcript and phenotype.

The aim was to check if SNPs reported in GWAS of complex traits significantly correlated with transcript levels of nearby genes i.e: testing whether the complex trait associated SNPs were eSNPs. The National Human Genome Research Institute (NHGRI) website (www.genome.gov/26525384) was used to assemble a list incorporating results from 190 GWAS (March 2005 - September 2008). This list included 411 SNPs (264 transcripts) significantly correlated with complex phenotypes such as diabetes, Crohn disease, celiac disease and asthma (Supplementary Table 2).

5.12.1 Confirmation of known eSNPs and identification of novel eSNPs

Expression profiles from whole blood in 320 KORA individuals (generated in this study) and LCL expression profiles from 90 Caucasian HapMap individuals (http://www.sanger.ac.uk/humgen/genevar/) were available. Genotypes from 500k Affymetrix microarrays and 2,2 millions SNPs using the Illumina array were available for the KORA and HapMap datasets respectively (Stranger, Nica et al. 2007). Therefore it was possible to systematically test the 411 SNPs with expression levels of the 264 transcripts in both KORA and HapMap.

15 eSNPs (10 in KORA, 7 in HapMap and 2 in both KORA and HapMap) were identified using linear regression analysis after applying a multiple testing correction of 5% FDR. 4 eSNPs out of 15 eSNPs had already been reported (1 in whole blood and 3 in LCL) while the remaining 11eSNPs were new eSNPs (Table 17a, 17b and Figure 35).

Table 17a-Confirmation of 4 eSNPs in KORA and HapMap

			Literature			KORA blood			HapMap CEU LCL		
Gene ID	Tissue	Trait	Reference	SNP	p-value	p-value	Beta	R^2	p-value	Beta	R^2
IL18RAP**	blood	Celiac disease	Hunt et al., 2008	rs917997	3.2×10^{-5}	4.06×10^{-16}	-0.46	0.19	0.31	0.09	0.01
C8ORF13**	LCL	SLE	Hom et al., 2008	rs13277113	5.0×10^{-35}	9.40×10^{-10}	0.06	0.11	1.24×10^{-7}	0.63	0.28
ORMDL3**	LCL	Asthma	Moffat et al., 2007	rs7216389	$<10^{-22}$	8.58×10^{-8}	0.19	0.09	2.10×10^{-8}	0.18	0.30
BLK**	LCL	SLE	Hom et al., 2008	rs13277113	9.0×10^{-27}	0.02	-0.10	0.02	1.80×10^{-6}	-0.55	0.23

** = significant with Bonferroni + FDR5%.

Table 17b-Identification of 11 new eSNPs in KORA and HapMap

Gene ID	Probe ID	SNP ID	p-value	Beta	R^2	Dataset	Trait	Literature
DCTN5**	2000711	rs420259	5.26×10^{-15}	0.17	0.17	KORA	Bipolar Disorder	WTCCC., 2007
EXOC2**	20056	rs6918152	8.05×10^{-7}	0.05	0.07	KORA	Hair colour	Han et al., 2008
HERC2**	1170324	rs916977	1.80×10^{-6}	0.09	0.07	KORA	Iris colour	Kayser et al., 2008
HERC2**	1170324	rs1667394	1.80×10^{-6}	0.09	0.07	KORA	Hair colour	Han et al., 2008
CAMK1D a**	6980685	rs12779790	4.68×10^{-5}	0.12	0.05	KORA	Type 2 Diabetes	Zeggini et al., 2008
CAMK1D a, b**	5900411	rs12779790	6.78×10^{-5}	0.13	0.05	KORA	Type 2 Diabetes	Zeggini et al., 2009
JAZF1*	6770075	rs864745	0.0012	-0.11	0.03	KORA	Type 2 Diabetes	Zeggini et al., 2010
AIM1*	4390438	rs783396	0.0015	0.11	0.03	KORA	Stroke	Matarin et al., 2008
GNA12**	GI_42476110-S	rs798544	6.90×10^{-7}	0.15	0.25	HapMap	Height	Gudbjartsson et al., 2008
MMAB**	GI_41053624-S	rs2338104	6.31×10^{-6}	0.11	0.21	HapMap	HDL-Cholesterol	Willer et al., 2008
ITGAM**	GI_6006013-S	rs9888739	5.89×10^{-5}	0.50	0.17	HapMap	SLE	Harley et al., 2008
PTPN2*	GI_18104978-I	rs2542151	0.0005	-0.18	0.13	HapMap	Crohn's disease	WTCCC., 2007

** = significant with Bonferroni + FDR5%. * = significant with FDR5%. a= Isoform 1. b= Isoform 2.

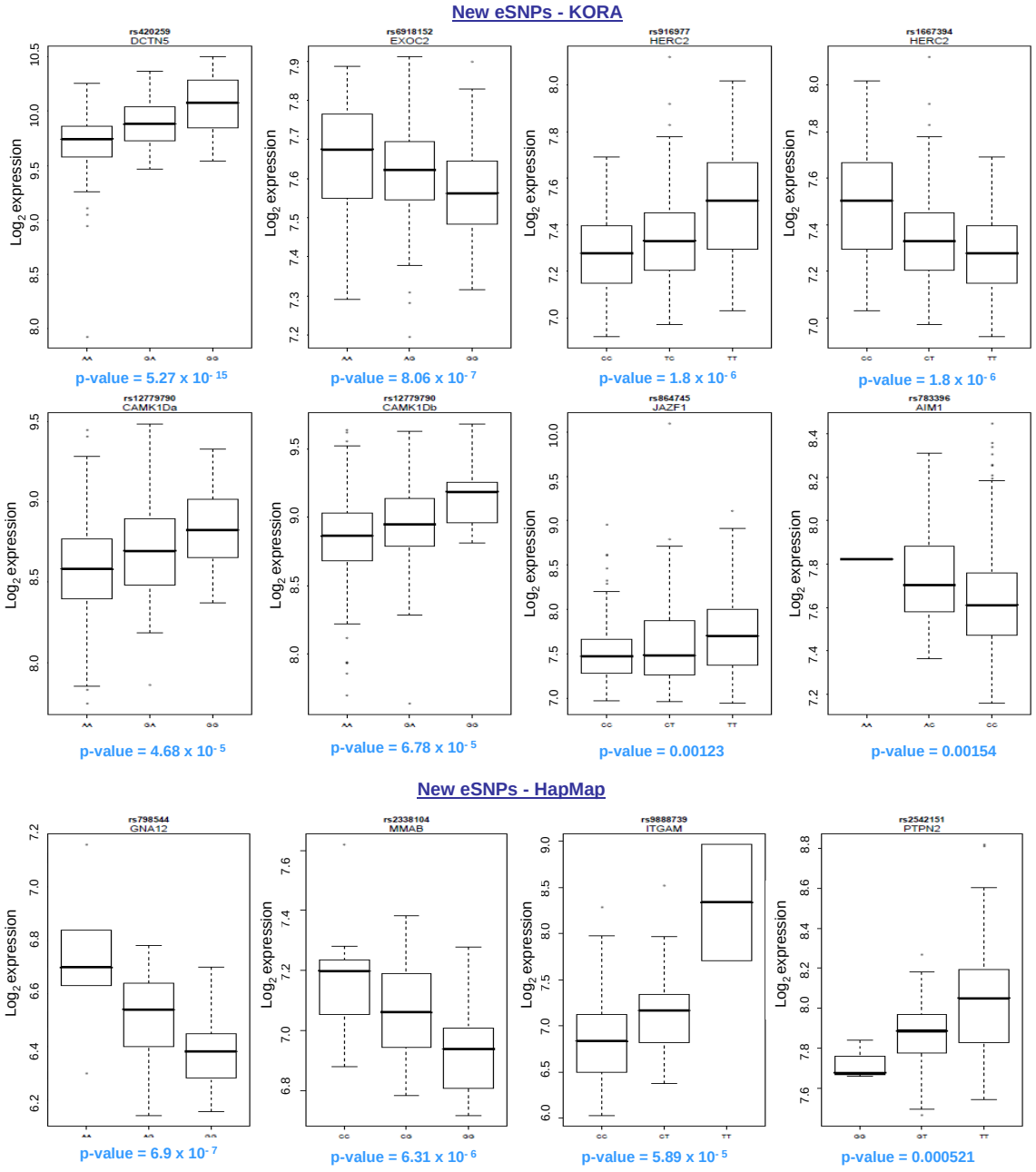

Figure 35-Boxplots of the new eSNPs: The boxplots depict log_2 expression levels (x axis) versus genotypes (y axis). From the known risk alleles for each SNP from the literature, it can be hypothesized that increased expression levels are associated with increased susceptibility towards type 2 diabetes for CAM1KD and JAZF1 and increased susceptibility towards SLE for ITGAM. For HERC2 and EXOC2, increased transcript levels resulted in black to red/brown hair colour. Increased expression of MMAB results in increased HDL-cholesterol. For DCTN5, PTPN2 and GNA12, decreased expression levels cause increased susceptibility towards BD, Crohn disease and height increase respectively. The exact risk allele for the susceptibility towards ischaemic stroke for AIM1 is unknown.

5.12.2 An example where expression profiles allowed prioritization of a candidate gene

In the WTCCC GWAS the strongest signal for bipolar disorder (BD) was at rs420259 on chromosome 16p12 (p-value: 6.3 x 10^{-8}) (2007). The authors noted several biologically interesting genes at this locus which could be associated with BD. These included PALB2 (involved in stability of key nuclear structures), NDUFAB1 (encoding a subunit of complex 1 of the mitochondrial respiratory chain) and DCTN5 (involved in intracellular transport). KORA expression profiles revealed a significant association of rs420259 with transcript levels of DCTN5 only (p-value: 5.27 x 10^{-15}), indicating the possible involvement of DCTN5 in the susceptibility to BD (Figure 36). Lower expression values were observed for individuals homozygous for the risk allele A of rs420259, indicating that lower expression of DCTN5 was associated with increased BD susceptibility. DCTN5 interacts with DISC-1, a gene implicated in susceptibility to BD and schizophrenia (Ozeki, Tomoda et al. 2003). The highly significant association of rs420259 with transcript levels of DCTN5 strengthens the hypothesis of DCTN5 as an interesting biological candidate for BD.

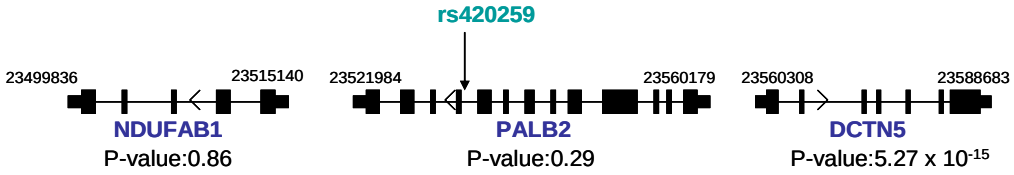

Figure 36-Significant association of rs420259 with expression levels of DCTN5: Expression profiles allowed prioritization of DCTN5 which was one of the three positional candidate genes identified in the GWAS of BD.

5.12.3 Testing for effects of cis and trans SNPs in the candidate genes

SNPs identified by GWAS are rarely the causal variants but might be in linkage disequilibrium with other causal SNPs which in turn might influence the expression of one or several transcripts. Furthermore there may be a subset of causal SNPs which might not be captured by GWAS due to statistical issues such as stringent multiple testing corrections applied. Therefore, in order to account for these, for the 264 transcripts from the above NHGRI list, the KORA cis and trans eQTL lists (from Chapter 5.11) were

inspected to search for cis and trans SNPs in the genome which influenced expression levels of the transcript.

As denoted in Figure 30, the SNPs significantly associated with the trait in published GWAS were termed “GWAS SNPs”, the GWAS SNPs significantly associated with the expression levels in the above subsection were termed “eSNPs” and cis/trans SNPs significantly associated with expression levels of the GWAS candidate genes in the KORA expression dataset were referred to as “cSNPs” and “tSNPs” in this section.

For 9 transcripts significant cSNPs were observed (Table 18). For 5 of these 9 transcripts no eSNPs were observed and for 4 of these 9 transcripts eSNPs were identified in the previous section. For B3GALT4, HLA-DRB1, KIAA1598, PTPN1 and SLC24A4 where no eSNPs were observed but only cSNPs were identified, no linkage disequilibrium information available for the SNPs hence it was difficult to draw conclusions.

For ORMDL3 and EXOC2 where both eSNPs and cSNPs were observed, the strength of association of the transcript for the eSNP and cSNP were comparable (similar p-values). For ORMDL3, there was high linkage disequilibrium between the cSNP and eSNP two SNPs ($R^2 = 0.87$) while for EXOC2 there was moderate linkage disequilibrium between the cSNP and eSNP two SNPs ($R^2 = 0.25$). For these SNPs, it could be hypothesized that the GWAS identified the functional variants.

For DCTN5 and IL18RAP where both eSNPs and cSNPs were observed, the strength of association of the transcripts with the cSNPs was much higher than that with the eSNP, hence it could be postulated that the cSNP and not the GWAS SNP might be the functional SNP (Figure 37).

In summary, for 24 out of 411 tested SNPs, possible functional SNPs were identified which significantly influenced the expression levels. These included 4 previously reported eSNPs, 11 novel eSNPs and 9 cSNPs. These results support the notion that SNPs associated with complex traits in GWAS might not be the functional SNPs and highlight the importance of expression profiles in providing evidence for functional variants. In this study, significant associations for those cases were revealed where the SNP directly influenced transcript levels of the genes, hence providing evidence for a causal mechanism. Obviously, more work is required to confirm the causal variant(s) and

gene(s) at each observed loci, but it is nevertheless informative to provide evidence on some of the likely functional candidate genes.

Table 18-Examples where expression profiles revealed cis SNPs to be significantly associated with transcript levels of GWAS candidate genes

Transcript	cis SNP	KORA cisSNP P-value	GWAS SNP	KORA eSNP P-value	LD, R^2	Complex trait	Reference
B3GALT4	rs462618	6.5×10^{-15}	rs2254287	>0.05	0.02	LDL cholesterol	Willer et al, 2008
HLA-DRB1	rs9272723	2.7×10^{-39}	rs2395148	>0.05	0	Juvenile arthritis	Behrens et al, 2008
KIAA1598	rs11598817	5.9×10^{-8}	rs4776472	>0.05	0	Heart failure	Larson et al, 2007
PTPN1	rs4602269	1.3×10^{-7}	rs17696736	>0.05	0	Type 1 diabetes	WTCCC, 2007
SLC24A4	rs4900132	3.4×10^{-7}	rs4904868	>0.05	0	Pigmentation	Sulem et al, 2007
ORMDL3	rs869402	6.8×10^{-8}	rs7216389	8.5×10^{-8}	0.87	Asthma	Moffat et al, 2007
EXOC2	rs6918152	4.3×10^{-7}	rs6918152	8×10^{-7}	0.25	Hair colour	Han et al, 2008
DCTN5	rs35635	9.2×10^{-23}	rs420259	5.2×10^{-15}	0.64	Bipolar disorder	WTCCC, 2007
IL18RAP	rs4851004	7.9×10^{-22}	rs917997	4×10^{-16}	0.29	Celiac disease	Hunt et al, 2008

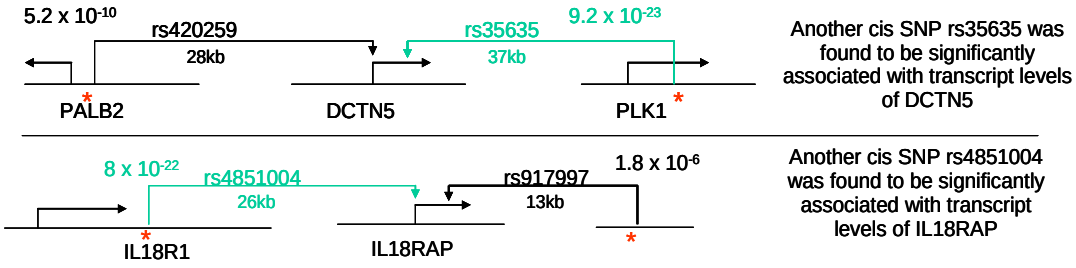

Figure 37-Examples where expression profiles uncovered possible functional variants unidentified by GWAS: Cis SNPs in the vicinity of the GWAS SNP were found to be significantly correlated with expression levels of DCTN5 and IL18RAP.

5.13 Use of gene expression to functionally validate GWAS candidate genes

Gene expression data can be used for functional validation of candidate genes identified in GWAS. In this context, the genome-wide expression profiles generated from the KORA individuals in this study helped to validate two candidate genes identified in independent GWAS for uric acid and mean platelet volume.

5.13.1 Functional validation of SLC2A9 influencing uric acid concentrations

A GWAS had been carried out in 1,644 individuals from the KORA F3 population. 335,152 high quality Affymetrix SNPs had been tested for associations with uric acid levels. A quantitative trait locus in a 500-kb region with high linkage disequilibrium had been identified, consisting of 40 autosomal SNPs. 26 of 40 significant SNPs (p-value<1.5 x 10^{-7}) mapped within the transporter gene SLC2A9. The strongest signals had been observed for SNPs in introns 4 and 6 of SLC2A9 (p-values: 3.39x 10^{-11} and 1.62 x 10^{-12}). Sequencing of all exons in 48 male and 48 female samples selected equally from the extremes of the serum uric acid distribution had resulted in the detection of two synonymous changes in exons 2 and 8 and two missense variants in exons 6 and 8.

To investigate the transcript levels of SLC2A isoforms in blood relative to serum uric acid concentrations, I analyzed genome-wide expression profiles from a subgroup of 117 KORA samples available then. It is known that alternative splicing of SLC2A9 results in two isoforms, each with differential targeting and tissue specificity.

Five probes present on the Illumina Sentrix WG6-v2 microarray were examined: two recognizing the two distinct isoforms of SLC2A9, one recognizing both isoforms, and two corresponding to the neighboring genes DRD5 and WDR1. The sample size was too small to show a significant genetic effect of SLC2A9 SNPs on intensity of transcription signals. However, the probe hybridizing to the SLC2A9 isoform 2 transcript showed a significant association with uric acid concentrations (Figure 38).

The uric acid variance explained by SLC2A9 expression levels was about 8% for isoform 2. For the isoform 2 of SLC2A9, gender-specific analyses showed a stronger association in women (p-value: 0.005; effect: 6.813) compared to men (p-value: 0.151; effect: 3.490).

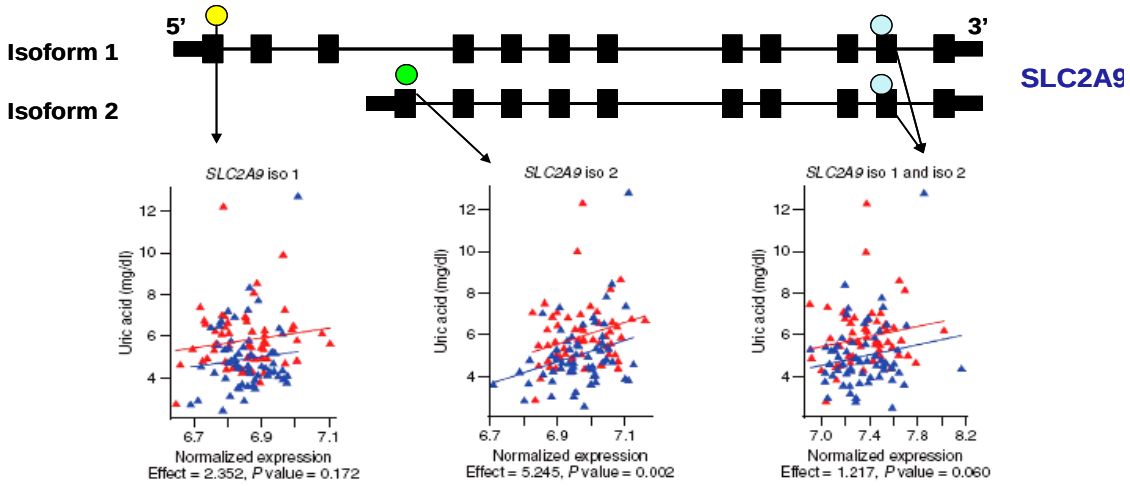

Figure 38-Isoform-specific gene expression analysis: One SLC2A9 probe was common to both isoforms (blue dots), while the other two probes were isoform-specific (yellow and green dot). Expression levels of SLC2A9 isoform 2 significantly correlated with urate levels, p-value of 0.002.

An association between SLC2A9 genotypes and urate concentrations and between SLC2A9 genotypes and gout was reported. The proportion of the variance of serum uric acid concentrations explained by genotypes was about 1.2% in men and 6% in women, and the percentage accounted for by expression levels was much higher; ranging from 3.5% in men and 15% in women (Doring, Gieger et al. 2008).

SLC2A9 is a predicted glucose as well as fructose transporter (Scheepers, Schmidt et al. 2005). Alternative splicing of SLC2A9 results in two proteins: GLUT9 and GLUT9ΔN, each exhibiting differential targeting and tissue specificity. GLUT9 is present in the proximal kidney cell membranes, liver, placenta, lung, leukocytes, chondrocytes and brain, while GLUT9ΔN is prominently expressed in the kidney in both humans and mice (Augustin, Carayannopoulos et al. 2004). The expression profiles generated in this study helped to focus on GLUT9ΔN and suggest a possible role of this protein in urate excretion.

5.13.2 Functional validation of WDR66 associated with MPV in a GWAS

A GWAS in the KORA F3 population had identified 3 SNPs strongly associated with mean platelet volume (MPV): rs7961894 within WDR66, rs12485738 upstream of ARHGEF3 and rs2138852 upstream of TAOK1. Together, the 3 loci accounted for 4-5% of MPV variance. Since the SNP in WDR66 accounted for 2.0% of the MPV variance, its coding sequence was analyzed in 382 samples. 20 new variants, a haplotype with 3 coding and 1 SNP at the transcription start site associated with MPV were found (p-value: 6.8×10^{-5}).

The strong correlation of the WDR66 SNP prompted an investigation of the transcript levels of WDR66 in 323 KORA expression profiles generated in this study. No association between SNP rs7961894 and WDR66 transcript level was observed, but a significant association of the levels of the WDR66 transcript with MPV was seen (p-value: 0.01, Figure 39) using the linear regression model. No correlations between gene expression and genotypes for the other 2 SNPs identified in the GWAS were observed. Based on the small samples size of expression profiles available, the analysis had limited power. The correlation of WDR66 expression with MPV supports the hypothesis that WDR66 is involved in the determination of MPV (Meisinger, Prokisch et al. 2009). Hence the expression profiles generated in this study allowed functional validation of two candidate genes: SLC6A9 associated with urate levels and WDR66 associated with MPV.

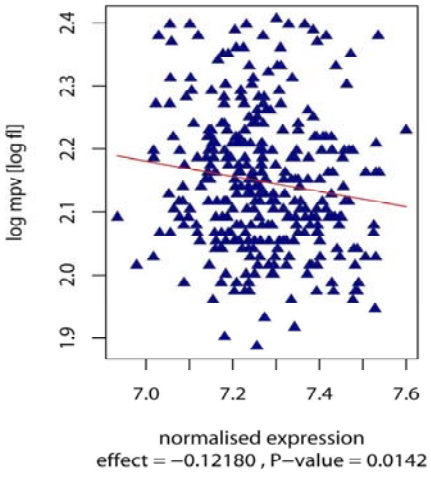

Figure 39-Association of mean platelet volume and expression of WDR66: KORA expression profiles showed a significant association of mean platelet volume with transcriptional profiles of WDR66.

5.14 Identification of novel regulatory pathway

Gene expression can allow inference of regulatory pathways and networks. Several studies have shown that it is feasible to infer signal transduction pathway activity, in individual samples, from gene expression data (Breslin, Krogh et al. 2005). Simple gene-gene interactions may provide evidence for gene clusters and aid in the discovery of new associations and complex biological pathways.

5.14.1 Use of expression profiles to identify IgE regulation pathway

A GWAS for IgE levels in the 1,530 KORA S3/F3 individuals followed by a replication in 3,890 KORA F4 individuals had revealed strong associations of rs2427837, located in the 5' region of FCER1A (α chain of the IgE high affinity receptor, p-value: 7.08×10^{-19}) (Weidinger, Gieger et al. 2008). Sequencing of all FCER1A exons with adjacent intronic sequences in 48 males and 48 females selected equally from the extremes of the serum IgE distribution had revealed two new mutations, each present in only one individual as well as confirmed 3 already annotated SNPs. None of the novel mutations were predicted to have functional consequences.

There is continuous cycling of the IgE receptor subunits from intracellular storage pools to the surface and there is substantial expression of the alpha subunit (FCER1A) after stimulation with IL-4 which requires de novo protein synthesis (Kraft and Kinet 2007). This induction is stimulated by the transcription factor GATA-1 which has a binding site in the putative promoter of FCER1A.The minor allele of rs2251746 was previously shown to be associated with higher FCER1A expression via enhanced GATA-1 binding (Hasegawa, Nishiyama et al. 2003).

Since expression of FCER1A requires IL-4 and transcription factor GATA-1, I decided to test for the known stimulation pathway using gene expression profiles generated in this study. Whole blood expression profiles of 320 KORA individuals showed a significant dependency of FCER1A expression on IL-4 expression (p-value: 0.0087) and GATA-1 expression (p-value: 1.4×10^{-4}), thereby confirming the known biological pathway. Moreover, a highly significant dependency of FCER1A expression on GATA-2 transcript levels was observed (Figure 40, p-value: 7.8×10^{-27}). This finding might indicate a novel regulatory mechanism of FCER1A expression via GATA-2 in whole blood.

GATA-1 is expressed in erythroid, megakaryocytic cells, mast cells and testis (Tsai, Martin et al. 1989), while GATA-2 is expressed in hematopoietic stem and progenitor cells, endothelial cells, central nervous system, placenta, fetal liver and fetal heart (Tsai, Keller et al. 1994; Orlic, Anderson et al. 1995). Despite the unique expression patterns of GATA-1 and GATA-2, substantial interplay exists between these two transcription factors. The extent of overlapping functional domains between GATA-1 and GATA-2 is so high that until now it has been very difficult to assign specific roles to the two genes (Grass, Boyer et al. 2003). The whole blood expression profiles indicate that GATA-2 gene might be involved in the regulatory pathway of IgE production (Weidinger, Gieger et al. 2008).

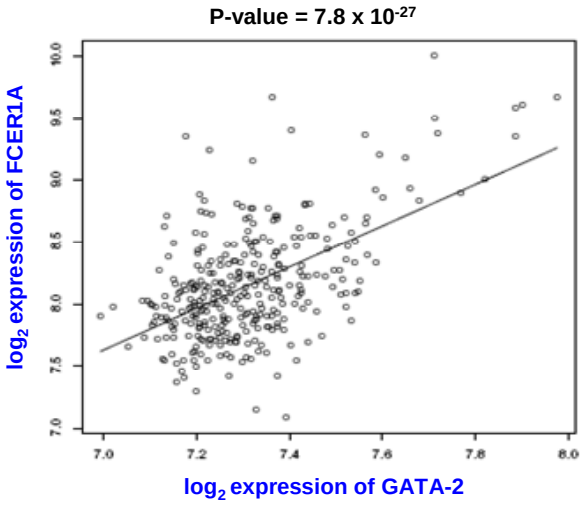

Figure 40-Dependency of FCER1A on GATA-2: Expression profiles revealed a highly significant dependency of FCER1A expression on GATA-2 expression in whole blood (p-value: 7.8 x 10^{-27}).

6.0 Discussion and conclusions

Natural variation in human gene expression has started to be explored only lately (Enard, Khaitovich et al. 2002). There is experimental evidence that gene expression levels in humans differ not only among diverse cell types within an individual but also between different individuals (Schadt, Monks et al. 2003). This observation resulted in investigation of gene expression as a quantitative phenotype. Genome-wide association studies (GWAS) have identified polymorphic genetic variants influencing gene expression levels (Morley, Molony et al. 2004). Most of the investigations of gene expression in humans performed so far have focused primarily on lymphoblast cell lines due to the limited availability of other cell types and tissues (Dermitzakis and Stranger 2006).

6.1 Advantages and disadvantages of using whole blood in transcriptomics

In this study genome-wide gene expression data was generated from whole blood. The key reason for using peripheral blood (whole blood) as a marker to pursue "blood transcriptomics" is that blood sampling is part of a routine physical examination and is easily accessible. Peripheral blood cells are advantageous because they share more than 80% of the transcriptome with nine tissues including brain, colon, heart, kidney, liver, lung, prostate, spleen and stomach (Liew, Ma et al. 2006). Blood cells function as transporters and mediators of immune response and coagulation, making whole blood a valuable resource for studying immune-related diseases. Furthermore, blood contacts and interacts with all human tissues, conveying bioactive molecules ranging from oxygen, nutrients, metabolites, cytokines and hormones (Mohr and Liew 2007).

The disadvantage of studying natural tissues such as whole blood is that they comprise of a multitude of different cell types which might be present in varying ratios and consequently result in a heterogeneous cell mixture. In general, gene expression assayed in humans may be under the influence of external factors, thereby generating noisy data which might interfere with results of genetic studies (Pritchard, Coil et al. 2006). The central question of whole blood transcriptomics is to address the value of using a mixture of cells versus a single cell type ((Dermitzakis and Stranger 2006; Goring, Curran et al. 2007).

In contrast to whole blood, lymphoblast cell lines (LCLs) have shown to be an accurate representation of the *in vivo* state (Dermitzakis and Stranger 2006). The existence of a single cell type reduces the range of factors influencing gene expression, thereby increasing the power for genetic investigations (Dermitzakis and Stranger 2006; Goring, Curran et al. 2007). The drawbacks of using LCLs are that gene expression in LCLs represents Epstein Barr Virus (EBV) infection of B-cells, which might affect the expression of some genes in an uncontrolled manner and influence certain biological processes, biasing the outcome of the analysis (Liu, Walter et al. 2006). LCLs may also exhibit extreme clonality with random patterns of monoallelic expression in single clones (Plagnol, Uz et al. 2008).

These are the several advantages and disadvantages of using different tissues and cell types for analysis of gene expression variation. The ultimate goal would to establish a large, comprehensive public resource of gene expression patterns across different tissues and across different human populations.

6.2 Establishment of the KORA gene expression dataset

In this study, genome-wide expression data from whole blood of 497 KORA individuals was generated, resulting in 497 x 48,701 data points. Low levels of population stratification in the KORA population have demonstrated it to be a valuable asset in association studies of complex diseases as well as pharmaco-genetic studies (Steffens, Lamina et al. 2006). In large datasets such as one established in this study, a major concern is that small systemic differences are capable of obscuring true associations being sought (WTCCC 2007). To ensure high quality gene expression data, quality control checks such as use of the Illumina BEADSTUDIO control summary reports and Bioanalyzer analysis of RNA integrity were applied to identify samples with low signal intensities on the microarray and/or degraded input RNA. Of 497 samples analyzed at start, 116 samples failing quality control filters were excluded from further analysis. The high correlation between the biological and technical replicates (0.96-0.99) indicated high reproducibility and robustness of the Illumina microarray procedures such as RNA extraction, amplification and hybridization.

Globin mRNA constitutes a significant portion of whole blood (~70% of whole blood mRNA). It has been suggested that globin mRNA might dilute messages from low

frequency cell populations such as lymphocytes and monocytes whilst masking other gene expression profiles, subsequently resulting in loss of low abundance transcripts. Affymetrix microarray platforms have incorporated the globin reduction step into their protocol, while for the Illumina microarray platforms this question was not adequately addressed. In this study, globin reduction was not carried out as the pilot experiment showed that this procedure introduced artifacts which altered gene expression in a non-systematic manner. Several studies confirmed these results and demonstrated that globin reduction resulted in loss of reproducibility at the cost of a slight increase in sensitivity (Liang, Li et al. 2006; Dumeaux, Borresen-Dale et al. 2008).

6.2.1 Use of the KORA dataset to measure variability of gene expression

Variation in transcript levels has been suggested to have a heritable component and can be measured using techniques such as microarrays (Cheung, Jen et al. 2003). The extent of this variation was investigated across the entire genome to identify genes whose transcript levels greatly differed among individuals and genes whose expression was stable among individuals. The overall variability across 13,701 transcripts in 381 individuals was low with a mean variance of 0.10 and median variance of 0.05 (ranging between 0.005-4.6). For several of the highest variable genes such as the highly polymorphic HLA-DRB1 locus and the Y-specific RPS4Y1 locus there is biological evidence of variation. HLA-DRB1 is a component of the major histocompatibilty complex. One of the hallmarks of the major histocompatibility complex is the high polymorphism and intralocus variability of its loci at the sequence level (Klein and Figueroa 1986). In this study the HLA-DRB1 was shown to be highly variable at the transcript level too. RPS4Y1 is located in the male-specific region of the Y chromosome and not in the pseudoautosomal region (Skaletsky, Kuroda-Kawaguchi et al. 2003). Since there were both males and females assayed in this study, it is not surprising that the male-specific gene RPS4Y1 emerged as one of the top variable gene since it differed between the two groups. For further genes such as DEFA1 and DEFA3 there is evidence of structural variation since they are known copy numbers variants (Ballana, Gonzalez et al. 2007). The least variable genes belonged to categories such as nucleic acid binding genes, transcription factors and cell junction genes. The least variable categories represent categories such as nucleic acid binding and transcription factors whose

functions are essential and hence the gene expression of transcripts belonging to this category is relatively stable. The highest variable genes belonged to classes of cytoskeletal genes, defense/immune genes, and signaling genes. The highest variable genes in unrelated individuals may reflect normal individual variation of gene expression (which might be due to genetic polymorphisms affecting gene expression) or may reflect various environmental exposures or biological processes.

6.2.2 Gender-specific gene expression signatures in the KORA dataset

Gender is one determinant of variation in physiology, morphology and disease susceptibility in humans (Whitney, Diehn et al. 2003). Many immunological and inflammatory diseases such as SLE and neuropsychiatric disorders such as depression and attention deficit hyperactivity have a striking gender bias in incidence and severity (Cutolo, Sulli et al. 1995; Verthelyi, Petri et al. 2001). The KORA gene expression profiles were employed to identify gender-specific gene expression signatures. The Welch's t-test (an adaptation of Student's t-test for two samples having possibly unequal variances) was used to search for genes whose expression differed significantly between male and female donors. 24 significantly different genes were identified, 18 of which were localized on the sex chromosomes. Y chromosomal genes were expected to differ between the genders while expression differences for X chromosomal genes between the two sexes indicate escape of X-inactivation. 8 of the 18 sex chromosome genes found to differ between the two genders in this study overlapped with gender-specific genes found in other studies in humans and mice (Whitney, Diehn et al. 2003; Vawter, Evans et al. 2004; Debey, Zander et al. 2006). None of the 6 autosomal genes associated with gender had been previously reported. The fact that only 6 genes differing between males and females were autosomal genes indicated that the two sexes did not differ greatly in gene expression levels in whole blood.

6.2.2.1 Establishment of a gender predictor

To assess whether gene expression differences were enough to classify men and women into distinct groups, a class-predictor was built using the gender-specific genes. The best predictor was obtained using the Y-specific RPS4Y1 gene, resulting in an accuracy of 95%. This predictor could not be improved by adding the other 23 gender-specific genes.

Gender prediction may serve as a quality control to check for sample mixing. For individuals whose gene expression levels for the gender-specific genes do not correspond to others of the same gender, caution must be taken. Theoretically, gender misclassified individuals can be excluded for downstream analysis. For the RPSY41 predictor, men and women showed a threshold-effect of RPS4Y1 expression and the misclassified individuals exhibited intermediate expression levels of RPS4Y1, thereby confirming that there was no experimental sample mixing. The possibility of sex reversal in individuals who were gender misclassified cannot be ruled out.

Previously a class predictor was built from peripheral blood mononuclear cells , based on 3 sex chromosomal genes, resulting in a 86% accuracy (Debey, Zander et al. 2006). The whole blood gender-prediction described here proceeded in a prediction accuracy of 95%, demonstrating the power of this approach to detect gender-specific changes.

To question whether males and females could be classified using non-gonadal gene expression, another predictor was built using the transcriptional profiles of the 6 gender-specific autosomal genes, resulting in a prediction rate of 74% accuracy. So far, to my knowledge, no report of gender determination using autosomal gene expression profiles has been described.

6.3 Age -specific gene expression signatures in the KORA dataset

Gene expression levels in many organisms change during the aging process and the advent of microarrays has allowed genome-wide patterns of transcriptional changes associated with aging to be studied in both model organisms and various human tissues (Hekimi and Guarente 2003; Fraser, Khaitovich et al. 2005). Identification of age-related genes might contribute towards the better understanding of molecular process of aging as well as help comprehend age-related disorders such as neurodegenerative diseases.

Within a cohort age range of 50-83 years in this study, 11 transcripts were found to be significantly associated with age using a linear regression model. Ten of these showed a negative correlation in age, while only VNN 3 showed a positive correlation with age. While there was no evidence of biological significance for ten of the age-specific genes, VNN3 had been reported to show a 2-6 fold inducible expression on stress induction (Berruyer, Martin et al. 2004). VNN3 is a member of the vanin family of proteins whose

exact function is not known. One study reported that vanin proteins possess pantotheinase activity, which may play a role in processes pertaining to tissue repair in the context of oxidative stress (Bomprezzi, Ringner et al. 2003). This is a noteworthy finding, considering the long known free radical theory providing genetic support between mechanisms of oxidative stress and ageing (Weedon, Lango et al. 2008). The free radical theory of aging holds that aging is at least in part due to deleterious side effects of aerobic respiration (Harman 1956). Specifically, mitochondrial activity leading to the production of reactive oxygen species (ROS) could damage many cellular components, including DNA, lipids, and proteins (Weedon, Lango et al. 2008). The free radical theory has gained widespread support from studies in a plethora of model organisms showing that decreasing ROS levels leads to an increase in lifespan indicate that ROS can strongly modulate the aging process (Hekimi and Guarente 2003). The positive correlation between VNN3 expression and age observed in this study could suggest an increase in ROS with an increase in age.

Since age-specific genes were identified, the question was whether these could be used to predict the age of an individual. Using the eleven age- specific gene signatures, an age-predictor was built to predict the age of the donors. For 25% of individuals, the difference between the real and predicted age was less than 2.5 years, for 50% of the people the difference was between 2.5-8 years and for the remaining 25% of individuals the difference was more than 8 years. Other age predictors built on human teeth resulted in a mean error of 5 years with confidence intervals ranging from 7-14 years in one study and resulted in a predictive success of +/- 5 years in about 45-48% of cases in another study The ages of the studied individuals ranged from 13-76 years in both studies (Drusini, Calliari et al. 1991; Tramini, Bonnet et al. 2001).

Age prediction might reflect the biological age rather than the chronological age of the individuals studied. Furthermore, if the survival times of the surveyed individuals will be known in the near future, then the human survival data could be matched with gene expression profiles to predict longevity. Despite the interesting prospects of this work, the power of this study to detect age-related gene-expression patterns was limited due to the narrow age range of the sampled individuals (50-83 years). It would be interesting to apply this age-predictor to larger sample sizes with broader age ranges.

6.4 Identification of cis and trans eQTLs

Genetic variants influencing gene expression in whole blood were assessed in this report. Of 371 identified eQTLs, 77% were cis eQTLs while only 23% were trans eQTLs, an observation consistent with previous reports showing that a major portion of regulatory variation was attributable to cis regulation (Schadt, Monks et al. 2003; Morley, Molony et al. 2004). Identification of fewer trans eQTLs is probably due to the fact that trans effects are more indirect and therefore are usually weaker effects, requiring a larger cohort with substantial power for detection (Stranger, Nica et al. 2007). For the KORA eQTLs identified in this study, since only whole blood was interrogated, variation manifested only in other cell types is not represented.

Despite differences between LCLs and whole blood, comparisons of the KORA with HapMap (Stranger, Forrest et al. 2007) showed an overlap ~35% of eQTLs (32% cis and 3% of trans eQTLs). The larger overlap of cis eQTLs is in concordance with previous reports that cis regulation was stable and consistent across different cell types and tissues (Hubner, Wallace et al. 2005). The lesser extent of overlap of trans eQTLs is due to the HapMap study design where the authors had selected only 25,000 putative functional SNPs for their trans analyses. An overlap of >30% of eQTLs between different tissues including adipose, LCLs, whole blood and liver has been previously demonstrated and confirmed in this study (Stranger, Forrest et al. 2007; Emilsson, Thorleifsson et al. 2008). The remaining 70% of the unshared fraction reflects the whole blood specific regulatory variation. Of the overlapping eQTLs, > 97% exhibited allelic effects in the same direction in both populations thereby demonstrating robust replication across the two populations despite the small sample sizes surveyed. A further 2% of overlapping eQTLs showing discordant direction of the allelic effect could be explained by differential allele frequencies across the KORA and HapMap. Taken together, this amounted to a > 99% replication of the overlapping eQTLs between KORA and HapMap and a <1% false discovery rate. Such a large extent of overlap in the replicated eQTLs provides confidence in the signals detected in this study.

Different studies use different definitions of cis-windows (100kb, 500kb, 1Mb), various multiple testing methods (ranging from the stringent Bonferroni to the not so stringent

FDR 5% to a computationally challenging Permutation method) and different statistical tools (linear regression, ANOVA) to analyze eQTLs, making comparisons across experiments difficult (Table 19). The larger the sample sizes and the greater the number of transcripts and SNPs analyzed, the higher is the power of the GWAS to detect genetic association. Simultaneously, the more tests performed, the higher the chance of false positives and the greater is the requirement to correct for multiple testing. The definition of the cis-window plays a vital role in determination of significant cis eQTLs. For larger cis-windows, more SNPs per transcript are tested and more stringent multiple testing corrections are required. In this study a cis interval of 100 kb was used since previous studies have shown that 90% of the cis SNPs are located within 100kb from the gene (Stranger, Forrest et al. 2007; Emilsson, Thorleifsson et al. 2008). Guidelines to define statistical interpretation of GWAS and publicly available datasets such as the HapMap and the 1000 Genomes project are required to make comparisons of data across different studies possible. Integration of eQTLs with next generation sequencing, metabolomic and proteomic analyses, epigenomic and functional studies may be a powerful tool for a systems biology approach to aid discovery of susceptibility loci (Schadt and Lum 2006).

Table 19-Different criteria used in published GWAS

Author	Date	Criteria used to define the cis interval up/downstream	Expression Platform	Number of transcripts (filtered)	Genotyping Platform (Number of SNPs)	Multiple Testing correction	Tissue (Sample Size)
Cheung et al.	2005	**50 kb** from gene boundaries	Affy Genome Focus Array	1000	HapMap release 14 770,394	Sidak	LCL 57
Stranger et al.	2005	**I Mb** from the midpoint of the gene	Custom Illumina	630 (374)	HapMap version 16b 753712	Bonferroni,FDR 5%, Permutation	LCL 60
Dixon et al.	2007	**100 kb** from gene boundaries	Affy HG-U133 Plus2.0	54675 (20599)	Illumina Sentrix Human-1 109157, 299116	Bonferroni	LCL 400
Spielman et al.	2007	**500 kb** of Transcriptional start site + 500 kb of 3' end of gene	Affy Genome Focus Array	8500 (4197)	HapMap release 19 2.2 million	Sidak	LCL 142
Stranger et al.	2007	**1 Mb** from probe midpoint. Genes>500kb, TSS used as midpoint	Illumina WG-6 v1	47294 (13643)	HapMap Phase II 2.2 million	0.001 Permutation threshold	LCL 270
Myers et al.	2007	**1 Mb** from 3' and 5' gene end	Illumina RefSeq8	24357 (14078)	Affy 500k 336140	0.001 Permutation threshold	Brain 193
Stranger et al.	2007	**1 Mb** from probe midpoint	Illumina WG-6 v1	47294 (14925)	HapMap Phase I 4358638	0.001 Permutation threshold	LCL 210
Kwan et al.	2008	**50 kb** from gene boundaries	Affy Exon 1.0 ST array	17897	HapMap Phase II 244029	FDR 5%	LCL 57
Emilsson et al.	2008	**1 Mb** from probe midpoint	Agilent Custom array	23720	Custom array 1732	FDR 5%	Adipose Blood 673, 1002
Goering et al.	2008	deCODE genetic map- **linear interpolation** to place markers based on physical location	Illumina WG-6 v1	47294 (20413)	Research Genetics Human Map Set v 6 & 8 432	FDR 5%	LCL 1240
Schadt et al.	2008	**I Mb** of TSS of gene	Agilent custom array	39280	Affy 500k, Illumina 650Y 782476	Bonferroni, FDR 5%	Liver 400
Mehta et al.	2009	**100 kb** from probe boundaries	Illumina WG-6 v2	48,701 (13767)	Affy 500k 335,152	Bonferroni	Blood 381

6.5 Use of the KORA gene expression resource to identify novel eSNPs

Genome-wide association studies have identified novel susceptibility loci across a wide spectrum of diseases ranging from cardiac diseases, age-related macular degeneration, obesity and diabetes (Skaletsky, Kuroda-Kawaguchi et al. 2003; Edwards, Ritter et al. 2005; Reiman, Webster et al. 2007). There is still a substantial gap between SNP associations from a GWAS and understanding how the locus contributes to the disease. In most of the published genetic association studies, there is no experimental evidence supporting the putative functional roles of given candidate genes in disease onset or progression (Schadt, Molony et al. 2008). The combination of GWAS and measurement of global gene expression allows mapping of genetic factors that underpin individual differences in quantitative levels of expression of many transcripts (Schadt, Lamb et al. 2005). The utility of gene expression to complement several genome-wide association results was demonstrated in this study.

Using the National Institutes of Health database of Catalog of Published Genome-Wide Association Studies (http://www.genome.gov), a list of 411 GWAS identified SNPs (corresponding to 264 transcripts) associated with complex traits such as cancer, diabetes, celiac disease and pigmentation was compiled. Testing of these SNPs with expression profiles of neighboring genes (i.e. testing for eSNPs) using the gene expression data from 381 KORA individuals and publicly available gene expression data from 60 HapMap individuals, revealed 15 eSNPs (4 already reported, 11 new).

For example, a meta-analysis of genome-wide expression data identified 6 novel susceptibility loci for type 2 diabetes (Zeggini, Scott et al. 2008). The strongest signals were for rs864745 in intron 1 of JAZF1 (p-value: 5×10^{-14}) and rs12779790, located ~63.5 kb from CAMK1D (p-value: 1.2×10^{-10}). Using gene expression data generated in this study, significant associations between rs864745 and JAZF1expression (p-value: 0.001) and rs12779790 and CAMK1D expression (p-value: 4.68×10^{-5}) were observed. Individuals homozygous for the risk alleles T and G for JAZF1 and CAM1KD respectively, exhibited elevated expression levels of the corresponding transcripts. Hence, it could be hypothesized that increased expression levels of CAM1KD and JAZF1 were associated with increased susceptibility towards type 2 diabetes.

To investigate for possible causal SNPs other than the GWAS reported SNPs, the KORA eQTL lists were probed to check if there were any cis or trans SNPs influencing the expression levels for the 264 candidate genes in the list. 9 cis SNPs were found to significantly influence transcriptional profiles of the genes.

In summary, for 15 of the 411 tested SNPs, possible functional SNPs were identified which were significantly associated with expression levels. This confirms that the GWAS identified the functional SNPs in these instances. Expression profiles allowed functional validation for those candidate genes where eSNPs were identified. The discovery of the 9 cis SNPs influencing expression levels of the candidate genes indicates that the GWAS might have not captured the functional SNP.

It has been demonstrated here that functional validation of candidate genes using gene expression profiles provides a more objective view into the role of the gene in a given phenotype-associated region. Assaying gene expression and genetic variation simultaneously in a large number of samples can be a powerful tool for unraveling the function of previously mapped susceptibility alleles underlying common complex diseases.

6.6 Functional validation of SLC2A9

Gene expression can be used as a tool to prioritize candidate genes identified in a genetic study in terms of functional validation (Goring, Curran et al. 2007). In this context, the KORA whole blood gene expression dataset was used to test a candidate gene, SLC2A9, which had been detected in a genome-wide association study to identify pathways in regulation of uric acid concentration. SLC2A9 is a predicted fructose and glucose transporter (Li, Sanna et al. 2007). Investigation of transcript levels of SLC2A9 isoforms in blood relative to serum uric acid concentrations resulted in identification of significant association of the SLC2A9 isoform 2 expression levels with uric acid concentrations (p-value: 0.002) .

The expression studies helped to focus the association signals to a specific isoform. SLC2A9 isoform 1 is expressed in several tissues such as kidney, placenta, liver, lung, leukocytes, chrondrocytes and brain, while SLC2A9 isoform 2 is prominently expressed in the kidney in both humans and mice (Augustin, Carayannopoulos et al. 2004) (Figure

41). Both isoforms are equally and sizably expressed in whole blood. The significant association with the shorter protein argues for a prominent role of the SLC2A9 isoform 2 in uric acid excretion in the kidney.

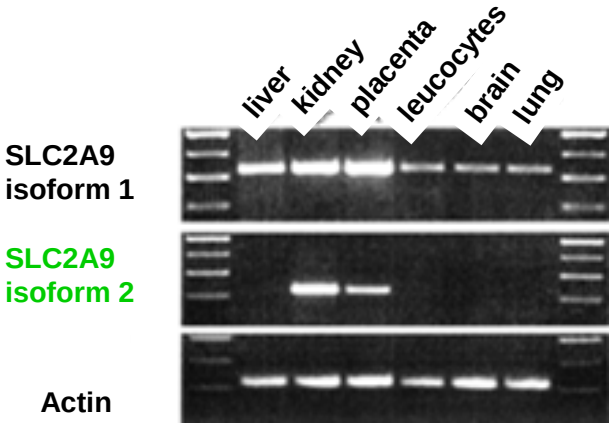

Figure 41-Expression of the two SLC2A9 isoforms: Isoform 2 of SLC2A9 is predominantly expressed in the kidney, thereby suggesting that this isoform might be involved in urate excretion via the kidney (Figure taken from Augustin et al. 2004).

The proportion of the variance of serum uric acid concentrations explained by expression levels was much higher than that explained by genotypes: 3.5% in men and 15% in women for expression, 1.2% in men and 6% in women for genotypes. The higher accountability of variance of serum urate levels in women is an interesting observation considering an early report in 1967, demonstrating a significant genetic component in the control of serum uric acid only among female twins (Boyle, Greig et al. 1967).

At the time this study was published, Vitart and colleagues too identified significant associations between SLC2A9 locus and urate levels in different populations (Vitart, Rudan et al. 2008). In their study, the authors assayed transporter activity in *Xenopus laevis* oocytes and demonstrated a 31-fold higher urate uptake by SLC2A9- expressing versus control oocytes. Furthermore, urate uptake was sevenfold higher for SLC2A9-expressing oocytes versus known urate transporter URAT1- expressing oocytes. It has been shown by others that URAT1 is potentially involved in 50% of urate reabsorption from glomerular filtrate by proximal tubules (Enomoto and Endou 2005). The results of Vitart and colleagues suggest that SLC2A9 may also contribute to this process.

A recent study demonstrated that urate is transported by SLC2A9 45-to 60-fold faster than glucose (Caulfield, Munroe et al. 2008). The identification of SLC2A9 as a high capacity urate transporter will facilitate production of new drug targets to lower uric acid levels in a range of conditions such as hyperuricemia, Lesch-Nyhan syndrome, gout and diabetes.

6.7 Genome-wide association studies - caveats and future perspectives

One major caveat of the design of genome-wide association studies is whether it is powerful enough to detect effects of both rare and common variants contributing to the trait of interest. It is a challenging task to collect large cohorts of well-characterized phenotypic quality and establish human panels of sufficient sizes with homogeneous allele frequencies and linkage disequilibrium patterns. These difficulties have been illustrated in the work of Reich et al, 2005 on multiple sclerosis, where an association on chromosome 1 in African-Americans could not be replicated in another sample of Afro-Caribbeans (Reich, Patterson et al. 2005).

Potential reasons for lack of reproducibility of association data could be:

- The association could be a false-positive association and hence cannot be replicated
- It could be a true association which cannot be replicated due to an underpowered follow-up study (essentially a false negative)
- A true association in one population which may not be true in another population due to genetic heterogeneity or different environmental background

Hence, caution must be exhibited when interpreting the results of a genetic association study. Significance thresholds in the order of $P<10^{-6}$ have been proposed for genome-wide association studies to rigorously account for the multiple tests performed in the course of the study (Dahlman, Eaves et al. 2002). GWAS findings that have not reached genome-wide significance may be genuine associations and could perhaps be uncovered by meta-analysis or SNP imputation (Zeggini, Scott et al. 2008).

There is a limit to how large population-based studies can get and there may be a class of variants that are too rare to be captured by GWAS but are not sufficiently high risk to be captured by population-based studies (Cambien and Tiret 2007). New approaches such as next generation sequencing technologies and bioinformatics methods might prove useful

in identification of these rare variants. For GWAS, larger sample sizes need to be used, biases should be taken into account, multiple-testing issues must be addressed and replication studies need to be carried out to allow a statistically powered yet economical experimental design (Newton-Cheh and Hirschhorn 2005; Wang, Barratt et al. 2005). To cite Mark Iles "The successes in finding common variants associated with common diseases are encouraging, but, as our findings show, we cannot yet be sure whether the common disease-associated variants found so far represent the tip of the iceberg or the bottom of the barrel"(Iles 2008).

6.8 Value of gene expression data

GWAS have identified susceptibility loci influencing a wide range of complex traits. Based on literature and available annotations of genes in the vicinity of SNPs, authors postulate the potential causal gene and its biological relevance to the trait. Majority of the SNPs identified by GWAS so far are intronic or in intergenic regions with unknown functionality. The challenge is the interpretation of GWAS results and confident assignment of the true causal variant(s). Although statistical approaches provide a robust assessment of significant observed association signals, functional data further supports and complements the initial hypotheses by providing a direct evaluation of biological processes. This highlights the need for further functional studies to pinpoint the causal variants and affected genes to aid the transition from candidate gene identification to translational progress.

Regulatory variation plays a key role in determining human phenotypic variation and is known to influence disease susceptibility. Integration of gene expression data with genotypic data allows prioritization of positional candidate genes, thereby providing a functional handle allowing a deeper understanding on the etiology of complex traits.

For transcriptomics, it would be ideal to study gene expression in the affected tissue such as brain in cases of neurodegenerative disorders or heart in case of cardiovascular diseases. Obtaining diseases tissue samples are subject to several ethical, legal and social issues. Post-mortem samples from tissues might retain their RNA quality and intact histological architecture but might be affected by gene expression changes accompanying death. Since obtaining such tissues might not be feasible, whole blood acts as a good

surrogate for baseline investigation of gene expression profiles. If gene expression signatures observed in other tissues such as brain, heart, muscle, liver, lung etc are also detected in whole blood; this would allow easy and quick analysis of expression profiles as a part of routine blood sampling.

National Institutes of Health (NIH) has only recently proposed an ambitious Genotype-Tissue Expression (GTEx) project, a database that will include expression analysis from 30 different tissues in 1,000 samples. Currently, this project is running in its 2-year pilot phase with a primary goal of testing the feasibility of collecting high-quality RNA and DNA from multiple tissues from 160 donors identified through low post-mortem autopsy or organ transplant.

In this study, the value of whole blood transcriptomics to address the usefulness of using a mixture versus a single cell type has been demonstrated. The KORA expression profiles generated in this study allowed functional validation of 2 candidate genes SLC2A9 isoform 2 and WDR66, identified in independent GWAS for serum uric acid levels and mean platelet volume respectively (Doring, Gieger et al. 2008; Meisinger, Prokisch et al. 2009). The expression profiles helped unravel a possible novel pathway of IgE regulation via transcription factor GATA-2 in whole blood (Weidinger, Gieger et al. 2008). Using whole blood expression profiles gender-specific profiles, age-specific signatures and eQTLs were observed. Identification of novel whole blood eQTLs not observed in other tissues highlights the power of using whole blood for expression analysis. Integration of gene expression generated in this study with available genotypic information allowed discovery of novel eSNPs, thereby uncovering the effects of variation in transcription on disease. The data presented here strongly suggest that to uncover tissue-specific expression profiles, it is essential to investigate gene expression in a multitude of different tissues and cells in the hope that we will discover as much of the regulatory variation as achievable.

7.0 Bibliography

Alizadeh, A. A., M. B. Eisen, et al. (2000). "Distinct types of diffuse large B-cell lymphoma identified by gene expression profiling." Nature **403**(6769): 503-11.

Allen, A. M. (1978). "Epidemiologic methods in dermatology, part 1: describing the occurrence of disease in human populations." Int J Dermatol **17**(3): 186-93.

Arking, D. E., A. Pfeufer, et al. (2006). "A common genetic variant in the NOS1 regulator NOS1AP modulates cardiac repolarization." Nat Genet **38**(6): 644-51.

Augustin, R., M. O. Carayannopoulos, et al. (2004). "Identification and characterization of human glucose transporter-like protein-9 (GLUT9): alternative splicing alters trafficking." J Biol Chem **279**(16): 16229-36.

Ballana, E., J. R. Gonzalez, et al. (2007). "Inter-population variability of DEFA3 gene absence: correlation with haplotype structure and population variability." BMC Genomics **8**: 14.

Baron, D., R. Houlgatte, et al. (2005). "Large-scale temporal gene expression profiling during gonadal differentiation and early gametogenesis in rainbow trout." Biol Reprod **73**(5): 959-66.

Berruyer, C., F. M. Martin, et al. (2004). "Vanin-1-/- mice exhibit a glutathione-mediated tissue resistance to oxidative stress." Mol Cell Biol **24**(16): 7214-24.

Bibikova, M., D. Talantov, et al. (2004). "Quantitative gene expression profiling in formalin-fixed, paraffin-embedded tissues using universal bead arrays." Am J Pathol **165**(5): 1799-807.

Bird, A. (2002). "DNA methylation patterns and epigenetic memory." Genes Dev **16**(1): 6-21.

Bomprezzi, R., M. Ringner, et al. (2003). "Gene expression profile in multiple sclerosis patients and healthy controls: identifying pathways relevant to disease." Hum Mol Genet **12**(17): 2191-9.

Bosserhoff, A. K., A. Hauschild, et al. (2000). "Elevated MIA serum levels are of relevance for management of metastasized malignant melanomas: results of a German multicenter study." J Invest Dermatol **114**(2): 395-6.

Botstein, D. and N. Risch (2003). "Discovering genotypes underlying human phenotypes: past successes for mendelian disease, future approaches for complex disease." Nat Genet **33 Suppl**: 228-37.

Botstein, D., R. L. White, et al. (1980). "Construction of a genetic linkage map in man using restriction fragment length polymorphisms." Am J Hum Genet **32**(3): 314-31.

Bouman, A., M. J. Heineman, et al. (2005). "Sex hormones and the immune response in humans." Hum Reprod Update **11**(4): 411-23.

Bourgain, C., E. Genin, et al. (2007). "Are genome-wide association studies all that we need to dissect the genetic component of complex human diseases?" Eur J Hum Genet **15**(3): 260-3.

Boyle, J. A., W. R. Greig, et al. (1967). "Relative roles of genetic and environmental factors in the control of serum uric acid levels in normouricaemic subjects." Ann Rheum Dis **26**(3): 234-8.

Brem, R. B., G. Yvert, et al. (2002). "Genetic dissection of transcriptional regulation in budding yeast." Science **296**(5568): 752-5.

Breslin, T., M. Krogh, et al. (2005). "Signal transduction pathway profiling of individual tumor samples." BMC Bioinformatics **6**: 163.
Butler, J. E. and J. T. Kadonaga (2002). "The RNA polymerase II core promoter: a key component in the regulation of gene expression." Genes Dev **16**(20): 2583-92.
Bystrykh, L., E. Weersing, et al. (2005). "Uncovering regulatory pathways that affect hematopoietic stem cell function using 'genetical genomics'." Nat Genet **37**(3): 225-32.
Cambien, F. and L. Tiret (2007). "Genetics of cardiovascular diseases: from single mutations to the whole genome." Circulation **116**(15): 1714-24.
Carmo-Fonseca, M. (2007). "How genes find their way inside the cell nucleus." J Cell Biol **179**(6): 1093-4.
Caulfield, M. J., P. B. Munroe, et al. (2008). "SLC2A9 is a high-capacity urate transporter in humans." PLoS Med **5**(10): e197.
Chabot, A., R. A. Shrit, et al. (2007). "Using reporter gene assays to identify cis regulatory differences between humans and chimpanzees." Genetics **176**(4): 2069-76.
Cheung, V. G., L. K. Conlin, et al. (2003). "Natural variation in human gene expression assessed in lymphoblastoid cells." Nat Genet **33**(3): 422-5.
Cheung, V. G., K. Y. Jen, et al. (2003). "Genetics of quantitative variation in human gene expression." Cold Spring Harb Symp Quant Biol **68**: 403-7.
Cho, R. J. and M. J. Campbell (2000). "Transcription, genomes, function." Trends Genet **16**(9): 409-15.
Crick, F. (1970). "Central dogma of molecular biology." Nature **227**(5258): 561-3.
Cutolo, M., A. Sulli, et al. (1995). "Estrogens, the immune response and autoimmunity." Clin Exp Rheumatol **13**(2): 217-26.
Dahlman, I., I. A. Eaves, et al. (2002). "Parameters for reliable results in genetic association studies in common disease." Nat Genet **30**(2): 149-50.
Dausset, J., H. Cann, et al. (1990). "Centre d'etude du polymorphisme humain (CEPH): collaborative genetic mapping of the human genome." Genomics **6**(3): 575-7.
de Bakker, P. I., M. A. Ferreira, et al. (2008). "Practical aspects of imputation-driven meta-analysis of genome-wide association studies." Hum Mol Genet **17**(R2): R122-8.
Debey, S., T. Zander, et al. (2006). "A highly standardized, robust, and cost-effective method for genome-wide transcriptome analysis of peripheral blood applicable to large-scale clinical trials." Genomics **87**(5): 653-64.
Dekel, B. (2003). "Profiling gene expression in kidney development." Nephron Exp Nephrol **95**(1): e1-6.
Dermitzakis, E. T. and B. E. Stranger (2006). "Genetic variation in human gene expression." Mamm Genome **17**(6): 503-8.
Deutsch, S., R. Lyle, et al. (2005). "Gene expression variation and expression quantitative trait mapping of human chromosome 21 genes." Hum Mol Genet **14**(23): 3741-9.
Devlin, B. and K. Roeder (1999). "Genomic control for association studies." Biometrics **55**(4): 997-1004.
Dixon, A. L., L. Liang, et al. (2007). "A genome-wide association study of global gene expression." Nat Genet **39**(10): 1202-7.

Doring, A., C. Gieger, et al. (2008). "SLC2A9 influences uric acid concentrations with pronounced sex-specific effects." Nat Genet **40**(4): 430-6.
Drusini, A., I. Calliari, et al. (1991). "Root dentine transparency: age determination of human teeth using computerized densitometric analysis." Am J Phys Anthropol **85**(1): 25-30.
Dumeaux, V., A. L. Borresen-Dale, et al. (2008). "Gene expression analyses in breast cancer epidemiology: the Norwegian Women and Cancer postgenome cohort study." Breast Cancer Res **10**(1): R13.
Edwards, A. O., R. Ritter, 3rd, et al. (2005). "Complement factor H polymorphism and age-related macular degeneration." Science **308**(5720): 421-4.
Elston, R. C. (1998). "Linkage and association." Genet Epidemiol **15**(6): 565-76.
Emilsson, V., G. Thorleifsson, et al. (2008). "Genetics of gene expression and its effect on disease." Nature **452**(7186): 423-8.
Enard, W., P. Khaitovich, et al. (2002). "Intra- and interspecific variation in primate gene expression patterns." Science **296**(5566): 340-3.
Enomoto, A. and H. Endou (2005). "Roles of organic anion transporters (OATs) and a urate transporter (URAT1) in the pathophysiology of human disease." Clin Exp Nephrol **9**(3): 195-205.
Felsenfeld, G. (2003). "Quantitative approaches to problems of eukaryotic gene expression." Biophys Chem **100**(1-3): 607-13.
Field, L. L., V. Bonnevie-Nielsen, et al. (2005). "OAS1 splice site polymorphism controlling antiviral enzyme activity influences susceptibility to type 1 diabetes." Diabetes **54**(5): 1588-91.
Fisher, R. A., F. R. Immer, et al. (1932). "The Genetical Interpretation of Statistics of the Third Degree in the Study of Quantitative Inheritance." Genetics **17**(2): 107-24.
FitzPatrick, D. R., J. Ramsay, et al. (2002). "Transcriptome analysis of human autosomal trisomy." Hum Mol Genet **11**(26): 3249-56.
Fraser, H. B., P. Khaitovich, et al. (2005). "Aging and gene expression in the primate brain." PLoS Biol **3**(9): e274.
Frayling, T. M. (2007). "Genome-wide association studies provide new insights into type 2 diabetes aetiology." Nat Rev Genet **8**(9): 657-62.
Frey, B. J., N. Mohammad, et al. (2005). "Genome-wide analysis of mouse transcripts using exon microarrays and factor graphs." Nat Genet **37**(9): 991-6.
Fung, H. C., S. Scholz, et al. (2006). "Genome-wide genotyping in Parkinson's disease and neurologically normal controls: first stage analysis and public release of data." Lancet Neurol **5**(11): 911-6.
Gabriel, S. B., S. F. Schaffner, et al. (2002). "The structure of haplotype blocks in the human genome." Science **296**(5576): 2225-9.
Gardina, P. J., T. A. Clark, et al. (2006). "Alternative splicing and differential gene expression in colon cancer detected by a whole genome exon array." BMC Genomics **7**: 325.
Giordano, M., M. Godi, et al. (2008). "A functional common polymorphism in the vitamin D-responsive element of the GH1 promoter contributes to isolated growth hormone deficiency." J Clin Endocrinol Metab **93**(3): 1005-12.

Golub, T. R., D. K. Slonim, et al. (1999). "Molecular classification of cancer: class discovery and class prediction by gene expression monitoring." Science **286**(5439): 531-7.
Goring, H. H., J. E. Curran, et al. (2007). "Discovery of expression QTLs using large-scale transcriptional profiling in human lymphocytes." Nat Genet **39**(10): 1208-16.
Grapes, L., M. Z. Firat, et al. (2006). "Optimal haplotype structure for linkage disequilibrium-based fine mapping of quantitative trait loci using identity by descent." Genetics **172**(3): 1955-65.
Grass, J. A., M. E. Boyer, et al. (2003). "GATA-1-dependent transcriptional repression of GATA-2 via disruption of positive autoregulation and domain-wide chromatin remodeling." Proc Natl Acad Sci U S A **100**(15): 8811-6.
Gros, F., H. Hiatt, et al. (1961). "Unstable ribonucleic acid revealed by pulse labelling of Escherichia coli." Nature **190**: 581-5.
Halperin, E., G. Kimmel, et al. (2005). "Tag SNP selection in genotype data for maximizing SNP prediction accuracy." Bioinformatics **21 Suppl 1**: i195-203.
Hamer, D. and L. Sirota (2000). "Beware the chopsticks gene." Mol Psychiatry **5**(1): 11-3.
Harman, D. (1956). "Aging: a theory based on free radical and radiation chemistry." J Gerontol **11**(3): 298-300.
Harris, H. (1970). "The expression of genetic information by somatic cell nuclei." J Gen Microbiol **63**(3): vi.
Hasegawa, M., C. Nishiyama, et al. (2003). "A novel -66T/C polymorphism in Fc epsilon RI alpha-chain promoter affecting the transcription activity: possible relationship to allergic diseases." J Immunol **171**(4): 1927-33.
Heap, G. A., G. Trynka, et al. (2009). "Complex nature of SNP genotype effects on gene expression in primary human leucocytes." BMC Med Genomics **2**: 1.
Hekimi, S. and L. Guarente (2003). "Genetics and the specificity of the aging process." Science **299**(5611): 1351-4.
Hemminki, K., A. Forsti, et al. (2008). "The 'common disease-common variant' hypothesis and familial risks." PLoS ONE **3**(6): e2504.
Hirschhorn, J. N., K. Lohmueller, et al. (2002). "A comprehensive review of genetic association studies." Genet Med **4**(2): 45-61.
Hoggart, C. J., E. J. Parra, et al. (2003). "Control of confounding of genetic associations in stratified populations." Am J Hum Genet **72**(6): 1492-1504.
Holle, R., M. Happich, et al. (2005). "KORA--a research platform for population based health research." Gesundheitswesen **67 Suppl 1**: S19-25.
Holstege, F. C. and R. A. Young (1999). "Transcriptional regulation: contending with complexity." Proc Natl Acad Sci U S A **96**(1): 2-4.
Hopper, J. L., D. T. Bishop, et al. (2005). "Population-based family studies in genetic epidemiology." Lancet **366**(9494): 1397-406.
Hubner, N., C. A. Wallace, et al. (2005). "Integrated transcriptional profiling and linkage analysis for identification of genes underlying disease." Nat Genet **37**(3): 243-53.
Iles, M. M. (2008). "What can genome-wide association studies tell us about the genetics of common disease?" PLoS Genet **4**(2): e33.

Iwanaga, R., H. Komori, et al. (2004). "Differential regulation of expression of the mammalian DNA repair genes by growth stimulation." Oncogene **23**(53): 8581-90.
Jeimy, S. B., N. Fuller, et al. (2008). "Multimerin 1 binds factor V and activated factor V with high affinity and inhibits thrombin generation." Thromb Haemost **100**(6): 1058-67.
Ji, W., J. N. Foo, et al. (2008). "Rare independent mutations in renal salt handling genes contribute to blood pressure variation." Nat Genet **40**(5): 592-9.
Jin, W., R. M. Riley, et al. (2001). "The contributions of sex, genotype and age to transcriptional variance in Drosophila melanogaster." Nat Genet **29**(4): 389-95.
Johnson, A. D., R. E. Handsaker, et al. (2008). "SNAP: a web-based tool for identification and annotation of proxy SNPs using HapMap." Bioinformatics **24**(24): 2938-9.
Kent, C., G. M. Carman, et al. (1991). "Regulation of eukaryotic phospholipid metabolism." Faseb J **5**(9): 2258-66.
Kim, H., R. Klein, et al. (2004). "Estimating rates of alternative splicing in mammals and invertebrates." Nat Genet **36**(9): 915-6; author reply 916-7.
Klein, J. and F. Figueroa (1986). "Evolution of the major histocompatibility complex." Crit Rev Immunol **6**(4): 295-386.
Kraft, S. and J. P. Kinet (2007). "New developments in FcepsilonRI regulation, function and inhibition." Nat Rev Immunol **7**(5): 365-78.
Kuhn, K., S. C. Baker, et al. (2004). "A novel, high-performance random array platform for quantitative gene expression profiling." Genome Res **14**(11): 2347-56.
Kullo, I. J. and K. Ding (2007). "Mechanisms of disease: The genetic basis of coronary heart disease." Nat Clin Pract Cardiovasc Med **4**(10): 558-69.
Kurimoto, K., Y. Yabuta, et al. (2007). "Global single-cell cDNA amplification to provide a template for representative high-density oligonucleotide microarray analysis." Nat Protoc **2**(3): 739-52.
Kwan, T., D. Benovoy, et al. (2008). "Genome-wide analysis of transcript isoform variation in humans." Nat Genet **40**(2): 225-31.
Lee, C. and M. Roy (2004). "Analysis of alternative splicing with microarrays: successes and challenges." Genome Biol **5**(7): 231.
Li, L., L. Ying, et al. (2008). "Interference of globin genes with biomarker discovery for allograft rejection in peripheral blood samples." Physiol Genomics **32**(2): 190-7.
Li, S., S. Sanna, et al. (2007). "The GLUT9 gene is associated with serum uric acid levels in Sardinia and Chianti cohorts." PLoS Genet **3**(11): e194.
Liang, S., Y. Li, et al. (2006). "Detecting and profiling tissue-selective genes." Physiol Genomics **26**(2): 158-62.
Liew, C. C., J. Ma, et al. (2006). "The peripheral blood transcriptome dynamically reflects system wide biology: a potential diagnostic tool." J Lab Clin Med **147**(3): 126-32.
Liu, J., E. Walter, et al. (2006). "Effects of globin mRNA reduction methods on gene expression profiles from whole blood." J Mol Diagn **8**(5): 551-8.
Liu, S. and R. B. Altman (2003). "Large scale study of protein domain distribution in the context of alternative splicing." Nucleic Acids Res **31**(16): 4828-35.

Meisinger, C., H. Prokisch, et al. (2009). "A genome-wide association study identifies three loci associated with mean platelet volume." Am J Hum Genet **84**(1): 66-71.
Modrek, B. and C. Lee (2002). "A genomic view of alternative splicing." Nat Genet **30**(1): 13-9.
Modrek, B., A. Resch, et al. (2001). "Genome-wide detection of alternative splicing in expressed sequences of human genes." Nucleic Acids Res **29**(13): 2850-9.
Mohr, S. and C. C. Liew (2007). "The peripheral-blood transcriptome: new insights into disease and risk assessment." Trends Mol Med **13**(10): 422-32.
Morgan, T. H. (1915). "Localization of the Hereditary Material in the Germ Cells." Proc Natl Acad Sci U S A **1**(7): 420-9.
Morley, M., C. M. Molony, et al. (2004). "Genetic analysis of genome-wide variation in human gene expression." Nature **430**(7001): 743-7.
Newton-Cheh, C. and J. N. Hirschhorn (2005). "Genetic association studies of complex traits: design and analysis issues." Mutat Res **573**(1-2): 54-69.
Orlic, D., S. Anderson, et al. (1995). "Pluripotent hematopoietic stem cells contain high levels of mRNA for c-kit, GATA-2, p45 NF-E2, and c-myb and low levels or no mRNA for c-fms and the receptors for granulocyte colony-stimulating factor and interleukins 5 and 7." Proc Natl Acad Sci U S A **92**(10): 4601-5.
Ozeki, Y., T. Tomoda, et al. (2003). "Disrupted-in-Schizophrenia-1 (DISC-1): mutant truncation prevents binding to NudE-like (NUDEL) and inhibits neurite outgrowth." Proc Natl Acad Sci U S A **100**(1): 289-94.
Pan, W., S. C. Choi, et al. (2008). "Wnt3a-mediated formation of phosphatidylinositol 4,5-bisphosphate regulates LRP6 phosphorylation." Science **321**(5894): 1350-3.
Petretto, E., J. Mangion, et al. (2006). "Integrated gene expression profiling and linkage analysis in the rat." Mamm Genome **17**(6): 480-9.
Pfeufer, A., S. Jalilzadeh, et al. (2005). "Common variants in myocardial ion channel genes modify the QT interval in the general population: results from the KORA study." Circ Res **96**(6): 693-701.
Pinzar, E., Y. Kanaoka, et al. (2000). "Prostaglandin D synthase gene is involved in the regulation of non-rapid eye movement sleep." Proc Natl Acad Sci U S A **97**(9): 4903-7.
Plagnol, V., E. Uz, et al. (2008). "Extreme clonality in lymphoblastoid cell lines with implications for allele specific expression analyses." PLoS ONE **3**(8): e2966.
Pritchard, C., D. Coil, et al. (2006). "The contributions of normal variation and genetic background to mammalian gene expression." Genome Biol **7**(3): R26.
Pritchard, J. K. and N. J. Cox (2002). "The allelic architecture of human disease genes: common disease-common variant...or not?" Hum Mol Genet **11**(20): 2417-23.
Raghavan, A. and P. R. Bohjanen (2004). "Microarray-based analyses of mRNA decay in the regulation of mammalian gene expression." Brief Funct Genomic Proteomic **3**(2): 112-24.
Redondo, M. J., P. R. Fain, et al. (2001). "Genetics of type 1A diabetes." Recent Prog Horm Res **56**: 69-89.
Reich, D., N. Patterson, et al. (2005). "A whole-genome admixture scan finds a candidate locus for multiple sclerosis susceptibility." Nat Genet **37**(10): 1113-8.
Reiman, E. M., J. A. Webster, et al. (2007). "GAB2 alleles modify Alzheimer's risk in APOE epsilon4 carriers." Neuron **54**(5): 713-20.

Rucker, R. B. and C. McGee (1993). "Chemical modifications of proteins in vivo: selected examples important to cellular regulation." J Nutr **123**(6): 977-90.

Salehi, Z. and F. Mashayekhi (2007). "Eukaryotic translation initiation factor 4E (eIF4E) expression in the brain tissue is induced by infusion of nerve growth factor into the mouse cisterna magnum: an in vivo study." Mol Cell Biochem **304**(1-2): 249-53.

Schadt, E. E., J. Lamb, et al. (2005). "An integrative genomics approach to infer causal associations between gene expression and disease." Nat Genet **37**(7): 710-7.

Schadt, E. E. and P. Y. Lum (2006). "Thematic review series: systems biology approaches to metabolic and cardiovascular disorders. Reverse engineering gene networks to identify key drivers of complex disease phenotypes." J Lipid Res **47**(12): 2601-13.

Schadt, E. E., C. Molony, et al. (2008). "Mapping the genetic architecture of gene expression in human liver." PLoS Biol **6**(5): e107.

Schadt, E. E., S. A. Monks, et al. (2003). "Genetics of gene expression surveyed in maize, mouse and man." Nature **422**(6929): 297-302.

Scheepers, A., S. Schmidt, et al. (2005). "Characterization of the human SLC2A11 (GLUT11) gene: alternative promoter usage, function, expression, and subcellular distribution of three isoforms, and lack of mouse orthologue." Mol Membr Biol **22**(4): 339-51.

Schiebel, K., M. Winkelmann, et al. (1997). "Abnormal XY interchange between a novel isolated protein kinase gene, PRKY, and its homologue, PRKX, accounts for one third of all (Y+)XX males and (Y-)XY females." Hum Mol Genet **6**(11): 1985-9.

Schroeder, A., O. Mueller, et al. (2006). "The RIN: an RNA integrity number for assigning integrity values to RNA measurements." BMC Mol Biol **7**: 3.

Skaletsky, H., T. Kuroda-Kawaguchi, et al. (2003). "The male-specific region of the human Y chromosome is a mosaic of discrete sequence classes." Nature **423**(6942): 825-37.

Smith, D. J. and A. J. Lusis (2002). "The allelic structure of common disease." Hum Mol Genet **11**(20): 2455-61.

Srinivasan, K., L. Shiue, et al. (2005). "Detection and measurement of alternative splicing using splicing-sensitive microarrays." Methods **37**(4): 345-59.

Steffens, M., C. Lamina, et al. (2006). "SNP-based analysis of genetic substructure in the German population." Hum Hered **62**(1): 20-9.

Stranger, B. E., M. S. Forrest, et al. (2005). "Genome-wide associations of gene expression variation in humans." PLoS Genet **1**(6): e78.

Stranger, B. E., M. S. Forrest, et al. (2007). "Relative impact of nucleotide and copy number variation on gene expression phenotypes." Science **315**(5813): 848-53.

Stranger, B. E., A. C. Nica, et al. (2007). "Population genomics of human gene expression." Nat Genet **39**(10): 1217-24.

Struhl, K. (1999). "Fundamentally different logic of gene regulation in eukaryotes and prokaryotes." Cell **98**(1): 1-4.

Szklo, M. (1998). "Population-based cohort studies." Epidemiol Rev **20**(1): 81-90.

Takeuchi, F., K. Yanai, et al. (2005). "Linkage disequilibrium grouping of single nucleotide polymorphisms (SNPs) reflecting haplotype phylogeny for efficient selection of tag SNPs." Genetics **170**(1): 291-304.

Tanaka, T. (2005). "[International HapMap project]." Nippon Rinsho **63 Suppl 12**: 29-34.
Thoeringer, C. K., S. Ripke, et al. (2009). "The GABA transporter 1 (SLC6A1): a novel candidate gene for anxiety disorders." J Neural Transm **116**(6): 649-57.
Thomas, P. D., M. J. Campbell, et al. (2003). "PANTHER: a library of protein families and subfamilies indexed by function." Genome Res **13**(9): 2129-41.
Tramini, P., B. Bonnet, et al. (2001). "A method of age estimation using Raman microspectrometry imaging of the human dentin." Forensic Sci Int **118**(1): 1-9.
Trinklein, N. D., S. J. Aldred, et al. (2003). "Identification and functional analysis of human transcriptional promoters." Genome Res **13**(2): 308-12.
Tsai, F. Y., G. Keller, et al. (1994). "An early haematopoietic defect in mice lacking the transcription factor GATA-2." Nature **371**(6494): 221-6.
Tsai, S. F., D. I. Martin, et al. (1989). "Cloning of cDNA for the major DNA-binding protein of the erythroid lineage through expression in mammalian cells." Nature **339**(6224): 446-51.
Vawter, M. P., S. Evans, et al. (2004). "Gender-specific gene expression in post-mortem human brain: localization to sex chromosomes." Neuropsychopharmacology **29**(2): 373-84.
Venter, J. C., M. D. Adams, et al. (2001). "The sequence of the human genome." Science **291**(5507): 1304-51.
Verthelyi, D., M. Petri, et al. (2001). "Disassociation of sex hormone levels and cytokine production in SLE patients." Lupus **10**(5): 352-8.
Vitart, V., I. Rudan, et al. (2008). "SLC2A9 is a newly identified urate transporter influencing serum urate concentration, urate excretion and gout." Nat Genet **40**(4): 437-42.
Volkin, E. (2001). "The discovery of mRNA." Mutat Res **488**(2): 87-91.
Volkin, E. and L. Astrachan (1956). "Intracellular distribution of labeled ribonucleic acid after phage infection of Escherichia coli." Virology **2**(4): 433-7.
Waeber, G., J. Delplanque, et al. (2000). "The gene MAPK8IP1, encoding islet-brain-1, is a candidate for type 2 diabetes." Nat Genet **24**(3): 291-5.
Wang, W. Y., B. J. Barratt, et al. (2005). "Genome-wide association studies: theoretical and practical concerns." Nat Rev Genet **6**(2): 109-18.
Weedon, M. N., H. Lango, et al. (2008). "Genome-wide association analysis identifies 20 loci that influence adult height." Nat Genet **40**(5): 575-83.
Weidinger, S., C. Gieger, et al. (2008). "Genome-wide scan on total serum IgE levels identifies FCER1A as novel susceptibility locus." PLoS Genet **4**(8): e1000166.
Whitney, A. R., M. Diehn, et al. (2003). "Individuality and variation in gene expression patterns in human blood." Proc Natl Acad Sci U S A **100**(4): 1896-901.
Willer, C. J., S. Sanna, et al. (2008). "Newly identified loci that influence lipid concentrations and risk of coronary artery disease." Nat Genet **40**(2): 161-9.
Winkelmann, J. (2008). "Genetics of restless legs syndrome." Curr Neurol Neurosci Rep **8**(3): 211-6.
Wisniewski, H. G. and J. Vilcek (2004). "Cytokine-induced gene expression at the crossroads of innate immunity, inflammation and fertility: TSG-6 and PTX3/TSG-14." Cytokine Growth Factor Rev **15**(2-3): 129-46.

Wray, G. A., M. W. Hahn, et al. (2003). "The evolution of transcriptional regulation in eukaryotes." Mol Biol Evol **20**(9): 1377-419.

WTCCC (2007). "Genome-wide association study of 14,000 cases of seven common diseases and 3,000 shared controls." Nature **447**(7145): 661-78.

Yang, Y. H., S. Dudoit, et al. (2002). "Normalization for cDNA microarray data: a robust composite method addressing single and multiple slide systematic variation." Nucleic Acids Res **30**(4): e15.

Zeggini, E., L. J. Scott, et al. (2008). "Meta-analysis of genome-wide association data and large-scale replication identifies additional susceptibility loci for type 2 diabetes." Nat Genet **40**(5): 638-45.

8.0 Supplementary materials

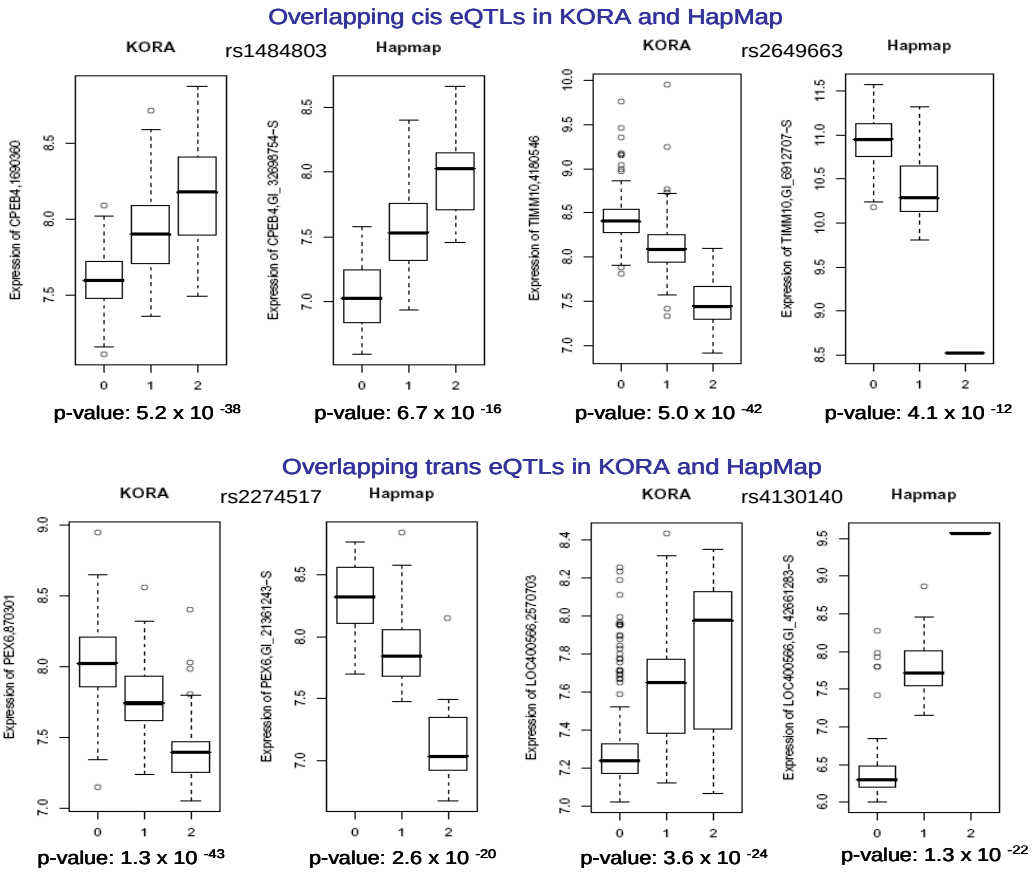

Supplementary Figure 1-Examples of 2 cis and 2 trans eQTLs which overlapped between KORA and HapMap GWAS: Boxplots indicate the same direction of effect of the SNPs on gene expression in both KORA and HapMap.

Supplementary Table 1-Differences in SNP effect on gene expression in KORA and HapMap

Transcript	SNP	KORA p-value	HapMap p-value	KORA effect size	HapMap effect size	eQTL	KORA SNP major allele	HapMap SNP major allele	Cause of opposite SNP effect
DPYSL4	rs7915260	7.7×10^{-8}	1.2×10^{-9}	-0.08	0.48	cis	C	A	opposite DNA strand orientation
DPYSL4	rs7896248	6.3×10^{-8}	1.2×10^{-9}	-0.08	0.48	cis	G	T	opposite DNA strand orientation
MRPL43	rs701835	3.2×10^{-25}	6.0×10^{-9}	0.27	-0.28	cis	A	T	opposite DNA strand orientation
MRPL43	rs4919510	4.5×10^{-23}	3.9×10^{-8}	26	-27	cis	G	C	difference in allelic frequency
MRPL43	rs3824783	4.8×10^{-28}	1.2×10^{-8}	0.28	-0.28	cis	C	G	opposite DNA strand orientation
MRPL43	rs3740488	4.7×10^{-26}	7.4×10^{-9}	0.28	-0.3	cis	A	A	possible false positive
MYOM2	rs2099746	7.1×10^{-9}	3.8×10^{-8}	-0.52	0.3	cis	A	T	opposite DNA strand orientation
MYOM2	rs6986035	1.0×10^{-9}	3.8×10^{-8}	-0.54	0.3	cis	C	G	difference in allelic frequency
ORMDL3	rs1008723	1.3×10^{-7}	2.1×10^{-8}	-0.18	0.18	cis	G	T	difference in allelic frequency
ORMDL3	rs869402	6.8×10^{-8}	2.3×10^{-8}	-0.19	0.19	cis	T	T	possible false positive
C20ORF22	rs3746337	2.5×10^{-8}	3.5×10^{-8}	0.04	-0.4	cis	C	T	difference in allelic frequency
SPG6	rs11640186	1.2×10^{-8}	1.5×10^{-10}	-0.1	0.14	cis	C	G	difference in allelic frequency
PEX6	rs6941212	5.6×10^{-36}	6.6×10^{-21}	0.3	-0.56	trans	A	C	opposite DNA strand orientation

Supplementary Table 2-Assembled GWAS list used to test for eSNP in KORA and HapMap

First Author	Date	Disease/Trait
Kiemeney	14. Sep 08	Urinary bladder cancer
Raychaudhuri	14. Sep 08	Rheumatoid arthritis
Hazra	07. Sep 08	Plasma level of vitamin B12
Di Bernardo	31. Aug 08	Chronic lymphocytic leukemia
Kugathasan	31. Aug 08	Inflammatory bowel disease
Weidinger	22. Aug 08	Serum IgE levels
Ferreira	17. Aug 08	Bipolar disorder
Graham	01. Aug 08	Systemic lupus erythematosus
Julia	01. Aug 08	Rheumatoid arthritis
O'Donovan	30. Jul 08	Schizophrenia
Schormair	27. Jul 08	Restless legs syndrome
Franke	21. Jul 08	Sarcoidosis and Crohn disease
Liu	10. Jul 08	Treatment response to TNF antagonists
Pare	04. Jul 08	Soluble ICAM-1
Sarasquete	01. Jul 08	Osteonecrosis of the jaw
Turner	30. Jun 08	Response to diuretic therapy
Barrett	29. Jun 08	Crohn's disease
Behrens	24. Jun 08	Juvenile idiopathic arthritis
Bouatia-Naji	19. Jun 08	Fasting plasma glucose
Cooper	05. Jun 08	Warfarin maintenance dose
Chen	04. Jun 08	Fasting plasma glucose
Uhl	04. Jun 08	Smoking cessation
Volpi	03. Jun 08	Response to iloperidone treatment (QT prolongation)
Brown	18. Mai 08	Melanoma
Sulem	18. Mai 08	Skin sensitivity to sun
Han	16. Mai 08	Black vs. red hair color
Maris	09. Mai 08	Neuroblastoma
Melzer	09. Mai 08	Protein quantitative trait loci
Valdes	08. Mai 08	Knee osteoarthritis
Chambers	04. Mai 08	Waist circumference and related phenotypes
Loos	04. Mai 08	Body mass index
Richards	29. Apr 08	Bone mineral density
Styrkarsdottir	29. Apr 08	Bone mineral density (spine)
Walsh	25. Apr 08	Schizophrenia
Reiner	24. Apr 08	C-reactive protein
Ridker	24. Apr 08	C-reactive protein
Ober	09. Apr 08	YKL-40 levels
Gudbjartsson	06. Apr 08	Height
Lettre	06. Apr 08	Height
Weedon	06. Apr 08	Height
Liu	04. Apr 08	Psoriasis
Amos	03. Apr 08	Lung cancer
Hung	03. Apr 08	Lung cancer
Thorgeirsson	03. Apr 08	Nicotine dependence
Tenesa	30. Mrz 08	Colorectal cancer
Tomlinson	30. Mrz 08	Colorectal cancer
Zeggini	30. Mrz 08	Type 2 diabetes
Capon	25. Mrz 08	Psoriasis
Sullivan	18. Mrz 08	Schizophrenia
Gold	11. Mrz 08	Breast cancer
Kirov	11. Mrz 08	Schizophrenia
Doring	09. Mrz 08	Serum urate
Vitart	09. Mrz 08	Serum urate
Hunt	02. Mrz 08	Celiac disease
Shifman	15. Feb 08	Schizophrenia
Eeles	10. Feb 08	Prostate cancer
Gudmundsson	10. Feb 08	Prostate cancer
Thomas	10. Feb 08	Prostate cancer (aggressive)
Sandhu	09. Feb 08	LDL cholesterol
Uda	05. Feb 08	Fetal hemoglobin levels
Kong	02. Feb 08	Recombination rate (males)
Kayser	24. Jan 08	Iris color
Harley	20. Jan 08	SLE
Hom	20. Jan 08	Systemic lupus erythematosus
Kozyrev	20. Jan 08	Systemic lupus erythematosus
Hakonarson	15. Jan 08	Type 1 diabetes
Kathiresan	13. Jan 08	Triglycerides
Kooner	13. Jan 08	Triglycerides
Sanna	13. Jan 08	Height
Willer	13. Jan 08	HDL cholesterol
Willer	13. Jan 08	Triglycerides
Wallace	10. Jan 08	Serum urate
van Es	16. Dez 07	Amyotrophic lateral sclerosis
Cronin	07. Dez 07	Amyotrophic lateral sclerosis
Suzuki	17. Nov 07	Coronary spasm in women
Li	09. Nov 07	Serum urate
Plenge	04. Nov 07	Rheumatoid arthritis
Webster	01. Nov 07	Alzheimer's disease

First Author	Date	Disease/Trait
Sulem	21. Okt 07	Freckles
Stokowski	15. Okt 07	Skin pigmentation b
Broderick	14. Okt 07	Colorectal cancer
Cervino	08. Okt 07	Lupus
Benjamin	19. Sep 07	Select biomarker traits
Fox	19. Sep 07	Waist circumference traits
Gottlieb	19. Sep 07	Sleepiness
Hwang	19. Sep 07	Urinary albumin excretion
Kiel	19. Sep 07	Bone mineral density
Larson	19. Sep 07	Major CVD
Levy	19. Sep 07	Blood pressure
Lunetta	19. Sep 07	Morbidity-free survival
Meigs	19. Sep 07	Diabetes related insulin traits
Murabito	19. Sep 07	Prostate cancer
Newton-Cheh	19. Sep 07	Electrocardiographic traits
O'Donnell	19. Sep 07	Other subclinical atherosclerosis traits
Seshadri	19. Sep 07	Cognitive test performance
Vasan	19. Sep 07	Exercise treadmill test traits
Wilk	19. Sep 07	Mean forced vital capacity
Yang	19. Sep 07	Hemostatic factors and hematological phenotypes
van Es	07. Sep 07	Amyotrophic lateral sclerosis
Plenge	05. Sep 07	Rheumatoid arthritis
Raelson	05. Sep 07	Crohn's disease
Menzel	02. Sep 07	F-cell distribution
Weedon	02. Sep 07	Height
Thorleifsson	09. Aug 07	Exfoliation glaucoma
Franke	08. Aug 07	Irritable bowel syndrome
Maeda	01. Aug 07	Diabetic nephropathy
Shifman	31. Jul 07	Neuroticism
Hafler	29. Jul 07	Multiple sclerosis
Moffatt	26. Jul 07	Asthma
Scuteri	20. Jul 07	Obesity-related traits
Stefansson	19. Jul 07	Restless legs syndrome
Samani	18. Jul 07	Coronary disease
Winkelmann	18. Jul 07	Restless legs syndrome
Buch	15. Jul 07	Gallstones
Hakonarson	15. Jul 07	Type 1 diabetes
Tomlinson	08. Jul 07	Colorectal cancer
Zanke	08. Jul 07	Colorectal cancer
Gudbjartsson	01. Jul 07	Atrial fibrillation/atrial flutter
Gudmundsson	01. Jul 07	Prostate cancer
van Heel	10. Jun 07	Celiac disease
Reiman	07. Jun 07	Alzheimer's disease
WTCCC	07. Jun 07	Bipolar disorder
WTCCC	07. Jun 07	Coronary disease
WTCCC	07. Jun 07	Crohn's disease
WTCCC	07. Jun 07	Hypertension
WTCCC	07. Jun 07	Rheumatoid arthritis
WTCCC	07. Jun 07	Type 1 diabetes
WTCCC	07. Jun 07	Type 2 diabetes
Parkes	06. Jun 07	Crohn's disease
Todd	06. Jun 07	Type 1 diabetes
Easton	27. Mai 07	Breast cancer
Hunter	27. Mai 07	Breast cancer
Stacey	27. Mai 07	Breast cancer
Baum	08. Mai 07	Bipolar disorder
Matarin	06. Mai 07	Stroke
Helgadottir	03. Mai 07	Myocardial infarction
Saxena	26. Apr 07	Type 2 diabetes
Scott	26. Apr 07	Type 2 diabetes
Steinthorsdottir	26. Apr 07	Type 2 diabetes
Zeggini	26. Apr 07	Type 2 diabetes
Rioux	15. Apr 07	Crohn's disease
Frayling	12. Apr 07	Body mass index
Hanson	01. Apr 07	End-stage renal disease
Yeager	01. Apr 07	Prostate cancer
Lencz	20. Mrz 07	Schizophrenia
Libioulle	05. Mrz 07	Crohn's disease
Schymick	20. Feb 07	Amyotrophic lateral sclerosis
Sladek	11. Feb 07	Type 2 diabetes
Bierut	07. Dez 06	Nicotine dependence
Duerr	26. Okt 06	Inflammatory bowel disease
DeWan	19. Okt 06	Wet age-related macular degeneration
Fung	28. Sep 06	Parkinson's disease
Arking	30. Apr 06	QT interval prolongation
Maraganore	09. Sep 05	Parkinson's disease
Klein	10. Mrz 05	Age-related macular degeneration

9.0 List of abbreviations

- °C : degrees celsius
- ATP : adenosine triphosphate
- CDCV : common disease common variant
- cDNA : complementary deoxyribonucleic acid
- CEPH/CEU : Centre d'Etude du Polymorphisme Humain
- cRNA : complementary ribonucleic acid
- Cy3 : cyanine 3
- DNA : deoxyribonucleic acid
- EBV : epstein-barr virus
- eQTL : expression quantitative trait loci
- F3/4 : follow-up 3/4
- GINI : German infant nutritional intervention program
- GWAS : genome wide association studies
- Hyb : hybridization
- IgE : immunoglobulin E
- ISAAC : International study of asthma and allergy in childhood
- kb : kilo base
- KORA : Cooperative health research in the region Augsburg
- LCL : lymphoblast cell line
- LD : linkage disequilibrium
- LISA : Influences of lifestyle-related factors on the immune system and the development of allergies in childhood study.
- LOWESS : Locally weighted scatter plot smoothing

- Mb : Mega base
- MCR : Major histocompatibility region
- mg/dl : milligrams per deciliter
- ml : milliliter
- mpv : mean platelet volume
- mRNA : messenger ribonucleic acid
- ng : nanogram
- PAM : Prediction analysis for microarray
- PCR : Polymerase chain reaction
- QC : Quality control
- RIN : RNA integrity number
- RNA : Ribonucleic acid
- rpm : revolutions per minute
- RT-PCR : Real-time polymerase chain reaction
- S3/4 : Survey 3/4
- SAPHIR : Salzburg atherosclerosis prevention program in subjects at high individual risk
- SHIP : Study of health in Pomerania
- SLE : Systemic lupus erythematosus
- SNPs : Single nucleotide polymorphisms
- UTR : Untranslated region
- µl : micro liter

10.0 Acknowledgements

Behind every successful PhD student is a group of people who made it possible. This section is dedicated to all those people who made it possible for me.

First of I would like to extend my heartfelt gratitude to both Professor Thomas Meitinger and Dr.Holger Prokisch for giving me the opportunity to work under their wings. Professor Meitinger I would like to thank for all his guidance and critical but always useful comments on my work. It was an honor to work under him and gain from his vast knowledge and expertise. I thank Holger Prokisch for his excellent supervision and enthusiasm and for valuable comments and inputs. I thank Katharina Heim for the statistical analyses and for putting up with my millions of questions and requests. I thank Professor Bertram Müller-Myhsok for his expert advice on the final statistical analyses. I am thankful to Prof. H.-E Wichmann and the entire KORA team for giving me access to the KORA resources. I would like to mention my gratitude towards Professor Adamski for all his help and support. I am very grateful to Professor Fries and Professor Gierl for their help and for agreeing to be my examiners. Furthermore, I acknowledge the efforts of all the reviewers who have taken the time to read this thesis.

My gratitude extends to my work colleagues Uwe Ahting (for all his guidance in the lab and beyond), Marieta Borzes (who never let me feel homesick), Anna Benet-Pages and Nuria (for the help, encouragement and discussions), Bettina Ries (to let me to ein igeln in her office). The love and support of all my friends and family especially my aunt Anima Kapadia, best friend Swapna Lagisetty and cousin Priya Patil helped me through these three years of my PhD.

I owe my deepest gratitude to Yogesh Bhanu (for always helping me, believing in me and most importantly for his endless patience when it was most needed).

All this would have never been possible without the love and support of my mother Minal Mehta and my father Deepak Mehta (who guided me through every step in my career and life). I am forever indebted to my parents for their understanding. They are my pillars of support and it is their encouragement which allows me to go on.

Saving the best for last, I would finally like to thank my nani (grandma) Susheela Choksi for standing by me always.

nature genetics

SLC2A9 influences uric acid concentrations with pronounced sex-specific effects

Angela Döring[1,10], Christian Gieger[1,2,10], Divya Mehta[3], Henning Gohlke[1], Holger Prokisch[3,4], Stefan Coassin[5], Guido Fischer[1], Kathleen Henke[6], Norman Klopp[1,2], Florian Kronenberg[5], Bernhard Paulweber[7], Arne Pfeufer[3,4], Dieter Rosskopf[6], Henry Völzke[8], Thomas Illig[1], Thomas Meitinger[3,4], H-Erich Wichmann[1,2] & Christa Meisinger[1,9]

Serum uric acid concentrations are correlated with gout and clinical entities such as cardiovascular disease and diabetes. In the genome-wide association study KORA (Kooperative Gesundheitsforschung in der Region Augsburg) F3 500K ($n = 1,644$), the most significant SNPs associated with uric acid concentrations mapped within introns 4 and 6 of *SLC2A9*, a gene encoding a putative hexose transporter (effects: –0.23 to –0.36 mg/dl per copy of the minor allele). We replicated these findings in three independent samples from Germany (KORA S4 and SHIP (Study of Health in Pomerania)) and Austria (SAPHIR; Salzburg Atherosclerosis Prevention Program in Subjects at High Individual Risk), with *P* values ranging from 1.2×10^{-8} to 1.0×10^{-32}. Analysis of whole blood RNA expression profiles from a KORA F3 500K subgroup ($n = 117$) showed a significant association between the *SLC2A9* isoform 2 and urate concentrations. The *SLC2A9* genotypes also showed significant association with self-reported gout. The proportion of the variance of serum uric acid concentrations explained by genotypes was about 1.2% in men and 6% in women, and the percentage accounted for by expression levels was 3.5% in men and 15% in women.

There is strong evidence that, in addition to environmental components, a strong genetic control influences the regulation of blood uric acid concentrations[1,2]. However, two linkage scans on uric acid concentrations or gout did not identify a significant locus[2,3]. We carried out a genome-wide association study (GWAS) with a sufficient number of replication samples to enable identification of hitherto unconsidered pathways in the regulation of uric acid concentrations. As marked differences in serum uric acid concentrations between men and women have been reported[4], we carried out sex-specific analysis of the data.

For the GWAS in the KORA F3 500K study population, we genotyped 1,644 individuals with the Affymetrix 500K Array Set. For statistical analysis, we selected SNPs by including only high-quality genotypes to reduce the number of false-positive signals. A total of 335,152 SNPs passed all quality-control measures and were tested for associations with uric acid concentrations (**Fig. 1a**).

We identified a quantitative trait locus (QTL) in a 500-kb region with high linkage disequilibrium (LD) including 40 autosomal SNPs with *P* values below the genome-wide significance level of 1.5×10^{-7}. All SNPs were located on the short arm of chromosome 4, in the region 4p15.3–16.1. From these 40 SNPs, 26 were located within the transcribed region of *SLC2A9*, which covers 100 kb. SNPs in introns 4 and 6 showed the strongest signals. Nearly all other significant SNPs were located upstream of *SLC2A9* in the intergenic region between *SLC2A9* and *ZNF518B*, with the exception of one SNP located in *WDR1* (**Fig. 1b–d** and **Table 1**). *P* values ranged from 8.6×10^{-8} to 1.6×10^{-12}. The effect estimates were –0.23 to –0.36 mg/dl per copy of the minor allele, which translates into a difference of up to –0.7 mg/dl in uric acid concentrations between the two homozygote groups (**Table 1**). No further genome-wide significant association was observed in any other region. In addition, we carried out a conditional analysis in the 500-kb region for which we selected the best SNP, rs7442295, conditioning on it to search for other SNPs with independent information. No other SNP was significant after correction for multiple testing.

We replicated the GWA results in three independent study samples. Twenty SNPs were initially chosen from the 500-kb region and genotyped in KORA S4. All 12 SNPs that reached genome-wide

[1]Institute of Epidemiology, Helmholtz Zentrum München, German Research Center for Environmental Health, 85764 Neuherberg, Germany. [2]Institute of Medical Informatics, Biometry and Epidemiology, Ludwig-Maximilians-Universität, 81377 Munich, Germany. [3]Institute of Human Genetics, Helmholtz Zentrum München, German Research Center for Environmental Health, 85764 Neuherberg, Germany. [4]Institute of Human Genetics, Klinikum rechts der Isar, Technical University Munich, 81765 Munich, Germany. [5]Division of Genetic Epidemiology, Department of Medical Genetics, Molecular and Clinical Pharmacology, Innsbruck Medical University, 6020 Innsbruck, Austria. [6]Department of Pharmacology, Ernst-Moritz-Arndt University, 17487 Greifswald, Germany. [7]First Department of Internal Medicine, St. Johann Spital, Paracelsus Private Medical University, 5020 Salzburg, Austria. [8]Institute for Community Medicine, Ernst-Moritz-Arndt University, 17487 Greifswald, Germany. [9]Central Hospital of Augsburg, MONICA (Monitoring Trends and Determinants of Cardiovascular Disease)/KORA (Kooperative Gesundheitsforschung in der Region Augsburg) Myocardial Infarction Registry, 86156 Augsburg, Germany. [10]These authors contributed equally to this work. Correspondence should be addressed to C.M. (christa.meisinger@helmholtz-muenchen.de).

Received 22 October 2007; accepted 1 February 2008; published online 9 March 2008; doi:10.1038/ng.107

© 2008 Nature Publishing Group http://www.nature.com/naturegenetics

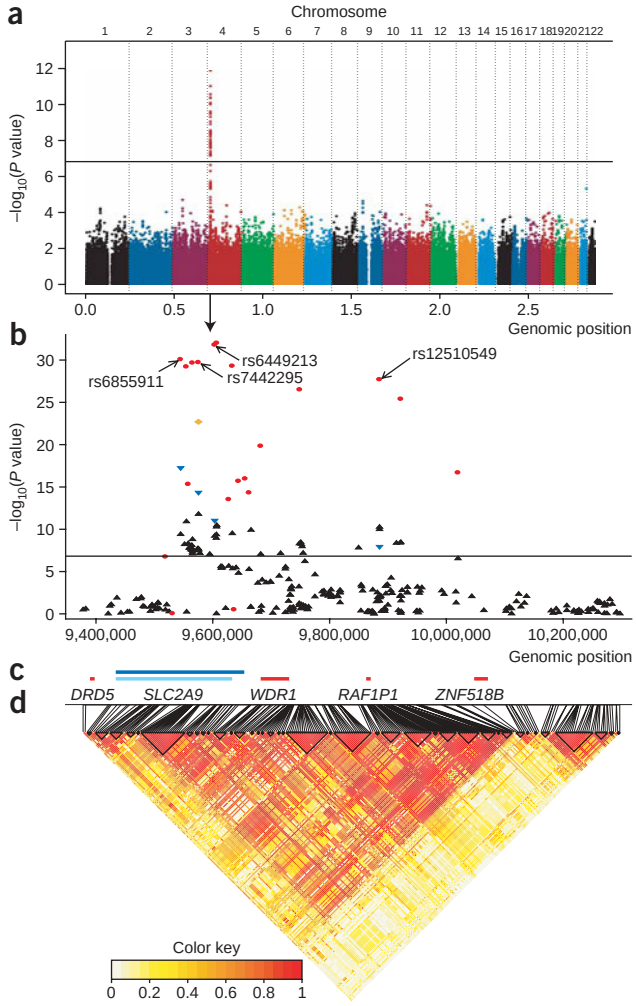

Figure 1 Summary of genome-wide association and replication results. (**a**) Genome-wide association study for uric acid concentrations on a population-based sample of 1,644 individuals. The *x* axis represents the genomic position (in Gb) of 335,152 SNPs; the *y* axis shows $-\log_{10}(P)$. After correcting for multiple testing, we found that 40 SNPs on chromosome 4 attained statistical significance. (**b**) *P* value diagram showing association signals near *SLC2A9*. The *x* axis represents the genomic position on chromosome 4. The *y* axis shows $-\log_{10}(P)$ of KORA F3 500K (black), KORA S4 (red), SAPHIR (blue) and SHIP (brown). (**c**) Gene regions are indicated by bars, with *SLC2A9* isoform 1 in light blue and *SLC2A9* isoform 2 in dark blue. (**d**) Pairwise LD diagram of the region on chromosome 4 covering the genes *DRD5, SLC2A9, WDR1, RAF1P1* and *ZNF518B*. Pairwise LD, measured as D′, was calculated from KORA F3 500K; blocks were determined using the method of Gabriel as implemented in HAPLOVIEW. Shading represents the magnitude of pairwise LD, with a white-to-red gradient reflecting lower to higher D′ values.

significance in the original scan were also significantly associated with uric acid in KORA S4, with *P* values ranging from 4.8×10^{-16} to 1.0×10^{-32} (given a corrected significance level of 0.002; **Fig. 1b**). Effect estimates of the significant SNPs were comparable and even slightly higher compared to those in the KORA F3 500K sample, with the exception of one SNP (**Table 1**). Among the three nonsynonymous SNPs in the exons of *SLC2A9*, only one in exon 9 (rs2280205) was significant ($P = 1.83 \times 10^{-7}$; **Table 1**). Haplotype analysis showed significantly lower uric acid concentrations for a haplotype carrying all minor alleles (haplotype frequency 7.5%) compared to the most common haplotype carrying all major alleles (haplotype frequency 35.7%). The effect size of –0.429 ($P = 8.44 \times 10^{-15}$) was slightly larger than the effects in the single-SNP analyses (**Supplementary Methods** and **Supplementary Table 1** online).

For replication of the KORA S4 results in SAPHIR, we selected four SNPs: two in the center (rs6449213 in intron 4 and rs7442295 in intron 6 of *SLC2A9*) and one at each margin of the 500-kb LD region (rs6855911 and rs12510549). We did not select the best SNP, rs7669607 ($P = 1.01 \times 10^{-32}$), from the KORA S4 replication, as we observed a violation of Hardy-Weinberg equilibrium ($P = 2.84 \times 10^{-9}$). All four SNPs were highly significantly associated with serum uric acid concentrations, with *P* values ranging from 1.2×10^{-8} to 5.6×10^{-18}. All effect estimates had the same direction and magnitude as in KORA S4. For replication in SHIP, the selected SNP rs7442295 was statistically significant, with a *P* value of 1.53×10^{-24} and an effect estimate in concordance with KORA S4 and SAPHIR. Finally, we carried out a combined analysis of all samples. SNP rs7442295, which was replicated in all studies, showed a *P* value of 3.0×10^{-70}; the three other SNPs, replicated in KORA S4 and SAPHIR, showed *P* values between 10^{-44} and 10^{-50}. The effect estimates were between –0.332 and –0.349 mg/dl (**Table 2**).

Through sex-stratified analyses, we observed a markedly stronger effect in females compared to males in all studies. Considering the combined analysis, we found the effect estimates to be about –0.25 mg/dl in men, and –0.45 mg/dl in women. In accordance, the proportion of the variance explained was about 1.2% in men and 6% in women in the combined analyses (**Table 2**). Adjustment for serum creatinine did not change the results; for further correlates, the variances explained were even higher (see **Supplementary Table 2** online). The haplotype analysis by sex showed that, in women, the haplotype carrying all minor alleles was again maximally associated with uric acid ($P = 8.19 \times 10^{-19}$), with an effect estimate of –0.588 mg/dl that reduced the uric acid concentration per copy more than twice as much as in men. Only one haplotype with a frequency of about 2% in both sexes showed no sex effect (**Supplementary Methods** and **Supplementary Table 1**).

All four SNPs replicated in KORA S4 and SAPHIR showed significant associations with self-reported gout in KORA S4. The odds ratios (ORs) per risk allele were in the range of 0.60 and 0.67, with slightly lower ORs for women. In SHIP, we found the same results for rs7442295 (**Table 3**). This corresponds to an OR of 0.36–0.45 in homozygotes for the major allele compared to homozygotes for the minor allele.

Sequence variation within the *SLC2A9* coding region is considerably higher than average, given that four synonymous and four nonsynonymous variants with allele frequencies between 8% and 48% have already been annotated. We sequenced all exons in 48 male and 48 female samples selected equally from the extremes of the serum uric acid distribution in 7,000 individuals (KORA F3 and S4). The common variants found in exons had *P* values in the same range compared to the intronic variants known from the GWA in this subsample. In addition to the common variants, we detected four rare variants: two synonymous changes in exons 2 and 8 and two missense variants in exons 6 and 8 (**Supplementary Table 3** online). The predicted amino acid changes, which occur in conserved regions of the protein, await functional characterization.

In a recently published expression dataset derived from lymphoblastoid cell lines of HapMap individuals[5], none of the uric acid–associated SNPs within intron 4 of *SLC2A9* or elsewhere in the region showed significant associations with *SLC2A9* expression (Illumina

© 2008 Nature Publishing Group http://www.nature.com/naturegenetics

Table 1 Summary of the GWAS (KORA F3 500K) and the replication study (KORA S4; additive model)

					GWAS (KORA F3 500K) (n = 1,644)				Replication (KORA S4) (n = 4,162)			
rs number	Position	Gene structure[a]	Gene	Selection criterion	MAF	Estimate (mg/dl)	*P* value	Genotyping efficiency (%)	MAF	Estimate (mg/dl)	*P* value	Genotyping efficiency (%)
rs2280205	9519021	Exon 9	*SLC2A9*	Nonsynonymous exchange					0.477	–0.137	1.83E–07	96.7
rs3733591	9531228	Exon 8	*SLC2A9*	Nonsynonymous exchange					0.189	–0.003	9.28E–01	90.2
rs6855911	9545008	Intron 7	*SLC2A9*	GWA	0.260	–0.303	3.93E–10	96.4	0.249	–0.350	8.79E–31	96.8
rs4697698	9551675	Intron 7	*SLC2A9*	GWA	0.476	–0.247	5.95E–09	100.0				
rs4697700	9554890	Intron 6	*SLC2A9*	GWA	0.236	–0.338	1.20E–11	96.5	0.243	–0.351	6.26E–30	97.1
rs998675	9557927	Intron 6	*SLC2A9*	GWA	0.480	–0.252	4.78E–09	98.1	0.477	–0.209	4.81E–16	96.9
rs12498956	9559803	Intron 6	*SLC2A9*	GWA	0.435	–0.243	1.68E–08	99.0				
rs13328050	9560218	Intron 6	*SLC2A9*	GWA	0.430	–0.246	1.39E–08	97.3				
rs4455410	9562395	Intron 6	*SLC2A9*	GWA	0.428	–0.239	2.47E–08	99.6				
rs9994266	9563548	Intron 6	*SLC2A9*	GWA	0.428	–0.244	1.53E–08	99.0				
rs7375599	9564016	Intron 6	*SLC2A9*	GWA	0.476	–0.245	7.70E–09	100.0				
rs7378340	9564296	Intron 6	*SLC2A9*	GWA	0.429	–0.237	2.93E–08	99.8				
rs4311316	9565069	Intron 6	*SLC2A9*	GWA	0.427	–0.231	7.68E–08	98.6				
rs4481233	9565177	Intron 6	*SLC2A9*	GWA	0.181	–0.333	1.54E–09	97.3	0.196	–0.375	2.21E–30	97.3
rs4314284	9565194	Intron 6	*SLC2A9*	GWA	0.430	–0.234	4.83E–08	99.6				
rs6839490	9574098	Intron 6	*SLC2A9*	GWA	0.430	–0.242	1.95E–08	99.0				
rs6449171	9575096	Intron 6	*SLC2A9*	GWA	0.430	–0.236	3.25E–08	99.6				
rs7442295	9575478	Intron 6	*SLC2A9*	GWA	0.218	–0.359	1.62E–12	98.2	0.220	–0.363	1.95E–30	97.3
rs6449174	9575520	Intron 6	*SLC2A9*	GWA	0.428	–0.237	2.72E–08	96.5				
rs7658170	9575691	Intron 6	*SLC2A9*	GWA	0.441	–0.243	2.09E–08	95.6				
rs6449178	9577782	Intron 6	*SLC2A9*	GWA	0.433	–0.231	6.70E–08	98.8				
rs17246501	9594808	Intron 5	*SLC2A9*	GWA	0.492	–0.227	8.49E–08	99.8				
rs6449213	9603313	Intron 4	*SLC2A9*	GWA	0.191	–0.328	6.09E–10	98.8	0.201	–0.385	1.64E–32	96.3
rs13111638	9605988	Intron 4	*SLC2A9*	GWA	0.198	–0.328	1.09E–09	95.6				
rs4529048	9606210	Intron 4	*SLC2A9*	GWA	0.249	–0.305	4.13E–10	96.7				
rs3733588	9606401	Intron 4	*SLC2A9*	GWA	0.240	–0.320	5.14E–11	96.9				
rs7669607[b]	9606899	Intron 4	*SLC2A9*	GWA	0.212	–0.338	3.39E–11	99.6	0.224	–0.357	1.01E–32	95.5
rs6827754	9627251	Intron 3	*SLC2A9*	GWA[c]	0.432	–0.201	2.21E–06	98.6	0.432	–0.195	3.06E–14	96.2
rs12509955	9633401	Intron 2	*SLC2A9*	GWA	0.212	–0.324	3.04E–10	100.0	0.220	–0.359	5.20E–30	97.3
rs6820230	9636640	Exon 2	*SLC2A9*	Nonsynonymous exchange					0.269	–0.029	3.22E–01	93.6
rs13146686	9644031	Intron 1	*SLC2A9*	GWA[c]	0.431	–0.183	1.49E–05	99.5	0.425	–0.214	2.11E–16	97.5
rs11734375	9655396	Intergenic	*SLC2A9,WDR1*	Putative transcription factor binding site					0.466	–0.215	1.09E–16	95.7
rs13120348	9662253	Intergenic	*SLC2A9,WDR1*	GWA[c]	0.439	–0.192	5.32E–06	100.0	0.429	–0.205	4.87E–15	96.8
rs7671266	9665474	Intergenic	*SLC2A9,WDR1*	GWA	0.211	–0.332	1.23E–10	99.1				
rs4320137	9682067	Intergenic	*SLC2A9,WDR1*	GWA	0.155	–0.309	8.55E–08	99.9	0.163	–0.330	1.49E–20	96.2
rs12509714	9716189	Intron	*WDR1*	GWA	0.430	–0.233	6.84E–08	96.8				
rs10939723	9748203	Intergenic	*WDR1,RAF1P1*	GWA	0.200	–0.311	4.91E–09	98.2				
rs11734783	9748203	Intergenic	*WDR1,RAF1P1*	GWA	0.181	–0.306	1.54E–08	99.9				
rs17198547	9750517	Intergenic	*WDR1,RAF1P1*	GWA	0.199	–0.314	3.43E–09	99.6				
rs17251963	9751659	Intergenic	*WDR1,RAF1P1*	GWA	0.194	–0.311	5.80E–09	99.2	0.199	–0.346	3.59E–27	99.5
rs4697714	9752884	Intergenic	*WDR1,RAF1P1*	GWA	0.200	–0.301	1.08E–08	99.8				
rs4640669	9754831	Intergenic	*WDR1,RAF1P1*	GWA	0.208	–0.283	6.39E–08	98.6				
rs10489070	9885450	Intergenic	*RAF1P1,ZNF518B*	GWA	0.207	–0.335	1.00E–10	99.9				
rs12510549	9885565	Intergenic	*RAF1P1,ZNF518B*	GWA	0.218	–0.331	5.43E–11	100.0	0.219	–0.344	2.06E–28	99.5
rs7689060	9914561	Intergenic	*RAF1P1,ZNF518B*	GWA	0.224	–0.296	4.20E–09	99.6				
rs12511337	9921070	Intergenic	*RAF1P1,ZNF518B*	GWA	0.201	–0.311	4.02E–09	99.5				
rs4698029	9921896	Intergenic	*RAF1P1,ZNF518B*	GWA	0.202	–0.311	3.43E–09	99.9	0.205	–0.335	4.19E–26	99.5
rs4698050	10019846	Intergenic	*RAF1P1,ZNF518B*	GWA[c]	0.243	–0.256	2.83E–07	99.6	0.235	–0.256	2.10E–17	99.5

All SNPs are located on chromosome 4.
[a]Numbering of SLC2A9 according to isoform 2. [b]HWE violation observed in KORA S4 replication. [c]Not genome-wide significant.

© 2008 Nature Publishing Group http://www.nature.com/naturegenetics

Table 2 Association between uric acid concentrations and selected SNPs in the GWAS sample and in the three replication samples stratified by sex

	KORA F3 500K			KORA S4			SAPHIR			SHIP			Combined		
SNP	Estimate	*P* value	Variance proportion (%)	Estimate	*P* value	Variance proportion (%)	Estimate	*P* value	Variance proportion (%)	Estimate	*P* value	Variance proportion (%)	Estimate	*P* value	Variance proportion (%)
							Total								
	$n = 1,644$			$n = 4,162$			$n = 1,719$			$n = 4,066$			$n = 7,525^a/11,591^b$		
rs6855911	–0.303	3.93E–10	2.4	–0.350	8.79E–31	3.3	–0.408	5.56E–18	4.3				–0.349	3.93E–52	3.1
rs7442295	–0.359	1.62E–12	3.1	–0.363	1.95E–30	3.2	–0.390	4.51E–15	3.5	–0.331	1.53E–24	3.5	–0.346	2.97E–70	2.7
rs6449213	–0.328	6.09E–10	2.3	–0.385	1.64E–32	3.5	–0.354	9.31E–12	2.7				–0.360	1.84E–47	2.8
rs12510549	–0.331	5.43E–11	2.1	–0.344	2.06E–28	2.9	–0.292	1.16E–08	1.9				–0.332	9.95E–44	2.5
							Men								
	$n = 813$			$n = 2,052$			$n = 1,081$			$n = 2,023$			$n = 3,946^a/5,969^b$		
rs6855911	–0.128	6.99E–02	0.4	–0.275	1.07E–08	1.6	–0.372	3.19E–09	3.2				–0.263	1.51E–14	1.5
rs7442295	–0.202	7.39E–03	0.9	–0.284	1.05E–08	1.6	–0.352	1.20E–07	2.6	–0.198	6.08E–05	2.6	–0.245	7.01E–17	1.2
rs6449213	–0.165	3.62E–02	0.5	–0.288	1.99E–08	1.6	–0.281	4.67E–05	1.5				–0.252	1.14E–11	1.2
rs12510549	–0.229	2.38E–03	1.1	–0.254	1.48E–07	1.3	–0.218	1.27E–03	1.0				–0.238	2.27E–11	1.1
							Women								
	$n = 831$			$n = 2,110$			$n = 638$			$n = 2,043$			$n = 3,579^a/5,622^b$		
rs6855911	–0.472	7.56E–13	6.3	–0.425	2.58E–30	6.2	–0.465	1.75E–11	6.9				–0.448	1.20E–51	6.4
rs7442295	–0.503	1.23E–13	6.5	–0.441	1.26E–29	6.1	–0.449	7.39E–10	5.9	–0.465	1.04E–29	5.9	–0.456	2.56E–74	5.8
rs6449213	–0.481	9.58E–12	5.5	–0.474	1.36E–32	6.7	–0.475	5.60E–10	5.9				–0.474	1.32E–49	6.1
rs12510549	–0.416	5.07E–10	4.6	–0.429	3.89E–28	5.6	–0.424	2.78E–08	4.8				–0.433	6.23E–44	5.3

[a]KORA F3 500K, KORA S4 and SAPHIR combined (rs6855911, rs6449213 and rs12510549). [b]KORA F3 500K, KORA S4, SAPHIR and SHIP combined (rs7442295).

probe ID, GI_9910553-S) or with the expression of any other gene in *cis* or in *trans* (all $P > 0.01$). In this published study, it was not possible to differentiate between the two isoforms of *SLC2A9*.

To investigate the transcript levels of *SLC2A* isoforms in blood relative to serum uric acid concentrations, we analyzed a subgroup of 117 samples from the study population for which genome-wide expression profiles were available. This subgroup had been selected randomly from the KORA F3 study population. We examined five hybridization probes: two recognizing the two distinct isoforms of *SLC2A9*, one recognizing both isoforms, and two corresponding to the

Table 3 Odds ratios for gout for SNPs associated with uric acid concentrations in KORA S4 and KORA F3 500 K combined (KORA) and in SHIP

		Total				Men				Women			
		Minor allele frequency				Minor allele frequency				Minor allele frequency			
SNP	Data	Cases	Controls	OR per risk allele 95% CI	*P* value	Cases	Controls	OR per risk allele 95% CI	*P* value	Cases	Controls	OR per risk allele 95% CI	*P* value
rs12510549	KORA	0.311	0.399	0.67 (0.574–0.803)	5.96E–06	0.321	0.402	0.70 (0.570–0.856)	5.55E–04	0.290	0.396	0.65 (0.481–0.867)	3.65E–03
rs6449213	KORA	0.260	0.366	0.61 (0.506–0.730)	9.59E–08	0.265	0.370	0.62 (0.496–0.774)	2.61E–05	0.304	0.454	0.59 (0.428–0.810)	1.15E–03
rs6855911	KORA	0.338	0.453	0.63 (0.534–0.742)	3.19E–08	0.353	0.452	0.66 (0.543–0.806)	4.04E–05	0.249	0.363	0.57 (0.422–0.761)	1.63E–04
rs7442295	KORA	0.299	0.402	0.63 (0.530–0.751)	2.21E–07	0.311	0.407	0.65 (0.529–0.806)	7.17E–05	0.273	0.397	0.59 (0.435–0.807)	8.88E–04
	SHIP	0.267	0.383	0.60 (0.459–0.781)	1.56E–04	0.284	0.386	0.63 (0.460–0.875)	5.48E–03	0.235	0.381	0.54 (0.335–0.861)	9.79E–03

Gout defined by medical anamnesis (having gout or elevated uric acid concentrations). The prevalence of gout is 6.4% in SHIP (8.6% in men and 4.4% in women) and 9.6% in KORA (13.6% in men and 6.0% in women). The difference is explained by the higher proportion of older persons in KORA.

© 2008 Nature Publishing Group http://www.nature.com/naturegenetics

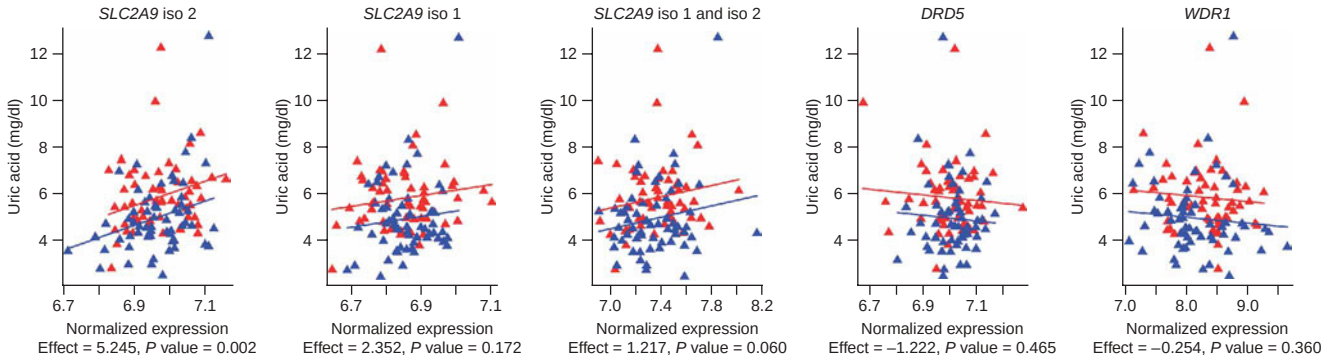

Figure 2 Transcription analysis of *SLC2A9* and association with serum uric acid concentrations. The indicated genes and probes were analyzed from genome-wide transcription profiles of 117 samples. The regression line is shown for females (blue) and males (red); female and male samples are indicated by blue and red triangles, respectively. *SLC2A9* is represented with three probes detecting the alternative first exons of isoforms 1 (iso 1, Illumina probe ID 1850100) and 2 (iso 2, ID 10128) and exon 12 (ID 4590201) at the distal end of both isoforms 1 and 2. The flanking genes *DRD5* (ID 7560053) and *WDR1* (ID 3610767) are represented with a single probe each.

neighboring genes *DRD5* and *WDR1*. The sample size was too small to show a significant genetic effect of *SLC2A9* SNPs on uric acid concentrations or intensity of transcription signals (**Supplementary Fig. 1** online). However, the probe hybridizing to the *SLC2A9* isoform 2 transcript showed a significant association with uric acid concentrations (**Fig. 2**). The uric acid variance explained by *SLC2A9* expression levels was about 8% for isoform 2; for this isoform of *SLC2A9* alone, sex-specific analyses showed a stronger association in women ($P = 0.005$; effect = 6.813) compared to men ($P = 0.151$; effect = 3.490).

Both identification and replication studies showed strongest associations of common alleles with serum uric acid concentrations and self-reported gout within introns 4 and 6 of *SLC2A9*. Smaller independent effects of other polymorphisms in the 500-kb region including *WDR1* and *ZNF518B* cannot be resolved. This result has recently been confirmed by a genome-wide study in a Sardinian population[6] and by the Wellcome Trust Case Control Consortium (WTCCC)[7]. Our explorative screen was not exhaustive; for instance, it did not include the SNPs in *SLC22A12* gene[8,9], which have been reported to influence uric acid concentrations.

SLC2A9 encodes a transporter protein that belongs to class II of the facilitative glucose transporter family[10]. Members of the GLUT family mediate sodium-independent specific hexose uptake into target cells by facilitated diffusion. A potential substrate of GLUT9 is fructose, as GLUT9 has the highest similarity with the fructose transporters GLUT5 and GLUT11 from the same subclass II in the SLC2A family[11,12]. Fructose intake had been identified as a determinant of uric acid concentrations some decades ago[13]. Fructose is phosphorylated by fructokinase in hepatocytes while generating ADP, which is used for rapid production of uric acid[14].

It has been shown that alternative splicing of *SLC2A9* results in two proteins, GLUT9 and GLUT9ΔN, each with differential targeting and tissue specificity[15]. Although GLUT9 is mainly localized to the membrane of proximal tubular kidney cells, the placenta, the liver, and to a lesser extent the lung, leukocytes, chrondrocytes and brain[15,16], GLUT9ΔN is prominently expressed in the kidney in both humans and mice[15,17].

Our expression studies help us to focus the association signals to a single protein, GLUT9, and allow discrimination between two annotated isoforms of this gene. Both isoforms are equally and sizably expressed in whole blood. The significant association with the shorter protein GLUT9ΔN argues for a prominent role of the *SLC2A9* isoform 2 in the regulation of urate concentrations. The association with the isoform 2 suggests an involvement of the protein in urate excretion, implying that GLUT9ΔN handles additional or alternative substrates to the ones suggested by protein family relations.

We report an association between *SLC2A9* genotypes and urate concentrations, between *SLC2A9* genotypes and gout, and between *SLC2A9* expression and uric acid, with stronger associations in women. Carriers of the major alleles of the most significant SNPs, especially homozygous individuals representing about 60% of our population (**Supplementary Table 4** online), are prone to developing high serum uric acid concentrations. Our expression analyses suggest an involvement of the protein in uric acid excretion in the kidney and open new avenues for a better understanding of the heritable basis of hyperuricemia.

METHODS

Subjects and study design. A detailed description of the GWAS population and the replication samples is given in **Supplementary Methods** and **Supplementary Table 5** online. The study populations represent samples from the general population with no indication of stratification after analysis of the genome-wide SNP dataset (see **Supplementary Methods**). For all studies, we obtained informed consent from participants and approval from the local ethical committees. The participants were of European origin.

KORA F3 500K and replication sample KORA S4. We recruited the study population for the GWAS (KORA F3 500K) and replication cohort S4 from the KORA S3 and S4 surveys. Both are independent population-based samples from the general population, comprising individuals living in the region of Augsburg, Southern Germany, aged 25–74 years, and examined in 1994–1995 (S3) and 1999–2001 (S4). In KORA S4, 4,261 persons participated (response 67%), and DNA was available from 4,162 participants. The standardized examinations applied in both surveys have been described in detail elsewhere[18]. For KORA F3 500K, we selected 1,644 subjects, who participated in a follow-up examination of S3 (F3), then comprising individuals aged 35–79 years.

SAPHIR. The Salzburg Atherosclerosis Prevention Program in Subjects at High Individual Risk (SAPHIR) is an observational study conducted in the years 1999–2002 involving 1,770 healthy unrelated subjects: 663 females from 50 to 70 years of age and 1,107 males from 40 to 60 years of age. Study participants were recruited by health screening programs in large companies in and around the city of Salzburg. At baseline, all study participants were subjected to a comprehensive program[19]. DNA was available from 1,719 persons.

SHIP. The third replication sample was recruited from the Study of Health in Pomerania (SHIP), which was conducted in the years 1997–2001. Study details

© 2008 Nature Publishing Group http://www.nature.com/naturegenetics

are given elsewhere[20]. We applied a two-stage sampling protocol that was adopted from the MONICA/KORA study. In total, 4,310 persons (68.8% of eligible subjects) aged 20 to 79 years participated, and DNA was available from 4,066 persons.

Uric acid measurements. We obtained nonfasting blood samples from study participants in KORA and SHIP and fasting samples from those in SAPHIR. Uric acid analyses were carried out in all studies on fresh samples using an uricase method (KORA S4 and SAPHIR: UA Plus, Roche; SHIP: Uric acid PAP, Boehringer; KORA F3 500K: URCA Flex, Dade Behring). A detailed description is given in **Supplementary Methods**.

Definition of gout in KORA and SHIP. We asked the following question in a standardized interview: "Did you suffer from gout or elevated uric acid levels in the past 12 months (Y/N)?" Furthermore, the participants were asked to bring all medications taken during the seven days preceding the interview. The medication data were registered online (KORA) or in a computer-assisted interview (SHIP). The drugs were categorized according to the Anatomical Therapeutical Chemical (ATC) classification index (see URLs section below). A participant was classified as having gout if he suffered from gout and/or elevated uric acid levels and/or took uricosuric or uricostatic drugs. The definition presents an overestimation of gout prevalence[21].

KORA F3 500K genotyping and quality control. Genotyping for KORA F3 500K was done using Affymetrix Gene Chip Human Mapping 500K Array Set consisting of two chips (Sty I and Nsp I). Genomic DNA was hybridized in accordance with the manufacturer's standard recommendations. Genotypes were determined using BRLMM clustering algorithm. We carried out filtering of both conspicuous individuals and SNPs to ensure robustness of association analysis. Details on quality criteria are described in **Supplementary Methods**.

SNP genotyping and quality control in the replication samples. For KORA S4, genotyping of SNPs was done with the iPLEX (Sequenom) method by means of matrix-assisted laser desorption ionization time-of-flight mass spectrometry method (MALDI-TOF MS, Mass Array, Sequenom) according to the manufacturer's instructions. For SAPHIR, genotyping was done within the Genotyping Unit of the Gene Discovery Core Facility at the Innsbruck Medical University, Austria using 5′-nuclease allelic discrimination (Taqman) assays (Applied Biosystems). For SHIP, the rs7442295 locus was amplified with the oligonucleotide primers 5′-GAATGTCTGCAGCAGGGAGGCAGTGGG ACTTGAG-3′ and 5′-CAAAAGTCCTTCCCTTCCTGGACTTGAATGAAGT C-3′. The 277-bp amplicon was digested with *Mbo*II, resulting in two fragments of 103 and 174 bp for the variant C allele.

In all studies, 5–15% of the samples were genotyped twice for quality control purposes; no discordant genotypes were found. In KORA S4, for 3 of 20 replicated SNPs, a deviation from Hardy-Weinberg equilibrium was observed ($P < 0.01$). In SAPHIR and SHIP, all replicated SNPs were in HWE. Details on genotyping are described in the **Supplementary Methods** and **Supplementary Table 6** online.

SNP selection for replication. The power of the replication in KORA S4, SAPHIR and SHIP was estimated for a difference in uric acid concentrations per allele between 0.2 and 0.4 mg/dl and a nominal significance level of 0.05. The power to detect a true association was above 85% in all replication samples.

For the replication in KORA S4, we selected SNPs that were significantly associated with uric acid concentrations at the genome-wide level. To capture the available genetic information, SNPs that did not reach genome-wide significance were added (**Supplementary Methods**). In addition, exonic and splice-site SNPs were included. For further replication in SAPHIR and SHIP, we selected highly significant SNPs of the KORA F3 500K and the KORA S4 replication.

Statistical analysis of genetic effects. In the KORA F3 500K sample, possible population substructures were analyzed (**Supplementary Methods**). We used additive genetic models assuming a trend per copy of the minor allele to specify the dependency of uric acid concentrations on genotype categories. All models were adjusted for age and gender. We used linear regression algorithms implemented in the statistical analysis system R (KORA F3 500K) and SAS version 9.1 (replications). To select significant SNPs in the genome-wide screening and the replications, we used conservative Bonferroni thresholds, which corresponded to a nominal level of 0.05. For the conditional analysis, the SNP with the lowest *P* value in the GWAS was selected and included in the linear regression as covariate. All other SNPs in the region were sequentially tested for significance. We carried out haplotype reconstruction and haplotype association analysis in the KORA S4 replication sample using the R-library HaploStats[22], which allows including all common haplotypes in the linear regression and incorporating age and sex as covariates. The most common haplotype served as reference. Details on haplotype analysis are described in **Supplementary Methods**. SNPs selected for replication in SAPHIR and SHIP were also analyzed by sex in all replication samples, and were additionally adjusted for further correlates of uric acid in KORA S4 (**Supplementary Table 2**). For each variable in the model, partial R (type II) were calculated to estimate the variance proportion explained. We conducted several sensitivity analyses in the replication study KORA S4. When excluding all persons under uricosuric or uricostatic medication ($n = 124$) from the analysis, and in a second step, all persons suffering from cancer ($n = 181$), we found that the associations were even stronger for the four SNPs, which were selected for further replication compared to the results from the full dataset.

Mutational analysis. *SLC2A9* exons were amplified with intronic primers (**Supplementary Table 7** online) and directly sequenced using a BigDye Cycle sequencing kit (Applied Biosystems). Genomic DNA (~30 ng) was subjected to PCR amplification carried out in a 15 µl volume containing 1× PCR Master Mix (Promega) and 0.25 µM of each forward and reverse primer under the following cycle conditions: initial step at 95 °C for 5 min, 30 cycles at 95 °C for 30 s, 58 °C (exon 1 62 °C) for 30 s and 72 °C for 30 s, and final extension at 72 °C for 5 min.

Gene expression analysis. We drew 2.5 ml of peripheral blood from individuals participating in the KORA study under fasting conditions. The blood samples were collected directly in PAXgene Blood RNA tubes (PreAnalytiX) between the hours of 10 a.m. and noon. The RNA extraction was done using the PAXgene Blood RNA Kit (Qiagen). We carried out RNA and cRNA quality control using the Bioanalyzer (Agilent), and quantification using Ribogreen (Invitrogen). We reverse transcribed 300–500 ng of RNA into cRNA and biotin-UTP–labeled the RNA using the Illumina TotalPrep RNA Amplification Kit (Ambion). We hybridized 1,500 ng of cRNA to the Illumina Human-6 v2 Expression BeadChip. Washing steps were carried out in accordance with Illumina protocol (technical note 1226030 Rev. B). We exported the raw data from the 'Beadstudio' software (Illumina) to R. The data were converted into logarithmic scores and normalized using the LOWESS method[23]. The association between uric acid concentration and normalized expression was computed with a linear regression adjusted for sex. Robustness of the significant association between uric acid concentrations and *SLC2A9* isoform 2 was shown by removing extreme uric acid concentrations from the analysis.

Bioinformatic analysis. All successfully replicated SNPs were subjected to an *in silico* analysis for putative transcription factor binding sites using the Genomatix Software Suite (Genomatix) as well as freely accessible bioinformatics tools (see URLs section below). The results are shown in **Supplementary Methods**.

URLs. Anatomical Therapeutical Chemical (ATC) classification index, http://www.whocc.no/atcddd/; Bioinformatics tools, http://pupasuite.bioinfo.cipf.es.

Note: Supplementary information is available on the Nature Genetics website.

ACKNOWLEDGMENTS

The MONICA/KORA Augsburg studies were financed by the Helmholtz Zentrum München, German Research Center for Environmental Health, Neuherberg, Germany and supported by grants from the German Federal Ministry of Education and Research (BMBF). Part of this work was financed by the German National Genome Research Network (NGFN). Our research was supported within the Munich Center of Health Sciences (MC Health) as part of LMUinnovativ. SHIP is part of the Community Medicine Research net (CMR) of the University of Greifswald, Germany, which is funded by the Federal Ministry of Education

© 2008 Nature Publishing Group http://www.nature.com/naturegenetics

and Research, the Ministry of Cultural Affairs as well as the Social Ministry of the Federal State of Mecklenburg-West Pomerania. The SHIP genotyping was supported by grant 03IP612 (InnoProfile) of the German Federal Ministry for Education and Research (BMBF). Part of the work on SAPHIR was supported by the 'Genomics of Lipid-associated Disorders – GOLD' of the Austrian Genome Research Programme (GEN-AU). We gratefully acknowledge the contribution of P. Lichtner, G. Eckstein, T. Strom and K. Heim and all other members of the Helmholtz Zentrum München genotyping staff in generating and analyzing the SNP and RNA dataset, as well as the contribution of A. Gehringer and M. Haak from the Division of Genetic Epidemiology, Innsbruck Medical University. We thank all members of field staffs who were involved in the planning and conduct of the MONICA/KORA Augsburg studies, the SHIP study and the SAPHIR study. Finally, we express our appreciation to all study participants.

AUTHOR CONTRIBUTIONS

Study design and biobanking KORA F3 500K: H.-E.W., T.M., C.G., T.I., C.M., A.P. and G.F.; study design and biobanking replication studies: H.V. (SHIP), B.P. and F.K. (SAPHIR), A.D. and H.-E.W. (KORA); statistical analysis: C.G. and A.D.; Affymetrix genotyping: T.M. and T.I.; genotyping in the replication studies: F.K., S.C., D.R., K.H., N.K. and H.G.; sequencing and gene expression analysis: T.M., D.M., H.P. and A.P.; phenotype assessment: H.V., B.P., A.D., C.M. and H.-E.W.; bioinformatical analysis: S.C., H.G.; manuscript writing: C.M., A.D, C.G., T.M., H.G., S.C. and F.K.

Published online at http://www.nature.com/naturegenetics
Reprints and permissions information is available online at http://npg.nature.com/reprintsandpermissions

1. Wilk, J.B. *et al.* Segregation analysis of serum uric acid in the NHLBI Family Heart Study. *Hum. Genet.* **106**, 355–359 (2000).
2. Yang, Q. *et al.* Genome-wide search for genes affecting serum uric acid levels: the Framingham Heart Study. *Metabolism* **54**, 1435–1441 (2005).
3. Cheng, L.S. *et al.* Genomewide scan for gout in Taiwanese aborigines reveals linkage to chromosome 4q25. *Am. J. Hum. Genet.* **75**, 498–503 (2004).
4. Fang, J. & Alderman, M.H. Serum uric acid and cardiovascular mortality the NHANES I epidemiologic follow-up study, 1971–1992. National Health and Nutrition Examination Survey. *J. Am. Med. Assoc.* **283**, 2404–2410 (2000).
5. Stranger, B.E. *et al.* Population genomics of human gene expression. *Nat. Genet.* **39**, 1217–1224 (2007).
6. Li, S. *et al.* The *GLUT9* gene is associated with serum uric acid levels in Sardinia and Chianti cohorts. *PLoS Genet.* **3**, e194 (2007).
7. Wallace, C. *et al.* Genome-wide association study identifies genes for biomarkers of cardiovascular disease: serum urate and dyslipidemia. *Am. J. Hum. Genet.* **82**, 139–149 (2008).
8. Graessler, J. *et al.* Association of the human urate transporter 1 with reduced renal uric acid excretion and hyperuricemia in a German Caucasian population. *Arthritis Rheum.* **54**, 292–300 (2006).
9. Shima, Y., Teruya, K. & Ohta, H. Association between intronic SNP in urate-anion exchanger gene, *SLC22A12*, and serum uric acid levels in Japanese. *Life Sci.* **79**, 2234–2237 (2006).
10. Joost, H.G. & Thorens, B. The extended GLUT-family of sugar/polyol transport facilitators: nomenclature, sequence characteristics, and potential function of its novel members. *Mol. Membr. Biol.* **18**, 247–256 (2001).
11. Burant, C.F., Takeda, J., Brot-Laroche, E., Bell, G.I. & Davidson, N.O. Fructose transporter in human spermatozoa and small intestine is GLUT5. *J. Biol. Chem.* **267**, 14523–14526 (1992).
12. Scheepers, A. *et al.* Characterization of the human *SLC2A11* (GLUT11) gene: alternative promoter usage, function, expression, and subcellular distribution of three isoforms, and lack of mouse orthologue. *Mol. Membr. Biol.* **22**, 339–351 (2005).
13. Stirpe, F. *et al.* Fructose-induced hyperuricaemia. *Lancet* **2**, 1310–1311 (1970).
14. Hallfrisch, J. Metabolic effects of dietary fructose. *FASEB J.* **4**, 2652–2660 (1990).
15. Augustin, R. *et al.* Identification and characterization of human glucose transporter-like protein-9 (GLUT9): alternative splicing alters trafficking. *J. Biol. Chem.* **279**, 16229–16236 (2004).
16. Richardson, S. *et al.* Molecular characterization and partial cDNA cloning of facilitative glucose transporters expressed in human articular chondrocytes; stimulation of 2-deoxyglucose uptake by IGF-I and elevated MMP-2 secretion by glucose deprivation. *Osteoarthritis Cartilage* **11**, 92–101 (2003).
17. Keembiyehetty, C. *et al.* Mouse glucose transporter 9 splice variants are expressed in adult liver and kidney and are up-regulated in diabetes. *Mol. Endocrinol.* **20**, 686–697 (2006).
18. Wichmann, H.E., Gieger, C. & Illig, T. KORA-gen–resource for population genetics, controls and a broad spectrum of disease phenotypes. *Gesundheitswesen* **67** Suppl. 1, S26–S30 (2005).
19. Heid, I.M. *et al.* Genetic architecture of the *APM1* gene and its influence on adiponectin plasma levels and parameters of the metabolic syndrome in 1,727 healthy Caucasians. *Diabetes* **55**, 375–384 (2006).
20. John, U. *et al.* Study of Health In Pomerania (SHIP): a health examination survey in an east German region: objectives and design. *Soz. Praventivmed.* **46**, 186–194 (2001).
21. Roddy, E., Zhang, W. & Doherty, M. The changing epidemiology of gout. *Nat. Clin. Pract. Rheumatol.* **3**, 443–449 (2007).
22. Lake, S.L. *et al.* Estimation and tests of haplotype-environment interaction when linkage phase is ambiguous. *Hum. Hered.* **55**, 56–65 (2003).
23. Yang, Y.H. *et al.* Normalization for cDNA microarray data: a robust composite method addressing single and multiple slide systematic variation. *Nucleic Acids Res.* **30**, e15 (2002).

© 2008 Nature Publishing Group http://www.nature.com/naturegenetics

A Genome-wide Association Study Identifies Three Loci Associated with Mean Platelet Volume

Christa Meisinger,[1,3,14] Holger Prokisch,[2,4,14] Christian Gieger,[1,5] Nicole Soranzo,[6,7] Divya Mehta,[2] Dieter Rosskopf,[8] Peter Lichtner,[2] Norman Klopp,[1] Jonathan Stephens,[12] Nicholas A. Watkins,[12] Panos Deloukas,[6] Andreas Greinacher,[9] Wolfgang Koenig,[13] Matthias Nauck,[10] Christian Rimmbach,[8] Henry Völzke,[11] Annette Peters,[1] Thomas Illig,[1] Willem H. Ouwehand,[6,12] Thomas Meitinger,[2,4] H.-Erich Wichmann,[1,5] and Angela Döring[1,*]

Mean platelet volume (MPV) is increased in myocardial and cerebral infarction and is an independent and strong predictor for postevent morbidity and mortality. We conducted a genome-wide association study (GWAS), the KORA (Kooperative Gesundheitsforschung in der Region Augsburg) F3 500K study, and found MPV to be strongly associated with three common single-nucleotide polymorphisms (SNPs): rs7961894 located within intron 3 of *WDR66* on chromosome 12q24.31, rs12485738 upstream of the *ARHGEF3* on chromosome 3p13-p21, and rs2138852 located upstream of *TAOK1* on chromosome 17q11.2. We replicated all three SNPs in another GWAS from the UK and in two population-based samples from Germany. In a combined analysis including 10,048 subjects, the SNPs had p values of 7.24×10^{-48} for rs7961894, 3.81×10^{-27} for rs12485738, and 7.19×10^{-28} for rs2138852. These three quantitative trait loci together accounted for 4%–5% of the variance in MPV. In-depth sequence analysis of *WDR66* in 382 samples from the extremes revealed 20 new variants and a haplotype with three coding SNPs and one SNP at the transcription start site associated with MPV ($p = 6.8 \times 10^{-5}$). In addition, expression analysis indicated a direct correlation of *WDR66* transcripts and MPV. These findings may not only enhance our understanding of platelet activation and function, but may also provide a focus for several novel research avenues.

Platelets are anucleate blood cells and play an important role in atherogenesis and atherothrombosis, two key processes underlying cardiovascular disease.[1,2] MPV is increased in myocardial (MIM 608446, MIM 608557) and cerebral (MIM 601367, MIM 606799) infarction and is an independent and strong predictor for postevent morbidity and mortality.[3,4] Platelets are formed from polyploid bone marrow precursor cells, the megakaryocytes, through a process of proplatelet formation. The volume of platelets is tightly regulated but the precise molecular machinery that controls it is only partially understood and involves outside-in signals emanating from extracellular matrix proteins and growth factors.[5]

There is ample evidence that the blood cell indices under which is also MPV have a high level of heritability. In twin studies, heritability estimates for hemoglobin levels and the counts of white blood cells and platelets ranged from 0.37 to 0.89.[6] Studies in baboons and rodents confirmed these findings and found (not surprisingly) that also the volumes of red cells and platelets are under genetic control.[7]

We conducted a genome-wide association study (GWAS) in individuals sampled from the KORA (Kooperative Gesundheitsforschung in der Region Augsburg) F3 500K study population. The study population for the GWAS was recruited from the MONICA S3 survey, a population-based sample from the general population living in the region of Augsburg, Southern Germany, which was carried out in 1994/95. The standardized examinations applied in this survey including 4856 participants aged 25 to 74 years (response 75%) have been described in detail elsewhere.[8,9] In a follow-up examination of S3 in 2004/05 (KORA F3), 3006 subjects participated. For KORA F3 500K we selected 1644 subjects of these participants then aged 35 to 79 years, including 1606 individuals with MPV values available. Genotyping was performed with the Affymetrix Gene Chip Human Mapping 500K Array Set as described in Döring et al.[10] In brief, on SNP level from a total of 500,568 SNPs, we excluded for the purpose of this analysis all SNPs on chromosome X, leaving 490,032 autosomal SNPs for the GWA screening step. The X chromosome SNPs were excluded from the analysis because the X chromosome has to be treated differently from the autosomes (note that the Affymetrix Chip used does not assay the Y chromosome). Because most loci on the X chromosome are subject to X chromosome inactivation, it can not be predicted which allele is active. Furthermore, because there is only one copy of X in males, sample sizes and accordingly

[1]Institute of Epidemiology, [2]Institute of Human Genetics, Helmholtz Zentrum München, German Research Center for Environmental Health, 85764 Neuherberg, Germany; [3]Central Hospital of Augsburg, MONICA/KORA Myocardial Infarction Registry, 86156 Augsburg, Germany; [4]Institute of Human Genetics, Technical University, 81765 Munich, Germany; [5]Institute of Medical Informatics, Biometry and Epidemiology, Ludwig-Maximilians-Universität, 81377 Munich, Germany; [6]Wellcome Trust Sanger Institute, Hinxton, Cambridge CB10 1SA, UK; [7]King's College London, Twin Genetic Epidemiology Unit, London SE1 7EH, UK; [8]Department of Pharmacology, Center for Pharmacology and Experimental Therapeutics, [9]Institute of Immunology and Transfusion Medicine, [10]Institute for Clinical Chemistry and Laboratory Medicine, [11]Institute for Community Medicine, Ernst-Moritz-Arndt University, 17487 Greifswald, Germany; [12]Department of Haematology, University of Cambridge and National Health Service Blood and Transplant (NHSBT), Cambridge CB2 0PT, UK; [13]University of Ulm Medical Center, Department of Internal Medicine-II, Cardiology, Ulm 89081, Germany
[14]These authors contributed equally to this work
*Correspondence: doering@helmholtz-muenchen.de
DOI 10.1016/j.ajhg.2008.11.015. ©2009 by The American Society of Human Genetics. All rights reserved.

power are different from the autosomes. From the 490,032 autosomal SNPs, 335,152 (68.39%) SNPs passed all quality control criteria and were selected for the subsequent association analyses. Criteria leading to exclusion were genotyping efficiency <95% (N = 49,325) and minor allele frequency (MAF) <5% (N = 101,323). An exact Fisher test has been used to detect deviations from Hardy-Weinberg equilibrium, and we excluded all SNPs with p values below 10^{-5} (N = 4,232) after passing the other criteria.[10]

We used three independent samples for replication. The first was a GWAS sample from the UK National Blood Services collection of Common Controls (UKBS-CC) typed with the same Affymetrix Chip. Details of genotyping and quality criteria are given in the original study.[11] In brief, the UKBS-CC collection is an anonymized collection of DNA samples from 3100 healthy blood donors. The collection has been established by the three British blood services of England, Scotland, and Wales as part of the Wellcome Trust Case Control Consortium (WTCCC) study.[11] Data from 1203 English individuals of panel 1 (UKBS-CC1) with available genotypes were used in this study, because no MPV data were available for the Scottish and Welsh samples.

The second replication cohort was recruited from the KORA S4 survey, an independent population-based sample from the general population living in the region of Augsburg, Southern Germany, conducted in 1999/2001. The standardized examinations applied in the survey (4261 participants, response 67%) have been described in detail elsewhere.[8,10] Genotyping of SNPs was performed with the iPLEX (Sequenom, San Diego, CA) method by means of matrix-assisted laser desorption ionization-time of flight mass spectrometry method (MALDI-TOF MS, Mass Array, Sequenom) according to the manufacturer's instructions. Details of genotyping and quality criteria are given elsewhere.[10]

The third replication sample, the Study of Health in Pomerania (SHIP), is a cross-sectional population-based health survey conducted between 1997 and 2001 in West Pomerania, a region in the northeastern part of Germany. The detailed objectives and the study design have been published elsewhere.[12] The final SHIP population comprising 4310 participants (response 68.8%) was invited to attend a 5-year follow-up examination, termed SHIP1, which was conducted between 2002 and 2006 (3300 participants; response 76.6%). For replication analysis, the SHIP1 population was included. The SNPs were genotyped with custom-made 5′ nuclease allelic discrimination (Taqman) assays (AppliedBiosystems, Foster City, CA). Quality control included the independent replication of 3% of genotypes and the inclusion of 2% negative controls on all DNA sample plates.

In all samples, MPV was measured on fresh venous EDTA blood with an automatic analyzer (Coulter STKS in KORA F3, KORA S4, and UKBS-CC1 and Sysmex SE-9000 analyzer in SHIP; reference MPV values were 7.8–11.0 fl in KORA F3, KORA S4, and UKBS-CC1 and 9.0–12.5 fl in SHIP).

A description of the GWA study population and the replication samples is given in Table S1 available online.

In all studies, informed consent was obtained from participants and the studies were approved by the local ethical committees.

We used additive genetic models assuming a trend per copy of the minor allele to test the association of MPV values and genotypes. MPV values were natural log transformed before analysis to approximate the normal distribution. All models were adjusted for age and gender, and additionally for collection center within the UK sample. We used linear regression algorithms as implemented in the statistical analysis packages R (KORA F3 500K), PLINK[13] (KORA F3 500K, UKBS-CC1), and SAS version 9.1 (KORA S4, SHIP). Imputation of genotypes in KORA F3 500K used to fine-map the replicated regions in Figures 1B–1D was performed with the software MACH based on HapMap II. Meta-analysis statistics were obtained with a weighted z-statistics method, where weights were proportional to the square root of the number of individuals examined in each sample and selected such that the squared weights sum was 1. Calculations were implemented in the METAL package. Combined betas and SEs were calculated with Inverse Variance meta-analysis, together with Cochran's Q and I^2 with R scripts.

To select significant SNPs in the genome-wide screening and in the replication studies, we used conservative Bonferroni thresholds that corresponded to an uncorrected significance level of 0.05. The associated quantile-quantile plot in Figure S1 shows good agreement with the null distribution.

The GWAS identified several genomic locations as potentially associated with MPV (Figure 1A). Of the 335,152 SNPs tested by regression analysis, 10 representing 8 distinct genetic regions reached p values below 10^{-5} (Table 1; Tables S2 and S3). One SNP rs7961894 ($p = 2.09 \times 10^{-11}$; Table 1; Figure 1B), located within intron 3 of the *WDR66* (WD repeat domain 66) gene at 12q24.31, reached genome-wide significance with a Bonferroni corrected significance level of 1.5×10^{-7}. The 10 SNPs were taken forward to replicate them in the UKBS-CC1 GWAS sample, and at the same time 8 SNPs (representing 8 different loci) were taken forward for replication in the KORA S4 Study. One of those SNPs could not be replicated in KORA S4 because of problems with the assay design (Table S3). The SNPs, which were successfully replicated in both studies, were rs7961894 in *WDR66*, rs12485738 on 30 and 56 kb distance from the transcription start sites of two short isoforms of the *ARHGEF3* gene at 3p13-p21 (Rho guanine nucleotide exchange factor 3) (MIM 612115), and rs2138852 upstream of the *TAOK1* gene at 17q11.2 (TAO Kinase 1; Figures 1B–1D; Table 1) (MIM 610266). None of the other tested SNPs reached significance in the UKBS-CC1 or KORA S4 sample given a corrected significance of 0.005 (Table S3). Finally, only the three loci that have been successfully replicated in both studies were taken forward to additional replication in the SHIP study where these SNPs again showed a significant association with MPV values (Table 1).

In further analysis in the GWA population, it was examined whether the three lead SNPs are associated with other

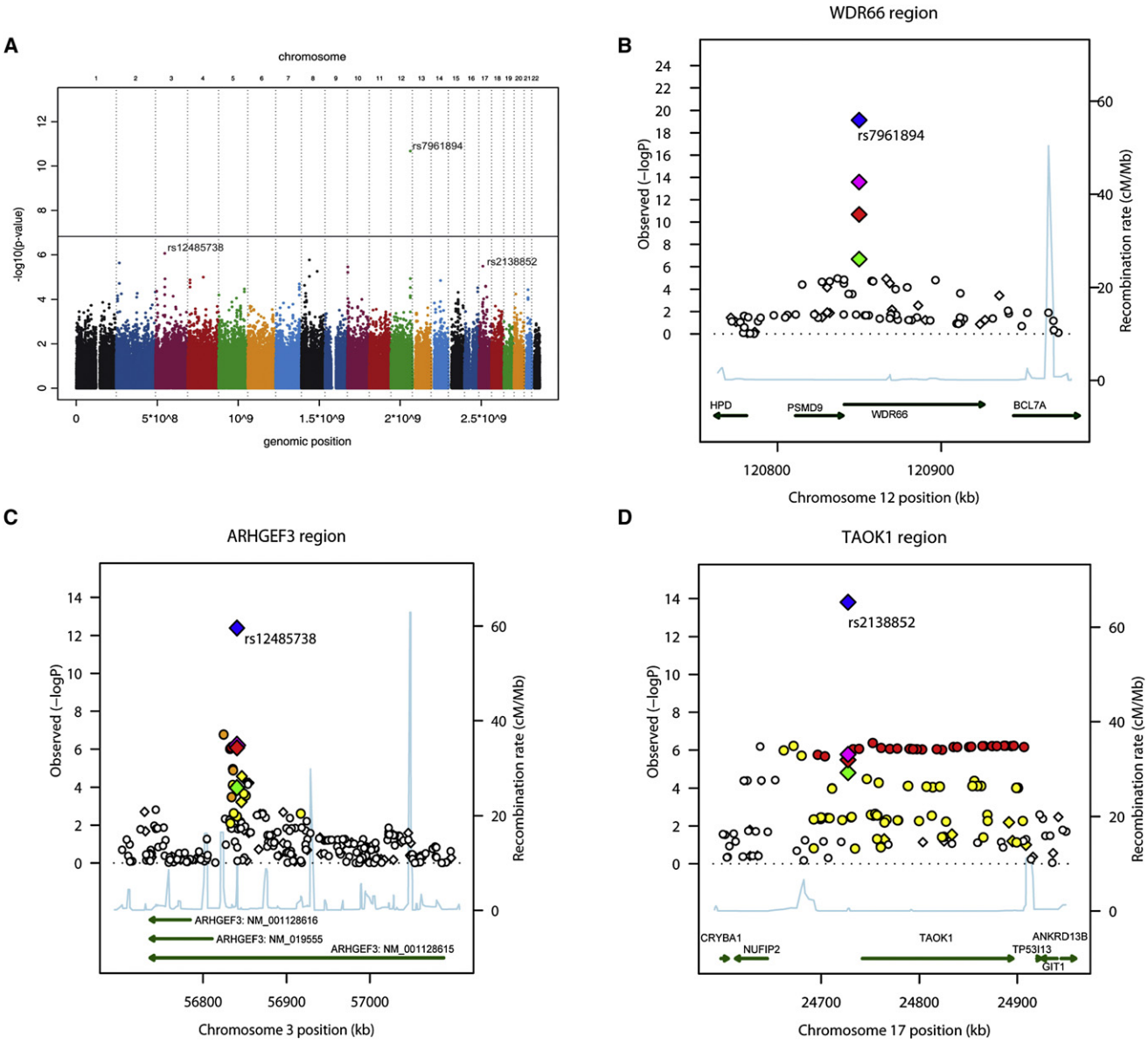

Figure 1. Summary of Genome-wide Association and Replication Results

(A) Genome-wide association study for log-transformed MPV on a population-based sample of 1606 individuals from the KORA F3 500K study. The *x* axis represents the genomic position (in Gb) of 335,152 SNPs; the *y* axis shows −log10(P). The horizontal line indicates the threshold for genome-wide significance at 1.5×10^{-7}. After correcting for multiple testing, we found that one SNP on chromosome 12 attained genome-wide statistical significance.

(B–D) p value plots showing the association signals in the region of *WDR66* on chromosome 12 (B), *ARHGEF3* on chromosome 3 (C), and *TAOK1* on chromosome 17 (D). −log10 p values are plotted as a function of genomic position (NCBI Build 36). Large diamonds indicate the p value for the lead SNP in KORA F3 500K (red), KORA S4 (blue), UKBS-CC1 (green), and SHIP (magenta). Proxies are indicated with diamonds for genotyped SNPs and circles for imputed SNPs of smaller size, with colors determined from their pairwise r^2 values from KORA F3 500K. Red diamonds indicate high LD with the lead SNP ($r^2 > 0.8$), orange diamonds indicate moderate LD with the lead SNP ($0.5 < r^2 < 0.8$), yellow indicates markers in weak LD with the lead SNP ($0.2 < r^2 < 0.5$), and white indicates no LD with the lead SNP ($r^2 < 0.2$). Recombination rate estimates (HapMap Phase II) are given in light blue, Refseq genes (NCBI) are displayed by green bars.

traits, such as white blood cell count, red blood cell count, mean corpuscular volume, hematocrit, and hemoglobin. None of the lead SNPs showed a significant association ($p < 0.05$) with any of these traits (data not shown).

In the combined sample of 10,048 individuals, the SNP rs7961894 reached a p value of 7.24×10^{-48} (effect per minor allele copy = 0.032 per log fl, CI 0.028–0.037), the SNP rs12485738 a p value of 3.81×10^{-27} (effect per minor allele copy = 0.015 per log fl, CI 0.012–0.017), and the third SNP (rs2138852) a combined p value of 7.19×10^{-28} (effect per minor allele copy = −0.015 per log fl, CI −0.018–−0.013).

The reference values were about 15% higher in SHIP than in the other studies, which is best explained by the different

Table 1. Association between Mean Platelet Volume and Three Lead SNPs in the GWAS and Three Replication Cohorts

	Chromosome	Position	Minor Allele	Major Allele	Genotyping Efficiency	p Value HWE	N (MAF in %)	Estimate (SE) (fl)	p Value	Variance Explained
rs12485738	3	56840816								
KORA 500K F3			A	G	98.6	0.706	1,584 (36.03)	0.019 (0.0038)	8.57×10^{-7}	1.52%
UKBS-CC1					99.9	0.449	1,219 (36.30)	0.017 (0.0043)	5.61×10^{-5}	1.27%
KORA S4					94.8	2.2×10^{-16}[a]	4,137 (30.14)	0.015 (0.0022)	4.02×10^{-13}	1.11%
SHIP					96.2	0.2922	3,024 (36.97)	0.012 (0.0024)	6.31×10^{-7}	0.87%
Combined[b]							9,964	0.015 (0.0014)	3.81×10^{-27}	
rs7961894	12	120849966								
KORA 500K F3			A	G	99.7	0.013	1,602 (11.92)	0.040 (0.0059)	2.09×10^{-11}	2.77%
UKBS-CC1					100.0	0.685	1,220 (11.32)	0.033 (0.0063)	3.04×10^{-7}	1.90%
KORA S4					97.9	0.937	4,070 (11.18)	0.034 (0.0037)	7.26×10^{-20}	2.04%
SHIP					98.2	0.3628	3,142 (11.14)	0.028 (0.0036)	2.61×10^{-14}	1.84%
Combined[b]							10,034	0.032 (0.0022)	7.24×10^{-48}[c]	
rs2138852	17	24727475								
KORA 500K F3			C	T	99.9	1.000	1,605 (49.33)	−0.017 (0.0037)	3.31×10^{-6}	1.34%
UKBS-CC1					99.5	0.307	1,220 (47.80)	−0.018 (0.0041)	1.62×10^{-5}	1.38%
KORA S4					99.8	0.5329	4,139 (47.17)	−0.018 (0.0023)	1.57×10^{-14}	1.42%
SHIP					96.2	0.1123	3,084 (48.21)	−0.011 (0.0024)	1.70×10^{-6}	0.74%
Combined[b]							10,048	−0.015 (0.0014)	7.19×10^{-28}	

Effect sizes (estimates and SE) are given for each copy of the minor allele and are expressed as natural logarithm of MPV.

[a] Violation of HWE equilibrium, also after regenotyping.

[b] No study heterogeneity (I2 range 0–43, p values > 0.05).

[c] The p value excluding the KORA S4 sample ($n = 5964$) is 1.087×10^{-29}.

analysis platforms with the Coulter-method (KORA, UKBS-CC1) or light scatter analysis (Sysmex SE-9000, SHIP). However, this fact may be negligible for the analysis, provided that the values are not differentially variable over the range. An internal comparison of the methods carried out in the SHIP project resulted in the regression equation Y (fl Sysmex SE-9000) = 1.000*X (fl Coulter-method) + 1.850, indicating that all values are shifted by the constant value of 1.850 upwards. We carried out an analysis corrected with MPV values for SHIP and found rather higher effect estimates for all three SNPs. We decided to use the conservative uncorrected values resulting in a slight underestimation of the effects.

Because the lead SNP in *WDR66* reached the best p value and accounted for about 2.0% of the MPV variance, we decided to analyze the coding sequence of *WDR66* in more detail (Tables S4 and S5). High-resolution melting analysis was used as mutation scanning technology to analyze the coding region of *WDR66*. *WDR66* exons were PCR amplified with intronic primers with ~5 ng genomic DNA with a final denaturation step at 94°C for 1 min (0.25 units Thermo-Start Taq DNA polymerase [Abgene], 1× LCGreen Plus [BIOKE], 0.25 μM of each primer; Table S5). High-resolution melting analysis was performed on a LightScanner instrument (Idaho Technology). In the presence of the saturating double-stranded DNA-binding dye, amplicons were slowly heated from 77°C until fully denatured (96°C) while the fluorescence was monitored. Melting curves were analyzed by LightScanner software (Idaho Technology), with normalized, temperature-shifted curves displayed as difference plots (−dF/dT). Detected samples with altered melting curves compared with the average of multiple wild-types were directly sequenced with a BigDye Cycle sequencing kit (Applied Biosystems).

We analyzed the sequence of all 21 coding exons and the 5′ UTR in 382 samples selected from the high and low extremes of the MPV distribution in 4000 individuals (KORA S4). We found variants or variation in 4 of the 9 coding SNPs, which were already annotated in dbSNP. None of these showed an association with MPV, but the A allele of the lead SNP rs7961894 was overrepresented in the high-MPV group ($p = 1.3 \times 10^{-6}$, Fisher's exact test for allele distribution, Figure 2; more detailed information in Table S4). In addition, we detected 10 nonsynonymous SNPs, one nonsense and five synonymous variants, a 15 bp and an 18 bp insertion, one 3′ UTR SNP and one SNP (C → T) a single bp upstream of the UCSC annotated 5′ end of the *WDR66* transcript (see Table S4). The latter variant (ss107795092) with a minor allele frequency (MAF) of 3.6% falls within a conserved region (LOD = 24, phastCons program) and is significantly overrepresented in the low-MPV group ($p = 6.8 \times 10^{-5}$). This variant is linked ($r^2 > 0.9$, see Table S6) with three other newly discovered coding SNPs (ss107795081-3, p.C304C, p.V307I, and p.R417Q) and they define—in the background of the G allele of the lead SNP rs7961894—a rare haplotype (MAF 2.5%). This haplotype may contribute to the significant association of rs7961894 with MPV, but the strongest association was found for the lead SNP followed by ss107795092 alone.

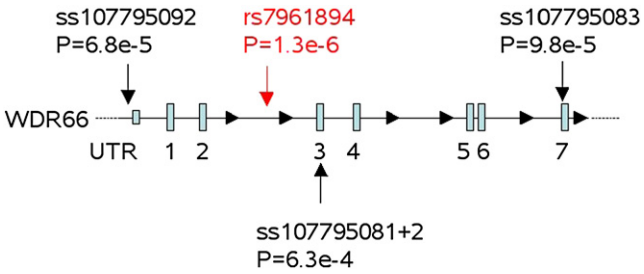

Figure 2. Localization of MPV-Associated SNPs within the 5′ Part of the *WDR66* Gene

The p values given are based on Fisher's exact test in 382 samples from the most extreme (high and low) MPV distribution in KORA S4.

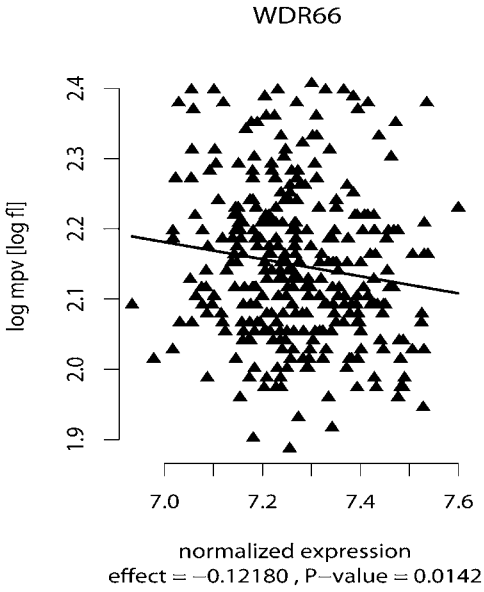

Figure 3. Expression Analysis of *WDR66* and Association with Log MPV

WDR66 expression was analyzed via whole-blood genome-wide transcription profiling in a subgroup of 323 KORA F3 samples with Illumina Human-6 v2 Expression BeadChip (probe ID 2630343).

The strong correlation of the SNP prompted us to investigate the transcript levels of *WDR66* in a randomly selected subgroup of 323 KORA F3 samples with whole-genome expression profiles available. Gene-expression analysis was performed with the Illumina Human-6 v2 Expression BeadChip as described in Döring et al.[10] In brief, blood samples were collected under fasting conditions in PAXgene (TM) Blood RNA tubes (PreAnalytiX) and RNA extraction was performed with the PAXgene Blood RNA Kit (QIAGEN). RNA was reverse transcribed and biotin-UTP labeled with the Illumina TotalPrep RNA Amplification Kit (Ambion). The raw data were exported from the Illumina "Beadstudio" Software to R, converted into logarithmic scores, and normalized.[10] We observed no association between intronic lead SNP rs7961894 and WDR66 transcript level, but a significant association of the levels of the *WDR66* transcript with MPV ($p = 0.01$, Figure 3) via the linear regression model. In addition, we looked at correlation between gene expression and genotypes for the other two lead SNPs and found no significant association. Based on the small samples size for the expression studies, the analysis has a limited power. However, the lacking association between the intronic SNP and WDR expression argues against a direct effect on WDR66 expression. On the other side, the correlation of WDR66 expression with MPV supports the hypothesis that WDR66 is involved in the determination of MPV.

In summary, we identified three loci associated with MPV, a quantitative trait that is increasingly recognized as being associated with the post-MI event risk of major complications. These three loci accounted for about 5% of the variance in MPV values in the normal population. All three genes are plausible biological candidates that could modify the process of platelet formation. The process of proplatelet formation is critically dependent on reorganization of cytoskeletal components and localized apoptosis seems to play an important role.[5,14] WD-repeat proteins are present in all eukaryotes but not in prokaryotes. It is hypothesized that they are involved in the regulation of cellular functions ranging from signal transduction and transcription regulation to cell-cycle control and apoptosis.[15] Our expression experiment indicates a direct correlation of *WDR66* transcript level and MPV. Previous studies have shown that *ARHGEF3* (*XPLN*), which encodes the rho guanine-nucleotide exchange factor 3 (RhoGEF3), is expressed in the brain, skeletal muscle, heart, kidney, and platelets as well as macrophage and neuronal cell tissues.[16] RhoGEFs activate RhoGTPases, which play an important role in many cellular processes such as regulation of cell morphology, cell aggregation, cytoskeletal rearrangements, and transcriptional activation.[17]

TAOK1, which is expressed in a wide variety of different tissues that include brain, heart, lung, testis, skeletal muscle, placenta, thymus, prostate, and spleen, encodes the TAO kinase 1 peptide (hTAOK1 also known as MARKK or PSK2) a microtubule affinity-regulating kinase that has been identified recently as an important regulator of mitotic progression, required for both chromosome congression and checkpoint-induced anaphase delay.[18] TAOK1 activates c-Jun N-terminal kinase (JNK) and induces apoptotic morphological changes that include cell contraction, membrane blebbing, and apoptotic body formation.[19]

In conclusion, to our knowledge we identified the first three quantitative trait loci associated with MPV in the general population. Identification of primary genetic determinants of MPV may not only enhance our understanding of platelet activation and function, but may also provide a focus for several novel research avenues.

Supplemental Data

Supplemental Data include one figure and six tables and can be found with this article online at http://www.ajhg.org/.

Acknowledgments

The MONICA/KORA Augsburg studies were financed by the Helmholtz Zentrum München, German Research Center for Environmental Health, Neuherberg, Germany, and supported by grants from the German Federal Ministry of Education and Research (BMBF). Part of this work was funded by the German National Genome Research Network (NGFN) and the European Union-sponsored project Cardiogenetics (LSH-2005-037593). Our research was supported within the Munich Center of Health Sciences (MC Health) as part of LMUinnovativ. SHIP is part of the Community Medicine Research net (CMR) of the University of Greifswald, Germany, which is funded by the Federal Ministry of Education and Research, the Ministry of Cultural Affairs, as well as the Social Ministry of the Federal State of Mecklenburg-West Pomerania. The SHIP genotyping was supported by the future fund of the state government of Mecklenburg-Vorpommern (UG 07 034). The establishment and genotyping of the UKBS-CC1 collection was funded by the Wellcome Trust and by a National Institutes of Health Research Grant to NHSBT. We thank the staff of the DNA Collections and Genotyping Facilities at the Wellcome Trust Sanger Institute for sample preparation. We gratefully acknowledge the contribution of G. Eckstein, T. Strom and K. Heim, A. Löschner, R. Hellinger, and all other members of the Helmholtz Zentrum München genotyping staff in generating and analyzing the SNP and RNA data set and G. Fischer and B. Kühnel for data management and statistical analyses. We thank all members of field staffs who were involved in the planning and conduct of the MONICA/KORA Augsburg, UKBS-CC1, and SHIP studies. Finally, we express our appreciation to all study participants. No conflict of interest relevant to this article was reported.

Received: September 30, 2008
Revised: November 14, 2008
Accepted: November 21, 2008
Published online: December 24, 2008

Web Resources

The URLs for data presented herein are as follows:

Genome browser, http://genome.ucsc.edu/
Markov Chain Haplotyping Package, http://www.sph.umich.edu/csg/abecasis/mach/
METAL Package, http://www.sph.umich.edu/csg/abecasis/Metal.index.html
Online Mendelian Inheritance in Man (OMIM), http://www.ncbi.nlm.nih.gov/Omim/
The R project for Statistical Computing, http://www.r-project.org/
Sequenom, http://www.sequenom.com
SNP database, http://www.ncbi.nlm.nih.gov/SNP/

References

1. Davi, G., and Patrono, C. (2007). Platelet activation and atherothrombosis. N. Engl. J. Med. *357*, 2482–2494.
2. Tsiara, S., Elisaf, M., Jagroop, I.A., and Mikhailidis, D.P. (2003). Platelets as predictors of vascular risk: is there a practical index of platelet activity? Clin. Appl. Thromb. Hemost. *9*, 177–190.
3. Martin, J.F., Bath, P.M., and Burr, M.L. (1992). Mean platelet volume and myocardial infarction. Lancet *339*, 1000–1001.
4. Bath, P., Algert, C., Chapman, N., Neal, B., and PROGRESS Collaborative Group.. (2004). Association of mean platelet volume with risk of stroke among 3134 individuals with history of cerebrovascular disease. Stroke *35*, 622–626.
5. Kaushansky, K. (2008). Historical review: megakaryopoiesis and thrombopoiesis. Blood *111*, 981–986.
6. Garner, C., Tatu, T., Reittie, J.E., Littlewood, T., Darley, J., Cervino, S., Farrall, M., Kelly, P., Spector, T.D., and Thein, S.L. (2000). Genetic influences on F cells and other hematologic variables: a twin heritability study. Blood *95*, 342–346.
7. Mahaney, M.C., Brugnara, C., Lease, L.R., and Platt, O.S. (2005). Genetic influences on peripheral blood cell counts: a study in baboons. Blood *106*, 1210–1214.
8. Löwel, H., Döring, A., Schneider, A., Heier, M., Thorand, B., Meisinger, C., and MONICA/KORA Study Group.. (2005). The MONICA Augsburg surveys—basis for prospective cohort studies. Gesundheitswesen *67* (*Suppl 1*), S13–S18.
9. Wichmann, H.E., Gieger, C., Illig, T., and MONICA/KORA Study Group.. (2005). KORA-gen–resource for population genetics, controls and a broad spectrum of disease phenotypes. Gesundheitswesen *67* (*Suppl 1*), S26–S30.
10. Döring, A., Gieger, C., Mehta, D., Gohlke, H., Prokisch, H., Coassin, S., Fischer, G., Henke, K., Klopp, N., Kronenberg, F., et al. (2008). SLC2A9 influences uric acid concentrations with pronounced sex-specific effects. Nat. Genet. *40*, 430–436.
11. Wellcome Trust Case Control Consortium. (2007). Genome-wide association study of 14,000 cases of seven common diseases and 3,000 shared controls. Nature *447*, 661–678.
12. John, U., Greiner, B., Hensel, E., Lüdemann, J., Piek, M., Sauer, S., Adam, C., Born, G., Alte, D., Greiser, E., et al. (2001). Study of Health In Pomerania (SHIP): a health examination survey in an east German region: objectives and design. Soz. Praventivmed. *46*, 186–194.
13. Purcell, S., Neale, B., Todd-Brow, K., Thomas, L., Ferreira, M.A., Bender, D., Maller, J., Sklar, P., de Bakker, P.I., Daly, M.J., et al. (2007). PLINK: a toolset for whole-genome association and population-based linkage analysis. Am. J. Hum. Genet. *81*, 559–575.
14. Chang, Y., Bluteau, D., Debili, N., and Vainchenker, W. (2007). From hematopoietic stem cells to platelets. J. Thromb. Haemost. (*Suppl 1*), 318–327.
15. Neer, E.J., Schmidt, C.J., Nambudripad, R., and Smith, T.F. (1994). The ancient regulatory-protein family of WD-repeat proteins. Nature *371*, 297–300.
16. Arthur, W.T., Ellerbroek, S.M., Der, C.J., Burridge, K., and Wennerberg, K. (2002). XPLN, a guanine nucleotide exchange factor for RhoA and RhoB, but not RhoC. J. Biol. Chem. *277*, 42964–42972.
17. Thiesen, S., Kübart, S., Ropers, H.H., and Nothwan, H.G. (2000). Isolation of two novel human RhoGEFs, ARHGEF3 and ARHGEF4, in 3p13–21 and 2q22. Biochem. Biophys. Res. Commun. *273*, 364–369.
18. Draviam, V.M., Stegmeier, F., Nalepa, G., Sowa, M.E., Chen, J., Liang, A., Hannon, G.J., Sorger, P.K., Harper, J.W., and Elledge, S.J. (2007). A functional genomic screen identifies a role for TAO1 kinase in spindle-checkpoint signalling. Nat. Cell Biol. *9*, 556–564.
19. Zihni, C., Mitsopoulos, C., Tavares, I.A., Baum, B., Ridley, A.J., and Morris, J.D. (2007). Prostate-derived sterile 20-like kinase 1-alpha induces apoptosis. JNK- and caspase-dependent nuclear localization is a requirement for membrane blebbing. J. Biol. Chem. *282*, 6484–6493.

OPEN ACCESS Freely available online

PLoS GENETICS

Genome-Wide Scan on Total Serum IgE Levels Identifies *FCER1A* as Novel Susceptibility Locus

Stephan Weidinger[1,2☯*], Christian Gieger[3,4☯], Elke Rodriguez[2], Hansjörg Baurecht[2,5], Martin Mempel[1,2], Norman Klopp[3], Henning Gohlke[3], Stefan Wagenpfeil[5,6], Markus Ollert[1,2], Johannes Ring[1], Heidrun Behrendt[2], Joachim Heinrich[3], Natalija Novak[7], Thomas Bieber[7], Ursula Krämer[8], Dietrich Berdel[9], Andrea von Berg[9], Carl Peter Bauer[10], Olf Herbarth[11], Sibylle Koletzko[12], Holger Prokisch[13,14], Divya Mehta[13,14], Thomas Meitinger[13,14], Martin Depner[12], Erika von Mutius[12], Liming Liang[15], Miriam Moffatt[16], William Cookson[16], Michael Kabesch[12], H.-Erich Wichmann[3,4], Thomas Illig[3]

1 Department of Dermatology and Allergy, Technische Universität München, München, Germany, **2** Division of Environmental Dermatology and Allergy, Helmholtz Zentrum München, Neuherberg and ZAUM-Center for Allergy and Environment, Technische Universität München, München, Germany, **3** Institute of Epidemiology, Helmholtz Zentrum München, German Research Center for Environmental Health, Neuherberg, Germany, **4** Institute of Medical Informatics, Biometry and Epidemiology, Ludwig-Maximilians-Universität München, München, Germany, **5** IMSE Institute for Medical Statistics and Epidemiology, Technische Universität München, München, Germany, **6** Graduate School of Information Science in Health (GSISH), Technische Universität München, München, Germany, **7** Department of Dermatology and Allergy, University of Bonn, Bonn, Germany, **8** IUF–Institut für Umweltmedizinische Forschung at the Heinrich-Heine-University, Düsseldorf, Germany, **9** Marien-Hospital, Wesel, Germany, **10** Department of Pediatrics, Technische Universität München, München, Germany, **11** Department of Human Exposure Research and Epidemiology, UFZ–Centre for Environmental Research Leipzig, Leipzig, Germany, **12** University Children's Hospital, Ludwig-Maximilians-Universität München, München, Germany, **13** Institute of Human Genetics, Helmholtz Zentrum München, German Research Center for Environmental Health, Neuherberg, Germany, **14** Institute of Human Genetics, Klinikum rechts der Isar, Technische Universität München, München, Germany, **15** Center for Statistical Genetics, Department of Biostatistics, School of Public Health, Ann Arbor, Michigan, United States of America, **16** National Heart and Lung Institute, Imperial College London, London, United Kingdom

Abstract

High levels of serum IgE are considered markers of parasite and helminth exposure. In addition, they are associated with allergic disorders, play a key role in anti-tumoral defence, and are crucial mediators of autoimmune diseases. Total IgE is a strongly heritable trait. In a genome-wide association study (GWAS), we tested 353,569 SNPs for association with serum IgE levels in 1,530 individuals from the population-based KORA S3/F3 study. Replication was performed in four independent population-based study samples (total n = 9,769 individuals). Functional variants in the gene encoding the alpha chain of the high affinity receptor for IgE (*FCER1A*) on chromosome 1q23 (rs2251746 and rs2427837) were strongly associated with total IgE levels in all cohorts with *P* values of 1.85×10^{-20} and 7.08×10^{-19} in a combined analysis, and in a post-hoc analysis showed additional associations with allergic sensitization ($P=7.78\times10^{-4}$ and $P=1.95\times10^{-3}$). The "top" SNP significantly influenced the cell surface expression of FCER1A on basophils, and genome-wide expression profiles indicated an interesting novel regulatory mechanism of FCER1A expression via GATA-2. Polymorphisms within the *RAD50* gene on chromosome 5q31 were consistently associated with IgE levels (*P* values 6.28×10^{-7}–4.46×10^{-8}) and increased the risk for atopic eczema and asthma. Furthermore, *STAT6* was confirmed as susceptibility locus modulating IgE levels. In this first GWAS on total IgE *FCER1A* was identified and replicated as new susceptibility locus at which common genetic variation influences serum IgE levels. In addition, variants within the *RAD50* gene might represent additional factors within cytokine gene cluster on chromosome 5q31, emphasizing the need for further investigations in this intriguing region. Our data furthermore confirm association of *STAT6* variation with serum IgE levels.

Citation: Weidinger S, Gieger C, Rodriguez E, Baurecht H, Mempel M, et al. (2008) Genome-Wide Scan on Total Serum IgE Levels Identifies *FCER1A* as Novel Susceptibility Locus. PLoS Genet 4(8): e1000166. doi:10.1371/journal.pgen.1000166

Editor: Vivian G. Cheung, University of Pennsylvania, United States of America

Received May 12, 2008; **Accepted** July 15, 2008; **Published** August 22, 2008

Copyright: © 2008 Weidinger et al. This is an open-access article distributed under the terms of the Creative Commons Attribution License, which permits unrestricted use, distribution, and reproduction in any medium, provided the original author and source are credited.

Funding: The study was funded by the German Ministry of Education and Research (BMBF) as part of the National Genome Research Network (NGFN), the Wellcome Trust, the German Ministry of Education and Research (BMBF), and the European Commission as part of GABRIEL (a multidisciplinary study to identify the genetic and environmental causes of asthma in the European Community). Furthermore the study was supported by the Genetic Epidemiological Modelling Center Munich (GEM Munich). The MONICA/KORA Augsburg studies were financed by the Helmholtz Zentrum München, German Research Center for Environmental Health, Neuherberg, Germany and supported by grants from the German Federal Ministry of Education and Research (BMBF). The research was supported within the Munich Center of Health Sciences (MC Health) as part of LMUinnovativ. The GINI/LISA studies were funded by grants of the BMU (for IUF, FKZ 20462296), and Federal Ministry for Education, Science, Research, and Technology (No. 01 EG 9705/2 and 01EG9732; No. 01 EE 9401-4) and additional financial support from the Stiftung Kindergesundheit (Child Health Foundation). S.Weidinger and S.Wagenpfeil are supported by research grants KKF-07/04 and KKF-27/05 of the University Hospital Rechts der Isar, Technische Universität München. The first author in addition is supported by a grant from the Wilhelm-Vaillant-Stiftung.

Competing Interests: The authors have declared that no competing interests exist.

* E-mail: weidinger@lrz.tum.de

☯ These authors contributed equally to this work.

Author Summary

High levels of serum IgE are considered markers of parasite and helminth exposure. In addition, they are associated with allergic disorders, play a key role in anti-tumoral defence, and are crucial mediators of autoimmune diseases. There is strong evidence that the regulation of serum IgE levels is under a strong genetic control. However, despite numerous loci and candidate genes linked and associated with atopy-related traits, very few have been associated consistently with total IgE. This study describes the first large-scale, genome-wide scan on total IgE. By examining >11,000 German individuals from four independent population-based cohorts, we show that functional variants in the gene encoding the alpha chain of the high affinity receptor for IgE (*FCER1A*) on chromosome 1q23 are strongly associated with total IgE levels. In addition, our data confirm association of *STAT6* variation with serum IgE levels, and suggest that variants within the *RAD50* gene might represent additional factors within cytokine gene cluster on chromosome 5q31, emphasizing the need for further investigations in this intriguing region.

Introduction

High levels of IgE have been considered for many years as markers of parasite and helminth exposure to which they confer resistance [1]. In Western lifestyle countries with less contact, however, elevated IgE levels are associated with allergic disorders [2]. Only recently, it has been established that IgE antibodies also play a key role in anti-tumoral defence [3] and are crucial mediators of autoimmune diseases [4], thus challenging the traditional Th1/Th2 dogma.

High total serum IgE levels are closely correlated with the clinical expression and severity of asthma and allergy [5,6]. The regulation of serum IgE production is largely influenced by familial determinants, and both pedigree- and twin-based studies provided evidence of a strong genetic contribution to the variability of total IgE levels [7,8]. Genetic susceptibility of IgE-responsiveness is likely to be caused by a pattern of polymorphisms in multiple genes regulating immunologic responses[9], but so far only very few loci could be established consistently and robustly, most notable *FCER1B*, *IL-13* and *STAT6* [10,11].

Family and case-control studies indicated that total serum IgE levels are largely determined by genetic factors that are independent of specific IgE responses and that total serum IgE levels are under stronger genetic control than atopic disease [8,12,13,14]. An understanding of the genetic mechanisms regulating total serum IgE levels might also aid in the dissection of the genetic basis of atopic diseases. In an attempt to identify novel genetic variants that affect total IgE levels, we conducted a genome-wide association study (GWAS) in 1,530 German adults and replicated the top signals in altogether 9,769 samples of four independent study populations.

Results

Genome-wide Association Scan

For the GWAS 1,530 individuals from the population-based KORA S3/F3 500 K study with available total IgE levels were typed with the Affymetrix 500 K Array Set. For statistical analysis, we selected SNPs by including only high-quality genotypes to reduce the number of false positive signals. A total of 353,569 SNPs passed all quality control measures and were tested for associations with IgE levels. Figure 1 summarizes the results of the KORA S3/F3 500 K analysis. No single SNPs reached genome-wide significance, but the scan pointed to the gene encoding the alpha chain of the high affinity receptor for IgE (*FCER1A*) on chromosome 1 (Figure 1A). Particularly the quantile-quantile-plot of the *P* values illustrates observed significant associations beyond those expected by chance (Figure 1B).

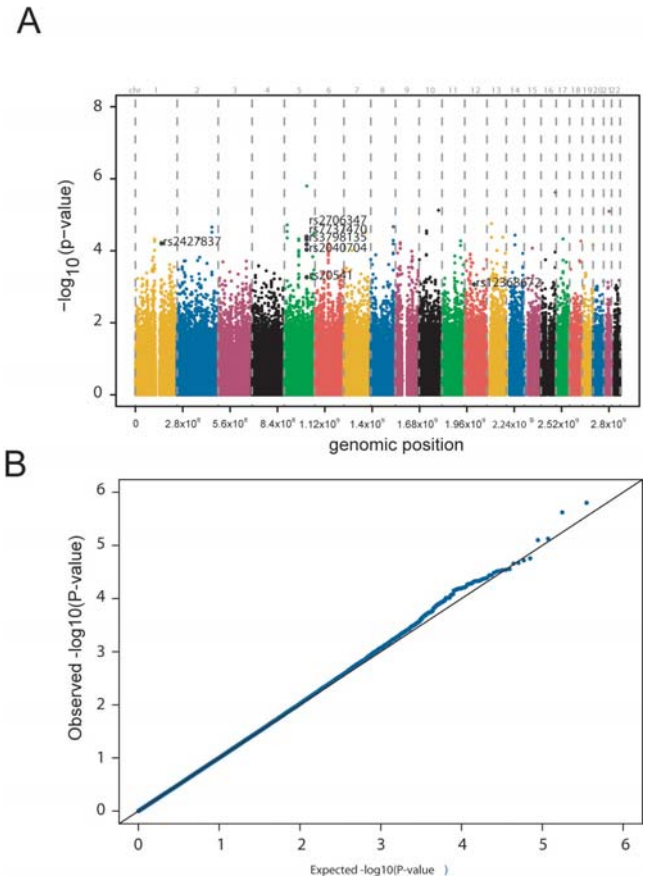

Figure 1. Results of the KORA S3/F3 500 K analysis. a) Genome-wide association study of chromosomal loci for IgE levels: the analysis is based on a population-based sample of 1530 persons. The x-axis represents the genomic position of 353,569 SNPs, and the y-axis shows −log10 (*P* value). b) Quantile-quantile plot of *P* values: Each black dot represents an observed statistic (defined as the −log10(*P* value)) versus the corresponding expected statistic. The line corresponds to the null distribution.
doi:10.1371/journal.pgen.1000166.g001

Replication and Fine-Mapping

For replication in the independent population-based KORA S4 cohort (N = 3,890), we used the following inclusion criteria: (i) $P<10^{-4}$ in the genome wide analysis (39 SNPs, 35 expected); (ii) $P<10^{-3}$ with at least one neighboring SNPs (±100 kb) with $P<10^{-3}$ (45 SNPs). The specific results for all SNPs in the GWAS and KORA S4 are given in supplementary table S3. Six SNPs were significantly associated with total IgE levels in KORA S4 with *P* values ranging from 2.47×10^{-4} to 3.23×10^{-9} (given a Bonferroni-corrected significance level of 5.10×10^{-4}). The strongest associations were observed for rs2427837 ($P=3.23\times10^{-9}$), which is located in the 5′ region of *FCER1A*, and rs12368672 ($P=2.03\times10^{-6}$), which is located in the 5′ region of *STAT6*. In addition, all 4 *RAD50* SNPs which had been selected in the GWAS could be replicated.

Effect estimates of the SNPs in *FCER1A* and *STAT6* were only slightly lower compared to those in the KORA S3/F3 500 K

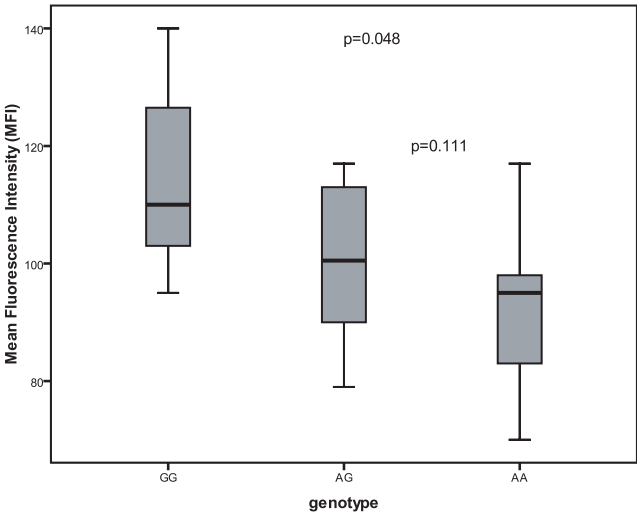

Figure 2. Expression of the FCER1 alpha chain on IgE-stripped basophils. PBMCs were isolated from individuals displaying high sIgE levels and FCER1 alpha chain expression was measured after stripping IgE from its receptor by lactic acid buffer incubation by FACS. Results are expressed as mean fluorescence intensity for FCER1A in the basophile gate. Significance was calculated using the Student's-t-test.
doi:10.1371/journal.pgen.1000166.g002

sample whereas clearly lower effects were observed for the SNPs in *RAD50*. The rare allele "G" of the top ranked SNP rs2427837 in *FCER1A* had an estimated effect per copy of −0.212 based on the logarithm of total IgE. This translates into an estimated decrease of 19.1% in total serum IgE level for the heterozygote genotype and 34.6% for the rare homozygote genotype, which was significantly associated with an increased FCER1A expression on IgE-stripped basophils (Figure 2).

The estimated effect of the *STAT6* SNP rs12368672 was 0.156 resulting in an increase of total IgE of 16.9% and 36.6% for the heterozygote and rare homozygote genotype, respectively. The most significant SNP in the *RAD50* gene (rs2706347) had an effect estimate of 0.143 ($P = 2.26\times10^{-4}$) with an associated increase in total IgE of 15.4% and 33.1%. Altogether the variance of total IgE level explained by genotypes of the three replicated regions was about 1.9%.

To fine-map the regions of strong association in greater detail, we selected additional SNPs covering the *FCER1A* and *RAD50* gene region based on HapMap data from individuals of European ancestry. In addition, two previously described promoter SNPs of *FCER1A* (rs2251746, rs2427827) [15,16], as well as 2 SNPs in the *RAD50* hypersensitive site 7 (RHS7) in intron 24 (rs2240032, rs2214370)[17] were included. In total, 14 SNPs were genotyped in KORA S4. We found the strongest association in the proximal promoter region of the *FCER1A* gene, at rs2251746, which was in strong LD ($r^2 = 0.96$) with rs2427837 (Table 1 and Figure 3). The contribution of the two alleles of rs2251746 in homozygotes and heterozygotes is given in Figure S1. Their effect is observed across the full range of IgE values. The strongest observed association of SNP rs2251746 and the distribution of the SNPs in the region are shown in Figure 3A. None of the *RAD50* SNPs in the fine-mapping showed distinctly stronger association with total IgE (Figure 3B). We additionally sequenced all *FCER1A* exons with adjacent intronic sequences in 48 male and 48 female samples selected equally from the extremes of the serum IgE distribution in 3,890 individuals from the KORA S4 cohort. We identified two new mutations, each present in one individual only, and concurrently confirmed three SNPs already annotated in public databases (dbSNP) with validated minor allele frequencies in Europeans. None of the novel mutations were predicted to have functional consequences (for details see Text S1 and Tables S5 and S6). Haplotype analysis for the *FCER1A* gene showed lower total IgE levels with effect estimates ranging from −0.18 to −0.32 for a haplotype described by the rare "G" allele of rs2427837 and the rare "C" allele of rs2251746 (haplotype frequency 26.4%) in comparison to all other common haplotypes carrying both major alleles (Table S7).

For further replication of the KORA S4 results in the population-based children cohorts GINI (n = 1,839), LISA (n = 1,042) and ISAAC (n = 2,998) the top 6 SNPs: rs2251746, rs2427837, rs2040704, rs2706347, rs3798135, rs7737470 and rs12368672 were tested for association with total serum IgE levels. In GINI, all SNPs except rs12368672 yielded significant *P* values ranging from 0.029 to 8.14×10^{-6}. After correction for multiple testing SNP rs2706347 is slightly above the significance level. In LISA, the two *FCER1A* polymorphisms rs2251746 and rs2427837 were strongly associated ($P = 4.18\times10^{-5}$ and 6.58×10^{-5}), while the *RAD50* SNPs showed consistent trends, but no statistical significance. In ISAAC, the effect estimates of the two *FCER1A* SNPs were distinctly smaller than in the other replication samples but in the same direction and significantly associated with *P* values of 2.11×10^{-4} for rs2251746 and of 4.27×10^{-4} for rs2427837. The *RAD50* SNPs showed effect estimates in concordance with the other replication samples but were only borderline significant. Additional analysis of markers in the *RAD50-IL13* region in a subset of 526 children from the ISAAC replication cohort (for details see Table S9) indicated presence of one linkage disequilibrium (LD) block, which encompasses the entire *RAD50* gene and extends into the promoter region of the *IL13* gene, whereas rs20541 showed low levels of LD with *RAD50* variants (r2<0.3) (Figure S2)

In the combined analysis of all replication samples both selected *FCER1A* SNPs ($P = 1.85\times10^{-20}$ and 7.08×10^{-19} for rs2251746 and rs2427837, respectively) and *RAD50* SNPs ($P = 6.28\times10^{-7}$–4.46×10^{-8}) were significantly associated with IgE levels. Effect estimates were consistent throughout all replication cohorts.

Association Analysis with Dichotomous Traits

In a *post hoc* analysis of the KORA S4 and ISAAC replication cohorts, *FCER1A* polymorphisms rs2251746 and rs2427837 showed association with allergic sensitization ($P = 7.78\times10^{-4}$ and 1.95×10^{-3} in KORA, $P = 0.025$ and 0.032 in ISAAC), while there were no significant associations for the dichotomous traits asthma, rhinitis and atopic eczema (AE). However, the number of cases for these traits was relatively low. We therefore additionally typed a cohort of 562 parent-offspring trios for AE from Germany and a population of 638 asthma cases and 633 controls from UK. In these cohorts we observed weak associations of *RAD50* variants with eczema ($P = 0.007$–0.01) and with asthma ($P = 0.017$–0.002, Table S8).

Discussion

In this large-scale population-based GWAS with follow-up investigations in 9,769 individuals from 4 independent population-based study samples we show that functional variants of the gene encoding the alpha chain of the high affinity receptor for IgE (*FCER1A*) are of major importance for the regulation of IgE levels.

The high affinity receptor for IgE represents the central receptor of IgE-induced type I hypersensitivity reactions such as the liberation of vasoactive mediators including serotonin and

Table 1. Association between total IgE and selected SNPs in the GWAS sample and in the four replication samples.

		GWAS KORA S3/F3			Replication KORA S4			Replication GINI			Replication LISA			Replication ISAAC			Combined		
		n = 1,530			n = 3,890			n = 1,839			n = 1,042			n = 2,998			n = 9,769		
Gene	SNP	Est.	P value	Est. %	Est.	P value	Est. %	Est.	P value	Est. %	Est.	P value	Est. %	Est.	P value	Est. %	Est.	P value	Est. %
FCER1A	rs2511211				−0.206	9.28E-08	−18.59												
FCER1A	rs10489854				0.153	2.85E-02	16.52												
FCER1A	rs2494262				0.122	1.67E-04	12.99												
FCER1A	rs2427837	−0.235	6.19E-05	−20.94	−0.212	3.23E-09	−19.12	−0.219	2.51E-05	−19.64	−0.280	6.58E-05	−24.56	−0.145	4.27E-04	−13.53	−0.202	7.08E-19	−18.27
FCER1A	rs12565775				0.119	2.45E-02	12.56												
FCER1A	rs2427824				0.082	2.52E-02	8.49												
FCER1A	rs3845625				0.085	5.09E-02	8.82												
FCER1A	rs2427827				0.120	2.45E-04	12.72												
FCER1A	rs2251746				−0.227	6.07E-10	−20.29	−0.236	8.14E-06	−20.99	−0.290	4.18E-05	−25.17	−0.153	2.11E-04	−14.16	−0.213	1.85E-20	−19.21
RAD50	rs2069812				−0.052	1.42E-01	−4.98												
RAD50	rs2706347	0.236	4.05E-05	26.62	0.143	2.26E-04	15.43	0.122	2.91E-02	13.02	0.118	1.01E-01	12.56	0.095	2.70E-02	9.96	0.120	6.28E-07	12.80
RAD50	rs6884762				0.034	7.22E-01	3.46												
RAD50	rs17772565				−0.096	2.27E-01	−9.17												
RAD50	rs17772583				−0.058	1.24E-01	−5.62												
RAD50	rs3798135	0.227	6.58E-05	25.48	0.142	2.32E-04	15.20	0.173	2.00E-03	18.91	0.107	1.37E-01	11.26	0.101	1.75E-02	10.64	0.129	6.69E-08	13.82
RAD50	rs2040704	0.221	9.25E-05	24.73	0.140	2.47E-04	14.97	0.158	4.40E-03	17.14	0.111	1.21E-01	11.73	0.112	8.22E-03	11.83	0.130	4.46E-08	13.90
RAD50	rs7737470	0.231	4.81E-05	25.99	0.142	2.27E-04	15.28	0.163	3.70E-03	17.70	0.100	1.64E-01	10.55	0.087	4.13E-02	9.12	0.123	3.35E-07	13.07
RAD50	rs2240032				0.137	4.01E-04	14.67												
RAD50	rs2214370				0.136	5.95E-01	14.54												
STAT6	rs12368672	0.167	8.52E-04	18.18	0.156	2.03E-06	16.93	0.016	7.34E-01	1.65	0.075	2.44E-01	7.78				0.108	1.52E-05	11.44

doi:10.1371/journal.pgen.1000166.t001

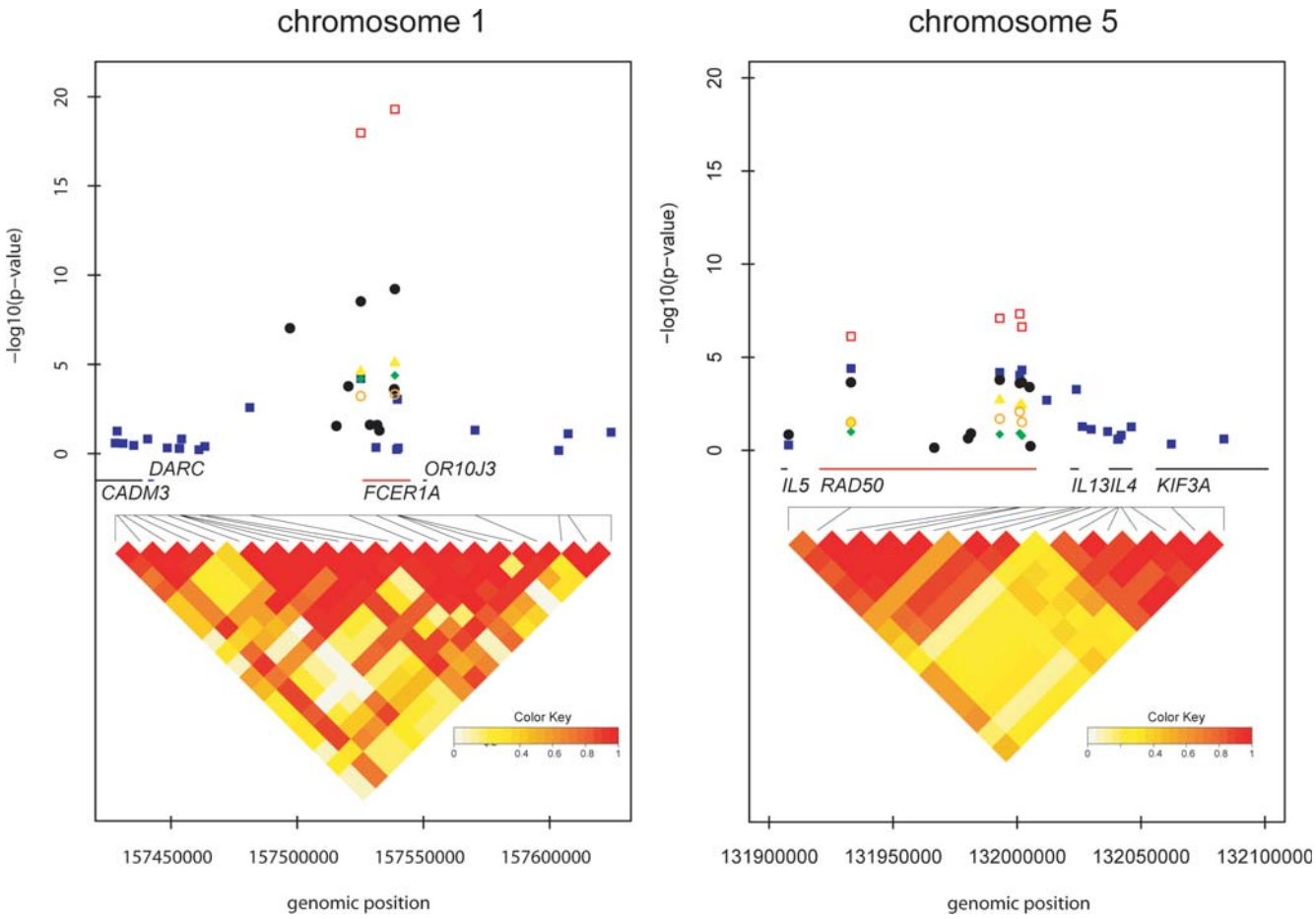

Figure 3. P value and pairwise linkage disequilibrium diagram of the region on chromosome 1q23, area of *FCER1A* (panel A), and chromosome 5q31, area of *RAD50* (panel B). Pairwise LD, measured as D′, was calculated from KORA S3/F3 500 K. Shading represents the magnitude of pairwise LD with a white to red gradient reflecting lower to higher D′ values. Gene regions are indicated by colored bars. *P* value diagram: The x-axis represents the genomic position. The y-axis shows −log10 (*P* values) of KORA S3/F3 500 K (blue), KORA S4 (black), GINI (yellow), LISA (green), ISAAC (orange), combined replication samples (red).
doi:10.1371/journal.pgen.1000166.g003

histamine, but also for the induction of profound immune responses through the activation of NFkappa B and downstream genes [18]. It is usually expressed as a $\alpha\beta\gamma_2$ complex on mast cells and basophils, but additionally as a $\alpha\gamma_2$ complex on antigen-presenting cells (APCs) as shown for dendritic cells and monocytes [18]. Interestingly, in APCs, IgE-recognition of allergens also leads to facilitated allergen uptake via FCER1 and thereby contributes to a preferential activation of Th2-subsets of T-cells. Its expression is substantially influenced by the binding of IgE to either form of the receptor as bound IgE apparently protects the receptor from degradation and thus enhances surface expression without *de novo* protein synthesis. Of note, binding of IgE in the two different complexes only uses the alpha subunit of the receptor lacking contact sites with the beta or gamma subunits. Consequently, the expression level of the alpha subunit is crucial for IgE levels on immune cells [18].

Previous studies suggested linkage of atopy to the gene encoding the β chain of the high-affinity IgE receptor (*FCRER1B*) [19]. FCER1B plays a critical role in regulating the cellular response to IgE and antigen through its capacity to amplify FCER1 signalling and regulate cell-surface expression [18], and there have been several studies which reported an association of *FCER1B* variants and atopy-related traits but conflicting results for total IgE [20,21,22,23,24,25,26,27,28]. In a more recent study, no association between *FCER1B* tagSNPs and IgE levels was observed [22]. The 500 k random SNP array contained only one SNP within as well as 31 SNPs within a 100-kb region around this gene, which were not significantly associated with total IgE. However, we cannot rule out that we missed relevant variants in this gene.

In the present study we identified *FCER1A* as susceptibility locus in a genome-wide association scan and replicated association of the *FCER1A* polymorphism rs2427837 with serum IgE levels in a total of 9,769 individuals from 4 independent population-based cohorts with a combined *P* value of 7.08×10^{-19}. This SNP is in complete LD with the *FCER1A* polymorphism rs2251746, for which we observed a combined *P* value of 1.85×10^{-20}.

Besides the continuous cycling of the IgE receptor subunits from intracellular storage pools to the surface, there is also a substantial expression of the alpha subunit after stimulation with IL-4 which requires *de novo* protein synthesis [18]. This induction is stimulated by the transcription factor GATA-1, which has a binding site in the putative promoter region of the *FCER1A* gene. Notably, in a previous study with Japanese individuals it could be shown that the minor allele of the polymorphism rs2251746 is associated with higher FCER1A expression through enhanced GATA-1 binding [15]. In line with this we observed an increased cell surface expression of FCER1A on IgE-stripped basophils from individuals homozygous for the "G" allele at rs2427837 (Figure 2). Analysis of

the correlation of FCER1A expression with IgE levels in 320 KORA samples where whole genome blood expression profiles were available revealed no significant effect. However, FCER1A expression showed a significant dependency on IL-4 ($P = 0.0087$) and GATA-1 expression ($P = 1.4 \times 10^{-4}$), confirming the known stimulation pathway. Interestingly, we found a highly significant dependency of FCER1A expression on GATA-2 transcript levels ($p = 7.8 \times 10^{-27}$). While whole blood expression levels could easily obscure the situation in basophils, this finding might indicate a novel regulatory mechanisms of FCER1A expression via GATA-2 [18].

The large (>50 kb) *RAD50* gene, which encodes an ubiquitously expressed DNA repair protein, is located within the Th2-cytokine locus on chromosome 5q31, which has been linked with total IgE [29]. It contains multiple conserved non-coding sequences with presumed regulatory function [30]. Remarkably, evidence has been provided for the presence of a locus control region (LCR) within a 25 kb segment of the 3′ region of this gene, which plays an important role in the regulation of Th2 cytokine gene transcription [31]. The core of this LCR is constituted by four *RAD50* hypersensitive sites (RHS) in intron 21 (RHS4-6) and 24 (RHS7) [17,32,33]. The finding of an association between *RAD50* variants and IgE levels is new and biologically compelling. However, it has to be considered that so far *RAD50* has not emerged as candidate, but that several known candidate genes for atopy-related traits map to this region with strong linkage disequlibrium, especially *IL13*, which is one of the strongest and widely replicated candidate genes [10,11]. Notably, two functional *IL13* polymorphisms, *IL13*-1112CT (rs1800925) in the promoter region and *IL13*+2044GA (*IL13* Arg130Gln, rs20541) in Exon 4, have been shown to be associated with a range of atopy-related disorders. *IL13*+2044GA (rs20541) did not pass our selection criteria, and *IL13*-1112CT (rs1800925) is not contained in the Affymetrix 500 K Array Set. Additional analysis of markers in this region including these two SNPs showed one LD block encompassing the entire *RAD50* gene and extending into the *IL13* promoter region, whereas rs20541 showed low levels of LD with *RAD50* SNPs (Figure S2). Thus, we cannot reliably differentiate the specific source of the signal between *RAD50* and *IL13* in our data. Functional studies are needed to assess whether *RAD50* is a true causal gene and to identify the causal genetic variants modulating IgE levels in this region.

The identification and positive replication of the *STAT6* locus, which is located in one of the most frequently identified genomic regions linked to atopy-related phenotypes [34], serves as positive control for the experiment. Our results confirm previous candidate studies which showed that genetic variants in the gene encoding STAT6, a key regulatory element of the TH2 immune response, contribute to the regulation of total serum IgE [35,36].

Other previously reported candidate genes for total IgE showed no or only weak signals in our genome-wide scan (Tables S10 and S11). However, it has to be considered that there are only very few genes that have been associated in the first place to IgE such as *STAT6*, whereas most reported candidate genes for total IgE were investigated in asthma or eczema cohorts [10,11]. In addition, there have been queries with regard to replication for many of the genes reported. Thus, our data obtained in a population-based and ethnically homogeneous sample (South German Caucasians) are not readily comparable with previous candidate gene studies. Furthermore some previously implicated variants were covered insufficiently by the 500 k random SNP array (Table S10).

In summary, in this first GWAS on total IgE *FCER1A* was identified and replicated as new susceptibility locus at which common genetic variation influences serum IgE levels. In addition, our data suggest that variants within the *RAD50* gene might represent additional factors within cytokine gene cluster on chromosome 5q31, emphasizing the need for further investigations in this intriguing region.

Methods

Subjects and Study Design

A detailed description of the GWAS population and the replication samples is given in Text S1 and Table S1. In all studies informed consent has been given, and all studies have been approved by the local ethical committees. The participants were of European origin.

KORA S3/F3 500 K and Replication Sample KORA S4

The study population for the GWAS (KORA S3/F3 500 K) and the first replication cohort were recruited from the KORA S3 and S4 surveys. Both are independent population-based samples from the general population living in the region of Augsburg, Southern Germany, and were examined in 1994/95 (KORA S3) and 1999/2001 (KORA S4). The standardized examinations applied in both surveys have been described in detail elsewhere [37]. In the KORA S3 study 4,856 subjects (participation rate 75%), and in KORA S4 in total 4,261 subjects have been examined (participation rate 67%). 3,006 subjects participated in a follow-up examination of S3 in 2004/05 (KORA F3). For KORA S3/F3 500 K we selected 1,644 subjects of these participants in the age range 25 to 69 years including 1,530 individuals with total IgE level available. From KORA S4, DNA samples from 3,890 individuals with total IgE level were available. Total and specific IgE antibodies to aeroallergens (S×1) were measured using RAST FEIA CAP system (Pharmacia, Freiburg, Germany). Specific sensitization was defined as specific IgE levels ≥0.35KU/l (CAP class > = 1).

GINI and LISA Replication Samples

GINI (German Infant Nutritional Intervention Program) and LISA (Influences of lifestyle-related factors on the immune system and the development of allergies in childhood study) are two ongoing population-based birth cohorts conducted in Germany. A detailed description of screening and recruitment has been provided elsewhere [38]. Briefly, the GINI birth cohort comprises 5,991 newborns, who were recruited between January 1996 and June 1998 in 16 maternity wards in Wesel and Munich, Germany. Children with a positive medical history of atopic disease were invited to a randomized clinical trial with hydrolyzed formulae [39]. The LISA birth cohort study includes 3,097 neonates who were recruited between December 1997 and January 1999 in Munich, Leipzig and Wesel, Germany. Blood samples were collected from 1,962 (51%) and 1,193(50%) children from the GINI and LISA study, respectively, at age 6. Total IgE was determined by standardized methods with CAP-RAST FEIA (Pharmacia Diagnostics, Freiburg, Germany).

ISAAC Replication Sample

Between 1995 and 1996, a cross sectional study was performed in Munich and in Dresden, Germany as part of the International Study of Asthma and Allergy in Childhood phase II (ISAAC II) to assess the prevalence of asthma and allergies in all schoolchildren attending 4th class in both cities (age 9 to 11 years) [40]. Serum measurements for total and specific IgE were performed according to standardized procedures as previously described [40]. Allergic sensitization was defined as positive prick test reaction to at least one out of six common aeroallergens. Within the study population

of 5,629 children, all children of German origin with DNA and total IgE level available were included in this analysis (n = 2,998).

KORA S3/F3 500 K Genotyping and Quality Control

Genotyping for KORA S3/F3 500 K was performed using Affymetrix Gene Chip Human Mapping 500 K Array Set consisting of two chips (Sty I and Nsp I). Genomic DNA was hybridized in accordance with the manufacturer's standard recommendations. Genotypes were determined using BRLMM clustering algorithm. We performed filtering of both conspicuous individuals and single nucleotide polymorphisms (SNPs) to ensure robustness of association analysis. Details on quality criteria are described in Text S1 and Table S2.

SNP Selection for Replication and Fine-Mapping

The power of the replication was estimated for a difference in log total IgE per allele of 0.2 and a nominal significance level of 0.05. The power to detect a true association was above 85% in KORA S4, GINI and ISAAC; whereas in LISA it was about 55%. No single SNPs in the GWAS reached genome-wide significance using a Bonferroni threshold of 1.4×10^{-7}. To fine map the replicated loci in KORA S4 we selected tagging SNPs and used the pairwise tagging algorithm ($r^2>0.8$) implemented in HAPLOVIEW 3.3 (HapMap data release #22, March 2007, on NCBI B36 assembly, dbSNP b126) and additionally selected putative functional SNPs in *FCER1A* and *RAD50*.

SNP Genotyping and Quality Control in the Replication Samples

In all replication samples genotyping of SNPs was realized with the iPLEX (Sequenom San Diego, CA, USA) method by means of matrix assisted laser desorption ionisation-time of flight mass spectrometry method (MALDI-TOF MS, Mass Arraay, Sequenom, San Diego, CA, USA) according to the manufacturers instructions. In KORA S4 for 7 of 84 replicated SNPs a deviation from Hardy-Weinberg-Equilibrium was observed (P value<0.01). In LISA, GINI and ISAAC all replicated SNPs were in HWE. Details on genotyping are described in Text S1 and Table S4.

Mutational Analysis by Cycle Sequencing

FCER1A exons were amplified with intronic primers (Tables S5 and S6) and were directly sequenced using a BigDye Cycle sequencing kit (Applied Biosystems). Genomic DNA (~30 ng) was subjected to PCR amplification carried out in a 15 µl volume containing 1× PCR Master Mix (Promega), 0.25 µM of each forward and reverse primer under the following cycle conditions: initial step at 95°C for 5 min, for 30 cycles at 95°C for 30 s, 58°C (exon 1 62°C) for 30 s, and 72°C for 30 s; and final extension at 72°C for 5 min.

Statistical Analysis of Genetic Effects

In the KORA S3/F3 500 K sample possible population substructures were analyzed (Text S1). Additive genetic models assuming a trend per copy of the minor allele were used to specify the dependency of logarithmic values of total IgE levels on genotype categories. The result is a multiplicative model on the original scale of total IgE with effects interpreted in percental changes. All models were adjusted for gender and in the adult cohorts we adjusted additionally for age. We used a linear regression algorithm implemented in the statistical analysis system R (http://www.r-project.org/) and SAS (Version 9.1.). To select significant SNPs in the genome-wide screening and the replications we used conservative Bonferroni thresholds which corresponded to a nominal level of 0.05. Haplotype reconstruction and haplotype association analysis was performed in the KORA S4 replication sample using the R-library *HaploStats* that allows including all common haplotypes in the linear regression and incorporating age and gender as covariates. The most common haplotype served as reference. Details on haplotype analysis are described in Text S1.

Gene Expression Analysis

Peripheral blood (2.5 ml) was drawn from individuals participating in the KORA study under fasting conditions. The blood samples were collected between 10–12am directly in PAXgene (TM) Blood RNA tubes (PreAnalytiX). The RNA extraction was performed using the PAXgene Blood RNA Kit (Qiagen). RNA and cRNA quality control was carried out using the Bioanalyzer (Agilent) and quantification was done using Ribogreen (Invitrogen). 300–500 ng of RNA was reverse transcribed into cRNA and biotin-UTP labeled using the Illumina TotalPrep RNA Amplification Kit (Ambion). 1,500 ng of cRNA was hybridized to the Illumina Human-6 v2 Expression BeadChip. Washing steps were carried out in accordance with the Illumina technical note # 11226030 Rev. B. The raw data were exported from the Illumina "Beadstudio" Software to R. The data were converted into logarithmic scores and normalized using the LOWESS method [41]. The association between *FCER1A* gene expression (independent variable) and IgE level (dependent variable) was computed using the linear regression model adjusted for gender.

Supporting Information

Figure S1 Box plot comparing the total IgE levels for the genotypes at rs2251746. The x axis represents the three genotype groups: TT (major homozygote), CT (heterozygote) and CC (minor homozygote). The y axis is the total IgE level on a logarithmic scale. Plot was created in R using the box plot function from the graphics package.
Found at: doi:10.1371/journal.pgen.1000166.s001 (0.38 MB TIF)

Figure S2 Patterns of pairwise LD between the SNPs at the RAD50-IL13 locus.
Found at: doi:10.1371/journal.pgen.1000166.s002 (0.03 MB TIF)

Table S1 Description of study populations.
Found at: doi:10.1371/journal.pgen.1000166.s003 (0.05 MB DOC)

Table S2 KORA S3/F3 500K SNP exclusion. Detailed breakdown of SNPs that were monomorphic or did not pass quality control and therefore did not enter analysis.
Found at: doi:10.1371/journal.pgen.1000166.s004 (0.04 MB DOC)

Table S3 Details on the association analysis of SNPs selected for replication (additive model).
Found at: doi:10.1371/journal.pgen.1000166.s005 (0.25 MB DOC)

Table S4 Genotyping details on replication and fine-mapping stages.
Found at: doi:10.1371/journal.pgen.1000166.s006 (0.15 MB DOC)

Table S5 Primers used to amplify the exons of *FCER1A*.
Found at: doi:10.1371/journal.pgen.1000166.s007 (0.04 MB DOC)

Table S6 Mutational analysis of *FCER1A* exons.
Found at: doi:10.1371/journal.pgen.1000166.s008 (0.04 MB DOC)

Table S7 Associations between *FCERA1* haplotypes and IgE levels in KORA S4. Results correspond to the single SNP analyses where presence of A (rs2427837) and C (rs2251746) alleles at respective positions were strongly associated.
Found at: doi:10.1371/journal.pgen.1000166.s009 (0.05 MB DOC)

Table S8 Association analysis of FCERA1 and RAD50 variants with AE in 562 German AE trios and with asthma in 638 UK asthma cases and 633 controls.
Found at: doi:10.1371/journal.pgen.1000166.s010 (0.06 MB DOC)

Table S9 Extended SNP analysis in the RAD50-IL13 region in a subset of 526 children from the ISAAC replication cohort and association with total IgE levels.
Found at: doi:10.1371/journal.pgen.1000166.s011 (0.05 MB DOC)

Table S10 Genes that have been associated with total IgE ordered by their chromosomal position.
Found at: doi:10.1371/journal.pgen.1000166.s012 (0.16 MB DOC)

Table S11 Affymetrix SNPs in selected candidate genes for total IgE, which yielded a nominal p-value <0.05 in the GWAS. Genes are ordered by their chromosomal position.
Found at: doi:10.1371/journal.pgen.1000166.s013 (0.14 MB DOC)

Text S1 Supplementary information.
Found at: doi:10.1371/journal.pgen.1000166.s014 (0.10 MB DOC)

Acknowledgments

We are extremely grateful to all the patients and families who took part in this study, the professionals who helped in recruiting them, and the KORA, ISAAC, GINI and LISA teams, which include interviewers, computer and laboratory technicians, clerical workers, research scientists, volunteers, managers, receptionists and nurses. We also acknowledge the contribution of P. Lichtner, G. Eckstein, T. Strom and K. Heim and other members of the Helmholtz Zentrum München genotyping staff in generating and analyzing the SNP and RNA datasets.

Author Contributions

Conceived and designed the experiments: S Weidinger, N Klopp, T Meitinger, HE Wichmann, T Illing. Performed the experiments: E Rodriguez, M Mempel, N Klopp, H Prokisch, D Mehta. Analyzed the data: S Weidinger, C Gieger, H Baurecht, H Gohlke, S Wagenpfeil, M Depner, L Liang, T Illing. Contributed reagents/materials/analysis tools: S Weidinger, H Gohlke, M Ollert, J Ring, H Behrendt, J Heinrich, N Novak, T Bieber, U Krämer, D Berdel, A von Berg, CP Bauer, O Herbarth, S Koletzko, T Meitinger, E von Mutius, MF Moffatt, W Cookson, M Kabesch, HE Wichmann. Wrote the paper: S Weidinger, C Gieger, MF Moffatt, M Kabesch, T Illing.

References

1. Cooper PJ, Ayre G, Martin C, Rizzo JA, Ponte EV, et al. (2008) Geohelminth infections: a review of the role of IgE and assessment of potential risks of anti-IgE treatment. Allergy 63: 409–417.
2. Gould HJ, Sutton BJ (2008) IgE in allergy and asthma today. Nat Rev Immunol 8: 205–217.
3. Gould HJ, Mackay GA, Karagiannis SN, O'Toole CM, Marsh PJ, et al. (1999) Comparison of IgE and IgG antibody-dependent cytotoxicity in vitro and in a SCID mouse xenograft model of ovarian carcinoma. Eur J Immunol 29: 3527–3537.
4. Dimson OG, Giudice GJ, Fu CL, Van den Bergh F, Warren SJ, et al. (2003) Identification of a potential effector function for IgE autoantibodies in the organ-specific autoimmune disease bullous pemphigoid. J Invest Dermatol 120: 784–788.
5. Limb SL, Brown KC, Wood RA, Wise RA, Eggleston PA, et al. (2005) Adult asthma severity in individuals with a history of childhood asthma. J Allergy Clin Immunol 115: 61–66.
6. Burrows B, Martinez FD, Halonen M, Barbee RA, Cline MG (1989) Association of asthma with serum IgE levels and skin-test reactivity to allergens. N Engl J Med 320: 271–277.
7. Jacobsen HP, Herskind AM, Nielsen BW, Husby S (2001) IgE in unselected like-sexed monozygotic and dizygotic twins at birth and at 6 to 9 years of age: high but dissimilar genetic influence on IgE levels. J Allergy Clin Immunol 107: 659–663.
8. Strachan DP, Wong HJ, Spector TD (2001) Concordance and interrelationship of atopic diseases and markers of allergic sensitization among adult female twins. J Allergy Clin Immunol 108: 901–907.
9. Xu J, Postma DS, Howard TD, Koppelman GH, Zheng SL, et al. (2000) Major genes regulating total serum immunoglobulin E levels in families with asthma. Am J Hum Genet 67: 1163–1173.
10. Vercelli D (2008) Discovering susceptibility genes for asthma and allergy. Nat Rev Immunol 8: 169–182.
11. Ober C, Hoffjan S (2006) Asthma genetics 2006: the long and winding road to gene discovery. Genes Immun 7: 95–100.
12. Dizier MH, Hill M, James A, Faux J, Ryan G, et al. (1995) Detection of a recessive major gene for high IgE levels acting independently of specific response to allergens. Genet Epidemiol 12: 93–105.
13. Lebowitz MD, Barbee R, Burrows B (1984) Family concordance of IgE, atopy, and disease. J Allergy Clin Immunol 73: 259–264.
14. Palmer LJ, Burton PR, Faux JA, James AL, Musk AW, et al. (2000) Independent inheritance of serum immunoglobulin E concentrations and airway responsiveness. Am J Respir Crit Care Med 161: 1836–1843.
15. Hasegawa M, Nishiyama C, Nishiyama M, Akizawa Y, Mitsuishi K, et al. (2003) A novel -66T/C polymorphism in Fc epsilon RI alpha-chain promoter affecting the transcription activity: possible relationship to allergic diseases. J Immunol 171: 1927–1933.
16. Shikanai T, Silverman ES, Morse BW, Lilly CM, Inoue H, et al. (2002) Sequence variants in the FcepsilonRI alpha chain gene. J Appl Physiol 93: 37–41.
17. Lee GR, Spilianakis CG, Flavell RA (2005) Hypersensitive site 7 of the TH2 locus control region is essential for expressing TH2 cytokine genes and for long-range intrachromosomal interactions. Nat Immunol 6: 42–48.
18. Kraft S, Kinet JP (2007) New developments in FcepsilonRI regulation, function and inhibition. Nat Rev Immunol 7: 365–378.
19. Cookson WO, Young RP, Sandford AJ, Moffatt MF, Shirakawa T, et al. (1992) Maternal inheritance of atopic IgE responsiveness on chromosome 11q. Lancet 340: 381–384.
20. Hizawa N, Yamaguchi E, Jinushi E, Kawakami Y (2000) A common FCER1B gene promoter polymorphism influences total serum IgE levels in a Japanese population. Am J Respir Crit Care Med 161: 906–909.
21. Hizawa N, Yamaguchi E, Jinushi E, Konno S, Kawakami Y, et al. (2001) Increased total serum IgE levels in patients with asthma and promoter polymorphisms at CTLA4 and FCER1B. J Allergy Clin Immunol 108: 74–79.
22. Maier LM, Howson JM, Walker N, Spickett GP, Jones RW, et al. (2006) Association of IL13 with total IgE: evidence against an inverse association of atopy and diabetes. J Allergy Clin Immunol 117: 1306–1313.
23. Traherne JA, Hill MR, Hysi P, D'Amato M, Broxholme J, et al. (2003) LD mapping of maternally and non-maternally derived alleles and atopy in FcepsilonRI-beta. Hum Mol Genet 12: 2577–2585.
24. Ulbrecht M, Eisenhut T, Bonisch J, Kruse R, Wjst M, et al. (1997) High serum IgE concentrations: association with HLA-DR and markers on chromosome 5q31 and chromosome 11q13. J Allergy Clin Immunol 99: 828–836.
25. Shirakawa T, Li A, Dubowitz M, Dekker JW, Shaw AE, et al. (1994) Association between atopy and variants of the beta subunit of the high-affinity immunoglobulin E receptor. Nat Genet 7: 125–129.
26. Shirakawa T, Mao XQ, Sasaki S, Enomoto T, Kawai M, et al. (1996) Association between atopic asthma and a coding variant of Fc epsilon RI beta in a Japanese population. Hum Mol Genet 5: 1129–1130.
27. Hoffjan S, Ostrovnaja I, Nicolae D, Newman DL, Nicolae R, et al. (2004) Genetic variation in immunoregulatory pathways and atopic phenotypes in infancy. J Allergy Clin Immunol 113: 511–518.
28. Palmer LJ, Rye PJ, Gibson NA, Moffatt MF, Goldblatt J, et al. (1999) Association of FcepsilonR1-beta polymorphisms with asthma and associated traits in Australian asthmatic families. Clin Exp Allergy 29: 1555–1562.
29. Marsh DG, Neely JD, Breazeale DR, Ghosh B, Freidhoff LR, et al. (1994) Linkage analysis of IL4 and other chromosome 5q31.1 markers and total serum immunoglobulin E concentrations. Science 264: 1152–1156.
30. Loots GG, Locksley RM, Blankespoor CM, Wang ZE, Miller W, et al. (2000) Identification of a coordinate regulator of interleukins 4, 13, and 5 by cross-species sequence comparisons. Science 288: 136–140.
31. Lee GR, Fields PE, Griffin TJ, Flavell RA (2003) Regulation of the Th2 cytokine locus by a locus control region. Immunity 19: 145–153.

A common *FADS2* promoter polymorphism increases promoter activity and facilitates binding of transcription factor ELK1

E. Lattka[1], S. Eggers[1], G. Moeller[2], K. Heim[3], M. Weber[3], D. Mehta[3], H. Prokisch[3, 4], T. Illig*[1], J. Adamski[2,5]

[1] Institute of Epidemiology,

[2] Institute of Experimental Genetics, Genome Analysis Center,

[3] Institute of Human Genetics, Helmholtz Zentrum München, German Research Center for Environmental Health, Neuherberg, Germany

[4] Institute of Human Genetics, Klinikum Rechts der Isar, Technische Universität München, München, Germany

[5] Lehrstuhl für Experimentelle Genetik, Technische Universität München, Freising-Weihenstephan, Germany

* Corresponding author: T. Illig
Helmholtz Zentrum München
German Research Center for Environmental Health
Institute of Epidemiology
Ingolstädter Landstrasse 1
85764 Neuherberg
Germany
Phone: +49-89-3187-4249
Fax: +49-89-3187-4567
Mail: illig@helmholtz-muenchen.de

Running title: Functional analysis of *FADS2* gene polymorphisms

Downloaded from www.jlr.org by on October 23, 2009

Abbreviations: FADS - fatty acid desaturase, HUFA - highly unsaturated fatty acid , SNP - single nucleotide polymorphism, DIP - deletion/insertion polymorphism, LD - linkage disequilibrium, SREBP - sterol regulatory element binding protein, PPAR - peroxisome proliferator activated receptor, TFBS - transcription factor binding site, C20:4n-6 or arachidonic acid - all-cis-5,8,11,14-eicosatetraenoic acid, C22:6n-3 or docosahexaenoic acid - 22:6(ω-3), all-cis-docosa-4,7,10,13,16,19-hexaenoic acid

ASBMB JOURNAL OF LIPID RESEARCH JLR

Downloaded from www.jlr.org by on October 23, 2009

Abstract

Fatty acid desaturases play an important role in the formation of omega-6 and omega-3 highly unsaturated fatty acids (HUFAs). The composition of HUFAs in the human metabolome is important for membrane fluidity and for the modulation of essential physiological functions such as inflammation processes and brain development. Several recent studies reported significant associations of single nucleotide polymorphisms (SNPs) in the human *FADS* gene cluster with HUFA levels and composition. The presence of the minor allele correlated with a decrease of desaturase reaction products and an accumulation of substrates.

We performed functional studies with two of the associated polymorphisms (rs3834458 and rs968567) and showed an influence of polymorphism rs968567 on *FADS2* promoter activity by luciferase reporter gene assays. Electrophoretic mobility shift assays proved allele-dependent DNA-binding ability of at least two protein complexes to the region containing SNP rs968567. One of the proteins binding to this region in an allele-specific manner was shown to be the transcription factor ELK1. These results indicate that rs968567 influences *FADS2* transcription and offer first insights into the modulation of complex regulation mechanisms of *FADS2* gene transcription by SNPs.

Keywords: delta-6 desaturase, fatty acid metabolism, desaturation, single nucleotide polymorphism

Downloaded from www.jlr.org by on October 23, 2009

Introduction

Fatty acids are among other metabolites essential components of the human metabolome. In cells, phospholipids containing highly unsaturated fatty acids (HUFAs) such as arachidonic acid (all-cis-5,8,11,14-eicosatetraenoic acid or C20:4n-6) and docosahexaenoic acid (22:6(ω-3), all-cis-docosa-4,7,10,13,16,19-hexaenoic acid or C22:6n-3) have a positive effect on the fluidity of cell membranes. On the molecular level, HUFAs fulfil several other central functions like acting as second messengers in intracellular signalling pathways or regulating transcription. On the physiological level, HUFAs are important for brain development, acquisition of cognitive behaviours and development of visual functions in early life. In addition, HUFAs are precursors for eicosanoids (leukotriens and prostaglandins) which play an important role in inflammatory processes (1).

The production of HUFAs from dietary fatty acids includes several desaturation and elongation steps. The desaturases involved in this reaction cascade, delta-6 desaturase and delta-5 desaturase, are the rate-limiting enzymes. Both are expressed in the majority of human tissues, with highest levels in liver and to a smaller amount in brain, heart and lung (2, 3). Delta-6 desaturase inserts a double bond at position 6 and after an elongation step, delta-5 desaturase inserts an additional double bond at position 5 of the elongated fatty acid chain. These conversions result in the formation of either arachidonic acid (C20:4n-6) in the omega-6 pathway or of eicosapentaenoic acid (C20:5n-3) in the omega-3 pathway. These molecules are either converted into eicosanoids or further elongated and desaturated, again with the help of the delta-6 desaturase (1). The importance of delta-6 desaturase for the formation of HUFAs and their influence on membrane integrity and fluidity was shown in a recent study by Stoffel et al. who generated a *fads2* -/- mouse (4). In this animal model, membrane polarity of Sertoli and ovarian follicle cells was completely disturbed due to the lack of HUFAs in knockout mice caused by the delta-6 desaturase deficiency. Furthermore, both male and female mice were infertile and eicosanoid synthesis was disturbed. However, the administration of a HUFA-rich diet (either C20:4n-6 or C20:5n-3/C22:6n-3) enabled the *fads2* -/- mice to overcome the genetic defect, restored the fatty acid pattern in membrane lipids and rescued spermatogenesis as well as normal follicle development. Similarly, eicosanoid synthesis was restored by administration of arachidonic acid. Similar effects were observed in another *fads2* -/- mouse by Stroud et al. (5).

These studies showed that the level and composition of HUFAs in the body highly depends on the conversion rate of the delta-6 desaturase, which is in turn regulated by supply with

Downloaded from www.jlr.org by on October 23, 2009

ASBMB JOURNAL OF LIPID RESEARCH

dietary fatty acids and hormone signalling. The effect of dietary fatty acids on desaturase transcription regulation is mediated by two transcription factors, SREBP1 and PPARA (6). The feedback regulation mechanisms by which dietary fatty acids act on SREBP1 processing and stability which in turn influences *FADS2* gene expression have been investigated intensively (7-11). The induction of desaturases by PPARA was shown to occur both by indirect and direct mechanisms (12-15). Besides the mediation of fatty acid effects, SREBP1 may also mediate the insulin effect on *FADS2* gene expression, as was observed in experimentally-induced diabetic rats (16, 17).

Although dietary and hormonal influences seem to play an important role in transcription regulation of delta-6 desaturase, genetic factors are important as well for influencing the level and composition of HUFAs in human tissues. Of special interest is the *FADS* gene cluster on chromosome 11, with a head-to-head orientation of the *FADS1* and the *FADS2* genes, which encode the delta-5 and delta-6 desaturase, respectively. A third putative desaturase gene, *FADS3*, is located in the 6.0 kb telomeric side from the *FADS2* gene in a tail-to-tail orientation (18). Several candidate gene studies reported an association of a number of single nucleotide polymorphisms (SNPs) in the *FADS* gene cluster with fatty acid composition in human tissues (19-22). These results were strengthened recently by our study, which for the first time compared genome-wide SNP data with metabolomics data and replicated the previous findings by this new approach (23). Additionally, several genome-wide association studies meanwhile reported an association of FADS polymorphisms with polyunsaturated fatty acids (24) and more complex lipid traits like low-density lipoprotein, high-density lipoprotein and triglycerides (25-27).

In the first association study (19), the minor alleles of 11 SNPs located in and around the *FADS1* and *FADS2* genes were associated with enhanced levels of desaturase substrates in serum phospholipids. In contrast, levels of desaturase products (especially arachidonic acid, with a genetically explained variance of 28%) were lower. The same significant associations were found for haplotype analyses. This observation speaks for a strong influence of the genetic variants on the activity of the desaturases. Until now, functional data on the described polymorphisms were not available. The aim of this study was to identify causative SNPs within the *FADS1/FADS2* haplotype and we therefore performed functional analyses of polymorphisms in the *FADS2* promoter region to gain insight into regulatory mechanisms of the *FADS2* gene resulting from the presence of these polymorphisms on the transcriptional level. Based on their close proximity to the translation start site of *FADS2*, we selected the one base pair deletion/insertion polymorphism (DIP) rs3834458 (position -942) and the SNP

Downloaded from www.jlr.org by on October 23, 2009

rs968567 (-299). In addition, both polymorphisms are located in a CpG-rich region predicted to contain interesting binding sites for transcription factors known to be involved in fatty acid metabolism such as SREBP1 and PPARA.

ASBMB JOURNAL OF LIPID RESEARCH

Downloaded from www.jlr.org by on October 23, 2009

Material and Methods

Bioinformatic analysis of transcription factor binding sites

The prediction of transcription factor binding sites (TFBS) in promoter sequences was performed using the Genomatix MatInspector software with standard settings for the highest matrix similarity (28). This programme uses a large library of weight matrices based on known *in vivo* binding sites to predict TFBS in nucleotide sequences.

Plasmid constructions

To obtain constructs for luciferase assays, the *FADS2* promoter sequence from position -1014 to -1 relative to the translation start site was amplified by PCR from human genomic DNA. The PCR product was first cloned into the vector pGEM T-Easy (Promega) and then subcloned into the reporter vector pGL4.12 (Promega). Constructs containing all possible combinations of major and minor alleles of rs3834458 (T/Del, position -942) and rs968567 (C/T, position -299) were obtained by PCR mutagenesis. Truncated constructs (containing region -414 to -1 and -214 to -1) were generated by PCR from the original respective plasmids and subsequent cloning into pGL4.12. All constructs were verified by sequencing.

Luciferase reporter assays

HeLa, HEK293 and HepG2 cells were seeded at a density of $1x10^5$ cells per well in 12-well plates in MEM or D-MEM medium with stable L-glutamine (PAA Laboratories), respectively, containing 10% FBS (PAA Laboratories) and 1% penicillin/streptomycin (Gibco) and incubated over night. All cell lines were transfected with 500 ng of the promoter construct per assay using FuGene6 (Roche Diagnostics) according to the manufacturer's instructions in an appropriate ratio of FuGene/DNA. For normalisation, 50 ng of the pGL4.74 vector (Promega), which constitutively expresses *Renilla* luciferase, were cotransfected. Transfected cells were incubated for 32 hours at 37 °C in a 5 % CO_2 atmosphere. Cells were then washed once in PBS buffer before 200 µl of 1X Passive Lysis Buffer (Promega) were added. After gentle shaking for 30 minutes, the plate containing the lysed cells was frozen at -80 °C over night. After thawing, luciferase activity was measured. For this, 50 µl of both Dual Luciferase Reporter Assay System reagents (Promega) were added successively to 20 µl of the lysate according to the manufacturer's instructions. Measurements were done in a Tecan GeniosPro microplate reader. Calculation of the intensity ratios of *Firefly* to *Renilla* luciferase

Downloaded from www.jlr.org by on October 23, 2009

ASBMB JOURNAL OF LIPID RESEARCH JLR

activity resulted in the relative promoter activity of the constructs. The significance of difference in promoter activity between the constructs was tested by independent-samples t-test using the SPSS 16.0 software.

Nuclear protein extraction and electrophoretic mobility shift assays

Confluent HeLa cells grown in T75 flasks were harvested and nuclear proteins were extracted with the NE-PER® Nuclear and Cytoplasmic Extraction Reagents (Pierce) according to the manufacturer's instructions. For electrophoretic mobility shift assays, oligonucleotides containing predicted transcription factor binding sites surrounding the DIP rs3834458 and the SNP rs968567 were designed and purchased from the company Metabion. The oligo sequences are summarised in Table 1. 20 pmol of double-stranded oligos containing either the major or the minor allele were 5'-end labelled with γ-^{32}P-ATP (Hartmann Analytic) and T4 Polynucleotide Kinase (Fermentas) according to the manufacturer's protocol. Unincorporated label was separated from labelled DNA by gel filtration on G-25 columns (GE Healthcare). Binding reaction was carried out with or without different concentrations of unlabelled competitor oligonucleotides using 15 µg of nuclear extract in 1x binding buffer (20 mM Tris/HCl pH 7.9, 50 mM NaCl, 1 mM EDTA, 10 % glycerol, 0.05 % NP40, 2.5 mM DTT) with 1 µg poly dI-dC (Roche Diagnostics) and 20 fmol of labelled probe in a total volume of 20 µl for 30 minutes at room temperature. Protein-DNA complexes were separated on 10 % non-denaturing polyacrylamide gels by electrophoresis in 1x TBE buffer. The gels were dried and radioactivity was visualised by autoradiography on Kodak films.

Gene expression analysis

Correlation analysis of peripheral blood gene expression was performed in 322 KORA F3 samples with whole-genome expression profiles available. A detailed description of the KORA F3 study, which is a population-based study comprising individuals living in the region of Augsburg, has been given elsewhere (29). Gene expression analysis was performed with the Illumina Human-6 v2 Expression BeadChip as described earlier (30). Raw data from the Illumina 'Beadstudio' software were exported to R. Data were logarithmised and normalised using the LOWESS method (31). Associations between the expression of two genes were computed with a linear regression model. Correlations were determined using the Pearson correlation coefficient.

Downloaded from www.jlr.org by on October 23, 2009

ASBMB JOURNAL OF LIPID RESEARCH JLR

DNA affinity purification and immunoblotting

Oligonucleotides for DNA affinity purification contained four repeats of the predicted transcription factor binding sites surrounding SNP rs968567 to ensure maximal binding efficiency (see Table 2). Double-stranded oligonucleotide binding sites were constructed by annealing 26 pmol of complementary single-stranded 5'-end biotinylated oligonucleotides containing the -299 major C allele or the -299 minor T allele in annealing buffer (89.6 mM Tris-HCl pH 9.0, 448.2 mM KCl and 13.4 mM $MgCl_2$). Oligonucleotides with four repeats of an experimentally verified ELK1 binding site were generated accordingly as positive control. Proteins binding to the oligonucleotides were purified using streptavidin-coated Dynabeads M-280 (Invitrogen). Briefly, 26 pmol of double-stranded biotinylated oligonucleotides were coupled to 250 µg (25 µl) of the streptavidin magnetic beads according to the manufacturer's protocol. 50 µg of HeLa nuclear extract were applied to the DNA-magnetic beads complex and incubated in protein binding buffer (4.6 mM Tris-HCl pH 8.0, 18.4 mM KCl, 0.02 % NP-40, 0.37 % glycerol, 4.8 mM DTT, 22.9 µM $ZnSO_4$ with 9.7 mM $MgCl_2$) for 10 minutes at room temperature. Non-specific DNA binding was inhibited by the subsequent addition of 2.5 µg poly[d(I-C)] (Roche) and incubation for additional 20 minutes. Afterwards, the supernatant containing unbound proteins was removed by use of a magnetic separator and the beads with the DNA-protein complexes were washed three times with wash buffer (9.9 mM Tris-HCl pH 8.0, 39.6 mM KCl, 0.05 % NP-40, 0.8 % glycerol, 10 mM DTT, 49.5 µM $ZnSO_4$). Bound proteins were eluted from the magnetic beads by use of a high ionic strength elution buffer (9.5 mM Tris-HCl pH 8.0, 1.9 M KCl, 0.048 % NP-40, 0.76 % glycerol, 10 mM DTT, 47.5 µM $ZnSO_4$ and 10 mM $MgCl_2$), separated on a 10% Tris-tricine SDS-PAGE gel and subsequently blotted onto a PVDF membrane (Pall). Incubation with ELK1 antibody (SC-355 X, Santa Cruz, 1:500 in PBS containing 0.5% milk powder) was carried out at 4°C over night. As secondary antibody, a peroxidase-conjugated goat anti-rabbit IgG (A-6154, Sigma, 1:5000 in PBS containing 0.5% milk powder) was used with an incubation time of one hour at room temperature. Peroxidase reaction was carried out using the Western Lightning Chemiluminescence Reagent Plus (PerkinElmer) and specific ELK1 bands were visualised by exposing Kodak films.

Downloaded from www.jlr.org by on October 23, 2009

Results

Bioinformatic analyses predict the allele-dependent presence of different transcription factor binding sites in the SNP-containing FADS2 promoter regions

Bioinformatic analyses using the Genomatix software predicted transcription factors with the highest core matrix similarities and revealed that our DIP (deletion/insertion polymorphism) of interest (rs3834458, position -942) is located in close proximity to predicted SREBP1 and PPARA binding sites, with the SREBP binding element being 48 bp and the PPAR/RXR binding element 12 bp away. Several other binding sites for transcription factors are predicted for the region containing the DIP rs3834458: C/EBP-beta in 6 bp distance from the DIP, and PAX4/PAX6 and BCL6 directly spanning the -942 position. Interestingly, the BCL6 binding site is only present, when the sequence contains the -942 major T allele, and lost when the deletion mutation is present, because the -942 major T allele is part of the binding site core sequence of BCL6 (Figure 1a and c).

The promoter region surrounding SNP rs968567 (position -299) is also predicted to contain several transcription factor binding sites. Once more, a PPAR/RXR binding site is located in the neighbourhood of the SNP only 12 bp away. Three additional binding sites are predicted for the sequence containing the -299 minor T allele: ELK1, STAT1 and STAT3, which are not present for the -299 major C allele (Figure 1b). Again, the -299 minor T allele is part of the matrix core sequences of all three transcription factor binding sites (Figure 1d).

Luciferase reporter gene assays reveal an influence of SNP rs968567 on promoter activity

To determine the functional effects of the two polymorphisms (rs3834458, T/Del, -942 and rs968567, C/T, -299) on transcriptional regulation, luciferase reporter gene assays were conducted to measure promoter activity (Figure 2). Three different human cell lines (HepG2, HEK293 and HeLa) were transiently transfected with the promoter constructs or the empty reporter vector pGL4.12 as control. Three individual experiments for each construct and cell line were performed and promoter activity was measured in triplicates for each construct and experiment. Luciferase activity was slightly lower for all constructs containing the -942 minor deletion mutation compared to the constructs containing the -942 major T allele. This was a modest statistically not significant effect, however, with a decrease in luciferase activity of around 20 % averaged over all tested cell lines and constructs. The replacement of the -299 major C allele of rs968567 by the -299 minor T allele resulted in a two to three-fold increase of luciferase activity in HeLa and HepG2 cells in full-length as well as truncated constructs.

Downloaded from www.jlr.org by on October 23, 2009

ASBMB JOURNAL OF LIPID RESEARCH

This effect was statistically significant in HepG2 ($p<2.0E-05$) and HeLa ($p<1.0E-6$) cells, but not in HEK293 cells. Altogether, the results indicate a strong regulatory function of polymorphism rs968567 in different cell lines.

Electrophoretic mobility shift assay (EMSA) demonstrates altered DNA-binding ability of nuclear proteins to the FADS2 promoter due to SNP rs968567

Next we asked, if the polymorphisms effect the DNA-binding ability of nuclear proteins. HeLa nuclear protein extracts were subjected to binding to oligonucleotides representing the region surrounding SNP rs968567 with either the -299 major C allele or the -299 minor T allele, and DNA-protein complexes were analysed by electrophoretic mobility shift assays (Figure 3). Specific binding of nuclear protein to the respective oligonucleotide was tested by adding increasing amounts of competing unlabelled oligonucleotide probe, containing the respective other allele. Two bands corresponding to shifted complexes showed different intensity, depending on which allele was present. Both bands showed weaker intensity when the labelled oligonucleotide with the C allele was present, whereas a higher intensity was achieved, when the labelled oligonucleotide contained the T allele. Competition of labelled C allele with unlabelled T allele resulted in a significant decrease of band intensities already at low concentrations of competitor. The upper band was still visible at very high competitor concentrations, whereas the lower band vanished completely. In contrast, competition for protein binding of labelled T allele with unlabelled C allele resulted in slightly decreased band intensities only at high concentrations of competitor. At the highest competitor concentration, the lower band vanished as well, but the upper band was much stronger than in the vice versa competition experiment. These effects were observed in two independent experiments. The results indicate that the -299 T allele increases binding affinity of the tested promoter region for at least two protein complexes. The same experiment was conducted with oligonucleotides containing the major and minor alleles of the rs3834458 polymorphism. Only very weak band intensities, hinting to very weak binding of two nuclear proteins, could be observed and no significant difference of competing effects between oligonucleotides was found (data not shown).

Gene expression analysis shows statistically significant association between expression levels of FADS2 and ELK1

Because we have found a significant impact on promoter activity and binding of nuclear protein complexes only for SNP rs968567 and not for DIP rs3834458, we focused on the

Downloaded from www.jlr.org by on October 23, 2009

ASBMB JOURNAL OF LIPID RESEARCH JLR

region surrounding SNP rs968567 for further characterisation. Prediction of transcription factor binding sites in this region results in three binding sites when the rs968567 minor T allele is present in the sequence: ELK1, STAT1 and STAT3. Regression analysis between *FADS2* whole blood mRNA expression levels and expression levels of these three transcription factors in 322 subjects revealed a statistically significant association between mRNA expression levels of *FADS2* and *ELK1* with a p-value of 2.29E-13 and an effect size of 0.36 (Figure 4 a). No significant p-values were obtained for the correlation of *FADS2* with *STAT1* and *STAT3* expression levels. To test the plausibility of this approach, regression analyses of *FADS2* expression levels with *PPARA* and *SREBP1*, two transcription factors already known to be involved in *FADS2* transcription regulation, were performed as positive controls. The expression levels of both transcription factors were significantly associated with *FADS2* expression (*PPARA*: p=4.22E-12, effect size=0.35 and *SREBP1*: p=2.93E-28, effect size=0.52) and by this proved the reliability of our expression data. We furthermore tested the association between *FADS2* and *ELK1* gene expression dependent on the rs968567 genotype. The effect size of association between *FADS2* and *ELK1* in homozygous carriers of the rs968567 major C allele (n=229) was 0.3 (p=4.13E-8). In heterozygous (CT) and homozygous minor T allele carriers (n=93) it reached 0.36 (p=8.47E-6), and in homozygous minor T allele carriers alone (n=8) the effect size increased to 0.84 (p=0.0055) (Figure 4 b). These results strongly point to ELK1 as a newly identified regulator of *FADS2* gene expression with a higher impact of ELK1 in carriers of the rs968567 minor T allele.

DNA affinity purification with immunoblotting reveals allele-specific binding of ELK1 to the region surrounding SNP rs968567

Our gene expression analyses in a population-based study revealed a significant association between expression levels of *FADS2* mRNA and *ELK1* mRNA in whole blood, with a higher effect size in carriers of the rs968567 minor T allele. Additionally, the Genomatix MatInspector software predicted allele-specific binding of ELK1 to the region surrounding SNP rs968567. We therefore tested the binding of ELK1 protein to the respective sequence by performing DNA affinity purification of nuclear proteins from HeLa nuclear extract using biotinylated oligonucleotides representing the region surrounding SNP rs968567 with either the -299 major C allele or the -299 minor T allele. An oligonucleotide containing an experimentally verified ELK1 binding site (32) was used as positive control. The supernatant and wash fractions containing unbound proteins as well as the elution fraction with the bound proteins were immunoblotted and a specific antibody against human ELK1 was used to detect

Downloaded from www.jlr.org by on October 23, 2009

presence of ELK1 protein in the fractions (Figure 5). A specific band corresponding to ELK1 was present in the elution fraction of the positive control, showing that ELK1 from HeLa nuclear extract is able to bind to its consensus sequence under the used buffer conditions and experimental setup. The appearance of ELK1 in the elution fraction of the -299 minor T allele, which was lacking in the elution fraction of the -299 major C allele, confirms binding of ELK1 to the *FADS2* promoter sequence exclusively when the minor T allele is present.

ASBMB JOURNAL OF LIPID RESEARCH

Downloaded from www.jlr.org by on October 23, 2009

Discussion

Disorders of delta-6 desaturase activity affect essential physiological functions

Recent association studies showed an association of delta-6 and delta-5 desaturase gene polymorphisms with HUFA level and composition in different human tissues, accompanied by an accumulation of desaturase substrates and a decline in desaturase products (19-23). This suggests that the desaturase activity is not only regulated by nutritional and hormonal influences, but also by genetic factors. The observed change of HUFA levels and composition in different human tissues due to the polymorphisms might alter several important physiological processes and is thought to modulate the development of complex diseases. The effect of *FADS* polymorphisms on brain development has been shown by Caspi et al. (33), who reported a modulation of the positive effect of breastfeeding on development of intelligence by polymorphisms in the *FADS* gene cluster in two independent birth cohorts. The importance of an intact delta-6 desaturase function on eicosanoid synthesis and membrane lipid composition was underlined by previous reports of two different *fads2* knockout mice (4, 5). The assumption that there is a direct effect of *FADS* polymorphisms on the outcome of fatty acid-related diseases, has been supported by Schaeffer at al. (19), who reported an association of the *FADS* gene cluster with allergic rhinitis and atopic eczema, however, without statistical significance after correction for multiple testing. Another study recently reported an association of *FADS* genotypes with inflammation and coronary artery disease (34). All these observations hint at a strong role of delta-6 desaturase in regulating fatty acid composition in human tissues to maintain health. Approaches to investigate the influence of genetic polymorphisms on the regulation of the human enzyme activity are therefore needed to understand the role of delta-6/delta-5 desaturases in the development of fatty acid-related complex diseases.

Detection of a critical polymorphism-containing region that influences delta-6 desaturase activity

Many studies have reported associations of several SNPs in the *FADS* gene cluster with HUFA levels and composition in different human tissues and have contributed to the understanding of the influence of SNPs on the regulation of fatty acid synthesis (19-23). However, the causative functional variant(s) are not known up to date. The analysis of linkage disequilibrium (LD) structures in the *FADS* gene cluster suggests that all polymorphisms in this region are in very high linkage disequilibrium and most of them are highly correlated.

Downloaded from www.jlr.org by on October 23, 2009

The real functional variant(s) could therefore cause associations of all other SNPs being in high LD, and cannot be directly identified by association studies for this reason. Functional approaches are needed to determine the effect of the associated SNPs on the molecular level and by this identify the causative variant(s).

By performing luciferase reporter gene assays, we showed that one of the two analysed *FADS2* promoter polymorphisms (rs968567) is located in a region that seems to be important for transcription regulation. While the minor deletion mutation of rs3834458 had only a little, statistically not significant effect on promoter activity, the minor T allele of rs968567 highly increased promoter activity compared to the construct containing both major alleles. The effect was the same in all three tested cell lines, however, the response in HEK293 cells was lower and not statistically significant for both polymorphisms. Because transcription regulation is tissue-dependent (35), this is likely due to the tissue-specific expression pattern of involved transcription factors. In order to investigate if altered binding of transcriptions factors to the polymorphism-containing regions is the cause for the observed effects in the luciferase assays, molecular interactions were analysed by electromobility shift assays. Bioinformatic analyses predicted several putative binding sites in the polymorphism-containing regions, and we consequently checked their functionality for protein binding. Indeed, several protein complexes were shown to bind to the regions of interest by EMSA. In the case of rs968567, a clear allele-specific binding affinity of at least two protein complexes was shown by using a competitive method. The minor T allele of rs968567 facilitated the binding in comparison to the major C allele. No differential binding affinity could be shown for the region containing rs3834458. All these observations speak for a strong influence of the rs968567 polymorphism on transcription regulation of the *FADS2* gene.

Identification of ELK1 as a potential new regulator of FADS2 gene transcription

In this study it was shown that the *FADS2* promoter region surrounding SNP rs968567 exhibits promoter activity, which increases when the major C allele of SNP rs968567 is replaced by the minor T allele. We assumed that this effect could be caused by allele-specific differential binding affinity of transcription factors. An *in silico* analysis of transcription factor binding sites predicted three additional binding sites (ELK1, STAT1 and STAT3) in the sequence when the major C allele of rs968567 was replaced by the minor T allele. This was substantiated by EMSA experiments that revealed allele-specific binding of at least two nuclear protein complexes to this promoter region. Linear regression analysis of whole blood mRNA levels of the predicted transcription factors and expression levels of *FADS2* mRNA

Downloaded from www.jlr.org by on October 23, 2009

resulted in a highly significant association between *ELK1* and *FADS2*, with a much higher effect size in subjects being homozygous for the rs968567 minor T allele. We used the correlation of *PPARA* and *SREBP1* with *FADS2* as positive control, because these two transcription factors are known to activate *FADS2* transcription (1). The significant association results of our positive controls approve reliability of the expression data and substantiate the significant association between *ELK1* and *FADS2*. ELK1 is a member of the ETS domain family of transcription factors, was first cloned in 1989 (36) and is primarily known for its role in the transcriptional regulation of immediate early genes including *c-fos* (37) and *egr-1* (38) by forming ternary complexes with serum response factor on the serum response elements of gene promoters (39). To our knowledge, a role of ELK1 in lipid metabolism has not been reported until now. We tested binding of ELK1 protein to the predicted binding site in the *FADS2* gene promoter by DNA affinity purification and subsequent immunoblotting. Specific ELK1 bands in the elution fraction were only present when the major C allele of SNP rs968567 was replaced by the minor T allele. This effect is in clear accordance with the Genomatix MatInspector prediction and identifies ELK1 as a putative new regulator of *FADS2* gene transcription in an allele-specific manner**.** The fact that correlation analysis between *FADS2* and *ELK1* mRNA expression gives significant results for both alleles (however with lower effect size for the major C allele) suggests that ELK1 also binds to the *FADS2* promoter in the presence of the –299 major C allele, but with lower affinity so that we were not able to detect ELK1 protein in that case in our immunoblotting experiment. Another possibility would be an additional functional ELK1 binding site in another region of the *FADS2* gene, of which several are predicted by Genomatix MatInspector.

Controversial impact of the rs3834458 deletion polymorphism on promoter activity

Nwankwo et al. published a study in 2003 (40), which already dealt with functional investigations of the rs3834458 polymorphism. The authors aimed to identify the molecular mechanism of *FADS2* deficiency in skin fibroblasts from a patient with severe symptoms like corneal ulceration, growth failure, skin abnormalities and photophobia previously shown to be caused by a deficiency of delta-6 desaturase (41). By sequencing the *FADS2* promoter region of DNA derived from patient fibroblasts and comparing the sequence to DNA from three healthy controls, they identified a thymidine insertion in the patient DNA, which corresponds to the T allele of rs3834458. Luciferase reporter gene assays in a mouse fibroblast cell line (NIH/3T3) with promoter sequences derived from patient (T allele present) and healthy

Downloaded from www.jlr.org by on October 23, 2009

control (T deletion) fibroblasts resulted in significantly decreased promoter activity when the T allele was present. This result could not be replicated in neither of our three tested human cell lines. Possible explanations could be that Nwankwo et al. used a mouse fibroblast cell line (NIH/3T3) for their assays, which might express a different set of transcription factors compared to our human cell lines or that another unrecognized polymorphism in the tested sequences caused the effect in the study of Nwankwo et al.

Conclusion and outlook

In this study we showed that polymorphism rs968567 influences *FADS2* gene promoter activity and alters DNA-binding affinity of nuclear proteins. One of the proteins binding to this region in an allele-specific manner was shown to be the transcription factor ELK1. Further experiments are required to completely characterise the interaction of ELK1 with the *FADS2* gene promoter or other functional elements in the gene and its impact on *FADS2* gene expression *in vivo*.

ASBMB JOURNAL OF LIPID RESEARCH JLR

Downloaded from www.jlr.org by on October 23, 2009

Functional validation of complex trait- associated SNPs using transcriptomics

Divya Mehta, Katharina Heim, Thomas Illig, H-E Wichmann, Thomas Meitinger, Holger Prokisch.

Abstract

GWAS have proven to be successful in uncovering genetic risk factors and unraveling new biological pathways, however they have been unable to pinpoint with certainty the causal gene(s) at the observed loci. Furthermore, the mechanisms of action by which associated loci influence disease or other complex traits in most cases remains unclear. Rarely does the associated variant change the coding sequence. In most cases the SNP influences gene activity. Genome-wide association study of gene expression can be used to address this question.

We generated expression profiles from whole blood of 320 KORA individuals with 500k genotypes available. Using these expression profiles, we systematically analyzed all SNPs so far found to be associated with disease or Quantitative Trait Loci for their potential to effect transcription level of the neighboring genes. We compared the results with published lymphocyte cell line data sets (Stranger et al, 2007, Dixon et al, 2008) and liver expression data (Schadt et al, 2008). Altogether, 7.4% of the analyzed loci were found to be regulated by the identified SNP. A substantial overlap of eQTLs between different datasets was observed despite the different tissues of origin and different microarray platforms used in the studies. We have demonstrated that whole blood expression profiles serve as a useful resource to refine loci identified in GWAS and to address the causality of the target loci.

CURRICULUM VITAE

Name: Miss Divya Deepak Mehta

Age - 26

Term address

Haus nummer 2

31 Pariser Strasse

Munich 81667

Germany

Mobile: 0049-17621649800

Email: mehta@mpipsykl.mpg.de , divs5@hotmail.com

Home address

2/42 Nanik Nivas

91-A B.Desai Road

Mumbai – 400 026

India

Tel: 0091- 22-23673421

Nationality: Indian

■ **Education:**

2009-2011	• Postdoctoral researcher, Max Planck Institute of Psychiatry, Munich. • Research Group – Molecular genetics of Depression.
2005-2008	• PhD student, Institute of Human Genetics, GSF/Helmholtz Research Center, Munich. Group of Prof.Dr.Thomas Meitinger. • Project Title – Genome wide association study to search for SNPs (Single Nucleotide Polymorphisms) affecting gene expression in the KORA population.
2003-2004	• Degree- MSc In Human Molecular Genetics, Imperial College of Science, Technology and Medicine, University of London. • Grade: **Ist Class** with **Distinction** in MSc Thesis. **Final Research Project** – Genetic Influence of Dopamine 4 Receptor on the etiology of Schizophrenia and treatment response at Kings College, London.
2000–2003	• Degree - BSc (Honours) Genetics, University of Sheffield. Grade: 2:2. **Final research project**: Culture and characterization of neural cell types from human embryonic stem cells. Supervisor: Prof.Harry.D.M.Moore.
1998–2000	• Standard12 Higher Secondary Certificate Examination (equivalent to A Level), Jai Hind Institute of Science and Technology, India. Physics 94%, Chemistry 89%, Biology 89%, Maths 70%, English 71%, Hindi 68%. Overall → 80% (**Distinction**)
1986–1998	• Standard10 Indian Certificate of Secondary Education **(**equivalent to GCSE), Villa Theresa High School, India English 92%, Hindi 86%, History, Geography and Civics 88%, Mathematics 90%, Science (Physics, Chemistry and Biology) 86%, Accounts 92%. Overall → 90% (**Distinction**)

■ **Other examinations/certificates:**

- EMBO certificate in Statistical analysis, 2007, U.K.
- Certificate in the 6th Bioinformatics Course 2005, Bertinoro, Italy.
- TOEFL score of 623 out of 660.
- 4 year training at Aakar Bharati Academy of Art, Bombay and certificates in the Elementary and Intermediate Drawing Board Examinations.
- Two-time winner of the Value for Education award.

■ **Scholarship and awards:**

- **University of Sheffield competitive academic scholarship** for 3 years.
- **FEBS Youth Travel Fund** to give a presentation at the FEBS Advanced Course "Mitochondrion in Health and Disease" in Aussois, France.
- **GfH travel grant** to enable me to give a presentation at the European Society of Human Genetics conference in Barcelona.
- **ESHG fellowship** to attend advanced course in Genetic Epidemiology in Paris,France.

■ **Work experience**:

- **May 2007:** Participated in the DAAD-RISE Summer Internship program. I mentored a student from Cornell University, U.S.A, for 3 months.
- **June 2005:** Worked on a 5 months research project at the University of Göttingen, Germany. Project : differential mRNA and protein expression of 3 candidate genes in a knockout mouse for Epilepsy.
- **October 2004:** Worked in the Genetics Diagnostic Laboratory at the Jaslok hospital in Mumbai.
- **September 2002:** Orientation program Meet and Greet assistant at the University of Sheffield: the aim was to greet the new international students and help with queries. This was very challenging and involved a lot of commitment, organization, communication skills and teamwork.
- **June 2002:** Worked in the Genomics laboratory at Nicholas Piramal, one of India's largest pharmaceutical companies. It was a short research project that involved PCR amplification of the CYP2D6 gene. This was in conjunction with a Pharmacogenomics project on 'Development of SNP database for a panel of candidate genes involved in drug response in the Indian population'.
- **Voluntary Work-** Organized a special Olympics program for mentally handicapped people. NASEOH (National Society for Equal Opportunities for the Handicapped) and LIFE (Let Individuals Feel for Everyone) certificates for raising funds for the less privileged.

■ **Extra curricular activities:**

- University of Sheffield 2002-2003 – Elected Secretary of the International Students Committee. We were in charge of over 5,000 International students and 50 different social and cultural societies.
- University of Sheffield 2001-2002 -Elected International Representative of the Hindu Students Forum.
- Winner of the School Debate Competition- Democracy versus Dictatorship.
- Won several certificates and medals in District Roller Skating Tournaments.
- Winner of many certificates in Art, Drawing and Painting competitions.

■ **Invited talks:**

1) November 2008: Philadelphia, U.S.A. – Platform presentation at the American Society of Human Genetics

2) June 2008: Barcelona, Spain- European Society of Human Genetics conference.

3) October 2007: Cambridge, U.K. - EMBO course in microarray analysis.

4) August 2007: Munich, Germany – Ludwig MaximiliansUniversität.

5) April 2007: Aussois, France – Mitochondria in life, death and disease, FEBS advanced lecture course.

■ **Poster presentations:**

1) November 2006: Munich, Germany- Bioinformatics Munich: From genomes to systems biology.

2) November 2006: Heidelberg, Germany-NGFN conference.

3) August 2007: Boston, U.S.A. – American Chemical Society National Meeting.

■ **Publications:**

1. SLC2A9 influences uric acid concentrations with pronounced sex-specific effects. Angela Döring*, Christian Gieger*, **Divya Mehta**, et al, *Nature Genetics* 40, 430 - 436 (2008).
2. Genome-Wide Scan on Total Serum IgE Levels Identifies FCER1A as Novel Susceptibility Locus. Weidinger et al, *PloS Genetics*, 2008.
3. A genome-wide association study identifies three loci associated with mean platelet volume, Meisinger, Prokisch et al, *AJHG*, 2009
4. A common FADS2 promoter polymorphism increases promoter activity and facilitates binding of transcription factor ELK1, Lattka et al, *Journal of Lipid Research*, 2009.
5. Single cell expression profiling of dopaminergic neurons in Parkinson disease, Elstner et al, *Annals of Neurology*, 2009.
6. Functional validation of eQTLs, *in preparation*.